

Patel, Nikhil (2014) Nutrition manipulation during development and its impact of metabolic homeostasis in the adult offspring. PhD thesis, University of Nottingham.

**Access from the University of Nottingham repository:**

[http://eprints.nottingham.ac.uk/13958/1/Nikhil\\_Patel\\_PhD\\_Print\\_Version.pdf](http://eprints.nottingham.ac.uk/13958/1/Nikhil_Patel_PhD_Print_Version.pdf)

**Copyright and reuse:**

The Nottingham ePrints service makes this work by researchers of the University of Nottingham available open access under the following conditions.

This article is made available under the University of Nottingham End User licence and may be reused according to the conditions of the licence. For more details see:  
[http://eprints.nottingham.ac.uk/end\\_user\\_agreement.pdf](http://eprints.nottingham.ac.uk/end_user_agreement.pdf)

**A note on versions:**

The version presented here may differ from the published version or from the version of record. If you wish to cite this item you are advised to consult the publisher's version. Please see the repository url above for details on accessing the published version and note that access may require a subscription.

For more information, please contact [eprints@nottingham.ac.uk](mailto:eprints@nottingham.ac.uk)

# Nutrition manipulation during development and its impact of metabolic homeostasis in the adult offspring

By Nikhil Patel, BSc (Dual Hons), MSc (Hons)

Thesis submitted to the University of Nottingham for  
the degree of Doctor of Philosophy

December 2012



# Abstract

---

Latest epidemiological data suggests 1.5 billion adults worldwide are either overweight or obese. With increasing weight and obesity, adipocytes increase in size. The enlargement of adipocytes has been associated with low grade chronic inflammation via elevated adipokine secretion. Previous epidemiological studies in humans and experimental studies in animals have shown that during different periods of pregnancy (gestation) the offspring that are born to maternal nutritional manipulation are more susceptible to developing metabolic diseases in later adult life. Therefore, the aim of this thesis was to investigate the role of maternal nutritional manipulation on adipose tissue depots and in particular the consequences the effect on markers of adipokine secretion.

Studies were conducted on both large and small animals (i.e. sheep and rats). Sheep studies focused on mid to late and late gestation periods of maternal nutritional restriction. Rat studies concentrated on long term fructose feeding during pregnancy and its effect on both the mother and offspring. Gene expression analysis identified an up-regulation in inflammatory related genes in pericardial and subcutaneous adipose tissue in the sheep studies. This was also seen in the rat studies with protein and gene expression displaying an up-regulation of inflammatory and metabolic related genes and proteins.

The main conclusion of my thesis is that after following maternal nutrient restriction, females appear to be much more sensitive to inflammatory and metabolic adaptations compared to males, possibly due to sex hormones playing a role. Whilst fructose feeding during pregnancy concluded the possibility of homeorhesis playing a protective role against potentially detrimental inflammatory pathways being activated in the mothers, the offspring however displayed signs of low level chronic inflammation in the retroperitoneal depot from early infancy to later adult life.

# Acknowledgements

---

Firstly, I would like to thank my funding organisations, the Medical Research Council and the University of Alberta, Canada whose financial support allowed me to complete my studies and PhD in Nottingham and Edmonton. I am also most grateful for the generous travel grants awarded to me by the University of Nottingham and Physiological Society which enabled me to present my work at both national and international scientific conferences.

My sincerest thanks go to my project supervisors Professors Michael Symonds, Dr. Helen Budge and Professor Rhonda Bell for providing excellent support, direction and advice throughout my study period. Many thanks go to all the staff and students within the Academic Division of Child Health and Obstetrics and Gynaecology Department at the Queen's Medical Centre, Nottingham who have made my time at the University of Nottingham both enjoyable and productive.

Special thanks to Dr Sylvain Sebert who performed all the animal experimentation work including the sheep handling and husbandry, data generation and collection for the animal activity and morphometric measurements, and finally all tissue and plasma sample collection for subsequent laboratory analysis. Also thanks to Pablo Fainberg, Mark Pope, Julianna Roda, Neele Dellschaft, Abha Hoedl, Chris Linker, Ian Bloor, and Victoria Wilson for their excellent technical support and expertise which allowed me to conduct my experimental analysis with confidence and proficiency.

Finally, I would like to thank my family and friends for all their support during the years of my studies, in particular my wife Jalpa and best friend's Inder, Ravi, and Jeetan along with Joey Diaz, Joe Rogan, Carl Sagan, Richard Feynman and Neil deGrasse Tyson for being providing great inspirational talks during my final phase of writing.

# Contents

---

<b>Abstract .....</b>	<b>3</b>
<b>Acknowledgements .....</b>	<b>5</b>
<b>Declaration .....</b>	<b>19</b>
<b>Abbreviations .....</b>	<b>20</b>
<b>List of Figures .....</b>	<b>23</b>
<b>List of Tables .....</b>	<b>31</b>
<b>Chapter 1 - Introduction .....</b>	<b>34</b>
1.1 Obesity .....	34
Table 1: International Classification of adult underweight, overweight and obesity according to BMI <sup>14</sup> .....	36
1.1.2 Worldwide Obesity .....	37
Figure 1.1 - <i>Percent of Obese (BMI &gt; 30) in U.S. Adults in 1985</i> <sup>7</sup> .....	38
Figure 1.2 - <i>Percent of Obese (BMI &gt; 30) in U.S. Adults in 2006</i> <sup>7</sup> .....	39
1.2 Metabolic Syndrome .....	40
1.3 Adipose Tissue .....	42
Figure 1.3 - <i>Stained microscopic images of brown (A) and white adipose tissue (B)</i> <sup>24</sup> .....	43
Figure 1.4 - <i>UCP-1 Thermogenesis. The uncoupling protein UCP1 is a proton carrier characteristic of brown adipose tissue. UCP1 uncouples the respiratory chain of ATP production, converting the metabolic energy in heat.</i> .....	46
1.4 White Adipose Tissue: .....	47
1.4.1 Adipose depots .....	48
1.4.2 Visceral fat .....	48
1.4.3 Subcutaneous fat .....	50
1.4.4 Epicardial Fat .....	51
1.5 Adipokines .....	52
1.5.1 Leptin .....	53
1.5.2 Tumour necrosis factor .....	54
1.5.3 IL-6 .....	57
1.5.4 Adiponectin .....	58

Figure 1.5 – *Adiponectin regions. Adiponectin belongs to the complement factor C1q-like superfamily of proteins and is composed of an N-terminal signal sequence (SS), a variable domain, a collagen-like (tail) domain and a C1q-like globular domain near the C-terminus*<sup>117</sup> .....59

Figure 1.6 – *Adiponectin complexes*<sup>125</sup>. *Adiponectin forms low-molecular weight (LMW) homotrimers and hexamers, and high-molecular weight (HMW) multimers of 12-18 monomers*<sup>126, 127</sup> .....60

Figure 1.7 – *Proposed molecular mechanisms of adiponectin*<sup>116</sup>. *The binding of adiponectin to its receptors provokes the activation of adenosine monophosphate AMPK and the activation of various signalling molecules, such as p38 mitogen-activated protein kinase MAPK, and PPAR. Activation of AMPK mediates pharmacological actions of adiponectin, including fatty acid oxidation, protein degradation, and glucose uptake.* .....62

1.5.5 Adiponectin Receptors .....63

1.5.6 Monocyte Chemotactic Protein-1 (MCP-1) .....65

1.5.7 Toll-like receptor (TLR).....66

1.5.8 Interleukin-18 .....66

1.5.9 Fat mass and obesity associated gene (FTO).....67

1.6 Endoplasmic reticulum stress pathways.....68

1.7 Nutrient Restriction .....69

1.7.1 Fetal nutritional programming of adult health and disease.....71

1.7.2 Low birth weight and “Catch-up growth” .....73

1.7.3 Effect of gender in nutrient restriction consequences.....74

1.7.4 Immune response with Inflammation .....75

1.7.5 Obesity induced inflammation .....77

1.7.6 Obesity and insulin resistance .....79

1.8 Fructose .....82

1.8.1 Fructose Intake .....82

1.8.2 Fructose Metabolism .....83

1.8.3 Hepatic Metabolism .....83

Figure 1.8 – *Fructose and glucose pathways. Fructose metabolism (grey arrows) differs from glucose (black arrows) due to 1) a nearly complete hepatic extraction and 2) different enzyme and reactions for its initial metabolic steps. Fructose taken up by the liver can be oxidized to CO<sub>2</sub> and then converted into lactate and glucose; glucose and lactate are subsequently either released into the circulation for extrahepatic metabolism or converted into hepatic glycogen or fat. The massive uptake and phosphorylation of fructose in the liver can lead to a large degradation of ATP to AMP and uric acid.* .....84



1.8.4 Long term effects of fructose .....	86
1.8.5 Dyslipidemia and de novo lipogenesis.....	87
1.8.6 Fructose and the pathogenesis of metabolic diseases.....	88
1.8.7 Fructose and weight gain.....	89
1.8.8 Fructose and cardiovascular issues .....	90
1.9 Fructose and Inflammation .....	91
1.9.1 Fructose and pregnancy .....	92
1.9.2 Main hypothesis and aims.....	94
<b>Chapter 2 – Methods .....</b>	<b>95</b>
2.1 Study Protocols .....	95
2.1.1 Sheep Study – early-to-mid gestational nutrient restriction.....	96
Figure 2.1 – <i>Sheep Study: Early to mid gestational nutrient restriction model.</i> <i>O=Obese group (100% of normal energy requirement given from 0 day of gestation, physical activity was restricted from 3 to 12 months during post-natal period to promote obesity). NR-O = Nutrient restricted-obese group (50% of normal energy requirements given from day 30 to 80 during gestation, physical activity was restricted from 3 to 12 months during post-natal period to promote obesity). L = Lean group ((100% of normal energy requirement given from 0 day of gestation, physical activity was not restricted during post-natal period) .....</i>	98
2.2 Sheep study – late gestational nutrient restriction .....	99
Figure 2.2 - <i>Sheep study: Late gestational nutrient restriction model. N = nutrient restricted (60% of normal energy requirements), R = fed to requirements (100% of normal energy requirements), A = fed to appetite (150% of normal energy requirements). During lactation, the N group were either raised as a singleton (-A = Accelerated growth raised without competition) or with a twin (-S = Standard growth raised as a twin). Post weaning phase, all groups were raised in an obesogenic environment.....</i>	105
2.3 Canada Studies .....	106
2.3.1 Rat Model .....	106
2.3.2 Fructose fed mothers study 2008.....	106
Figure 2.3 – <i>Rat Study: Fructose fed mothers model. FR group = Females fed 10% fructose water during pregnancy. CNTL group = females fed water. Both groups were fed chow (ad libitum) from the onset of mating.....</i>	108
2.3.3 Blood Collection.....	109
2.3.4 Cardiac puncture.....	110
2.3.5 Dissection.....	111
2.4 – Effect of Long Term Fructose Consumption .....	113

Figure 2.4 – <i>Rat Study: Effect of long term fructose consumption model. FR CHOW group were fed 10% fructose water during gestation and weaning while H2O CHOW group were fed water during gestation and weaning. Offspring for both groups fed only water and chow during post-natal period.</i> .....	115
2.5 Standard PCR .....	116
2.5.1 Hot Start PCR Procedure.....	117
2.5.2 Gel Electrophoresis & DNA Extraction.....	118
2.5.3 Gel Electrophoresis & DNA Extraction Procedure .....	119
2.5.4 RNA extraction.....	121
2.5.5 RNA Extraction Procedure .....	122
2.5.6 Nottingham Study.....	123
2.5.7 Alberta Study .....	124
2.6 Real Time PCR (real-time Polymerase Chain Reaction) .....	125
Figure 2.5 - <i>Real-Time PCR 18s samples using the StepOne Plus Real Time PCR System. Typical 'sigmoidal' curve in Q-PCR, the fluorescence signal crosses the threshold and increases exponentially until it reaches a plateau.</i> .....	128
Figure 2.6 - <i>Melting curve using the StepOne Plus Real Time PCR System. A typical melt curve from Q-PCR, the single peak indicates the specificity of product amplified.</i> .....	129
2.6.1 Primer Design .....	130
Table 2: List of primers used in the rat studies .....	132
2.6.2 Reverse Transcription (RT-PCR) .....	133
2.6.3 Reverse Transcription Procedure .....	134
2.6.4 Real-Time PCR Procedure .....	135
2.7 Histology .....	136
2.7.1 Histological tissue processing .....	137
2.7.2 Haematoxylin and eosin staining.....	138
2.7.3 H&E staining procedure.....	138
2.7.4 Immunohistochemistry.....	139
2.7.5 IHC procedure .....	141
2.8 Bicinchoninic acid total protein determination .....	142
2.8.1 BCA assay procedure .....	142
2.9 Electrochemiluminescence.....	144
Figure 2.8 - <i>Electrochemiluminescence mechanism uses SULFO-TAG labels, which emit light upon electrochemical stimulation initiated at the electrode surfaces of MSD assay plates.</i> .....	145

2.9.1 MSD Technology .....	146
2.9.2 ECL – MSD Multi-Array Procedure.....	147
2.9.3 Solution preparation.....	147
2.9.4 Calibrator and standard solutions .....	148
2.9.5 Analysis of results .....	150
Figure 2.9 – .....	150
2.9.6 Statistical analysis .....	151
<b>Chapter 3 – Early-to-mid gestational nutrient restriction.....</b>	<b>152</b>
3.1 Introduction and aims.....	152
3.2 Hypothesis .....	153
3.3 Material and methods .....	154
Figure 3.1 – <i>Sheep Study: Early to mid gestational nutrient restriction model.</i> <i>O=Obese group, NR-O = Nutrient restricted-obese group, L = Lean group.</i> .....	154
3.4 Results.....	155
3.4.1 The effects of maternal nutrient restriction between early to mid-gestation on pericardial fat mass .....	155
Figure 3.2 - <i>Pericardial fat mass (g) measurements of obese group (O, n=8) and nutrient restricted group (NR-O, n=12). Values are in mean ± SEM; statistical differences are donated by *, where *= p&lt;0.05. Analyses of pericardial fat mass (g) between the groups were treated with unpaired t-tests.</i> .....	155
Figure 3.2.1 – <i>Pericardial % total fat measurements of obese group (O, n=8) and nutrient restricted-obese group (NR-O, n=12). Values are in mean ± SEM; statistical differences are donated by *, where *= p&lt;0.05. Analyses of pericardial fat mass (g) between the groups were treated with unpaired t-tests.</i> .....	156
3.4.2 Pericardial gene expression of pro-inflammatory markers interleukin-6 (IL-6) and interleukin 18 (IL-18) .....	157
Figure 3.2.2 – <i>Interleukin-6 (IL-6) and Interleukin 18 (IL-18) mRNA expression values of the obese group (O, n=8) and nutrient restricted-obese group (NR-O, n=12). Values are in mean ± SEM; statistical differences are donated by * = p&lt;0.05 (unpaired t-test).</i> .....	157
3.4.3 Pericardial gene expression of 78 kDa glucose-regulated protein (GRP-78) and monocyte chemotactic protein-1 (MCP-1).....	158
Figure 3.2.3 – <i>GRP-78 and MCP-1 mRNA expression values of the obese group (O, n=8) and nutrient restricted-obese group (NR-O, n=12). Values are in mean ± SEM; statistical differences are donated by * = p&lt;0.05 (unpaired t-test).</i> .....	158
3.4.4 Pericardial gene expression of metabolic and inflammatory markers.....	159

Table 3: <i>Inflammatory and metabolic gene mRNA expression of O (obese group) and NR-O (nutrient-restricted obese group). Values are mean ±SEM. NS = no significant difference (unpaired t-test)</i> .....	159
3.5 Discussion .....	160
3.5.1 Fat mass accumulation following maternal nutrient restriction in juvenile obesity .....	161
3.5.2 Expression of inflammatory markers following maternal nutrient restriction in juvenile obesity.....	163
3.6 Conclusion.....	163
<b>Chapter 4 – Late gestational nutrient restriction .....</b>	<b>165</b>
4.1 Introduction and aims.....	165
4.2 Hypothesis .....	167
4.3 Materials and Methods .....	168
Figure 4.1 - <i>Late gestational nutrient restriction model, N = nutrient restricted (60% of normal energy requirements), R = fed to requirements (100% of normal energy requirements), A = fed to appetite (150% of normal energy requirements). During lactation, the N group were either raised as a singleton (-A = Accelerated growth raised without competition) or with a twin (-S = Standard growth raised as a twin). Post weaning phase, all groups were raised in an obesogenic environment. ....</i>	168
4.4 Results.....	169
4.4.1 The effects of a nutrient restricted environment and their impact on body weight and fat mass accumulation.....	169
Figure 4.1.1 - <i>Birth weight measured following late gestational maternal nutrition restriction. N = nutrient restricted (60% of normal energy requirements, n=16), R = fed to requirements (100% of normal energy requirements, n=9). Values are in mean ± SEM; statistical differences are denoted by * = p&lt;0.05 (unpaired t-test).</i>	169
Figure 4.1.2 – <i>Early post-natal growth displayed in a time course from birth to the end of lactation (90 days) for the RA group (fed to 100% of energy requirements, raised without competition, n=9), NA group (fed to 60% of energy requirements, raised without competition, n=8), and the NS group (fed to 60% of energy requirements, raised with competition, n=8). Values are in mean ± SEM; there were no statistical differences between the groups (Two way - ANOVA).</i> .....	170
Figure 4.1.3 – <i>Graph of weight taken at 17 months of age. RA group (fed to 100% of energy requirements, raised without competition, n=9), NA group (fed to 60% of energy requirements, raised without competition, n=8), and the NS group (fed to 60% of energy requirements, raised with competition, n=8). Values are in mean ± SEM; there were no statistical differences between the groups (ANOVA).</i> .....	171
Figure 4.1.4 – <i>Graph of total fat mass % taken at 17 months of age, RA group (fed to 100% of energy requirements, raised without competition, n=9), NA group (fed</i>	

to 60% of energy requirements, raised without competition, n=8), and the NS group (fed to 60% of energy requirements, raised with competition, n=8). Values are in mean  $\pm$  SEM; there were no statistical differences between the groups (ANOVA).

.....172

4.4.2 Maternal gestational nutrition restriction effect on gene expression of metabolic and inflammatory markers from subcutaneous adipose tissue.....173

Table 4: mRNA gene expression values of inflammatory and metabolic markers on RA group (fed to 100% of energy requirements, n=9) compared to NA group (fed to 60% of energy requirements, n=8). Values are in mean  $\pm$  SEM; NS = no significant difference, S =significance ( $p<0.05$ ) .....173

Figure 4.1.5 - An up-regulation of IL-6 mRNA expression values in females from RA group (fed to 100% of energy requirements, raised without competition, n=9) compared to NA group (fed to 60% of energy requirements, raised without competition, n=8). Values are in mean  $\pm$  SEM; statistical differences are donated by \* =  $p<0.05$  (unpaired t-test). .....174

Figure 4.1.6 - An up-regulation of FTO mRNA expression values in females from RA group (fed to 100% of energy requirements, raised without competition, n=9) compared to NA group (fed to 60% of energy requirements, raised without competition, n=8). Values are in mean  $\pm$  SEM; statistical differences are donated by \* =  $p<0.05$  (unpaired t-test). .....175

4.4.3 The effects of postnatal accelerated growth on gene expression of inflammatory on subcutaneous adipose tissue.....176

Table 5: mRNA gene expression values of inflammatory and metabolic markers on NS group (fed to 60% of energy requirements, n=8, raised with competition) compared to NA group (fed to 60% of energy requirements, n=9, raised without competition). Values are in mean  $\pm$  SEM; NS = no significant difference, S =significance ( $p<0.05$ , unpaired t-test).....176

Figure 4.1.7 - An up-regulation of adiponectin mRNA expression values in females from NS group (fed to 60% of energy requirements, raised with competition, n=9) compared to NA group (fed to 60% of energy requirements, raised without competition, n=8). Values are in mean  $\pm$  SEM; statistical differences are donated by \* =  $p<0.05$  (unpaired t-test). .....177

4.4.4 The effect of a maternal nutrient restricted environment during gestation followed by differing post-natal conditions on the development of adipose tissue .....178

Figure 4.1.8 – Representative of haematoxylin & eosin microscopic stained section of adipocytes from the RA group (fed to 100% of energy requirements, raised without competition, n=9) at x40 magnification. ....178

Figure 4.1.9 – Representative of haematoxylin & eosin microscopic stained section of adipocytes from the NA group (fed to 60% of energy requirements, raised without competition, n=8) at x40 magnification. ....179

Figure 4.2.0 – Representative of haematoxylin & eosin microscopic stained section of adipocytes from the NS group (fed to 60% of energy requirements, raised with competition, n=8) at x40 magnification. ....	179
Table 6: Adipocyte area ( $\mu\text{m}^2$ ) of subcutaneous adipose tissue from NS group (fed to 60% of energy requirements, raised with competition, n=9), NA group (fed to 60% of energy requirements, raised without competition, n=8). RA group (fed to 100% of energy requirements, without competition, n=9). Values are in mean $\pm$ SEM; NS = no significant difference (ANOVA). ....	180
4.4.5 Discussion .....	181
4.4.6 Nutrient restriction during late gestation and intra-uterine growth restriction .....	181
4.4.7 Changes in inflammatory gene expression.....	182
4.4.8 Accelerated post-natal growth and its effects on anti-inflammatory gene expression.....	185
4.4.9 Adipose tissue deposition and physiology.....	187
4.5.0 Conclusion.....	188
<b>Chapter 5 – Fructose fed mothers .....</b>	<b>189</b>
5.1 Introduction and aims.....	189
5.2 Hypothesis .....	189
5.3 Methods and materials.....	190
Figure 5.1 - Rat Study: Fructose fed mothers model. FR group = Females fed 10% fructose water during pregnancy. CNTL group = females fed water. Both groups were fed chow (ad libitum) from the onset of mating. ....	190
5.4 Results.....	191
5.4.1 The effect of fructose feeding during pregnancy on body weight .....	191
Figure 5.2 - Graph of weight taken at gestation day 20. FR group (n=18) = Females fed 10% fructose water during pregnancy. CNTL group (n=17) = females fed water during pregnancy. Both groups were fed chow (ad libitum) from the onset of mating. Values are in mean $\pm$ SEM; there were no statistical differences between the groups (Unpaired t-test). ....	191
5.4.2 Measurement of food and water intake during pregnancy .....	192
Table 7: Measurements food and water intake along with body weight and adipose weight of the FR group (fed 10% fructose water, n=18) and CNTL group (fed water, n=17), values are in mean $\pm$ SEM; statistical differences are denoted by * = $p < 0.05$ (unpaired t-test). ....	192
5.4.3 The effect of fructose intake during pregnancy on expression of metabolic markers.....	194
5.4.4 Gene expression of metabolic markers.....	194

Figure 5.2.1 - An up-regulation of leptin mRNA expression values of FR group (n=18) = Females fed 10% fructose water during pregnancy compared to CNTL group (n=17) = females fed water during pregnancy. Both groups were fed chow (ad libitum) from the onset of mating. Values are in mean  $\pm$  SEM; statistical differences are donated by \* = p<0.05 (unpaired t-test).....194

Figure 5.2.2 - An up-regulation of FTO mRNA expression values of FR group (n=18) = Females fed 10% fructose water during pregnancy compared to CNTL group (n=17) = females fed water during pregnancy. Both groups were fed chow (ad libitum) from the onset of mating. Values are in mean  $\pm$  SEM; statistical differences are donated by \* = p<0.05 (unpaired t-test).....195

Figure 5.2.3 - An up-regulation of adiponectin mRNA expression values of CNTL group (n=17) = females fed water during pregnancy compared to FR group (n=18) = Females fed 10% fructose water during pregnancy. Both groups were fed chow (ad libitum) from the onset of mating. Values are in mean  $\pm$  SEM; statistical differences are donated by \* = p<0.05 (unpaired t-test).....196

5.4.5 The effect of fructose intake during pregnancy on expression of pro-inflammatory markers .....197

5.4.6 Gene expression of inflammatory markers .....197

Figure 5.2.4 - An up-regulation of Nf-kB mRNA expression values of FR group (n=18) = Females fed 10% fructose water during pregnancy compared to CNTL group (n=17) = females fed water during pregnancy. Both groups were fed chow (ad libitum) from the onset of mating. Values are in mean  $\pm$  SEM; statistical differences are donated by \* = p<0.05 (unpaired t-test).....197

Figure 5.2.5 - An up-regulation of IL-18 mRNA expression values of FR group (n=18) = Females fed 10% fructose water during pregnancy compared to CNTL group (n=17) = females fed water during pregnancy. Both groups were fed chow (ad libitum) from the onset of mating. Values are in mean  $\pm$  SEM; statistical differences are donated by \* = p<0.05 (unpaired t-test).....198

Table 8: mRNA gene expression values of inflammatory and metabolic markers on FR group (fed 10% fructose water, n=18) compared to CNTL group (fed water, n=17,. Values are in mean  $\pm$  SEM; NS = no significant difference between the groups (unpaired t-test).....199

5.4.7 Plasma triglyceride concentration.....200

Figure 5.2.6 – Representative of triglyceride concentrations measured during pregnancy for FR group (n=18) = Females fed 10% fructose water during pregnancy compared to CNTL group (n=17) = females fed water during pregnancy. Values are in mean  $\pm$  SEM; statistical differences are donated by \* = p<0.05; \*\*\* = p<0.01(Two way ANOVA with repeated measures) .....200

5.5 Discussion .....201

5.5.1 Homeorhesis.....203

5.5.2 Pregnancy and inflammation.....	204
5.6 Conclusion.....	207
<b>Chapter 6 – Effect of long-term fructose consumption.....</b>	<b>209</b>
6.1 Introduction and aims.....	209
6.2 Hypothesis .....	209
6.3 Methods and materials.....	210
Figure 6.1 - <i>Rat Study: Effect of long term fructose consumption model. FR CHOW group were fed 10% fructose water during gestation and weaning while H2O CHOW group were fed water during gestation and weaning. Offspring for both groups FR CHOW (n=21) and H2O CHOW (n=24) fed only water and chow during post-natal period.</i> .....	210
6.4 Results.....	211
6.4.1 Long term body weight measurements and fat mass measure during fructose feeding in pregnancy in females.....	211
Table 9: <i>Measurements of body weight and adipose weight of the FR CHOW group (fed 10% fructose water, n=18) and H2O CHOW group (fed water, n=17) were taken during the study, values are in mean ± SEM; statistical differences are denoted by * = p&lt;0.05 (unpaired t-test).</i> .....	211
6.4.2 Long term body weight measurements and fat mass measure during fructose feeding in pregnancy in males.....	212
Table 10: <i>Measurements of body weight and adipose weight of the FR CHOW group (fed 10% fructose water, n=18) and H2O CHOW group (fed water, n=17) were taken during the study in males, values are in mean ± SEM; statistical differences are denoted by * = p&lt;0.05 (unpaired t-test).</i> .....	212
6.4.3 Measurement of food and water intake during pregnancy .....	213
Table 11: <i>Measurements food and water intake along with body weight and total Kcal intake of the FR group (fed 10% fructose water, n=18) and CNTL group (fed water, n=17) in mothers during pregnancy, values are in mean ± SEM; statistical differences are denoted by * = p&lt;0.05 (unpaired t-test).</i> .....	213
6.4.4 The effect of fructose intake during pregnancy on expression of inflammatory markers on 3 month old offspring.....	214
6.4.5 Gene expression of inflammatory markers on reproductive adipose tissue	214
Table 12: <i>mRNA gene expression values of inflammatory and metabolic markers on FR CHOW (fed 10% fructose water, n=7) compared to H2O CHOW group (fed water, n=9) in reproductive adipose tissue at 3 months of age, Values are in mean ± SEM; NS = no significant difference.</i> .....	214
6.4.6 Gene expression of inflammatory markers on retroperitoneal adipose tissue .....	215



Table 13: *mRNA gene expression values of inflammatory and metabolic markers on FR CHOW (fed 10% fructose water, n=7) compared to H2O CHOW group (fed water, n=9) in retroperitoneal adipose tissue at 3 months of age, Values are in mean ± SEM; NS = no significant difference. S =significance (p<0.05, unpaired t-test) ....215*

6.4.7 Gene expression of inflammatory markers on retroperitoneal adipose tissue .....216

Figure 6.2 - *An up-regulation of Leptin, MCP-1, FTO, and NF-kB mRNA expression values of FR group offspring (n=8) compared to H2O group offspring (n=9) in retroperitoneal adipose tissue at 3 months of age. Values are in mean ± SEM; statistical differences are donated by \* = p<0.05 (unpaired t-test). .....216*

6.4.8 The effect of fructose intake during pregnancy on expression of inflammatory markers on 6 month old offspring .....217

Table 14: *mRNA gene expression values of inflammatory and metabolic markers on FR CHOW (fed 10% fructose water, n=7) compared to H2O CHOW group (fed water, n=9) in reproductive adipose tissue at 6 months of age, Values are in mean ± SEM; NS = no significant difference. S =significance (p<0.05, unpaired t-test) .....217*

6.4.9 Gene expression of inflammatory markers on retroperitoneal adipose tissue .....219

Table 15: *mRNA gene expression values of inflammatory and metabolic markers on FR CHOW (fed 10% fructose water, n=7) compared to H2O CHOW group (fed water, n=9) in retroperitoneal adipose tissue at 6 months of age, Values are in mean ± SEM; NS = no significant difference. S =significance (p<0.05, unpaired t-test) ....219*

6.4.10 Gene expression of inflammatory markers on retroperitoneal adipose tissue .....220

Figure 6.2 - *An up-regulation of CHOP, IL-1B, IL-18, IL-6, MCP-1, NF-kB and TLR4 mRNA expression values of FR group offspring (n=8) compared to H2O group offspring (n=9) in retroperitoneal adipose tissue at 6 months of age. Values are in mean ± SEM; statistical differences are donated by \* = p<0.05 (unpaired t-test). 221*

6.4.11 The effect of fructose intake during pregnancy on expression of inflammatory markers on 9 month old offspring .....222

Table 16: *mRNA gene expression values of inflammatory and metabolic markers on FR CHOW (fed 10% fructose water, n=7) compared to H2O CHOW group (fed water, n=9) in reproductive adipose tissue at 9 months of age, Values are in mean ± SEM; NS = no significant difference. S =significance (p<0.05, unpaired t-test) .....222*

6.4.12 Gene expression of inflammatory markers on retroperitoneal adipose tissue .....223

Table 17: *mRNA gene expression values of inflammatory and metabolic markers on FR CHOW (fed 10% fructose water, n=7) compared to H2O CHOW group (fed water, n=9) in retroperitoneal adipose tissue at 9 months of age, Values are in mean ± SEM; NS = no significant difference. S =significance (p<0.05, unpaired t-test) ....223*

6.5 Electrochemiluminescence protein results on 3 months and 9 months offspring of gestational fructose feeding on retroperitoneal adipose tissue .....	225
6.5.1 3 Month Retroperitoneal MSD multiplex arrays .....	225
Figure 6.3 - An up-regulation of IL-1B protein expression values of FR group offspring (n=8) compared to H2O group offspring (n=9) in retroperitoneal adipose tissue at 3 months of age. Values are in mean $\pm$ SEM; statistical differences are donated by * = $p < 0.05$ (unpaired t-test) .....	225
Figure 6.4 - IL-6 protein expression values of FR group offspring (n=8) compared to H2O group offspring (n=9) in retroperitoneal adipose tissue at 3 months of age. Values are in mean $\pm$ SEM; no statistical differences were observed (unpaired t-test) .....	226
Figure 6.5 – MCP-1 protein expression values of FR group offspring (n=8) compared to H2O group offspring (n=9) in retroperitoneal adipose tissue at 3 months of age. Values are in mean $\pm$ SEM; no statistical differences were observed (unpaired t-test) .....	227
Figure 6.6 – TNF- $\alpha$ protein expression values of FR group offspring (n=8) compared to H2O group offspring (n=9) in retroperitoneal adipose tissue at 3 months of age. Values are in mean $\pm$ SEM; no statistical differences were observed (unpaired t-test) .....	228
6.5.2 9 Month Retroperitoneal MSD multiplex arrays .....	229
Figure 6.7 – An up-regulation of IL-1B protein expression values of FR group offspring (n=6) compared to H2O group offspring (n=7) in retroperitoneal adipose tissue at 3 months of age. Values are in mean $\pm$ SEM; statistical differences are donated by * = $p < 0.05$ (unpaired t-test) .....	229
Figure 6.8 – An up-regulation of IL-6 protein expression values of FR group offspring (n=6) compared to H2O group offspring (n=7) in retroperitoneal adipose tissue at 3 months of age. Values are in mean $\pm$ SEM; statistical differences are donated by * = $p < 0.05$ (unpaired t-test) .....	230
Figure 6.9 – An up-regulation of MCP-1 protein expression values of FR group offspring (n=6) compared to H2O group offspring (n=7) in retroperitoneal adipose tissue at 3 months of age. Values are in mean $\pm$ SEM; statistical differences are donated by * = $p < 0.05$ (unpaired t-test) .....	231
Figure 6.10 – An up-regulation of TNF- $\alpha$ protein expression values of FR group offspring (n=6) compared to H2O group offspring (n=7) in retroperitoneal adipose tissue at 3 months of age. Values are in mean $\pm$ SEM; statistical differences are donated by * = $p < 0.05$ (unpaired t-test) .....	232
6.6 Triglyceride concentration, insulin plasma and glucose levels measured in gestational fructose fed offspring compared to the control group .....	233
Table 18: Measurements of triglyceride concentrations, insulin plasma, and glucose levels for the FR CHOW group (fed 10% fructose water) and H2O CHOW group (fed	

<i>water) were taken during the study, values are in mean ± SEM; NS = no significant difference. S =significance (p=&lt;0.05, unpaired t-test).</i> .....	233
6.7 Discussion .....	234
6.7.1 Body weight and fat mass measurements .....	235
6.7.2 Gene expression of inflammatory markers at 3, 6 and 9 months .....	239
6.8 Protein expression of inflammatory markers at 3, and 9 months.....	241
6.9 Conclusion.....	242
<b>Chapter 7 – Conclusions .....</b>	<b>243</b>
7.1 Conclusion.....	243
7.1.1 General aims .....	243
7.1.2 Impact of gestational nutrient restriction on the sheep model .....	243
7.1.3 Impact of gestational nutrient manipulation on the rat model .....	244
7.2 Study limitations .....	246
7.2.1 Sheep model .....	246
7.2.2 Rat model.....	246
7.3 Future work and perspectives .....	247
7.3.1 Non-pregnant group .....	247
7.3.2 Other adipose depots .....	247
7.3.3 Further protein work .....	247
7.3.4 Final Remarks.....	248
Final Remarks.....	248
<b>References.....</b>	<b>249</b>

# Declaration

---

The work in this thesis was performed within the Academic Child Health Division, School of Clinical Sciences, University of Nottingham and the University of Alberta, Edmonton between October 2007 and April 2012.

This thesis illustrates my own work, completed under the supervision of Professor Michael Symonds, Dr. Helen Budge and Rhonda Bell. This report is an accurate representation of the work performed and no other study reproducing this work, to my knowledge, has been carried out within the University of Nottingham.

Nikhil Patel

April 2012

# Abbreviations

---

**AdipoR1** – Adiponectin receptor 1  
**AdipoR2** – Adiponectin receptor 2  
**AMC** - Academic Medical Centre  
**AMP (cAMP)** - Cyclic adenosine monophosphate  
**ANOVA** – Analysis of variance  
**APC** - Antigen presenting cells  
**ATF6** - Activating transcription factor 6  
**ATP** – Adenosine triphosphate  
**AUC** – Area under the curve  
**BAT** – Brown adipose tissue  
**BCA** – Bicinchoninic Acid  
**BiP** – Binding immunoglobulin protein  
**BMI** – Body mass index  
**BSA** – Bovine serum albumin  
**CCR2** – Chemokine (C-C motif) receptor 2  
**CD14** – Cluster of differentiation 14  
**cDNA** – Complimentary deoxyribonucleic acid  
**Cl<sup>-</sup>** – Chloride ion  
**CLS** - Crown-like structure  
**CNS** – Central nervous system  
**COSHH** – Control of substances hazardous to health  
**CRF** – Corticotropin releasing factor  
**CRP** – C reactive protein  
**Ct/Cp** - cycle threshold/crossing point  
**CVD** – Cardiovascular disease  
**DAB** – 3,3 diaminobenzidine  
**DMSO** – Dimethyl sulfoxide  
**DNA** – Deoxyribonucleic acid  
**DNL** - de novo lipogenesis  
**dNTP** – Deoxyribonucleotide  
**dSAT** - Deep subcutaneous adipose tissue  
**DTT** - Dithiothreitol  
**DXA** – Dual x-ray absorptiometry  
**EARNEST** – Early nutrition programming project  
**EAT** - Epicardial adipose tissue  
**ECL** - Electrogenerated chemiluminescence  
**EDTA** – Ethylenediaminetetraacetic acid  
**ELISA** – Enzyme linked immunosorbent assay  
**ER** – Endoplasmic reticulum  
**ETC** – Electron transport chain  
**fAd** - Full-length adiponectin  
**FADD** – Fas associated with death domain  
**FADH2** - Flavin adenine dinucleotide  
**FFA** – Free fatty acids  
**FR** – Fructose fed group  
**FTO** - Fat mass and obesity associated gene

**gAd** - Globular adiponectin  
**GD** - Gestational day  
**gDNA** - genomic DNA  
**GLUT4** – Glucose transporter type 4  
**GR** – Glucocorticoid receptor  
**GRP78** - Glucose-regulated protein 78  
**GTT** – Glucose tolerance test  
**HDL** - High-density lipoprotein  
**H<sub>2</sub>O** – Water  
**H<sub>2</sub>O<sub>2</sub>** – Hydrogen peroxide  
**H&E** – Haematoxylin and eosin  
**HCl** – Hydrochloric acid  
**HCO<sub>3</sub><sup>-</sup>** – Bicarbonate ion  
**HFCS** - High fructose corn syrup  
**HIER** – Heat induced epitope retrieval  
**HMW** - High molecular mass  
**HPA** – Hypothalamic pituitary adrenal axis  
**HRP** - Horseradish peroxidase  
**HSE** – Health survey of England  
**ICAM1** – Intercellular adhesion molecule 1  
**IFN $\gamma$**  – Interferon gamma  
**IHC** - Immunohistochemistry  
**IL** - Interleukin  
**IKK** - I $\kappa$ B kinase  
**IR** - Insulin resistance  
**Ire1** - Ser/thr protein kinase  
**IRS-1** – Insulin receptor substrate 1  
**iSAT** - Inguinal SAT  
**JNK** - C-Jun N-terminal kinase  
**L** – Lean environment  
**LBP** – Lipid binding protein  
**LMW** - low-molecular mass  
**LPS** - Lipopolysaccharide  
**MAPK** - Mitogen-activated protein kinase  
**MCPI** – Monocyte chemoattractant protein 1  
**MHC** – Major histocompatibility complex  
**MIF** – Macrophage migration factor  
**MMW** - Medium-molecular mass  
**mRNA** – Messenger ribonucleic acid  
**MSD** – Meso Scale Discovery  
**mVAT** - Mesenteric VAT  
**NADH** - Nicotinamide adenine dinucleotide  
**Na<sup>+</sup>** – Sodium ion  
**NEFA** – Non esterified fatty acid  
**NF $\kappa$ B** – Nuclear factor kappa-light-chain-enhancer of activated B cells  
**NR-O** - Nutrient restricted obese  
**O** – Obesogenic environment  
**O<sub>2</sub>** – Oxygen  
**OXPHOS** - Oxidative phosphorylation

**PAI-1** - Plasminogen activator inhibitor type  
**PBS** – Phosphate buffered saline  
**PCR** – Polymerase chain reaction  
**PERK** - Protein kinase RNA-like endoplasmic reticulum kinase  
**PPAR $\gamma$**  – Peroxisome proliferator activated receptor gamma  
**QPCR** – Quantitative polymerase chain reaction  
**R** - Fed to requirement group  
**r18s** – Ribosomal 18s  
**rVAT** - Retroperitoneal  
**RNA** – Ribonucleic acid  
**ROS** – Reactive oxidative species  
**RTPCR** – Reverse transcription polymerase chain reaction  
**S** – Significant  
**SAT** - Subcutaneous adipose tissue  
**SGA** - small for gestational age  
**siRNA** - Small interfering RNA  
**SODD** - Silencer of death domains  
**Srebp1** - Sterol Regulatory Element-Binding Proteins  
**sSAT** - Superficial subcutaneous adipose tissue  
**T2DM** - Type 2 diabetes mellitus  
**TAE** – Tris-acetate-EDTA  
**TBA** – Thiobarbituric acid  
**TG** - Triglyceride  
**TLR** – Toll like receptor  
**TNF $\alpha$**  – Tumour necrosis factor alpha  
**TNFR1** – Tumour necrosis factor receptor 1  
**TNFR2** – Tumour necrosis factor receptor 2  
**TRADD** – TNF receptor associated death domain  
**TRAF2** - TNF receptor-associated factor 2  
**Tris** – Tris(hydroxymethyl)aminomethane  
**tRNA** – Transfer ribonucleic acid  
**TTBS** – Tris buffered saline with Tween®  
**TZD** - Thiazolidinedione  
**UCP-1** - Uncoupling Protein-1  
**UPR** - Unfolded protein response  
**USDA** - United States Department of Agriculture  
**VAT** - Visceral adipose tissue  
**VCAM1** – Vascular cell adhesion molecule 1  
**VEGF** – Vascular endothelial growth factor  
**VLDL** - Very low density lipoprotein  
**WAT** – White adipose tissue  
**WHO** – World health organisation

# List of Figures

---

Figure 1.1 - Percent of Obese (BMI > 30) in U.S. Adults in 1985 <sup>7</sup> .....	38
Figure 1.2 - Percent of Obese (BMI > 30) in U.S. Adults in 2006 <sup>7</sup> .....	39
Figure 1.3 - Stained microscopic images of brown (A) and white adipose tissue (B) <sup>24</sup> .....	43
Figure 1.4 - UCP-1 Thermogenesis. The uncoupling protein UCP1 is a proton carrier characteristic of brown adipose tissue. UCP1 uncouples the respiratory chain of ATP production, converting the metabolic energy in heat. ....	46
Figure 1.5 – Adiponectin regions. Adiponectin belongs to the complement factor C1q-like superfamily of proteins and is composed of an N-terminal signal sequence (SS), a variable domain, a collagen-like (tail) domain and a C1q-like globular domain near the C-terminus <sup>117</sup> . ....	59
Figure 1.6 – Adiponectin complexes <sup>125</sup> . Adiponectin forms low-molecular weight (LMW) homotrimers and hexamers, and high-molecular weight (HMW) multimers of 12-18 monomers <sup>126, 127</sup> . ....	60
Figure 1.7 – Proposed molecular mechanisms of adiponectin <sup>116</sup> . The binding of adiponectin to its receptors provokes the activation of adenosine monophosphate AMPK and the activation of various signalling molecules, such as p38 mitogen-activated protein kinase MAPK, and PPAR. Activation of AMPK mediates pharmacological actions of adiponectin, including fatty acid oxidation, protein degradation, and glucose uptake. ....	62
Figure 1.8 – Fructose and glucose pathways. Fructose metabolism (grey arrows) differs from glucose (black arrows) due to 1) a nearly complete hepatic extraction and 2) different enzyme and reactions for its initial metabolic steps. Fructose taken up by the liver can be oxidized to CO <sub>2</sub> and then converted into lactate and glucose; glucose and lactate are subsequently either released into the circulation for extrahepatic metabolism or converted into hepatic glycogen or fat. The massive uptake and phosphorylation of fructose in the liver can lead to a large degradation of ATP to AMP and uric acid. ....	84
Figure 2.1 – Sheep Study: Early to mid gestational nutrient restriction model. O=Obese group (100% of normal energy requirement given from 0 day of	



gestation, physical activity was restricted from 3 to 12 months during post-natal period to promote obesity). NR-O = Nutrient restricted-obese group (50% of normal energy requirements given from day 30 to 80 during gestation, physical activity was restricted from 3 to 12 months during post-natal period to promote obesity). L = Lean group ((100% of normal energy requirement given from 0 day of gestation, physical activity was not restricted during post-natal period)..... 98

Figure 2.2 - Sheep study: Late gestational nutrient restriction model. N = nutrient restricted (60% of normal energy requirements), R = fed to requirements (100% of normal energy requirements), A = fed to appetite (150% of normal energy requirements). During lactation, the N group were either raised as a singleton (-A = Accelerated growth raised without competition) or with a twin (-S = Standard growth raised as a twin). Post weaning phase, all groups were raised in an obesogenic environment. .... 105

Figure 2.3 – Rat Study: Fructose fed mothers model. FR group = Females fed 10% fructose water during pregnancy. CNTL group = females fed water. Both groups were fed chow (ad libitum) from the onset of mating. .... 108

Figure 2.4 – Rat Study: Effect of long term fructose consumption model. FR CHOW group were fed 10% fructose water during gestation and weaning while H2O CHOW group were fed water during gestation and weaning. Offspring for both groups fed only water and chow during post-natal period. 115

Figure 2.5 - Real-Time PCR 18s samples using the StepOne Plus Real Time PCR System. Typical ‘sigmoidal’ curve in Q-PCR, the fluorescence signal crosses the threshold and increases exponentially until it reaches a plateau.. 128

Figure 2.6 - Melting curve using the StepOne Plus Real Time PCR System. A typical melt curve from Q-PCR, the single peak indicates the specificity of product amplified..... 129

Figure 2.7 - RT-PCR process step by step. A random primer binds to single stranded mRNA and the sequence is elongated by a transcriptase enzyme to create cDNA. Template of double stranded cDNA is then amplified by classic PCR..... 133

Figure 2.8 - Electrochemiluminescence mechanism uses SULFO-TAG labels, which emit light upon electrochemical stimulation initiated at the electrode surfaces of MSD assay plates. .... 145

Figure 2.9 – Typical standard curve from an MSD plate. The blue dots indicate the standards used to generate the standard curve, red dots are samples plotted against the curve to calculate concentration based on signal..... 150

Figure 3.1 – Sheep Study: Early to mid gestational nutrient restriction model. O=Obese group, NR-O = Nutrient restricted-obese group, L = Lean group.. 154

Figure 3.2 - Pericardial fat mass (g) measurements of obese group (O, n=8) and nutrient restricted group (NR-O, n=12). Values are in mean ± SEM; statistical differences are denoted by \*, where \* = p<0.05. Analyses of pericardial fat mass (g) between the groups were treated with unpaired t-tests.155

Figure 3.2.1 – Pericardial % total fat measurements of obese group (O, n=8) and nutrient restricted-obese group (NR-O, n=12). Values are in mean ± SEM; statistical differences are denoted by \*, where \* = p<0.05. Analyses of pericardial fat mass (g) between the groups were treated with unpaired t-tests.156

Figure 3.2.2 – Interleukin-6 (IL-6) and Interleukin 18 (IL-18) mRNA expression values of the obese group (O, n=8) and nutrient restricted-obese group (NR-O, n=12). Values are in mean ± SEM; statistical differences are denoted by \* = p<0.05 (unpaired t-test). .... 157

Figure 3.2.3 – GRP-78 and MCP-1 mRNA expression values of the obese group (O, n=8) and nutrient restricted-obese group (NR-O, n=12). Values are in mean ± SEM; statistical differences are denoted by \* = p<0.05 (unpaired t-test). .... 158

Figure 4.1 - Late gestational nutrient restriction model, N = nutrient restricted (60% of normal energy requirements), R = fed to requirements (100% of normal energy requirements), A = fed to appetite (150% of normal energy requirements). During lactation, the N group were either raised as a singleton (-A = Accelerated growth raised without competition) or with a twin (-S = Standard growth raised as a twin). Post weaning phase, all groups were raised in an obesogenic environment. .... 168

Figure 4.1.1 - Birth weight measured following late gestational maternal nutrition restriction. N = nutrient restricted (60% of normal energy

requirements, n=16), R = fed to requirements (100% of normal energy requirements, n=9). Values are in mean  $\pm$  SEM; statistical differences are donated by \* =  $p < 0.05$  (unpaired t-test). ..... 169

Figure 4.1.2 – Early post-natal growth displayed in a time course from birth to the end of lactation (90 days) for the RA group (fed to 100% of energy requirements, raised without competition, n=9), NA group (fed to 60% of energy requirements, raised without competition, n=8), and the NS group (fed to 60% of energy requirements, raised with competition, n=8). Values are in mean  $\pm$  SEM; there were no statistical differences between the groups (Two way - ANOVA). ..... 170

Figure 4.1.3 – Graph of weight taken at 17 months of age. RA group (fed to 100% of energy requirements, raised without competition, n=9), NA group (fed to 60% of energy requirements, raised without competition, n=8), and the NS group (fed to 60% of energy requirements, raised with competition, n=8). Values are in mean  $\pm$  SEM; there were no statistical differences between the groups (ANOVA). ..... 171

Figure 4.1.4 – Graph of total fat mass % taken at 17 months of age, RA group (fed to 100% of energy requirements, raised without competition, n=9), NA group (fed to 60% of energy requirements, raised without competition, n=8), and the NS group (fed to 60% of energy requirements, raised with competition, n=8). Values are in mean  $\pm$  SEM; there were no statistical differences between the groups (ANOVA). ..... 172

Figure 4.1.5 - An up-regulation of IL-6 mRNA expression values in females from RA group (fed to 100% of energy requirements, raised without competition, n=9) compared to NA group (fed to 60% of energy requirements, raised without competition, n=8). Values are in mean  $\pm$  SEM; statistical differences are donated by \* =  $p < 0.05$  (unpaired t-test). ..... 174

Figure 4.1.6 - An up-regulation of FTO mRNA expression values in females from RA group (fed to 100% of energy requirements, raised without competition, n=9) compared to NA group (fed to 60% of energy requirements, raised without competition, n=8). Values are in mean  $\pm$  SEM; statistical differences are donated by \* =  $p < 0.05$  (unpaired t-test). ..... 175

Figure 4.1.7 - An up-regulation of adiponectin mRNA expression values in females from NS group (fed to 60% of energy requirements, raised with competition, n=9) compared to NA group (fed to 60% of energy requirements, raised without competition, n=8). Values are in mean  $\pm$  SEM; statistical differences are denoted by \* =  $p < 0.05$  (unpaired t-test). ..... 177

Figure 4.1.8 – Representative of haematoxylin & eosin microscopic stained section of adipocytes from the RA group ((fed to 100% of energy requirements, raised without competition, n=9) at x40 magnification. .... 178

Figure 4.1.9 – Representative of haematoxylin & eosin microscopic stained section of adipocytes from the NA group ((fed to 60% of energy requirements, raised without competition, n=8) at x40 magnification. .... 179

Figure 4.2.0 – Representative of haematoxylin & eosin microscopic stained section of adipocytes from the NS group ((fed to 60% of energy requirements, raised with competition, n=8) at x40 magnification. .... 179

Figure 5.1 - Rat Study: Fructose fed mothers model. FR group = Females fed 10% fructose water during pregnancy. CNTL group = females fed water. Both groups were fed chow (ad libitum) from the onset of mating. .... 190

Figure 5.2 - Graph of weight taken at gestation day 20. FR group (n=18) = Females fed 10% fructose water during pregnancy. CNTL group (n=17) = females fed water during pregnancy. Both groups were fed chow (ad libitum) from the onset of mating. Values are in mean  $\pm$  SEM; there were no statistical differences between the groups (Unpaired t-test)..... 191

Figure 5.2.1 - An up-regulation of leptin mRNA expression values of FR group (n=18) = Females fed 10% fructose water during pregnancy compared to CNTL group (n=17) = females fed water during pregnancy. Both groups were fed chow (ad libitum) from the onset of mating. Values are in mean  $\pm$  SEM; statistical differences are denoted by \* =  $p < 0.05$  (unpaired t-test)..... 194

Figure 5.2.2 - An up-regulation of FTO mRNA expression values of FR group (n=18) = Females fed 10% fructose water during pregnancy compared to CNTL group (n=17) = females fed water during pregnancy. Both groups were fed chow (ad libitum) from the onset of mating. Values are in mean  $\pm$  SEM; statistical differences are denoted by \* =  $p < 0.05$  (unpaired t-test)..... 195

Figure 5.2.3 - An up-regulation of adiponectin mRNA expression values of CNTL group (n=17) = females fed water during pregnancy compared to FR group (n=18) = Females fed 10% fructose water during pregnancy. Both groups were fed chow (ad libitum) from the onset of mating. Values are in mean  $\pm$  SEM; statistical differences are denoted by \* =  $p < 0.05$  (unpaired t-test). ..... 196

Figure 5.2.4 - An up-regulation of Nf-kB mRNA expression values of FR group (n=18) = Females fed 10% fructose water during pregnancy compared to CNTL group (n=17) = females fed water during pregnancy. Both groups were fed chow (ad libitum) from the onset of mating. Values are in mean  $\pm$  SEM; statistical differences are denoted by \* =  $p < 0.05$  (unpaired t-test)..... 197

Figure 5.2.5 - An up-regulation of IL-18 mRNA expression values of FR group (n=18) = Females fed 10% fructose water during pregnancy compared to CNTL group (n=17) = females fed water during pregnancy. Both groups were fed chow (ad libitum) from the onset of mating. Values are in mean  $\pm$  SEM; statistical differences are denoted by \* =  $p < 0.05$  (unpaired t-test)..... 198

Figure 5.2.6 – Representative of triglyceride concentrations measured during pregnancy for FR group (n=18) = Females fed 10% fructose water during pregnancy compared to CNTL group (n=17) = females fed water during pregnancy. Values are in mean  $\pm$  SEM; statistical differences are denoted by \* =  $p < 0.05$ ; \*\*\* =  $p < 0.01$  (Two way ANOVA with repeated measures) ..... 200

Figure 6.1 - Rat Study: Effect of long term fructose consumption model. FR CHOW group were fed 10% fructose water during gestation and weaning while H2O CHOW group were fed water during gestation and weaning. Offspring for both groups FR CHOW (n=21) and H2O CHOW (n=24) fed only water and chow during post-natal period. .... 210

Figure 6.2 - An up-regulation of Leptin, MCP-1, FTO, and NF-kB mRNA expression values of FR group offspring (n=8) compared to H2O group offspring (n=9) in retroperitoneal adipose tissue at 3 months of age. Values are in mean  $\pm$  SEM; statistical differences are denoted by \* =  $p < 0.05$  (unpaired t-test). ..... 216

Figure 6.2 - An up-regulation of CHOP, IL-1B, IL-18, IL-6, MCP-1, NF-kB and TLR4 mRNA expression values of FR group offspring (n=8) compared to H2O

group offspring (n=9) in retroperitoneal adipose tissue at 6 months of age. Values are in mean  $\pm$  SEM; statistical differences are denoted by \* =  $p < 0.05$  (unpaired t-test). ..... 221

Figure 6.3 - An up-regulation of IL-1B protein expression values of FR group offspring (n=8) compared to H2O group offspring (n=9) in retroperitoneal adipose tissue at 3 months of age. Values are in mean  $\pm$  SEM; statistical differences are denoted by \* =  $p < 0.05$  (unpaired t-test). ..... 225

Figure 6.4 - IL-6 protein expression values of FR group offspring (n=8) compared to H2O group offspring (n=9) in retroperitoneal adipose tissue at 3 months of age. Values are in mean  $\pm$  SEM; no statistical differences were observed (unpaired t-test). ..... 226

Figure 6.5 – MCP-1 protein expression values of FR group offspring (n=8) compared to H2O group offspring (n=9) in retroperitoneal adipose tissue at 3 months of age. Values are in mean  $\pm$  SEM; no statistical differences were observed (unpaired t-test). ..... 227

Figure 6.6 – TNF- $\alpha$  protein expression values of FR group offspring (n=8) compared to H2O group offspring (n=9) in retroperitoneal adipose tissue at 3 months of age. Values are in mean  $\pm$  SEM; no statistical differences were observed (unpaired t-test). ..... 228

Figure 6.7 – An up-regulation of IL-1B protein expression values of FR group offspring (n=6) compared to H2O group offspring (n=7) in retroperitoneal adipose tissue at 3 months of age. Values are in mean  $\pm$  SEM; statistical differences are denoted by \* =  $p < 0.05$  (unpaired t-test). ..... 229

Figure 6.8 – An up-regulation of IL-6 protein expression values of FR group offspring (n=6) compared to H2O group offspring (n=7) in retroperitoneal adipose tissue at 3 months of age. Values are in mean  $\pm$  SEM; statistical differences are denoted by \* =  $p < 0.05$  (unpaired t-test). ..... 230

Figure 6.9 – An up-regulation of MCP-1 protein expression values of FR group offspring (n=6) compared to H2O group offspring (n=7) in retroperitoneal adipose tissue at 3 months of age. Values are in mean  $\pm$  SEM; statistical differences are denoted by \* =  $p < 0.05$  (unpaired t-test). ..... 231

Figure 6.10 – An up-regulation of TNF- $\alpha$  protein expression values of FR group offspring (n=6) compared to H2O group offspring (n=7) in

retroperitoneal adipose tissue at 3 months of age. Values are in mean  $\pm$  SEM;  
statistical differences are denoted by \* =  $p < 0.05$  (unpaired t-test)..... 232

# List of Tables

---

Table 1: International Classification of adult underweight, overweight and obesity according to BMI <sup>1 4</sup> .....	36
Table 2: List of primers used in the rat studies.....	132
Table 3: Inflammatory and metabolic gene mRNA expression of O (obese group) and NR-O (nutrient-restricted obese group). Values are mean ±SEM. NS = no significant difference (unpaired t-test).....	159
Table 4: mRNA gene expression values of inflammatory and metabolic markers on RA group (fed to 100% of energy requirements, n=9) compared to NA group (fed to 60% of energy requirements, n=8). Values are in mean ± SEM; NS = no significant difference, S =significance (p<0.05).....	173
Table 5: mRNA gene expression values of inflammatory and metabolic markers on NS group (fed to 60% of energy requirements, n=8, raised with competition) compared to NA group (fed to 60% of energy requirements, n=9, raised without competition). Values are in mean ± SEM; NS = no significant difference, S =significance (p<0.05, unpaired t-test).....	176
Table 6: Adipocyte area (µm <sup>2</sup> ) of subcutaneous adipose tissue from NS group (fed to 60% of energy requirements, raised with competition, n=9), NA group (fed to 60% of energy requirements, raised without competition, n=8). RA group (fed to 100% of energy requirements, without competition, n=9). Values are in mean ± SEM; NS = no significant difference (ANOVA). .....	180
Table 7: Measurements food and water intake along with body weight and adipose weight of the FR group (fed 10% fructose water, n=18) and CNTL group (fed water, n=17), values are in mean ± SEM; statistical differences are donated by * = p<0.05 (unpaired t-test). .....	192
Table 8: mRNA gene expression values of inflammatory and metabolic markers on FR group (fed 10% fructose water, n=18) compared to CNTL group (fed water, n=17,. Values are in mean ± SEM; NS = no significant difference between the groups (unpaired t-test). .....	199
Table 9: Measurements of body weight and adipose weight of the FR CHOW group (fed 10% fructose water, n=18) and H2O CHOW group (fed water,	



n=17) were taken during the study, values are in mean  $\pm$  SEM; statistical differences are donated by \* =  $p < 0.05$  (unpaired t-test). ..... 211

Table 10: Measurements of body weight and adipose weight of the FR CHOW group (fed 10% fructose water, n=18) and H2O CHOW group (fed water, n=17) were taken during the study in males, values are in mean  $\pm$  SEM; statistical differences are donated by \* =  $p < 0.05$  (unpaired t-test)..... 212

Table 11: Measurements food and water intake along with body weight and total Kcal intake of the FR group (fed 10% fructose water, n=18) and CNTL group (fed water, n=17) in mothers during pregnancy, values are in mean  $\pm$  SEM; statistical differences are donated by \* =  $p < 0.05$  (unpaired t-test)..... 213

Table 12: mRNA gene expression values of inflammatory and metabolic markers on FR CHOW (fed 10% fructose water, n=7) compared to H2O CHOW group (fed water, n=9) in reproductive adipose tissue at 3 months of age, Values are in mean  $\pm$  SEM; NS = no significant difference. .... 214

Table 13: mRNA gene expression values of inflammatory and metabolic markers on FR CHOW (fed 10% fructose water, n=7) compared to H2O CHOW group (fed water, n=9) in retroperitoneal adipose tissue at 3 months of age, Values are in mean  $\pm$  SEM; NS = no significant difference. S = significance ( $p < 0.05$ , unpaired t-test)..... 215

Table 14: mRNA gene expression values of inflammatory and metabolic markers on FR CHOW (fed 10% fructose water, n=7) compared to H2O CHOW group (fed water, n=9) in reproductive adipose tissue at 6 months of age, Values are in mean  $\pm$  SEM; NS = no significant difference. S = significance ( $p < 0.05$ , unpaired t-test)..... 217

Table 15: mRNA gene expression values of inflammatory and metabolic markers on FR CHOW (fed 10% fructose water, n=7) compared to H2O CHOW group (fed water, n=9) in retroperitoneal adipose tissue at 6 months of age, Values are in mean  $\pm$  SEM; NS = no significant difference. S = significance ( $p < 0.05$ , unpaired t-test)..... 219

Table 16: mRNA gene expression values of inflammatory and metabolic markers on FR CHOW (fed 10% fructose water, n=7) compared to H2O CHOW group (fed water, n=9) in reproductive adipose tissue at 9 months of

age, Values are in mean  $\pm$  SEM; NS = no significant difference. S = significance ( $p < 0.05$ , unpaired t-test)..... 222

Table 17: mRNA gene expression values of inflammatory and metabolic markers on FR CHOW (fed 10% fructose water, n=7) compared to H2O CHOW group (fed water, n=9) in retroperitoneal adipose tissue at 9 months of age, Values are in mean  $\pm$  SEM; NS = no significant difference. S = significance ( $p < 0.05$ , unpaired t-test)..... 223

Table 18: Measurements of triglyceride concentrations, insulin plasma, and glucose levels for the FR CHOW group (fed 10% fructose water) and H2O CHOW group (fed water) were taken during the study, values are in mean  $\pm$  SEM; NS = no significant difference. S = significance ( $p < 0.05$ , unpaired t-test). ..... 233

# Chapter 1 - Introduction

---

## 1.1 Obesity

Obesity is often described as an atypical or disproportionate accumulation of fat. The accumulation of fat leads to an increased risk of metabolic diseases and impairment of health<sup>1 2</sup>. The World Health Organisation (WHO) measures obesity based on a body mass index (BMI). BMI is the measure of an adult's weight in relation to their height. More specifically weight in kilograms divided by the square of height in metres<sup>1</sup>.

### **BMI Index Equations:**

---

SI (International System of Units)

$$BMI = \frac{\text{weight (kg)}}{\text{height}^2(\text{m}^2)}$$

---

United States of America Units

$$BMI = \frac{\text{weight (lb)} \times 703}{\text{height}^2(\text{in}^2)}$$

---

An example measurement (based on SI units) would be an adult weighing 65kg with a height of 1.70m and a BMI of 22.5.

$$BMI = \frac{\text{weight (kg)}}{\text{height}^2(\text{m}^2)} = BMI = \frac{65}{1.7^2}$$

BMI was devised between 1830 and 1850 by a Belgian polymath named Adolphe Quetelet<sup>3</sup>. BMI is used by the WHO to define overweight and obesity as it provides the most efficient large population measurement tool for both sexes and all ages of adults.

The WHO defines “obesity” as  $\geq 30$ , whilst “overweight” is  $\geq 25$  but  $< 30$  (See Table 1)<sup>4</sup>.

BMI works for most adults but taller adults have been reported to have a BMI abnormally higher when compared to their actual body fat levels. This occurs as BMI is proportional to weight given a fixed height, body shape and density. Therefore, when BMI is calculated proportional to height for a fixed weight, body shape and density, BMI is inversely proportional to the square of the height. Therefore, if you take all body dimensions and double them, weight will increase with the cube of the height. BMI should remain the same but instead doubles. This irregularity can be explained with the observation that taller people are not just scaled up short people, they tend to have leaner frames in ratio to their height<sup>5</sup>.

**Table 1: International Classification of adult underweight, overweight and obesity according to BMI<sup>1 4</sup>**

<b>Classification</b>	<b>BMI(kg/m<sup>2</sup>)</b>
	<b>Principal cut-off points</b>
<b>Underweight</b>	<b>&lt;18.50</b>
<b>Severe thinness</b>	<16.00
<b>Moderate thinness</b>	16.00 - 16.99
<b>Mild thinness</b>	17.00 - 18.49
<b>Normal range</b>	<b>18.50 - 24.99</b>
<b>Overweight</b>	<b>≥25.00</b>
<b>Pre-obese</b>	25.00 - 29.99
<b>Obese</b>	<b>≥30.00</b>
<b>Obese class I</b>	30.00 - 34.99
<b>Obese class II</b>	35.00 - 39.99
<b>Obese class III</b>	≥40.00

### 1.1.2 Worldwide Obesity

The prevalence of obesity worldwide is increasing at an alarming rate. There are an estimated 400 million obese adults with 1.6 billion adults being overweight<sup>1</sup>. Obesity across Europe has also seen a sharp rise, with countries such as Croatia having 31% of its men obese and Albania has 36% of its females obese<sup>6</sup>. The United States is by far the fattest population in the Americas; within its population, 31% of adult males and 33% of adult females are obese<sup>6</sup>. Surveys carried out from 2006 – 2007 in America showed the frequency of obesity had risen from 15% during 1976-1980 to 32.9% during the 2003-2004 survey (See Figure 1.1 and 1.2)<sup>7</sup>.

Obesity is not just confined to adults. Childhood obesity is also increasing at a startling rate. BMI is calculated differently for children, it is referred to as BMI-for-age. BMI values for children change depending on sex and age<sup>8</sup>. Unlike the adult version where a score is given, BMI-for-age values are plotted against a specific graph. BMI for children concentrates on certain percentile in which the child falls in. The BMI-for-age graph displays lines of specific percentiles, similar to that of weight and height charts for children<sup>8</sup>.

BMI-for-age shows children being less than the 5<sup>th</sup> percentile are at risk of being underweight, 85<sup>th</sup> to the 95<sup>th</sup> percentile shows the child is at risk of being overweight. If the child is calculated to be greater than the 95<sup>th</sup> percentile then the child is overweight. A healthy child displays a result between the 15<sup>th</sup> and 85<sup>th</sup> percentile<sup>8</sup>.

One in ten children worldwide between the ages of 5-17 years old are overweight, a total of 155 million. Amongst these, 30-45 million children are



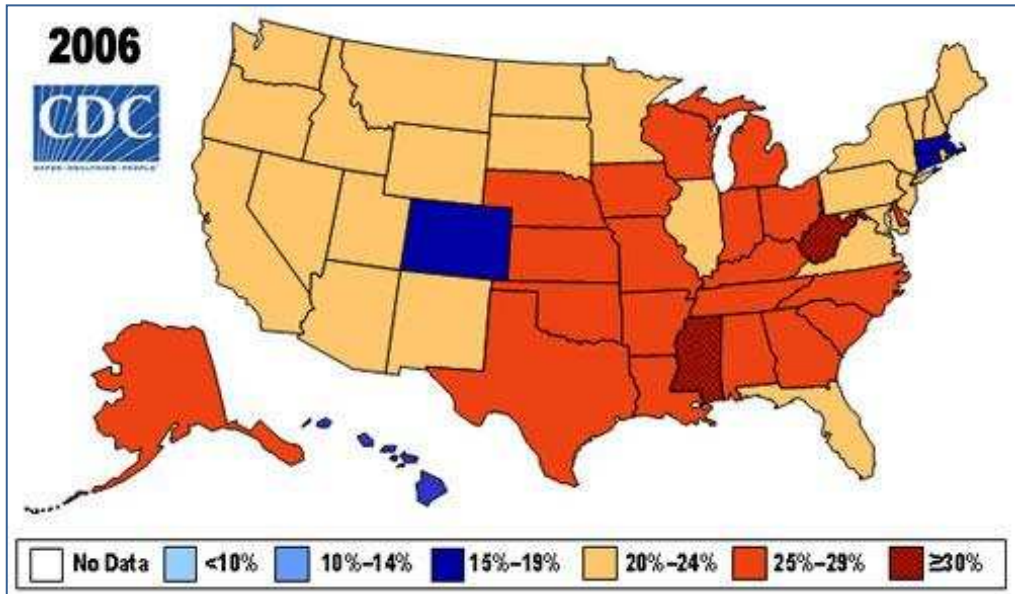


**Figure 2.2 - Percent of Obese (BMI > 30) in U.S. Adults in 2006<sup>7</sup>**



## 1.2 Metabolic Syndrome

Obesity has a profound impact on the human body and its metabolic system. Obesity increases the risk of health problems such as:

- Hypertension
- Insulin resistance and diabetes
- Cardiovascular disease
- Dyslipidemia
- Osteoarthritis
- Fatty liver disease

As obesity increases the risk of health problems such as those listed above, it essentially becomes a central player in the metabolic syndrome<sup>11</sup>. The syndrome is seen as a collection of factors including hypertension, central adiposity, glucose intolerance, insulin resistance and dyslipidemia which leads to cardiovascular disease and/or diabetes<sup>11</sup>. Metabolic syndrome has seen an increase in prevalence worldwide which many have linked to the increasing frequency of obesity worldwide<sup>12</sup>. The metabolic syndrome is also known as syndrome X, metabolic syndrome X, Reaven's syndrome, insulin resistance syndrome or CHAOS (Australia). Each of these different syndromes is defined with varying symptoms and, therefore, the definition given by the WHO is most commonly used<sup>12</sup>.

The WHO defines metabolic syndrome to have features such as high levels of blood glucose, increased blood triglycerides levels, decreased levels of HDL (high-density lipoprotein) cholesterol, increased blood pressure, and BMI over 30. When a person is exhibiting three or more of the features listed above, they have metabolic syndrome<sup>13</sup>.

Fat accumulation around the abdomen has been clearly linked to insulin resistance and plays a central role in the development of metabolic syndrome. Insulin resistance is the situation where regular levels of insulin can no longer generate a standard insulin response from liver cells, fat and muscle<sup>14</sup>. Due to the impairment of action from the fat, liver and muscle cells begin to lose the ability to control the regulation of insulin resulting in raised insulin<sup>14</sup>.

With insulin resistance playing a central role in metabolic syndrome, increased levels of plasma insulin and blood glucose are often seen as early indicators to a development of insulin resistance.

### 1.3 Adipose Tissue

The primary role of adipose tissue is to store energy in the form of fat but it also insulates and protects the body<sup>15</sup>. Adipose tissue is composed from many types of cells including fibroblasts, macrophages and endothelial cells but the highest proportions of cells that occupy adipose tissue are adipocytes. Adipocytes are essentially fat cells. They give adipose tissue the ability to store fat and also utilise fat into energy when required<sup>16</sup>. These specialised locations are often referred to as ‘adipose depots’.

There are two types of adipose tissue: brown adipose tissue (BAT) and white adipose tissue (WAT) (Figure 1.3).

**White Adipose Tissue (Unilocular Cells):** has a structure that consists of a large lipid droplet enclosed within a border of cytoplasm. Unlike brown adipose tissue, the nucleus of white adipocyte is flattened and situated on the edge of the cell<sup>17 18</sup>.

**Brown Adipose Tissue (Multilocular Cells):** has a polygonal structure with smaller lipid droplets spread throughout the cell. Brown adipocyte has more cytoplasm with the nucleus being round and located away from the edge of the cell. BAT acquires its brown colour from the significant amount of mitochondria present<sup>17 18</sup>.

Both BAT and WAT are able to store energy as triglycerides, the difference coming with white fat being able to release this energy in accordance to the requirements of the organism and brown fat transferring it as heat<sup>19</sup>. This

unique property gives BAT a decisive function in the regulation of body temperature, an important feature in hibernation, also in small and newborn mammals<sup>20</sup>.

Originally studies concerning BAT were focused on non shivering thermogenesis and thermoregulatory responses with WAT studies mainly focused on energy metabolism<sup>20</sup>. This however began to change with researchers investigating BAT in diet-induced thermogenesis led them to focus on its role in assorted conditions related with changes of energy balance<sup>21, 22, 23</sup>.

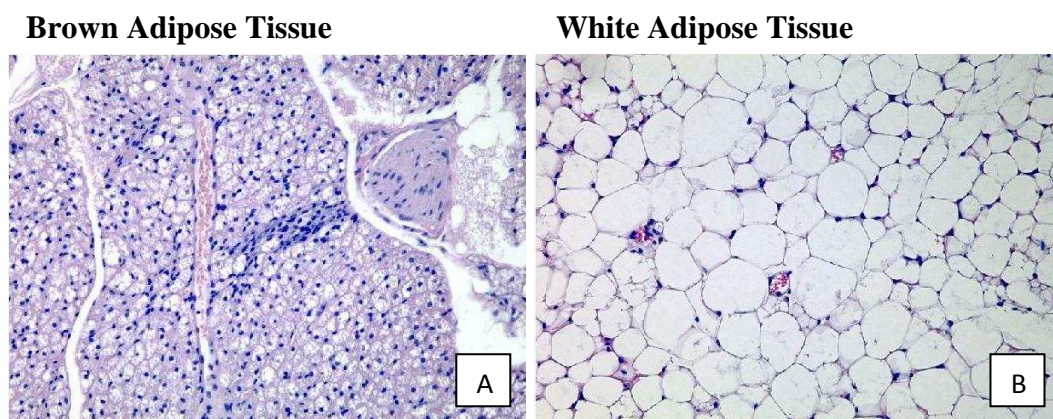


**Figure 3.3** - Stained microscopic images of brown (A) and white adipose tissue (B)<sup>24</sup>.

### **Brown Adipose Tissue**

The main function of BAT is to generate heat in newborn infants and hibernating mammals. Body heat is produced and maintained via the mitochondria located within the BAT<sup>18</sup>.

Chemiosmosis is a process that was first put forward by a British scientist, Peter Mitchell in 1961. The theory explains how ATP (adenosine triphosphate)

is synthesised in prokaryotes and eukaryotes. For eukaryotes, chemiosmosis occurs at the cristae (inner membrane of the mitochondria)<sup>25</sup>. The theory of chemiosmosis suggests that ATP is produced via energy stored in the form of a proton-motive force or proton gradients across membranes.

The process in which chemiosmosis occurs primarily involves two main components, the electron transport chain (ETC) and ATP Synthase. Chemiosmosis is coupled with oxidative phosphorylation<sup>26</sup>. In general, oxidative phosphorylation obtains electrons from NADH and FADH<sub>2</sub> and merges them with O<sub>2</sub>. This energy that is released from these redox reactions allows for the production of ATP from ADP<sup>26</sup>.

Brown adipose tissue has the unique ability to produce heat without the synthesis of ATP. Non-shivering thermogenesis is the main process for heat production for hibernating mammals and neonates<sup>27</sup>. Non-shivering thermogenesis is facilitated by UCP-1 (Uncoupling Protein-1). UCP-1 is an uncoupling protein located within the mitochondria of brown adipose tissue<sup>27</sup>.

## UCP1

UCP1 has the unique ability to supply a substitute route for protons to re-enter the matrix of mitochondria. This unorthodox pathway that is produced by UCP1 allows a short-cut for protons which are linked to the respiratory chain via the ATP synthase complex, this short-circuiting allows respiration to occur without ATP production. Therefore, heat is produced as respiration is allowed to be performed without ATP production (Figure 1.4)

UCP1 is exclusive to brown fat as it offers a mechanism by which vast amounts of heat can be produced. Activation of UCP1 occurs through a pathway which liberates fatty acids in brown fat cells. The pathway begins with the sympathetic nervous system which releases norepinephrine at its terminals<sup>28 29</sup>. Beta-3 adrenergic receptors which are situated on plasma membranes interact with the release of norepinephrine. This, in turn, activates adenylyl cyclase, a lyase enzyme<sup>30</sup>. Adenylyl cyclase synthesises the transformation of ATP to cyclic AMP (cAMP). cAMP then begins a further chain of activation in which protein kinase A is activated, that then proceeds to phosphorylate triacylglycerol lipase and becomes activated. The function of triacylglycerol lipase is to transform triacylglycerols into free fatty acids. Free fatty acids therefore activate UCP1<sup>30</sup>. During the end of thermogenesis, mitochondria oxidise the remaining free fatty acids. This is followed by the inactivation of UCP1 and, in turn, the brown fat cell restarts its regular energy-saving form<sup>30</sup>.

To summarise, BAT is heavily integrated with the generation and allocation of heat. Brown adipocytes have the ability to store triglycerides, though they differ from those of WAT through their vast number of mitochondria<sup>30</sup>.

Mitochondria in BAT are distinctly different from those found in liver or muscle. Mitochondria present in liver or muscle use electrochemical potential gradients within the mitochondrial membrane to generate ATP. BAT expresses UCP1; UCP1 is the main catalysis behind energy being expressed as heat instead of ATP<sup>30</sup>.

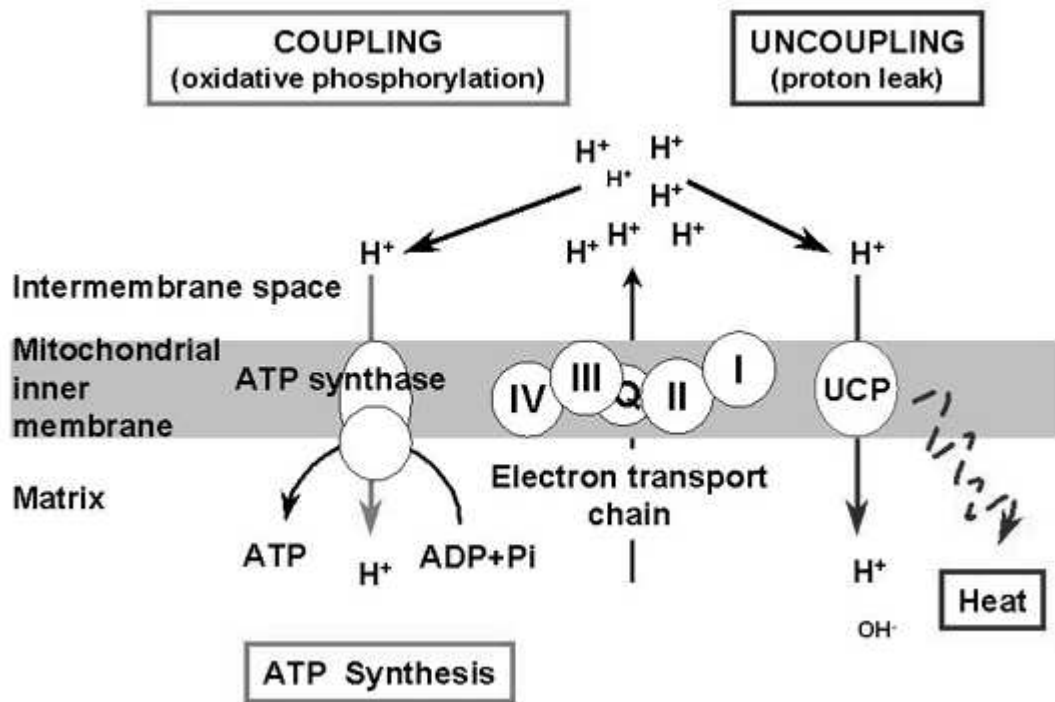


**Figure 4.4 - UCP-1 Thermogenesis.** The uncoupling protein UCP1 is a proton carrier characteristic of brown adipose tissue. UCP1 uncouples the respiratory chain of ATP production, converting the metabolic energy in heat.

#### **1.4 White Adipose Tissue:**

WAT is one of the most predominant tissue available in the organism, its main features comprise of fuel storage along with protection of organs from damage and acting as a thermal insulator. WAT is allocated into numerous depots, positioned internally and subcutaneously<sup>31</sup>. White adipose tissue in non-overweight, healthy humans is responsible for 25% of body weight in women and 20% in men<sup>32</sup>. The cells contain one large fat droplet, which due to its size, causes the nucleus to be compressed into a thin rim at the border. The cells also have receptors for growth hormones, norepinephrine, insulin, and glucocorticoids<sup>32</sup>.

One of the main functions of white adipose tissue is its ability to be used as a store of energy. WAT has the ability to accumulate excess dietary fat in the form of triglycerides and also release free fatty acids (FFAs) during moments of energy demand or starvation<sup>33</sup>. Lipolysis is defined as the breakdown of lipids and the hydrolysis of triglycerides into FFAs (FFAs are further degraded into acetyl units through beta oxidation).

WAT was simply known as a fuel storage depot until the discovery of leptin<sup>34</sup>. This gave the adipose tissue the recognition of an endocrine organ and fuelled sustained research into the role of adipose tissue which resulted in it being seen as an endocrine organ that was involved in many metabolic and physiological processes.



### **1.4.1 Adipose depots**

In the development of insulin resistance, total adipose tissue plays an important role, however it is theorised that certain fat depots maybe more heavily associated to risk factors for disease than others. The key adipose depots of significance are located in the abdomen and are split into SAT (subcutaneous adipose tissue) and VAT (visceral adipose tissue) with visceral adipose tissue further divided into mesenteric (a deep underlying depot which surrounds the intestine) and omental.

The allocation of VAT and SAT differs from person-to-person and is reliant on a variety of factors such as nutrition, age, sex, and the energy homeostasis of the adipose depots<sup>35</sup>. Even though many similarities exist, the differences between rodent and human adipose tissue should carry caution when deciding which depots to study and furthermore when extrapolating the findings between species<sup>36</sup>.

### **1.4.2 Visceral fat**

Visceral fat depots (particularly omental and mesenteric adipose tissue) characterise a major risk factor for the development and progression of T2DM (Type 2 Diabetes Mellitus) and CVD (Cardiovascular disease). Studies have shown that while total or subcutaneous tissue mass does not correlate with the development insulin resistance, visceral adipose tissue displays a positive correlation<sup>35, 37, 38</sup>. It is well known and comprehensively confirmed that the adipocytes of visceral fat tissue are significantly more lipolytically active than

subcutaneous adipocytes, which contributes furthermore to the plasma free fatty acid levels<sup>35, 39</sup>. In certain studies it was shown that diabetic obese individuals showed a significant downregulation of adiponectin and upregulation of leptin gene expression when comparing mesenteric VAT to SAT and omental VAT<sup>40</sup>.

Studies in rat focusing on mitochondrial content between epididymal (VAT) and human inguinal (SAT) adipocytes, showed a higher content of mitochondrial present in rat epididymal (VAT) adipocytes, as metabolic activity in cells are dependent on mitochondrial presence, this furthermore adds to the evidence of VAT adipocytes integral to energy homeostasis<sup>41</sup>. Further studies in adipose tissue taken from obese patients undergoing bariatric surgery, displayed higher relative oxidative phosphorylation (OXPHOS) activity in omental VAT then SAT<sup>42</sup>. It has been shown that subjects with a polymorphism within the UCP1 promoter reducing UCP1 gene expression are more susceptible to a high BMI, more significantly due to abdominal obesity<sup>43</sup>. This therefore adds weight to the conclusion that the amount of mitochondrial uncoupling and energy efficiency may indeed have an effect on obesity in WAT, in addition to BAT. High lipolytic activity could also be contributed due to the higher expression level of beta-adrenergic receptors in VAT<sup>44</sup>. In addition, glucose uptake (insulin-stimulated) was discovered to be higher in VAT when compared to SAT<sup>45</sup>. This results in excess visceral fat increasing the amount of free fatty acid being distributed to the liver, which therefore leads to increased very low-density lipoprotein particles and hepatic glucose output and in tandem leading to impairing the hepatic insulin response<sup>33</sup>.

Increased PPAR $\gamma$  mRNA expression has been shown in studies involving obese subjects<sup>45</sup>, additionally there was no difference in omental VAT and SAT tissues, and surprisingly PPAR $\gamma$  expression in mesenteric VAT was significantly higher in obese diabetic patients<sup>40</sup>. This authenticates the involvement of PPAR $\gamma$  in mesenteric adipose tissue lipolysis.

Studies in rodents have shown lipid synthesis to be higher in internal adipose tissue compared to SAT<sup>46</sup>. Further studies investigating gene expression in rat retroperitoneal (rVAT), inguinal SAT (iSAT), and mesenteric VAT (mVAT) displayed that the larger sized cells in rVAT expressed a higher amount of PPAR $\gamma$ , GLUT4, and Srebp1 mRNA expression compared iSAT and Mvat. The study was able to show overall that lipogenesis and lipolysis related genes combined with a low expression of fatty-acid oxidation related genes can give explanation to the high triglyceride turnover and therefore explain the differing behaviour of depots under physiological circumstances and its contribution in obesity-linked metabolic disorders<sup>47</sup>. The group was also able to show genes which were involved in lipid metabolism adjusted rapidly due to fasting in the internal rVAT depot in comparison to the SAT<sup>48</sup>.

### **1.4.3 Subcutaneous fat**

As stated in the chapter above, VAT is known as the highly metabolically active depot with strong associations to insulin-resistance and progression of metabolic disorders, SAT, however, is known better for its short-term and long term storage capacity. Therefore, this depot is crucial for the accumulation of TG in phases of excess energy intake and also at times of starvation, exercise,

fasting, or starvation to supply the organism with FFA's. As suggested for the role of SAT is to play a buffer throughout the intake of dietary lipids. By playing a buffer SAT protects other tissues against lipotoxic effects<sup>48</sup>.

SAT is anatomically divided by a stromal fascia (fascia superficialis) in humans, into deep subcutaneous adipose tissue (dSAT) and superficial subcutaneous adipose tissue (sSAT), both regions can be identified by their distinct histological characteristics. Studies have been able to show that sSAT is not linked to the risk of T2DM, whilst the depot sizes of dSAT have been significantly related to insulin-stimulated glucose utilization and also linked to fasting insulin levels along with total fat and VAT<sup>49, 50</sup>. When observing obese patients, the relationship between dSAT and insulin resistance is seen strongly in male patients<sup>51, 52</sup>. Studies researching expression and secretion of cytokines and hormones in lean patients, found dSAT to behave more like VAT than sSAT<sup>53</sup>. Further research in leptin indicates that SAT seems to have an exclusive role in its secretion, due to SATs the correlation with plasma leptin levels, which is in contrast to plasma insulin levels who draw a parallel with inter abdominal fat<sup>54</sup>. Rat studies have also been able to show gender-linked variance in SAT, with PPAR $\gamma$ 2 expression being higher in males than in females<sup>55</sup>.

#### **1.4.4 Epicardial Fat**

The visceral fat layer situated around the heart is called the epicardial adipose tissue (EAT). This depot is believed to be important in the safeguarding of coronary arteries along with utilizing fatty acids as a source of energy for the

cardiac muscle. It has been suggested that the release of adrenomedullin and adiponectin may have a protecting effect on the heart during mechanical or metabolic situations<sup>56</sup>.

Whilst being a protective force in certain situations, EAT has also been shown to act locally and influence the heart and vasculature via the secretion of pro-inflammatory cytokines and possibly lead to the contribution of coronary atherosclerosis<sup>57,58,59</sup>. Studies relating to carotid artery stiffness and their relationship to the amount of EAT have been observed in obese patients with hypertension whilst a correlation with waist circumference showed no significant link<sup>60</sup>.

## **1.5 Adipokines**

WAT adipocytes were seen to secrete many important hormones in addition to leptin, most importantly adiponectin. Leptin, adiponectin, plasminogen activator inhibitor type 1(PAI-1), tumour necrosis factor (TNF), resistin and many other proteins were notably termed as adipocytokines or most commonly called adipokines<sup>31</sup>. Adipokines have now totalled over 50 different molecular proteins. The adipokines are very distinct in each of their structure and function which gives them a unique ability collectively to regulate processes such as lipid metabolism, vascular function, insulin resistance and glucose tolerance<sup>61</sup>. Adipokines are also directly linked to immunity and inflammatory processes in the body, many cytokines secreted within an immune response can also be produced by adipose tissue, suggesting a role for adipose tissue in immunity and inflammation<sup>61</sup>.

### 1.5.1 Leptin

In 1994 Jeremy Friedman and his group from Rockefeller University published a paper which outlined a new gene in mice and humans, this gene was leptin<sup>34</sup>. Since then, leptin has been established as an essential element in energy homeostasis<sup>62</sup>. Leptin is produced by adipocytes in amounts relative to tissue mass<sup>62</sup>. It has a 167-amino acid structure and its gene, identified as Ob (Lep) gene (Ob meaning obese and Lep meaning leptin) is located on chromosome 17<sup>63</sup>. Leptin expresses its effects by binding to the transmembrane leptin receptor, named Ob-R<sup>64</sup>. In total there are 5 isoforms of the Ob-R receptor, the most well known is the Ob-Rb, that activates the Jak-Stat signal transduction pathway which in turn plays a vital role in the management of cellular reactions to growth factors and cytokines<sup>65-67</sup>.

The hypothalamus is the most significant site of action for leptin<sup>68</sup>. The ventromedial nucleus region of the hypothalamus is where leptin binds<sup>69</sup>. This specific area of the brain is known for its control over appetite. Leptin helps in the regulation of energy intake as well the control of some neuroendocrine relationships. Studies in deficiency syndromes have shown that leptin has a strong association with insulin resistance<sup>34</sup>. Deficiency or mutation of the leptin ob/ob gene, in mice results in metabolic symptoms such as obesity, hyperphagia and diabetes<sup>70</sup>. When leptin deficient mice are administered leptin

exogenously, these abnormalities are reversed, food intake is decreased and weight loss is observed, along with improved metabolic homeostasis<sup>70</sup>. Experiments with hyperglycemia and hyperinsulinemia in mice, leptin administered at supra-physiological doses showed a reversal of these symptoms but there was no significant decrease in weight loss<sup>34 70</sup>. This shows that leptin has an individual effect on insulin resistance which is separate from its effects on weight regulation.

### **1.5.2 Tumour necrosis factor**

Tumour necrosis factor (TNF) is an adipokine that is secreted by the adipose tissue; TNF is also involved with the immune system<sup>71 72</sup>. There are two types of TNF, alpha ( $\alpha$ ) and beta ( $\beta$ ). TNF- $\alpha$  is most commonly known for cell apoptosis and regulation of immune cells. TNF- $\alpha$  is a 17kDa protein that is synthesised into a 51kDa trimer which derives its name from its pro-apoptotic properties in tumour cells<sup>73</sup>. TNF- $\alpha$  is comprised of a transmembrane protein with stable homotrimers<sup>74 75</sup>. As TNF- $\alpha$  is essentially membrane bound, a TNF- $\alpha$  converting enzyme (TACE) releases TNF- $\alpha$  in a soluble form via proteolytic cleavage<sup>76</sup>.

Whilst adipose tissue synthesise a major proportion of TNF- $\alpha$ , the known producers of TNF- $\alpha$  are macrophages<sup>73</sup>. Along with being involved with apoptosis, TNF- $\alpha$  also stimulates the secretion of other adipokines such as IL-1, IL-6 and is involved in inflammation and immunity<sup>77</sup>. Within adipose tissue, TNF- $\alpha$  has effects on the liver, such as inducing insulin resistance by increasing serine-phosphorylation of insulin receptor substrate 1 (IRS-1)<sup>78</sup>.

This phosphorylation of IRS-1 leads to impaired insulin signalling<sup>79 80</sup>. TNF- $\alpha$  is highly expressed in visceral adipose tissue in comparison to subcutaneous adipose tissue<sup>81 82</sup>.

TNF- $\alpha$  has two receptors that it can bind to TNF-R1 and TNF-R2<sup>83 84</sup>. Both receptors are present in adipose tissue, though TNF-R2 is more prevalent in the immune system<sup>83 84</sup>.

When TNF- $\alpha$  binds to either TNF-R1 or TNF-R2 it leads to conformational changes in structure for the receptor<sup>85</sup>. The receptors form into a trimer shape into which fits TNF- $\alpha$ 's monomer structure<sup>86</sup>. The changes in receptor structure in binding the ligand lead to an uncoupling of the SODD (silencer of death domains) inhibitory protein<sup>87 88</sup>. The uncoupling means the adaptor protein TRADD (TNFRSF1A-associated via death domain) is activated and begins binding to the death domain<sup>89 90</sup>. This binding leads to activation from one of three pathways.

1. MAPK (Mitogen-activated protein kinase) pathway: JNK (C-Jun N-terminal kinase) is activated in the MAPK pathway by TNF, the JNK group is involved in pro-apoptotic properties, cell proliferation and differentiation<sup>91</sup>.
2. Death Signalling: With TRADD being activated it binds to FADD, this allows cysteine protease caspase-8 to be enrolled at a high concentrations. The high concentration of cysteine protease caspase-8 leads to autoproteolytic activation and removing of effector caspases which in turn leads to cell apoptosis<sup>92</sup>.



3. NF- $\kappa$ B pathway: NF- $\kappa$ B which is usually inhibited by I $\kappa$ B $\alpha$  (an inhibitory protein) is phosphorylated by protein kinase IKK (I $\kappa$ B kinase). The phosphorylation of I $\kappa$ B $\alpha$  by IKK allows NF- $\kappa$ B to be released and translocate to the nucleus and oversee the transcription of cell survival, proliferation, anti-apoptotic and inflammatory responses<sup>87</sup>  
88

TNF $\alpha$  plays a vital role in adipose tissue by suppressing the genes concerned with the consumption and storage of free fatty acids<sup>93 94</sup>. TNF $\alpha$  also suppresses genes implicated in the storage and uptake of glucose and adipogenesis<sup>95</sup>. TNF $\alpha$  has the ability to alter the expression of other adipokines such as adiponectin and IL-6<sup>96</sup>.

In the liver, TNF $\alpha$  has been reported to suppress the expression of genes involved with fatty acid oxidation, metabolism and glucose uptake<sup>97</sup>. TNF $\alpha$  is involved with impaired insulin signalling through two separate paths.

The first path involves TNF $\alpha$  activating serine kinases which lead to an increase in serine phosphorylation of insulin receptor substrates 1 and 2. The increased phosphorylation means that the substrates are unable to bind with insulin receptor kinases due to their inadequate state. Due to their inability to bind sufficiently to insulin receptor kinases, signalling is weakened<sup>78 98</sup>.

The second path involves TNF $\alpha$  playing an indirect role in impairing insulin signalling. TNF $\alpha$  impairs signalling by increasing serum levels of free fatty acids<sup>78 98</sup>.

### 1.5.3 IL-6

Interleukin 6 (IL-6) is a cytokine that has the ability to produce a variety of effects spanning from inflammation to insulin resistance<sup>99</sup>. IL-6 has a strong relationship with insulin resistance and plasma levels of IL-6 are positively associated with obesity and insulin resistance<sup>62</sup>. Adipose tissue secretes approximately 25% of all IL-6 synthesised in the body, with a range of cell types such as fibroblasts, skeletal muscle, immune cells and endothelial cells also contributing to its production<sup>99</sup>. Visceral depots have been shown to secrete more IL-6 compared to subcutaneous depots<sup>100</sup>. The location of visceral depots allows them to secrete directly into the portal circulation, thereby allowing IL-6 to have stronger metabolic effect on the liver<sup>101</sup>.

IL-6 circulates between sizes of 22 to 27 kDa and binds to an IL-6 transmembrane receptor resulting in a 2 protein complex forming, that complex binds to glycoprotein 130 (gp130) a transmembrane protein belonging to the cytokine receptor family. This three protein complex then permits signal transduction cascades<sup>62</sup>.

Epidemiological studies have shown that subjects with type 2 diabetes have elevated levels of IL-6, which are significantly lowered in adipose tissue and serum following weight loss<sup>102-105</sup>. Genetic studies illustrate a strong relationship between IL-6 genetic polymorphism and insulin resistance<sup>106</sup>. A possible mechanism through which IL-6 may present hepatic insulin resistance is by inhibition of the insulin receptor signal transduction cascade. This inhibition can lead to an induction of suppressor of cytokine signalling-3 SOCS-3<sup>101</sup>.

A recent study of IL-6 administration however concluded that it does not inhibit glucose homeostasis in healthy subjects as levels were not elevated to those seen in disease states<sup>107</sup>. Along with human studies, studies carried out on IL-6 deficient mice showed obesity and glucose intolerance was not prevented through IL-6 administration<sup>108</sup>.

Other possible effects of IL-6 include a decrease in the activity of lipoprotein lipase, thereby reducing the activity of triglyceride synthesis and then substrate availability. Secretion of adiponectin has also shown to be reduced by IL-6; this in turn leads to deterioration of insulin sensitivity<sup>109</sup>.

#### **1.5.4 Adiponectin**

Of all the adipokines expressed by adipose tissue, adiponectin is by far the most abundant with plasma protein levels averaging ~1 - 17µg/ml<sup>110</sup>. Adiponectin is synthesised by adipose tissue and secreted into the blood. It was originally identified by four different research groups, used different techniques to clone and identify the gene and leading to a host of names such as Acrp30, AdipoQ, apM1 and GBP28 being published for the same protein<sup>111-114</sup>. Finally, adiponectin was chosen as name for the protein.

Adiponectin's structure consists of four individual regions made up of a 244 amino acid polypeptide<sup>115</sup>. The four different regions all exhibit different properties, the first region is a short signal sequence region which allows the protein to secrete outside of the cell. The second region exhibits different properties depending on species<sup>116</sup>. The third region shows striking

resemblance to collagenous proteins and is often referred to as the collagen domain. The last region has been identified as the globular domain region (See Figure 1.5)<sup>116</sup>.

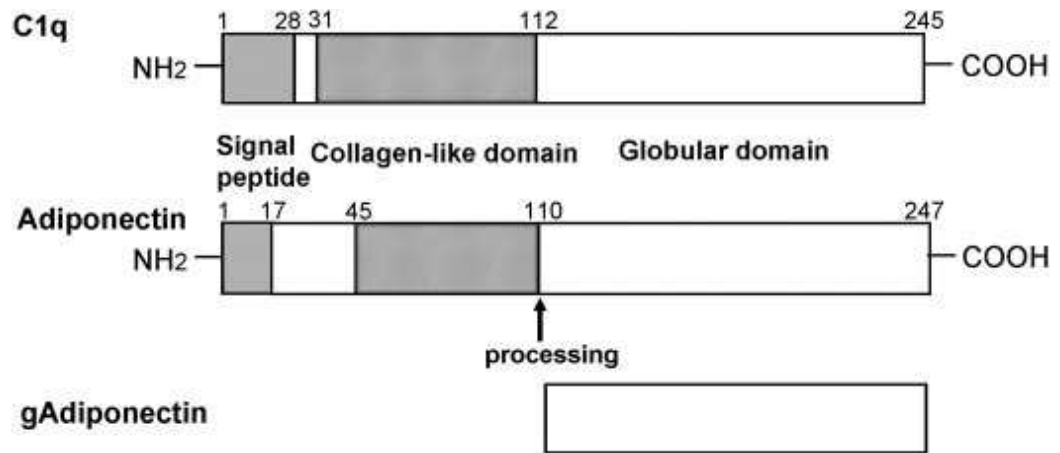


**Figure 5.5** – Adiponectin regions. Adiponectin belongs to the complement factor C1q-like superfamily of proteins and is composed of an N-terminal signal sequence (SS), a variable domain, a collagen-like (tail) domain and a C1q-like globular domain near the C-terminus<sup>117</sup>.

Adiponectin is present as a small globular form or in a full-length form. The dominant form is full-length adiponectin (fAd) and is present in nearly all plasma adiponectin<sup>116</sup>. The 3D structure of the globular domain of adiponectin shows a very high similarity to that of TNF $\alpha$  but there is no similarity in sequence between the two<sup>118</sup>. Recent evidence has shown a low concentration of globular adiponectin (gAd) in plasma resulting from proteolytic cleavage<sup>119</sup>. A recent study added more evidence to this hypothesis by showing that

activated monocytes with/without neutrophils secrete leukocyte elastase, is responsible for the cleavage of adiponectin to form globular adiponectin fragments<sup>120</sup>. Further studies have shown gAd that is cleaved from the fAd contains a C-terminal; this subsequent C-terminal gives gAd the ability to manipulate metabolic changes in skeletal muscle<sup>119 121 122</sup>.

The structure of adiponectin is vital to its understanding. Structural analysis of adiponectin helps to unlock the many pathways it regulates in the body. It produces a protein product of 30kDa that can lead to many complexes being formed such as trimeric complexes with low-molecular mass (LMW), hexamers with medium-molecular mass (MMW) and oligomers with high molecular mass (HMW) (Figure 1.6)<sup>123</sup>. Each different complex that is formed from the protein product exhibits different properties in various tissues<sup>124</sup>.

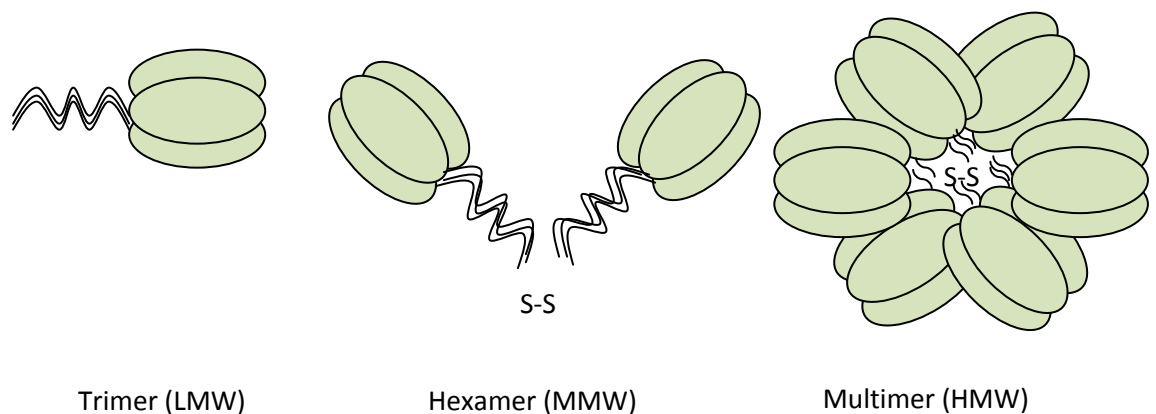


**Figure 6.6** – Adiponectin complexes<sup>125</sup>. Adiponectin forms low-molecular weight (LMW) homotrimers and hexamers, and high-molecular weight (HMW) multimers of 12-18 monomers<sup>126, 127</sup>.

Trimer formation (LMW): Trimers are formed through three monomers linking via their C-terminal globular domains. The trimer complex is then

secured into place by the triple helix structure of the three collagenous domains<sup>123 124</sup>.

Hexamer formation (MMW): Hexamers are formed through two trimers coming together at the Cys39 residues. Trimers are structurally held into position by the use of disulphide bonds<sup>123 124</sup>.

Multimer formation (HMW): HMW multimers are produced with multiple hexamers forming together with non-covalent interactions<sup>123 124</sup>.

Adiponectin levels are negatively correlated with BMI and are especially low in obese subjects. This is not reflected with the circulating levels of other adipokines, which seem to have an inverse relationship with obesity<sup>110</sup>.

Adiponectin influences many metabolic changes in the body. The two main processes with which adiponectin are associated with is glucose and lipid metabolism. With glucose metabolism, adiponectin affects gluconeogenesis and glucose uptake. Adiponectin has also shown to contribute towards increasing insulin sensitivity along with weight loss and a reduction in atherosclerotic formation<sup>128 129</sup>.

Adiponectin has, therefore, been thought to be anti-diabetic, anti-atherosclerotic and anti-inflammatory. Many of these properties can be attributed to its insulin sensitising effects<sup>130</sup>. Adiponectin activates the AMP kinase pathway and peroxisome-proliferatoractivated receptor  $\gamma$  (PPAR $\gamma$ ) to exert its metabolic effects. The pathways are activated in the liver and skeletal

muscle resulting in fatty acid oxidation and reduction of triglyceride content in liver and skeletal muscle (Figure 1.7)<sup>131 132</sup>.

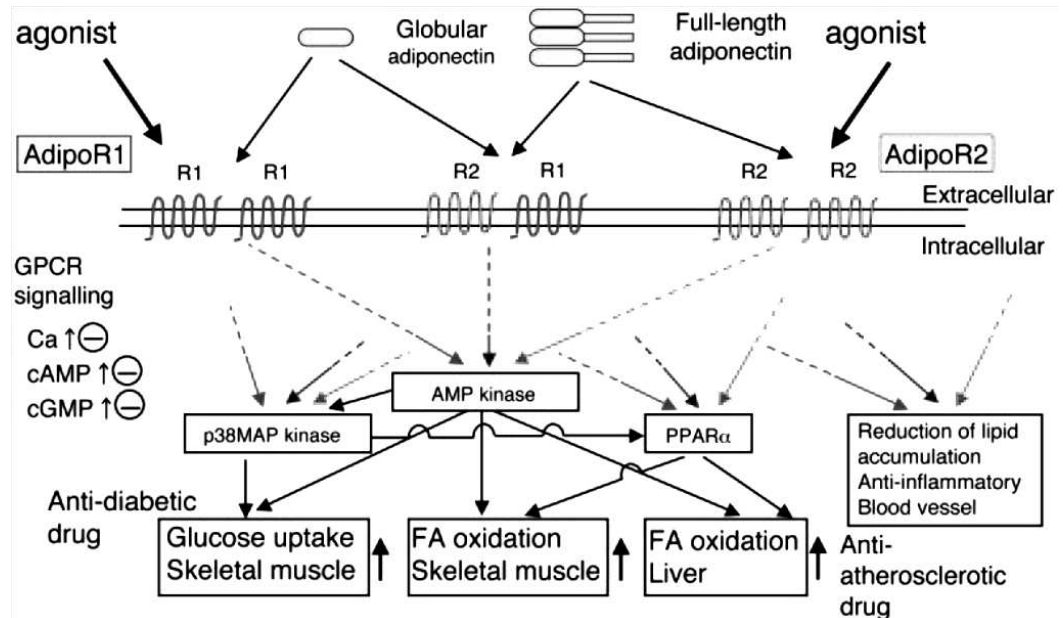


**Figure 7.7** – Proposed molecular mechanisms of adiponectin<sup>116</sup>. The binding of adiponectin to its receptors provokes the activation of adenosine monophosphate AMPK and the activation of various signalling molecules, such as p38 mitogen-activated protein kinase MAPK, and PPAR. Activation of AMPK mediates pharmacological actions of adiponectin, including fatty acid oxidation, protein degradation, and glucose uptake.

The presence of HMW, MMW and even LMW forms of circulating adiponectin have been detected in plasma, although the presence of gAd in the circulation is still debatable<sup>119 133</sup>. Transcription factors such as PPAR $\gamma$ , Sterol-regulatoryelement-binding protein (SREBP) and CCAAT/enhancer binding protein (C/EBP) have shown to regulate the adiponectin gene promoter<sup>134 135</sup>.

With diseases such as cardiovascular disease, metabolic syndrome, diabetes, lipodystrophy and insulin resistance all being associated with low levels of adiponectin, gender and ethnicity have now also been shown to effect adiponectin levels<sup>136-138</sup>.

As stated before adiponectin does not positively correlate with increasing fat mass and circulating adiponectin levels are notably lower in obese subjects in comparison to lean subjects, who have increased levels of adiponectin<sup>139-141</sup>. A possible mechanism to explain why adiponectin decreases as body fat mass rises is a possible feedback inhibitory system that accounts for the increased concentrations of adipokines as a possible reason for body fat mass gain, these adipokines possess an inhibitory influence over adiponectin gene expression (e.g. TNF $\alpha$  and IL-6)<sup>138</sup>.

### **1.5.5 Adiponectin Receptors**

Adiponectin has two identified transmembrane receptors responsible for its possible mechanisms of action. These are a distant relation to the G-protein coupled transmembrane family<sup>142 143</sup>. AdipoR1 was first identified through screening for gAd in the skeletal muscle and AdipoR2 was identified due to its close homology to AdipoR1. Both receptors display a different preference for adiponectin type<sup>143</sup>. AdipoR1 is primarily expressed in skeletal muscle with a strong affinity to gAd and a low affinity to fAd. AdipoR2 is mainly expressed in the liver with transitional affinity to fAd and gAd<sup>142</sup>. AdipoR1 was first identified through screening for gAd in skeletal muscle and AdipoR2 was



identified due to its close homology to AdipoR1<sup>142 143</sup>. AdipoR1 and AdipoR2 have been shown to be expressed in pancreatic  $\beta$ -cells, though further studies are required to confirm this<sup>144 145</sup>. Both receptors exert the effects of adiponectin on fatty acid oxidation, PPAR $\gamma$  ligand activity, glucose uptake and 5' AMPK pathway<sup>142 146-148</sup>.

Evidence supporting AdipoR1 and AdipoR2 for mediating fatty acid oxidation with globular and full-length adiponectin has been put forward through a study which uses siRNA (small interfering RNA) to suppress the expression of both receptors. This leads to a decrease in fatty acid oxidation from gAd and fAd in contrast to normal expression. The study highlighted that suppression of AdipoR1 and AdipoR2 that led to subsequent decreased levels of fatty acid oxidation leading to a conclusion that both receptors play a mediating effect on fatty acid oxidation<sup>142</sup>.

AdipoR1 protein has been shown to be heavily conserved in a variety of species from yeast to man. The seven transmembrane structural fixture in particular is heavily conserved through different species. The adiponectin receptors are known to play a role in the regulation of lipid metabolism which is mirrored with the yeast homolog YOL002c. Structural analysis of the receptors has revealed that the N terminal region was internal and the C terminal region external for both receptors. The structural geometry of AdipoR1 and AdipoR2 is reversed in all other existing G protein-coupled receptors<sup>142 149</sup>.

### **1.5.6 Monocyte Chemotactic Protein-1 (MCP-1)**

MCP-1 also known as Chemokine (C-C motif) ligand 2 (CCL2) or small inducible cytokine A2 is a protein which is encoded by the CCL2 gene in humans. MCP-1 is a small cytokine which is a part of the CC chemokines family. MCP-1 is a major player in the recruitment of memory T cells, monocytes and dendritic cells to the site of infection and tissue injury. MCP-1 is secreted as a protein precursor which contains a signal peptide of 23 amino acids along with a mature signal peptide of 76 amino acids and has a molecular weight of ~13 kDa and is a monomeric polypeptide<sup>150</sup>. MCP-1 binds to membrane surface of CCR2 proteins which are highly expressed on activated T cell and monocytes surfaces. The receptor complexes of MCP1-CCR2 are initially occupied in attracting monocytes, natural killer cells and T-lymphocytes to the sites of cellular injury or stress. Studies have shown MCP-1 to up-regulate the expression of IL-6 in epithelial cells and amplification in the expression of TNF- $\alpha$  concentration with increasing MCP-1 expression from in vitro models studies<sup>151</sup>. Studies investigating obesity and increased fat mass have displayed increased expression of MCP-1 subsequently leads to increased MCP-1 plasma concentrations<sup>151</sup>. Studies in obese mice specifically engineered for the over expression of MCP-1 gene have shown amplified macrophage infiltration in adipose tissue along with an increase in hepatic triglyceride levels and insulin resistance, whilst MCP-1 knockout studies have shown decreased insulin resistance<sup>151</sup>.

### **1.5.7 Toll-like receptor (TLR)**

Toll-like receptor (TLR) is a major regulator of both adaptive and innate immune responses. TLR signalling is involved with the activation of the innate immune system through lipotoxicity. TLR has been shown to play a strong molecular link between hyperlipidemia, known for its clinical feature in obesity and the initiation of the innate immune system<sup>152</sup>. TLR-4 is widely expressed in a range of cells, especially macrophages and adipocytes and forms an important ligand complex when in contact with free fatty acids<sup>152</sup>. Once activated, TLR-4 up-regulates the inflammatory expression in cytokines and stimulates insulin resistance. TLR's are seen to play a major role in other metabolic symptoms of obesity including hepatic steatosis and atherosclerosis<sup>153</sup>. TLR-4 has also been associated with macrophage infiltration and their expression levels exhibiting a positive correlation with the magnitude of increase in adipocyte hyperplasia and hypertrophy, therefore demonstrating a possible macrophage-related inflammatory response that may co-ordinate towards the development of obesity<sup>154</sup>.

### **1.5.8 Interleukin-18**

Interleukin-18 (IL-18) is a pro-inflammatory cytokine that is generated by macrophages and various other cells, with its receptor belonging to the IL-1R and TLR super-family. IL-18 shares a homologous structure to IL-1 but is

expressed by both non-immune and immune cells<sup>155</sup>. Studies have shown over-expression of IL-18 can lead to the development of severe pro-inflammatory disorders such as auto-immune diseases and inflammatory tissue damage<sup>156</sup>. Contrasting studies have shown IL-18 deficient mice exhibit obesity and insulin resistance in comparison to their wild type group and may exhibit a similar role to which IL-6 and TNF- $\alpha$  display in energy intake and insulin sensitivity<sup>156</sup>.

### **1.5.9 Fat mass and obesity associated gene (FTO)**

The FTO gene is located on chromosome 16 in humans with various variants of the gene showing correlation with obesity in humans. FTO is expressed in a wide range of tissues and in particular the hypothalamus, a region known for appetite regulation where its expression is highly concentrated<sup>157</sup>. Studies in mice have shown that FTO expression from the hypothalamus tissue is regulated by nutritional status, with starvation displaying a down-regulation in FTO expression<sup>158</sup>. These findings confirm the relationship between energy intake and FTO polymorphisms, leaving a possible suggestion that the product of the FTO gene is directly involved with energy balance regulation<sup>158</sup>. In addition the FTO gene is expressed in a wide range of tissues, including major tissues or organs that regulate energy metabolism and cardiovascular function<sup>158</sup>. The role that FTO plays in the regulation of these tissues and organs in their relationship to obesity and metabolic symptoms is still to be verified and remains unknown.

European epidemiological studies have identified variants of the FTO gene to be linked to obesity (allele SNPrs9939609). The study was able to conclude that carriers with one copy of the risk allele weighed 1.2kg more than people without any copies; subsequently carriers with two copies of the risk allele weighed approximately 3kg more and displayed a 1.67 fold higher risk of obesity<sup>159</sup>. FTO has also been shown to be linked with an increased risk of type 2 diabetes<sup>159</sup>. A study involving a combination of nutrient restriction (in utero) followed by juvenile obesity showed increased FTO gene expression in the hypothalamus, once again indicating its role in appetite control and obesity<sup>157</sup>.

### **1.6 Endoplasmic reticulum stress pathways**

Organelle dysfunction is a promising concept used to explain the wide collection of maladaptive responses in an obese state. To be more specific, endoplasmic reticulum (ER) stress proceeded with the activation of unfolded protein response (UPR). During obesity, stressed adipocytes activate the UPR pathway to promote cell survival by increasing the recruitment of crucial ER chaperones, such as glucose-regulated protein 78 (GRP78) to the site of stress in order to aid the restoration of cellular homeostasis<sup>160</sup>. GRP78 also known as binding immunoglobulin protein (BiP) is an ER chaperone located at the lumen of the ER<sup>161</sup>. When unfolded proteins build up in the ER, resident chaperones such as GRP78 become occupied, releasing transmembrane ER proteins involved in generating the UPR. These transmembrane proteins (PERK – PRK-like ER kinase, Ire1, and ATF6 – Activating transcription factor 6) span across the ER membrane, with their N-terminus situated in the lumen of the ER and

their C-terminus in the cytosol, thus supplying a bridge that connects these two compartments<sup>162</sup>. Under normal conditions the N-terminus of the ER proteins is held together by GRP78, therefore preventing their activation. However when misfolded proteins accumulate, GRP78 is released from holding together Ire1, PERK, and ATF6. This release leads to an Ire1 and PERK oligomerization within the ER membrane. Oligomerized Ire1 binds with TRAF2 (TNF receptor-associated factor 2), signalling downstream kinases that activate NF- $\kappa$ B and c-Jun, resulting in expression of gene associated with host defence (inflammatory)<sup>163, 164</sup>.

When the process fails to promote cell survival, the UPR pathway activates programmed cell death via the apoptosis pathway, through the activation of induction of the CHOP gene or through activation of the JNK pathway<sup>165 166</sup>.

With the accumulation of increased adipose tissue leading to obesity, it is accompanied by adipocyte cell death which displays a distinct gathering of mast cells and macrophages in the swelling of adipose tissue during obesity<sup>167</sup>. These macrophages are seen to fuse and form a syncytium around the multinucleate giant cells (also referred to as crown-like structures), displaying a trademark of chronic inflammation<sup>168</sup>.

## **1.7 Nutrient Restriction**

Growth of the fetus during their development in the mother is restricted by the amount of nutrients that are supplied via the placenta. When the nutrient supply rate does not meet requirements, development and growth rates are

altered. If the rate of nutrient supply is insufficient for long periods, the fetuses metabolic system makes alterations to compensate for the lack of nutrients<sup>169</sup>. Ultimately development of vital fetal organs and structure are often compensated for leaving the offspring to be born underweight and of a smaller size<sup>170</sup>.

The Dutch Famine Study of 1944 (or “Hongerwinter” or Hunger Winter) is a study that can be used to understand the implications of nutrient restriction<sup>171</sup>. During the end of World War II, certain areas within the Netherlands were subjected to insufficient food supplies leading to a famine during the midst of winter<sup>171</sup>. Food rationing was implemented to compensate for the lack of food supply. The food rations for adults were restricted to between 400-800 calories a day, a quarter of recommended daily intake<sup>171</sup>. The famine took place in a well developed and modern country which meant the famine was well documented and allowed scientists to study the famine in great detail and measure the effects of famine upon pregnant woman and their offspring.

A follow-up study to the Dutch famine of 1944 was completed by the AMC (Academic Medical Centre) in Amsterdam in collaboration with the University of Southampton. The study concluded that a significant amount of pregnant women dependent on their stage of pregnancy during the famine produced offspring who were underweight and smaller with greater susceptibility to metabolic diseases such as obesity, diabetes and mainly cardiovascular disease<sup>171-173</sup>.

The study is used to support the fetal origins of disease hypothesis which supports long term programming from in utero events<sup>174</sup>. The hypothesis was

formed from observations made from low birth weight which Barker contributed to maternal nutrition. Barker hypothesised maternal nutrition is the key cause of long-term health consequences such as cardiovascular disease<sup>174</sup><sup>175</sup>. The Dutch Famine follow-up of adult offspring is used to support Barker's hypothesis. The original idea of fetal programming was originally proposed by Lucas in 1991<sup>176</sup>.

The fetal origin of disease hypothesis has received support from epidemiological literature<sup>177</sup><sup>178</sup>. The hypothesis was first introduced back in 1992 by Hales and Barker who concluded that females who have to withstand deprived nutritional conditions during pregnancy have the ability to change the development of the unborn infant in such a way that it will be adept to survive in surroundings with a lack of nutritional resources i.e. The Thrifty Phenotype<sup>179</sup>.

The thrifty phenotype states babies who carry the thrifty phenotype and are born into a rich nutritional environment are more susceptible to obesity, diabetes, cardiovascular disease and other metabolic disorders. In contrast, babies which received a good nutritional intake during pregnancy and born into a rich nutritional environment will adapt better to the surroundings and therefore be less likely to encounter such problems<sup>180</sup>.

### **1.7.1 Fetal nutritional programming of adult health and disease**

For the development and growth of the offspring, the intrauterine environment plays a critical role. The frequency of adult disease increases in infants who



have a suboptimal growth in utero<sup>181, 182</sup>. When looking at the effects of early life nutrition on growth and development, “programming” was defined as the lasting consequences of a stimulus or insult during a sensitive period in early life<sup>183</sup>.

Changes in fetal physiology can be permanently influenced by events that occur during gestation. The bulk of morphological features are present prior to the birth and this is the prime period for plasticity or adaptation. Subsequent adaptations to in utero insults may have long term adverse consequences in later life. The theory proposed by the “fetal origins of adult disease hypothesis” is that fetal programming occurs when inadequate nutrition of the mother impairs fetal nutrient supply that leads to permanent physiological changes which can predispose to later cardiovascular disease, hypertension, impaired glucose tolerance and type 2 DM<sup>181, 182, 184</sup>.

Decreased glucose tolerance in adults has been linked to low birth weight. Decreased rates of fetal growth and impaired insulin-glucose metabolism have also been found in children and adolescents in several populations and in different countries<sup>172</sup>. A unique opportunity to study the fetal effects of severe maternal under nutrition during pregnancy in humans was provided by the Dutch famine, (late November 1944 to early May 1945)<sup>172</sup>. The official daily rations for the general population during this famine varied between 400 and 800 Kcal (1680 and 3360 KJ). For those 702 participants whose prenatal and birth records could be assessed and who were born between Nov 1, 1943 and February 28, 1947 in Amsterdam were included for the purposes of this study. For participants who were exposed to famine in different stages of gestation,

their glucose and insulin responses to a standard oral glucose test were compared with those born after this period (i.e. Controls). These results suggested that decreased glucose tolerance in adults is linked to prenatal exposure to famine, especially during late gestation. The research also suggested that even if the effect on fetal growth is small, insufficient nutrition may lead to permanent changes in insulin-glucose metabolism<sup>172, 185, 171</sup>.

It is now well recognised that either throughout or at specific stages of pregnancy, changes in the macronutrient or micronutrient composition of the maternal diet can have significant effects on the fetus<sup>171</sup>.

### **1.7.2 Low birth weight and “Catch-up growth”**

In developed countries, the infant undergoes a period of accelerated (“catch-up growth”) growth during early postnatal life when its nutrient supply is no longer constrained and where fetal growth restriction is generally the result of compromised placental nutrient transfer rather than a decreased intake of nutrients by the mother<sup>186</sup>. **Being born** into a plentiful postnatal environment is associated with higher accumulation of subcutaneous and visceral adipose tissue in a shorter period of time<sup>186, 187</sup>.

Various studies have indicated that for infants with a small gestational age, fast post-natal “catch-up” growth may have a negative effect on late metabolic health. However, it is still not known at which point after birth the accelerated growth may be detrimental, with some studies indicating to the immediate early post-natal period<sup>188, 189, 190, 191, 192</sup>. Several other findings have also indicated that

accelerated growth in childhood further increases the risk<sup>193, 194, 195</sup>. The lack of correction of catch-up growth for low birth weight could be a possible confounder in many previous studies. What may be important is the shift from an adverse and sparse nutritional intra-uterine environment into one of potentially excess nutrition that small for gestational age (SGA) infants at the time of birth go through. What may facilitate a more efficient nutritional uptake and energy metabolism and thereby higher post-natal growth rate is the potential state of cellular nutrient restriction in SGA infants at the time of birth<sup>196</sup>. A positive relationship was shown between weight gain during the first two weeks of life and insulin resistance in adolescence irrespective of birth-weight. This was discovered at age 13-16 years of preterm infants from a randomized intervention trial of neonatal nutrition<sup>192</sup>. Another study indicated that weight gain of term newborn infants from birth to six months was positively associated with metabolic risk at 17 years of age<sup>197</sup>.

### **1.7.3 Effect of gender in nutrient restriction consequences**

Different aspects have demonstrated gender-specific differences in fetal growth and development following nutritional manipulation in utero. What has also been previously noted a gender specific regulation of the fetal and adult hypothalamic-pituitary-adrenal (HPA)<sup>198</sup>. A distinct sex-specific bias has been exhibited in responses to challenges that have been shown to incur developmental consequences<sup>198</sup>. An example of this is when only the adult female offspring are affected after maternal restraint stress in rats during late gestation (resulting in maternal HPA axis activation). Males appear largely

unaffected. Another increase response is found in adult females following prenatal alcohol exposure also but the males once again are not affected, HPA axis activity<sup>198</sup>.

#### **1.7.4 Immune response with Inflammation**

The body is comprised of a network of molecular pathways which respond to immunity in a variety of ways. The immune network has two such complex pathways<sup>199</sup>:

1. Adaptive immune system (Immune memory pathway)
2. Innate immune system (Non-specific pathway).

These two systems protect the host organism against infection and are also vital in detecting differences between pathogens and host cells, in cases where both systems fail; auto-immune disease can transpire<sup>200</sup>. For instance, an antigen which infiltrates the external barrier and enters the host's body, the immune response for both humoral and cell-mediated are stimulated. Upon reaching the antigen, phagocytic cells (macrophages, monocytes, dendritic cells or neutrophils) surround and ingest the antigen, followed by a phagocytic apoptosis of the antigen<sup>199</sup>. To help in the development of the immune system, specific immune cells such as antigen presenting cells (APC) and major histocompatibility (MHC) form complexes present themselves to the antigen and initiate an immune response. The complexes use the surface of the MHC to bind with the invading antigen, whilst circulating T-cells use their receptors to

communicate and stimulate the adaptive immune system to release cytotoxic T-cells and B-cells<sup>201</sup>.

In the case of injury or stress the cells affected secrete chemical signals known as chemokines, proteins and cytokines that provoke an inflammatory response to protect the surrounding cells and tissue. This chemical response causes immune cells, which are involved in biochemical complement cascades, to be activated by antibodies and breakdown the targeted cell<sup>202</sup>. The immune response from the host to such agonists is to regulate cell-adhesion molecule and oxidative stress factor expression, cytokine secretion and cell death<sup>203</sup>. In certain cases, inflammatory responses can be under or over reactive to the situation which can cause additional tissue damage because of certain pro- and anti-inflammatory mediators uncoupling<sup>204</sup>.

### 1.7.5 Obesity induced inflammation

Obesity and hyperinsulinaemia are widely seen as established conditions that initiate the immune system to activate a chronic low level pro-inflammatory state. Excess or increased amounts of adipose tissue mass have shown to be positively correlated with the expression of pro-inflammatory gene, TNF- $\alpha$ <sup>205</sup>. This is a gene more commonly associated with regulation of immune cells, cell signalling and recruitment of cytokines but through obesity studies, it has been shown to have a role in insulin resistance. TNF- $\alpha$  is responsive to insulin and inhibits tyrosine phosphorylation of insulin receptor substrate-1 (IRS-1) thereby decreasing glucose intake<sup>205, 78</sup>. This demonstrates the complexity of adipose tissue and inflammatory networks that underline the mechanisms obesity and insulin resistance.

Concentrations of pro-inflammatory markers such as acute phase C-reactive protein (CRP) and other plasma cytokines have been shown to be correlated positively with increased adipose tissue mass<sup>206</sup>. This further reaffirms the relationship between obesity and inflammation. CRP is commonly associated with the development of cardiovascular disease (CVD) and is often used as a biomarker in assays for the early detection of CVD<sup>206</sup>. This also links the relationship between obesity and increased risks of morbidity through enhanced inflammation.

As previously described, adipose tissue is known to secrete and synthesise a wide variety of molecular signals. In an obese pro-inflammatory state the most interesting are the immune-mediating adipokines with IL-6 and IL-10 showing increased expression and circulating plasma concentrations<sup>207, 208, 209</sup>. MCP-1

along with its receptor C-C motif receptor 2 (CCR2) have also shown increased expression in an obese condition<sup>151</sup>. Both IL-6 and MCP-1 are also understood to be involved in the contribution to the developing of insulin resistance<sup>208, 151</sup>.

There are a wide variety of mechanisms that could promote inflammation in adipose tissue such as increased NEFA's, adipokine secretion and increasing triglycerides concentrations ensuing from adipocyte hypertrophy and hyperplasia. Adipocyte hypertrophy is positively correlated with increased apoptosis and development of crown-like structure (CLS)<sup>168</sup>. CLS have been linked with increased macrophage recruitment and signalling<sup>210</sup>.

The non-fat cell fraction of adipose tissue is hypothesised to be accountable for the majority of adipokine expression<sup>211</sup>. One of the main mechanisms hypothesised behind non-fat cell development in an obese state is through adipocyte enlargement caused by hypoxia and microcirculatory dysfunction<sup>212</sup>. Adipose tissue undergoing hypoxia leads to stimulation of vascular synthesis and up-regulation of vascular endothelial growth factor (VEGF) action, therefore increasing endothelial growth causing further macrophage and immune cell infiltration, leading to an inflammation feedback loop<sup>212</sup>.

To conclude, recent studies have shown that well established metabolic protein hormones adiponectin and leptin, which not only influence the regulation of appetite via direct signalling on the hypothalamus, but also alter immune responses in an obese state displaying inflammation through indirect and direct pathways<sup>213, 214</sup> (see Fig 1.10).

### **1.7.6 Obesity and insulin resistance**

Insulin is a carbohydrate and lipid metabolism signalling hormone, produced by the pancreas and is central to balancing blood glucose levels immediately after a meal. Blood glucose levels are increased from eating which leads to the stimulation of insulin release from pancreatic  $\beta$  cells. Insulin in turn causes cells in the muscle, adipose tissue and the liver to uptake glucose from the blood. The glucose is then converted to glycogen and stored within these tissues. The mechanism in by which insulin operates is by suppressing hepatic gluconeogenesis and by modulating entry and uptake of glucose through various glucose transporters, the major transporter being GLUT4<sup>215</sup>.

One of the main responsibilities of insulin is to regulate the release of glucose into cells, supplying the cells with energy. Cells which have become insulin resistant cannot uptake in glucose, fatty acids or amino acids<sup>216</sup>.

Insulin resistance (IR) can be defined as a physiological state to which cells fail to react to the normal behaviour of the hormone insulin. The body will produce insulin in a response to stimulus of increased glucose in the blood<sup>216</sup>. When the cells become resistant to insulin and are no longer able to use the hormone correctly, it leads to hyperglycemia. B-cells in the pancreas therefore increase their secretion of insulin, furthermore playing a role to hyperinsulinemia. This situation often remains unobserved and results in contributing to the conclusion of Type 2 Diabetes<sup>216</sup>.



Glucose uptake (and local storage of triglycerides and glucose as glycogen) is reduced in muscle and fat cells during insulin resistance, whilst insulin resistance in liver cells marks reduced glycogen synthesis and storage along with a breakdown to suppress production of glucose and release into the blood<sup>217, 218</sup>. Insulin resistance is usually defined to as reduced glucose-lowering effect of insulin, however many other roles of insulin are also affected. For example, fat cells are affected by a reduced uptake of circulating lipids and increased hydrolysis of stored triglycerides<sup>219, 218</sup>. This leads to an increased recruitment of stored lipids in these cells leads to elevated free fatty acids in the blood plasma. These high plasma levels of insulin and glucose due to insulin resistance are key elements to the progression of metabolic syndrome<sup>220, 218</sup>.

During an obese state, the insulin sensing pathway is disrupted, a problem seen in all tissues sensitive to insulin. The sensing pathway is impaired due to a down-regulation of the GLUT4 gene in insulin responsive tissues<sup>215</sup>. A combination of impaired glucose storage and decreased stimulation of insulin regulated glucose transport leads to insulin resistance. This state can then further develop into hyperglycaemia and a possible development of type II diabetes.

Obesity has been suggested to help in the progression of insulin resistance by playing a central role in the pathway to insulin resistance by reduction of binding to the insulin receptor, led by impaired phosphorylation of the insulin receptor and decreasing activity of tyrosine kinase in both adipose tissue and muscle<sup>215</sup>. Whilst many mechanisms are known for insulin resistance, obesity led insulin resistance are not fully known. Because of the complexity in

understanding all pathways stimulated by obesity it is hypothesised that the endocrine function of adipose tissue and increased levels of secretion of cytokines, NEFA's, glycerol and other various signalling markers from adipocytes in the obese state all promote insulin resistance<sup>221</sup>.

Insulin resistance has been well established to show a positive correlation to increased visceral fat mass and BMI. Many epidemiological studies have also been able to display that subsequent weight loss coupled with a decreased in central adipose tissue depot mass actually reverses insulin resistance and improves sensitivity<sup>222</sup>.

## **1.8 Fructose**

The most common naturally occurring sweeteners in our daily diet are glucose, sucrose and fructose. Glucose and fructose are monosaccharides that are present in small quantities in fruits and honey. Sucrose is a disaccharide which has a structure that consists of one molecule of fructose connected to one molecule of glucose through an  $\alpha$  1-4 glycoside bond and is found in significant amounts in sugarbeet and sugar cane<sup>223</sup>.

A potential nutritional problem that has developed over the past few decades has been the gradual increase in fructose consumption in the daily diet and has tracked the increase in obesity incidence in developed countries<sup>224</sup>. The widespread availability of fructose has increased in part due to its low cost and highly sweet taste, together with the introduction of high fructose corn syrup (HFCS) by major beverage companies in the early 1980's<sup>225</sup>.

### **1.8.1 Fructose Intake**

According to reports from the United States Department of Agriculture (USDA), sugar consumption per capita equalled to 90g/day in 1970<sup>226</sup>. At this time HFCS consumption was near enough to zero. As the production value of fructose decreased more beverage companies decided to implement the sugar as a cheaper equivalent to glucose, this coincided with the decrease in sucrose consumption.

### 1.8.2 Fructose Metabolism

Fructose ( $C_6H_{12}O_6$ ) has the same chemical composition of glucose but is structured differently giving it unique abilities. When entering the gut, fructose is transported into the enterocyte via GLUT 5, a specific fructose transporter, located at the tip of the enterocyte. Unlike glucose metabolism, fructose does not require ATP hydrolysis and is therefore self-regulating of sodium absorption. After entry into the enterocyte, fructose is diffused into blood vessels through a GLUT2 transporter<sup>227, 228</sup>. Studies in rodents have shown GLUT5 to be expressed relatively low until weaning but can be stimulated through fructose administration<sup>229</sup>. Ageing has also shown to be involved in fructose absorption; studies in aged rodents have exhibited decreased absorption rates in fructose and carbohydrates<sup>230</sup>.

### 1.8.3 Hepatic Metabolism

Once fructose is absorbed into the blood it is efficiently and quickly extracted by the liver (Figure 1.8). The glucose transporter GLUT2 is thought to be responsible for the transport of fructose into the liver<sup>231, 232</sup>. The majority of fructose once extracted into the liver is quickly metabolised into fructose-1-phosphate (P) by the highly specific enzyme fructokinase. Fructokinase has distinct properties such a low  $k_m$  (~0.5mM) and a high  $V_{max}$  (suggested rate of ~3 $\mu$ mol/min per gram of liver in human and rats)<sup>233, 234, 235</sup>. These unique

properties explain for the rapid rate of metabolism of fructose within liver cells.

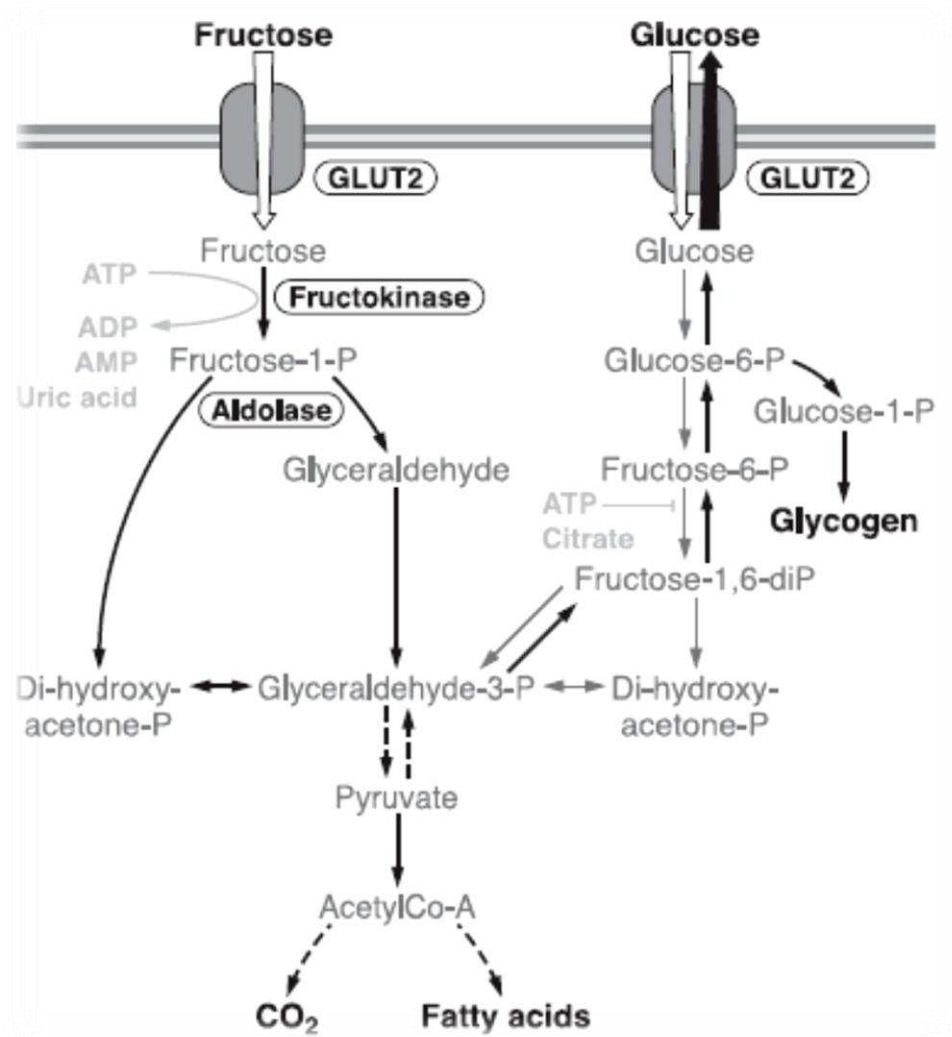


**Figure 8.8** – Fructose and glucose pathways. Fructose metabolism (grey arrows) differs from glucose (black arrows) due to 1) a nearly complete hepatic extraction and 2) different enzyme and reactions for its initial metabolic steps. Fructose taken up by the liver can be oxidized to CO<sub>2</sub> and then converted into lactate and glucose; glucose and lactate are subsequently either released into the circulation for extrahepatic metabolism or converted into hepatic glycogen or fat. The massive uptake and phosphorylation of

fructose in the liver can lead to a large degradation of ATP to AMP and uric acid.

Hepatic metabolism of glucose and fructose varies noticeably for many reasons. The first being, entry of glucose into the glycolytic pathway is regulated by glucokinase (also known as hexokinase IV). Glucokinase has a high  $K_m$  for glucose unlike the high low  $k_m$  of fructokinase and therefore the rate of phosphorylation for glucose in the liver varies in relation to portal glucose concentration<sup>236</sup>. Conversion of glucose-6-P to fructose-6-P is catalysed by enzyme phosphofructokinase, the activity of this enzyme is moderated by citrate and ATP, therefore controlling the reaction based on the energy level of the cell<sup>237</sup>. Overall the process of glucose being converted to pyruvate is regulated by insulin and the energy status of the cell. Insulin is involved in the stimulation of glucokinase gene expression and activation of glycolytic enzymes. In comparison to the conversion of fructose to triose-P, this process is self-governing and not dependent on insulin. Fructose conversion is also a quick process because of the low  $k_m$  of fructokinase and lack of a negative feedback of ATP or citrate. This process causes a temporary reduction in the amount of free phosphate and ATP presence in liver cells in reaction to fructose<sup>238, 239</sup>.

The remaining structure of fructose is the carbon atoms, which are processed into fatty acids within hepatocytes through a process known as de novo lipogenesis (DNL). The DNL pathway was first observed in rat in vivo studies and in rat hepatocytes where the administration of [<sup>14</sup>C] fructose displayed <sup>14</sup>C

being taken up into liver lipids<sup>240, 241, 242</sup>. Studies have shown stimulation of the hepatic DNL pathway through the administration of fructose or glucose-fructose complexes in humans via the observing of infused <sup>13</sup>C-labelled acetate in very low density lipoprotein (VLDL)<sup>243, 244</sup>. DNL is performed in most cells but adipocytes and liver cells are predominantly well tailored for this process. Studies have shown that DNL in the liver has damaging effects which include the increasing of serum triglyceride and intrahepatic lipid (steatosis) levels, both of which lead to nonalcoholic fatty liver disease and steatohepatitis<sup>245</sup>. Furthermore, increased hepatic DNL activity has been shown to be positively correlated with insulin resistance<sup>246</sup>.

#### **1.8.4 Long term effects of fructose**

The relationship between fructose intake and obesity has been somewhat controversial and is the subject of ongoing investigations<sup>247-249</sup>. To successfully evaluate the link between fructose consumption and obesity, the effect of fructose intake on total energy intake is a vital issue. Several studies have investigated the metabolic effects of replacing part of the carbohydrate diet with fructose for patients with type 2 diabetes mellitus as fructose metabolism does not require insulin secretion and has a low glycaemic rise. These studies were able to demonstrate that fructose intake was related to a substantial increase in plasma triglyceride concentration and reduced levels of high-density lipoprotein (HDL)-cholesterol<sup>250, 251, 252</sup>. Subsequent studies with animal models investigating the effects of diet supplemented with fructose or sucrose displayed that high-fructose/high-sucrose diets did exhibit harmful

cardiovascular and metabolic effects, such as insulin resistance, hyperuricemia, dyslipidemia, hypertension and weight gain<sup>253, 248, 249</sup>.

### **1.8.5 Dyslipidemia and de novo lipogenesis**

Studies have been well established to display that ingesting a high-fructose diet for longer than 1 week leads to increased plasma total-VLDL-triglyceride concentrations and cholesterol in patients with type 2 diabetes, insulin resistance and even in healthy volunteers<sup>251, 254, 255</sup>. This abnormal amount of lipids in the blood is often referred to as dyslipidemia, with studies showing a sustained level elevated insulin levels can increase the risk of developing dyslipidemia<sup>256</sup>.

Studies measuring plasma triglyceride kinetics in rats used high-glucose, -sucrose and -fructose diets concluded that both fructose and sucrose diets compared to the glucose diet lead to an increase in triglyceride production and a decrease in clearance of triglycerides<sup>257</sup>. Fructose is known to be highly lipogenic, as it supplies substantial quantities of hepatic triose-phosphate as precursors for fatty acid synthesis. It has been demonstrated in several studies that hepatic de novo synthesis was initiated following acute fructose intake and concluding that fructose also supplements to the production of both the glycerol and fatty-acyl components of VLDL-triglycerides<sup>258, 259</sup>.



Various studies have contributed in supporting the role played by fructose-induced hypertriglyceridemia in the stimulation of hepatic de novo lipogenesis. The two main observations that lend the most weight behind this process are the positive correlation demonstrated between partial hepatic de novo lipogenesis and fasting triglycerides in healthy patients fed an isocaloric, high-sugar diet or a hypercaloric, high-fructose diet<sup>260, 261</sup>. This study also illustrated that a 2-week infused diet with fish oil reduced fasting triglycerides and hepatic de novo lipogenesis in healthy patients previously overfed with fructose supplementation<sup>261</sup>.

In support of the increase of fasting plasma triglycerides as described above, a postprandial rise was also observed in plasma triglycerides when acute fructose was administered, this was explained by the weakened clearance of triglyceride-rich lipoprotein<sup>258</sup>, an effect also seen with chronic high fructose ingestion.

Studies in overweight women have yielded results that show fructose involvement during a 10 week period studying postprandial triglyceride levels to be enhanced due to the intake of fructose sweetened beverages; these fluctuations in postprandial triglyceride levels are evident to impaired triglyceride clearance from fructose intake<sup>262</sup>. This further reaffirms the theory that impaired triglyceride clearance leads to hyperlipidemia stimulated by high-fructose diets<sup>259</sup>.

### **1.8.6 Fructose and the pathogenesis of metabolic diseases**

In observation of the compelling evidence documented for the case that high fructose can stimulate in human and animal models a cascade of metabolic and cardiovascular changes it is justifiable to question whether fructose intake plays an important role in the development of metabolic disease within our populations

### **1.8.7 Fructose and weight gain**

To evaluate the effect of fructose on body weight gain, various cross-sectional studies have been reviewed recently, most notably studies involving sugar-sweetened beverages performed on children and adolescents<sup>263</sup>. Many of the studies involved did show a positive correlation between consumption of sugar-sweetened beverages and body weight<sup>264, 265, 266, 267</sup> but others failed to replicate these results<sup>268, 269, 270</sup>. Analysing these studies to produce a definite answer for the possible link between weight gain and fructose requires caution as many factors have to be taken into account, such as patterns of physical activity, patterns of feeding, socioeconomic status, education, etc.

Studies involving meta-analyses investigating the relationship between body weight and consumption of sugar-sweetened beverages also produced contradictory results. Meta-analysis involving 88 studies detailed a significant positive correlation between weight gain and consumption of sugar-sweetened beverages<sup>271</sup> whilst an alternative meta-analysis of 12 studies produced no correlation of weight gain<sup>272</sup>.

Results from intervention studies produced the clearest relationship between sugar-sweetened beverages and weight gain. An intervention study involving HFCS-sweetened beverages and aspartame-sweetened beverages (an artificial

non-calorie, non-saccharide sweetener) concluded in considerable weight gain from the HFCS group only<sup>273</sup>. In a study examining overweight patients receiving either sugar-sweetened beverages or non-calorie sweetened beverages (observed as a control group) resulted in significant weight gain and energy intake from the sugar-sweetened beverage group whilst there was no weight change in the control group<sup>274</sup>. Equally in relation to increased weight gain with sugar-sweetened beverages, several studies mainly involving adolescents and children with a daily reduction of sugar-sweetened beverages resulted in a significant decrease in body weight and energy intake<sup>275, 276, 277</sup>.

#### **1.8.8 Fructose and cardiovascular issues**

The Framingham Heart Study investigating the link between sugar-sweetened beverage consumption and cardiovascular risk factors was studied in over 6,000 subjects. The study was able to demonstrate that consumption of one or more sugar-sweetened beverage on a daily basis was significantly correlated with the occurrence of metabolic syndrome. The prevalence of metabolic syndrome for this study was characterised by three or more of the following symptoms: waist circumference of females (>35 inches) and males (40 inches), high triglyceride, blood pressure, fasting plasma glucose and low levels of HDL-cholesterol<sup>278</sup>. In addition, the study conducted a follow up of subjects who at the time of inclusion into the study did not exhibit metabolic syndrome but through consumption of one or more sugar-sweetened beverage on a daily basis resulted in an increased chance of developing metabolic syndrome<sup>278</sup>.

Studies conducted investigating cardiovascular risk over the past few decades have been able to identify several “unique markers” associated with cardiovascular disease. These include certain inflammatory cytokines or mediators such as TNF- $\alpha$ , IL-6 and other various adipokines, who have been positively correlated with sucrose intake in association with increased cardiovascular risk<sup>279</sup>.

### **1.9 Fructose and Inflammation**

Several studies in experimental animals have been able to demonstrate inflammation induced by fructose intake. For example, expression of the intracellular adhesion molecule (ICAM)-1, a leukocyte adhesion protein was shown to be induced in human aortic endothelial cells from fructose intake<sup>280</sup>. Concentrations of fructose that are normally achieved in daily human ingestion of a fructose-supplemented meal (1mM) has shown to rapidly induce both mRNA and protein expression of ICAM-1<sup>281</sup>. During inflammation, ICAM-1 is an adhesion molecule that allows the attachment of leukocytes to the endothelium and subsequently allows them to transmigrate into peripheral tissue. This cellular migration produces modifications of vascular permeability causing the transfer of solutes to peripheral tissues<sup>282</sup>.

Studies have shown that the expression of MCP-1 in various cell types is also induced through fructose intake<sup>283, 280</sup>. MCP-1 is seen as a key cytokine in the development of atherosclerosis and is involved in mediating an inflammatory response in symptoms related to metabolic syndrome.

A possible mechanism behind inflammatory markers such as MCP-1, IL-6 being induced by fructose intake can be explained through various factors such

as the development of dyslipidemia, insulin resistance, and excess uptake of fatty acids. Adipose tissue's main property is to process excess fatty acids supplemented by the diet and store them in the form of triglycerides. Triglycerides are later converted to energy during phases of starvation, the capacity for storing fat in adipose tissue is however limited. It is when these limits are breached that adipose tissue begins to malfunction in its capacity to regulate fat storage and acquire fatty acids which leads to elevated levels of fatty acids in circulation<sup>284</sup>. The increased fat mass from fructose intake leads to reduced adiponectin secretion in adipocytes and further stimulates the release of TNF- $\alpha$  and IL-6, due to the removal of any inhibitory controls<sup>138</sup>. These conditions lead to a possible elevated inflammatory response, in particular MCP-1, who as previously described, stimulates the recruitment of other monocytes and macrophages to the adipocyte of target<sup>285</sup>.

### **1.9.1 Fructose and pregnancy**

Studies involving fructose intake during pregnancy have been scarce, though early studies using fructose based diets of 78% and 50% during different periods of pregnancy have shown changes in maternal hypertriglyceridemia<sup>286, 287</sup>. These studies focused on high-fructose diets which are not common in human diet as fructose is consumed in lower concentrations because it is more widely used as a sweetener. Therefore a lower fructose concentration studies may yield different results, this was successfully researched in a study using 10% fructose during pregnancy and lactation<sup>288</sup>,

resulting in hyperinsulinemia during the weaning phase for the offspring and hyperglycemia and hyperinsulinemia for the mothers<sup>288</sup>.

In addition studies examining fructose intake during pregnancy have shown that when given with an otherwise nutritionally balanced diet results in raised increased insulin and plasma glucose concentrations along with body fat content<sup>288</sup>. The magnitude of effect can however differ between stages of gestation with hypoglycaemia and hypertriglyceridemia occurring in early gestation compared with hypotriglyceridemia in late gestation<sup>287</sup>.

A recent study was able to demonstrate the first findings of sex-specific effects on placental and offspring development induced by maternal fructose intake<sup>289</sup>. The study highlighted that fructose intake during pregnancy lead to maternal hyperinsulinemia and increased circulating plasma fructose and leptin levels exclusive to females. These changes were correlated with a reduction in placental weights in females also. No such changes were observed in male offspring leading to a sex-specific change during fetal development<sup>289</sup>.

These studies underline the need for further investigation in the effects of fructose in gestation as molecular techniques along with the understanding of adipocyte biology have advanced. Furthermore studies researching the impact of fructose intake during pregnancy have not been studied extensively.

### **1.9.2 Main hypothesis and aims**

The introduction chapter above has reviewed the theories and ideas behind nutritional manipulation during different periods of gestation and how this leads to adipose tissue dysfunction and the possible consequences this has in the development of metabolic diseases later in adult life. This thesis will detail both large and small animal models, with the sheep study focusing on nutrient restriction during early to mid gestation and late gestation followed by differing post natal conditions. The small animal study (wistar rats) focuses on long term fructose feeding during pregnancy on mothers and their offspring.

Current research on certain ectopic depots such as subcutaneous, retroperitoneal, epididymal, and pericardial adipose tissue is limited in their investigation relating to nutrient manipulation during pregnancy. Also with very little research focusing on fructose intake during pregnancy and its long term effects on the offspring has been studied, this study covers both a nutrient restricted environment and a nutrient rich environment during pregnancy, in two animal models.

The principal hypothesis for this thesis was that the presence of nutrient manipulation with differing post-natal environments in ovine and rodent models, will promote an elevated inflammatory state, arbitrated by physiological alterations in ectopic adipose tissue depots.

# Chapter 2 – Methods

---

## 2.1 Study Protocols

During the first phase of the PhD all laboratory experiments conducted in England were performed in the, Academic Division of Child Health at the University of Nottingham. All experimental practices followed national legislation alongside the ethical approval of the University of Nottingham. For all animal research performed the approval of the Home Office was obtained and all procedures conducted on animals were subject to the terms of the Animal Act.

The University of Nottingham administered a code of laboratory practice (the United Kingdom Control Substances Hazardous to Health, COSHH: SI No 1657, 1988) under which all laboratory procedures were undertaken. All experimental equipment was supplied from Laboratory Supplies with all chemicals and reagents unless stated otherwise supplied from Sigma-Aldrich Company (Gillingham, UK). For all other suppliers and standard solutions consumed in the laboratory, details can be found under the Appendix section.



### **2.1.1 Sheep Study – early-to-mid gestational nutrient restriction**

During the study all procedures carried out by Professor Michael Symonds and Dr. D. Gardner in accordance with the 1986 UK Animals Act of Scientific Procedure. Welsh mountain sheep were randomly allocated into one of three groups; nutrient restricted (NR-O), lean (L) and obese (O). During the experiment the Welsh mountain ewes were housed at the University of Nottingham Joint Animal Breeding Unit located at the Sutton Bonington Campus. All ewes selected for this experiment were of similar body composition and age; they were mated with Texel rams. To determine the fetal number present during pregnancy, ewes were scanned via ultrasound at 30 days of pregnancy, only ewes displaying twins (n=26) during ultrasound were further selected to take part in the study.

Pregnant ewes (n=12) allocated to the NR-O group were each fed 3.5MJ/day (50%) from days 30 to 80. Pregnant ewes in both C-O and L groups were given normal metabolic energy requirements of 7MJ/day (100%) with 7 sheep allocated to the O group (n=7) and 8 sheep to the L group (n=8). The metabolic energy requirements were restored back to 100% for all groups after 80 days of gestation to 12-13MJ/day. After birth, the offspring from all the groups were kept with their mothers for the lactation period of 10 weeks. Mothers were fed to requirements for lactation purposes.

Accelerometry ('Actiwatch', Linton Instrumentation, UK) was used to measure the physical activities of all the groups in periods of 30 seconds over a 24 hour period. This procedure was carried out during the period of the stocking environment. The results from this showed a great fourfold rate in

physical activity of the L group in comparison to the O group. Other observational activities taken during the study was food intake, this measurement was taken daily during the hours of 0800 and 0900h (the time of animal feeding was also during this period).

Strict guidelines were followed for the metabolic and nutritional requirements of the ewes during pregnancy. The guidelines were based on recommendations by the Agricultural and Food Research Council (1980). The daily nutritional dietary intake for the mothers was 1kg of loosely chopped hay and 200-500g of barley at an increasing fraction dependent on stage of pregnancy and nutritional group. All mothers were allowed unrestricted access to water with additional minerals and vitamins added into dietary intake throughout the pregnancy in accordance to guidelines stated above.

To promote obesity, O and NR-O groups between the 4<sup>th</sup> and 12<sup>th</sup> months after birth were given ad libitum concentrated pellets and confined into a space of 17 animals per 50m<sup>2</sup> to restrict physical activity (stocking environment). A total of twenty-two sheep were born (10 male and 12 female) from the control fed mothers. They were grouped randomly into either Obese or Lean control groups as listed above. Groups were assigned regardless of gender as previous observations in 1 year old sheep displayed no differences in metabolic responses<sup>290</sup>. Furthermore the maternal nutrient restricted group was also comprised of twenty-two newborns with 18 females and 6 male sheep. At the time of euthanasia (12 months of age), the sheep were humanely euthanased with an electric shock. Tissue samples were collected and snap frozen into liquid nitrogen and kept at -80°C , including pericardial adipose tissue, until

further analysis was required. Before any tissues were kept for preservation, all samples dissected were weighed.

	Prenatal			Birth	Lactation					Postnatal
	Days (Sheep gestation)				Months					
	0	30	80		0	3	6	9	12	
O (n:8)	*	*	*		*	Low physical activity to promote obesity				
NR-O (n:12)	*	NR	*		*	Low physical activity to promote obesity				
L (n:8)	*	*	*		*	Normal activity				

\* Fed meet to metabolic requirements (100%). NR – Restricted nutrient diet during 30-80 day gestation period (3.5MJ/day).

**Figure 9.1** – Sheep Study: Early to mid gestational nutrient restriction model. O=Obese group (100% of normal energy requirement given from 0 day of gestation, physical activity was restricted from 3 to 12 months during post-natal period to promote obesity). NR-O = Nutrient restricted-obese group (50% of normal energy requirements given from day 30 to 80 during gestation, physical activity was restricted from 3 to 12 months during post-natal period to promote obesity). L = Lean group ((100% of normal energy requirement given from 0 day of gestation, physical activity was not restricted during post-natal period)

## **2.2 Sheep study – late gestational nutrient restriction**

This study had all animal procedures were performed under the guidelines and accordance with the UK Animals (Scientific Procedures) Act (1986) and the UK Home Office. The animal experimentation procedures were all completed by Professor M.E Symonds, Dr D. Gardner and Dr S. Sebert. All experimental practices followed national legislation alongside the ethical approval of the University of Nottingham. For all animal research performed the approval of the Home Office was obtained and all procedures conducted on animals were subject to the terms of the Animal Act.

The University of Nottingham administered a code of laboratory practice (the United Kingdom Control Substances Hazardous to Health, COSHH: SI No 1657, 1988) under which all laboratory procedures were undertaken.

All experimental equipment was supplied from Laboratory Supplies with all chemicals and reagents unless stated otherwise supplied from Sigma-Aldrich Company (Gillingham, UK). For all other suppliers and standard solutions consumed in the laboratory, details can be found under the Appendix section. The experimental procedures performed in this study were performed under manufacturer or supplier instructions and where required the experiment was optimised by Dr S. Sebert, Dr L. Chan, Dr M. Hyatt, Dr D. Sharkey, Dr P. Fainberg, Dr I. Bloor and Mr M. Pope at the Academic Child Health department.

The Early Nutrition Programming Project 2007 (EARNEST, FP6, #FOOD-CT-2005-007030) was the second sheep study was conducted. The aim of the present study was to determine the extent to which exposure to a nutrient restricted diet in late gestation with or without accelerated postnatal growth may influence the development of metabolic related issues such as obesity and diabetes in early adult life.

The study was designed for experimental nutritional treatments at different developmental stages during pregnancy. Dietary and physical activity manipulation was performed at 3 different critical stages prenatal, lactation and post-natal development stages. During the prenatal stage mothers were fed either a high or low calorie diet during the late gestation period (110 days till term). The second stage was designed to examine the effect of being reared as a twin (i.e. with competition from a sibling for available food) or raised alone. The third stage of nutritional experimentation was post-weaning development which involved the offspring at 3 months of age being placed in environments of low and high physical activity till the age of 17 months of age. The environments of low and high activity were in place to nurture the development of obese and leans animals, respectively.

The sheep selected for this study were Bluefaced Leicester cross Swaledale ewes, a total of forty twin bearing sheep were chosen of similar age and body weight. The ewes were bred and housed at the University of Nottingham Joint Animal Breeding Unit located at the Sutton Bonington Campus. As previously

described above, ewes selected on the basis of being confirmed they are twin bearing, this was confirmed via ultrasound (as described above).

Forty pregnant ewes were divided equally into three groups for the first prenatal stage of experimental nutritional development. Ewes were randomly selected into either a nutritional restricted group (N), a fed to appetite group (A) or fed to requirements group (R). The N group had n=20 sheep, the A group had n=10 and the R also had n=10 sheep entering into their last 4-6 weeks of pregnancy (late gestation).

The nutritional restricted group (N) only received a recommended 60% of the normal daily nutritional daily energy requirement ( $0.46 \text{ MJ/kg}^{0.75}$  body weight at 110 dGA and  $0.72 \text{ MJ/kg}$  body weight at 140 dGA). The fed to appetite group (A) received 150% of the recommended normal daily nutritional requirements ( $1.15 \text{ MJ/kg}^{0.75}$  body weight at 110 dGA and  $1.80 \text{ MJ/kg}^{0.75}$  body weight at 140 dGA). The fed to requirements group (R) received 100% of the normal daily nutritional requirements ( $1.00 \text{ MJ/kg}^{0.75}$  body weight at 110 dGA and  $1.80 \text{ MJ/kg}^{0.75}$  body weight at 140 dGA). The daily nutritional and energy requirements for the pregnant ewes were calculated on guidelines based on the ARFC manual (1993) of 'Energy and Protein Requirements of Ruminants'

Once the lambs were born for all three group (N: n=40, R: n=20 and A: n=20) they were raised during the lactation period as either twins or raised alone by their respective mothers. All offspring raised as twins were labeled as 'S' (Standard growth), offspring raised alone by their mother were labeled as 'A' (Accelerated growth with no competition). During the lactation period all mothers were fed to requirements.

The final stage was post-weaning; at this point the ewes were allocated into either a lean environment (L) or an obesogenic environment (O). These environments were set up to establish the development of obesity through the effect of physical activity. The obesogenic environment had a stocking rate of 6 sheep per 19m<sup>2</sup> whilst the lean environment had a stocking rate of 6 sheep per 1125m<sup>2</sup>. Nutritional requirements during post-weaning were the same for all sheep, they were fed high concentrate pellets (12.6 MJ/kg) (Manor Farm Feeds, Oakham, UK) and a mixture of hay (8.8 MJ/kg) which constituted to 100% of the energy requirements recommended from the guidelines as instructed above. All sheep had their daily energy intake measured through food intake and refusal; all sheep diets also contained a balanced measurement of minerals and vitamins with sheep having unrestricted access to water.

As previously stated in the earlier nutritional intervention study, physical activity of the sheep was measured using Accelerometry ('Actiwatch', Linton Instrumentation, UK). Accelerometry was used to measure the physical activities of all the groups in periods of 30 seconds over a 24 hour period during their restricted or unrestricted physical activity stage. Collars placed around the necks of the sheep had probes placed over a 24 hour period, these probes recorded activity measurements at a rate of 32 times per second. The data collected from the probes was uploaded to a dedicated software programme (Actigraph, FL, USA) for analysis. The data showed a two to three-fold increase of activity between the obesogenic and lean environments.

Measurement of body weight were taken on a regular 3 day cycle, body weight was also measured at birth, throughout the first month of birth and on a weekly basis up to 3 months. All weight measurements were established with the use of weighing scales. Once the sheep reached 16 months of age both systolic and diastolic blood pressure readings were monitored along with a standard blood pressure reading taken whilst the animal was under sedation.

Other measurements were also taken in conjunction with those listed above; they included fat mass, bone density and free fat mass. These measurements were taken via dual x-ray absorptiometry (DXA) once the sheep reached 8 months and then finally at 16 months of age.

DXA measurements were taken by fasting sheep overnight and later sedated with an intramuscular injection (mixture of ketamine and xylazine). The sheep were scanned in a Lunar DPX-L bone densitometer (Lunar, Florida, USA) for 15 minutes each and after this procedure was completed, sheep were returned back to their respective holding pens once fully recovered. For correct validation of the DXA scan performed on the sheep, a whole body chemical analysis was therefore performed on 14 half carcasses. All carcasses were dried and cut into more manageable pieces after the DXA scan. For fat percentage and nitrogen content analysis, 250g of dried tissue was homogenised for use in the Gerhardt Soxtherm fat analyser (Wolf labs, York, UK) and FlashEA1112 nitrogen analyser (Thermo Scientific, Massachusetts, USA).

Nearing the conclusion of the study, all sheep underwent pre-mortem plasma sampling with various physiological evaluations. This was conducted



approximately 2 weeks prior to the end of the study where all sheep were located into individual holding pens for sampling and physiological tests.

All sheep were humanely euthanized during the hours of 0900h and 1100h via electrical stunning followed by exsanguination. During the process of euthanasia all major organs and tissues were weighed (including adipose depots and glands). Specific tissues were sampled for histological analysis and therefore fixed in 10% formalin. The remaining tissues and organs were dissected and snap frozen into liquid nitrogen and stored at -80°C for further analysis.

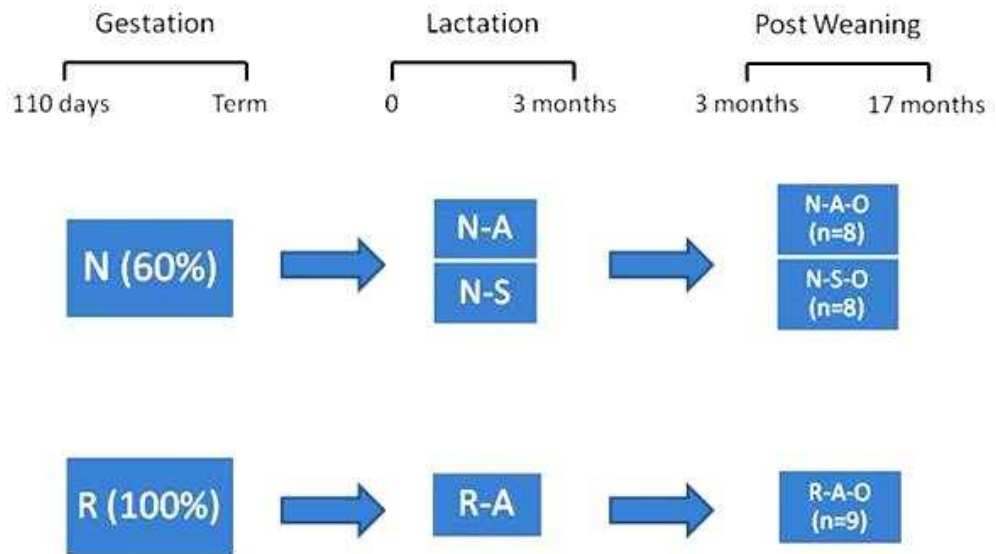


**Figure 10.2** - Sheep study: Late gestational nutrient restriction model. N = nutrient restricted (60% of normal energy requirements), R = fed to requirements (100% of normal energy requirements), A = fed to appetite (150% of normal energy requirements). During lactation, the N group were either raised as a singleton (-A = Accelerated growth raised without competition) or with a twin (-S = Standard growth raised as a twin). Post weaning phase, all groups were raised in an obesogenic environment.

## **2.3 Canada Studies**

### **2.3.1 Rat Model**

The laboratory rat of choice for this study was the Wistar Rat (*Rattus Norvegicus*). The Wistar rat is a strain of albino rats which belong to the species of *Rattus Norvegicus*. The Wistar strain was first produced in 1906 at the Wistar Institute, Philadelphia, Pa, USA. The strain was the first model organism developed for extensive use in a medical research field during a period where only *Mus musculus* was widely used in laboratories. The original colony of Wistar rats was developed by Henry Donaldson, Milton J. Greenman, and Helen Dean King, currently more than half of all Wistar rats used in laboratories have descended from this original strain<sup>291</sup>.

### **2.3.2 Fructose fed mothers study 2008**

Female Wistar rats (Charles Rivers, Montreal) were acclimated to the animal facility at the University of Alberta for one week with access to rat chow and regular drinking water ad libitum. Females were then mated to male Wistar rats overnight, with evidence of a vaginal sperm plug the following morning confirming gestational day (GD) zero. At this point, females were randomized into one of two treatment groups: regular drinking water (CONTROL, n=17) or a 10% fructose solution in regular drinking water (FRUCTOSE, n=18), for the duration of the pregnancy. Females were given standard rat chow (food, location) and their particular fluid ad libitum, with 24 hour food and fluid ingestion estimated on gestational days 7 and 14. These measurements were

made on individual rats, usually while their cage-partner was being mated. The animals were weighed on gestational days 0, 12, 19 and 20.

Whole blood was collected from the tail vein of conscious rats under mild restraint before mating and on gestational days 12 and 19. Blood samples were transferred to K<sub>2</sub> EDTA microtainer tubes (BD, Franklin Lakes, NJ USA) and plasma was recovered following centrifugation (5 minutes, 2400 rpm, Eppendorf 5415 Microcentrifuge, Brinkmann Instruments, Westbury, NY) before being transferred to clean tubes, frozen and held at -20°C until assayed for metabolites. On gestational day 20, animals were weighed, humanely euthanized and a blood sample was obtained using cardiac puncture. Tissues, including the retroperitoneal adipose depots, were dissected, snap frozen into liquid nitrogen and held at -80°C until commencement of PCR analysis. Before commencement of all treatments and procedures, approval was obtained from the Animal Care and Use Committee in the Faculty of Agricultural, Life and Environmental Sciences at the University of Alberta, in accordance with standards established by the Canadian Council of Animal Care.

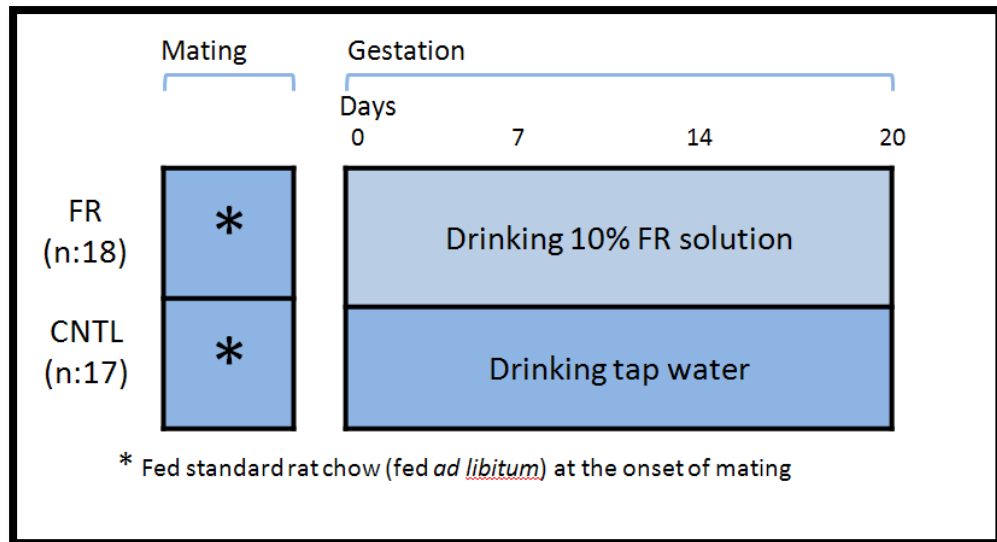


**Figure 11.3** – Rat Study: Fructose fed mothers model. FR group = Females fed 10% fructose water during pregnancy. CNTL group = females fed water. Both groups were fed chow (ad libitum) from the onset of mating.

### **2.3.3 Blood Collection**

For collecting regular blood samples from rats we chose a safe and simple method called tail vein sampling. This method is suitable for most strains and easy to perform with competent individuals. The number of attempts at sampling blood from the rats was minimised to 2 for each rat with alternate sides of the rats tail used for needle punctures. The vein we targeted was the lateral tail vein, it is best approached approximately 1/3 from the tip of the tail and it runs towards to the base of the tail. As it easier to access closer to the bottom of the tail as the skin thickens towards the rat's body. The vein is clearly visible when the tail is rotated either anti-clockwise or clockwise.

The procedure does require the warming of the rats prior to collecting blood from the tail. Heating the rat allows the blood vessels to dilate and therefore more visible for the injection to be placed, we used heat lamps with constant monitoring of the rats body temperature and behaviour. This procedure does have side effects on the rats such as dehydration (from salivation) and an increased metabolic rate which therefore could have an effect on the data collected from blood sampling.

We constantly moved the heat lamp around the housing of the rat to ensure no hot spots were produced and a uniform heating environment was achieved. To ensure the rat was comfort and restrained at all times we used a sterile cloth provided by the University Animal Housing Facility to securely wrap the rat

into a cone like shape with the tail end sticking out of the wrap. Alcohol swabs were used to clean the rat tail and a sterile 20G ½ needle (Becton Dickinson) with a 2ml syringe (Becton Dickinson) was used to puncture the epithelium of the tail. Before inserting the needle into the tail, a negative pressure was created by pulling back on the plunger slightly, this allowed for a dead space for blood to pool before withdrawing more blood from the tail. Once blood 1ml of blood had been collected, it was quickly transferred into a Microvette 300 (Sarstedt); this stopped the blood from coagulating during the procedure, all microvette's were placed on wet ice once blood had been successfully transferred from the needle. The rat was then calmly handled and its tail was cleaned with a warm swab and placed back into its original housing. This procedure is clearly easier to perform in younger rats as they tail skin is not harden as those of adult rats.

#### **2.3.4 Cardiac puncture**

During the euthanisation of rats cardiac puncture was performed on all rats. Cardiac puncture is a viable technique used to collect a large amount of blood. Depending on the age of the rat, 10-15 ml of blood was collected at time of euthanisation. All cardiac punctures are carried out before any other procedure is performed on the rat as the large amount of blood present in the heart can cause difficulties when dissecting tissues and extracting blood later in the procedure leads to coagulation of the blood. For all cardiac punctures a 23 ½ needle (Becton Dickinson), 5-10ml syringe (Becton Dickinson) and a Microvette 500 (Sarstedt) were used for collection. The rat is sprayed with

70% Ethanol along the chest and thorax whilst being laid on its back. The needle is inserted just below the diaphragm and angled to the left of the middle at a 10-30 degree angle. The needle is slowly inserted into the heart where a small bleb of blood will begin to collect in the syringe; slowly drawing back on the syringe will allow a large collection of blood to occur. All blood collected from euthanasia was placed on wet ice whilst other procedures occurred.

### **2.3.5 Dissection**

Each rat underwent the same euthanasia procedure at the end of his or her respective term. Rats were given their final weighing at the time of euthanasia; euthanasia was carried out through a small dose of isoflurane soaked on a cotton ball. The ball was safely enclosed into a glass holding bowl with an airtight seal to ensure all fumes stayed in. This bowl was used to anaesthetise the rats before cervical dislocation.

Restraining the rat on a flat surface and gripping the base tail with one hand and holding the head or the base of the neck with the other hand, and quickly pulling backward with the hand gripping the base tail performed cervical dislocation. To verify the dislocation was successful, a gap between the neck and spinal cord of 2-4mm can be felt. For larger adult rats a metal rod or wooden rod instrument were used to separate the spinal cord whilst gripping the tail, this required two or more people.



Once cervical dislocation was successful, cardiac puncture was performed as described above. To access all organs and tissues carefully, the rat was laid on its back against a non-slip surface; surgical scissors were used to cut shallowly and laterally above the urethral orifice and along both sides of the ribcage till a large flap of tissue is present. This flap can then be removed or pinned back to allow remove of organs and adipose tissues. Retroperitoneal, epididymal and uterine adipose tissue depots were carefully removed from each subject along with vital organs such as the liver, heart, kidneys and pancreas. All tissues and organs were directly labelled and snap frozen into liquid nitrogen and later transported into an -80°C freezer.

## **2.4 – Effect of Long Term Fructose Consumption**

All rats were housed within the University of Alberta, Animal Housing Facility and were Wistar rats (Charles River, Montreal). In total 8 female rats were supplied along with 4 male rats that were given 1 week to acclimatise to their new conditions and lower stress levels from the travel prior. Rats were caged in a Dynamic Containment Cage (DCC), which automatically monitored air pressure, air flow, filtering of allergens and carcinogenic and violate chemical agents, all bedding and cage washing occurred 3 times a week. They were all fed a chow diet (Purina 5001, USA) and given regular drinking water during their period of acclimatisation. Female rats were then mated with males overnight; positive pregnancy was detected by the presence of a successful vagina plug or through the presence of sperm.

The presence of sperm was carefully observed by inserting a plastic soft syringe (BD, Franklin Lakes, NJ USA) into the female rat's vagina and pipetting 0.1% saline solution (Fisher Scientific, USA) in and out. The next stage was viewing the saline solution under an optical microscope to view the presence of sperm. Sperm is positively identified as a small ball with a hooked tail protruding out.

Once the female rat was identified as being pregnant, this was designated as day zero, after which they were randomly assigned into one of two treatment groups; regular drinking water (H<sub>2</sub>O CHOW, n=4) or a 10% fructose solution in regular drinking water (FR CHOW, n=4), for the duration of the pregnancy and weaning period. Both groups consumed standard chow and had free access to their food and respective drinking water throughout.

Females were weighed pre- and post-mating and during gestational days 0, 12, 19 and 20. Food and water intake was estimated on gestational days 7 and 14 on each individual rats, usually while their cage-partner was being mated. Once female rats reached day 19 of their pregnancy, they were caged separately to allow for a stress free birth and avoidance of the other female cannibalizing the pups once born. Whole blood was collected from the tail vein of conscious rats under mild restraint before mating and on gestational days 12 and 19. Blood samples were collected in EDTA tubes (BD, Franklin Lakes, NJ USA), centrifuged, the plasma was then recovered and stored at -20°C for later analysis of glucose and insulin concentrations.

Females were housed in separate cages two days prior to parturition and were monitored twice daily to accurately count the amount of pups born to each mother. Due to the long term duration of the study, offspring numbers could not be predicted, as mothers could give birth from 1 to 12 pups. Offspring pups at 3 months; H2O CHOW n=9, FR CHOW n=7, at 6 months; H2O CHOW n=8, FR CHOW n=7, at 9 months; H2O CHOW n=7, FR CHOW n=6.

Pups stayed with their mothers for 3 weeks (weaning phase) before being housed in pairs of the same sex away from their mother. Mothers were humanely euthanized after each of their respective weaning phases was completed. Pups that were born as runts were also humanely euthanized at the time of birth.

Pups were randomly selected into 3, 6 and 9 month old groups, mothers that gave birth first had their pups selected for the 9 month group, followed by 6 months and 3 months, this allowed for correct time management. All pups

were fed chow and regular drinking water throughout after weaning. Once each rat was of an adult size, it was decided whether they could co-habit the same cage if their size was becoming restrictive. All rats were weighed weekly, with monthly blood collection.

On their final day rats were weighed, humanely euthanized and a blood sample was obtained using cardiac puncture. Tissues, including the retroperitoneal adipose depots, were expediently dissected and immediately frozen in liquid nitrogen. Tissues were stored at -80°C for further biological analysis. All experimental procedures and protocols were approved by the Animal Care and Use Committee in the Faculty of Agricultural, Life and Environmental Sciences at the University of Alberta, in accordance standards established by the Canadian Council of Animal Care.

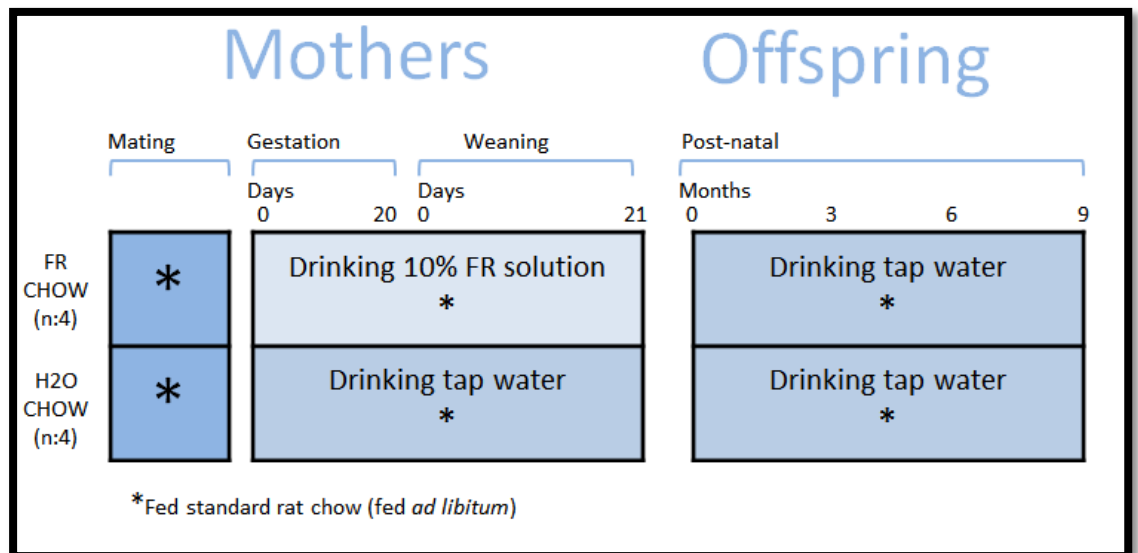


**Figure 12.4** – Rat Study: Effect of long term fructose consumption model. FR CHOW group were fed 10% fructose water during gestation and weaning while H2O CHOW group were fed water during gestation and weaning. Offspring for both groups fed only water and chow during post-natal period.

## 2.5 Standard PCR

Polymerase chain reaction was first published in 1983 when Kary Mullis whilst working for Cetus invented a process which he called PCR, this technique went on to become the most widely used process for DNA amplification and earning Kary Mullis a Nobel Prize in 1993 (Chemistry)<sup>292</sup>.

PCR bases itself on two oligonucleotide primers (that contain 5' and 3' sequences 20-30 nucleotides long); these primers flank the target DNA. Deoxynucleoside triphosphates (dNTPs) are also required as part of the process, magnesium chloride ( $MgCl_2$ ) is needed for the incorporation of dNTP, the final ingredient is the polymerase, Taq polymerase is the most commonly used due to high amplification ability in low concentrations<sup>293</sup>.

PCR is broken up into three basic steps consisting of a denaturation of the DNA (90-94°C) followed by annealing of the primers (45-70°C) and finally extension by the polymerase (70-75°C). This cycle occurs 30-40 times to produce a sufficient yield of PCR products. Each cycle of PCR produces an exponential increase of DNA; common formula attributed to PCR is  $2^n$ , with n being the number of cycles assigned in the procedure<sup>294</sup>.

### 2.5.1 Hot Start PCR Procedure

The programme used to synthesise DNA using standard PCR involves a three step process:

Time	Temperature	Process
4 minutes	105°C	Initiation
15 minutes	96°C	Activation

Time	Temperature	Process
30 seconds	94°C	Denaturation
30 seconds	60°C	Annealing
60 seconds	72°C	Extension
7 minutes	72°C	Extension

} 30-45 Cycles

Time	Temperature	Process
Infinite	8°C	Hold

Standard PCR reactions were set up to a final volume of 20µl. The reaction involves 1µl of cDNA sample, 1µl of reverse primer (18s), 1µl of forward primer (18s), 10µl of PCR master mix (ABgene Ltd., Epsom, UK) and 7µl of RNA free water (Ambion, Applied Biosystems, Warrington, UK).

Standard PCR was used to amplify the adiponectin gene. In order to identify the gene product was adiponectin, Qiagen gel extraction kit (Qiagen Co., West Sussex, UK) was performed to manufacturer's instructions. The extracted gel sample was sequenced and analysed through software called Chromas Lite (<http://www.technelyium.com.au>).

### **2.5.2 Gel Electrophoresis & DNA Extraction**

Products of PCR are analysed and identified by running the products through a gel matrix (polyacrylamide or agarose gel). The products move across the gel through electrophoresis. Electrophoresis allows for DNA fragments to move from a negative to a positive electrode, smaller fragments migrate quicker and larger fragments take longer to move, this allows for identification of PCR products from their fragment size<sup>295</sup>.

For visualisation of the DNA fragment, it is essential to add an intercalating DNA dye to the gel before setting, most commonly used is ethidium bromide. Ethidium bromide emits fluorescence when exposed under ultra-violet light, therefore any DNA fragments present within the gel matrix is shown with a fluorescent band.

To identify the correct size of each positive band present in the gel matrix, a DNA ladder is used to confirm the size of the bands. DNA ladders separate at regular base pair sizes to allow for unknown band sizes to be correctly calculated.

Extraction of DNA fragments from the gel for further procedures can be safely achieved through the use of commercially available kits. The Qiagen QIAquick Spin kit uses DNA affinity columns and several washing steps to remove any contamination from the extraction. DNA suspended in the membranes columns can be eluted with the elution buffer supplied or nuclease-free water.

### 2.5.3 Gel Electrophoresis & DNA Extraction Procedure

Gels were constituted to 2% of agarose gel grade (Invitrogen Life Technologies) by dissolving 2g of agarose gel powder into 50ml of 1xTAE buffer (diluted from a stock of 50x tris(hydroxymethyl)aminomethane base, EDTA buffer and acetic acid (Fisher Scientific)). This solution was heated till clear and mixed with 5 $\mu$ l of 10mg/ml ethidium bromide and then poured into a cast for setting. All PCR products were mixed with glycerol blue dye and placed next to a DNA ladder (100bp Blue eXtendec, Bioron, Ludwigshafen, Germany) in the cast gel. The gel was then run for ~1 hour at 100v using a BioRad PowerPac Basic (Hertfordshire, U.K). The gels were visualised using a UV trans-illuminator CCD camera (Fuji Film luminescent image analyser LAS-1000 v1.01). The bands that were emitting fluorescence were extracted out of the gel and purified using the QIAquick gel extraction kit (Qiagen).

Gel bands that were extracted were weighed and dissolved into 2.0ml eppendorf tubes in 300 $\mu$ l of GQ buffer per 100 $\mu$ g of gel band extracted for 10 minutes at 50°C. Once all the gel was dissolved, 100 $\mu$ l of isopropanol (Fisher Scientific) was added per 100 $\mu$ g of gel extracted and the mixture was vortexed. The solution was pipetted to a QIAquick spin column and centrifuged for 1 minute at 10,000g, any filtrate solution carried over was discarded. A further 500 $\mu$ l of GQ was added to the column and centrifuged for 1 minute at 10,000g, this was to remove any leftover agarose, and all filtrate was discarded once again.

700 $\mu$ l of PE buffer treated with ethanol was added to the column and left at room temperature for 5 minutes and then centrifuged for 1 minute at 10,000g



and any filtrate was discarded. The column was then transferred to a new 2ml eppendorf collection tube and centrifuged for 1 minute at 10,000g to allow for any residual PE buffer to be removed from the membrane. The column was then moved to a 1.5ml eppendorf tube, with the final step being the elution of DNA by pipetting 30µl of EB buffer (elution buffer) onto the column membrane and centrifuging for 1 minute at 10,000g.

To calculate the concentration and authenticity of the DNA products extracted, they were analysed by using the NanoDrop®ND-1000. To verify the authenticity of the DNA products from new primers they were sent to the University of Nottingham's Centre for Genetics and Genomics (Queen's Medical Centre, Nottingham, UK) for DNA sequencing and results were cross-referenced against the NCBI website online (National Centre for Biotechnology Information). All final DNA amplicons were aliquoted down to a diluted concentration of 1ng/µl and kept at -20°C until further use.

#### 2.5.4 RNA extraction

RNA extraction (Total Ribonucleic acid – RNA) is a vital step in performing various molecular techniques such as RT-PCR, Q-PCR and Real-Time PCR. All PCR techniques require sensitive and non-contaminated samples therefore all steps before, during and after RNA extraction and purification must be performed vigilantly.

RNA extraction from adipose tissue in all my studies were completed in the same principle method as described here. The technique used was a modified procedure of the one-step acid guanidinium thiocyanate-phenol-chloroform (TRI-Reagent solution – Invitrogen) RNA isolation method via the use of an RNA extraction kit (Qiagen)<sup>296, 297</sup>. Homogenisation of the tissue sample in the phenol-guanidinium thiocyanate monophasic solution causes inhibition and denaturing of RNase activity<sup>297</sup>.

With the subsequent addition of chloroform into the solution leads to a creation of three phase layers. The organic phase situated at the bottom contains dissolved proteins and lipids. The interphase which is a thin layer in the middle contains dissolved DNA and the clear aqueous phase at the top is entirely constituted of dissolved RNA<sup>296, 297</sup>. The aqueous phase is separated from the solution and further treated with ethanol; this washing treatment allows the RNA ( $\geq 100\mu\text{g}$ ) to correctly bind to the membrane in the RNA centrifuge column. Depending on the manufacturer's instructions various washing steps are performed with guanidium salt-based buffers, these washing steps eliminates possible contaminants carried over from the phenol-guanidinium thiocyanate monophasic solution. The final wash is performed with nuclease-

free water. Once the RNA is extracted, it has to be quantified to calculate the concentration of the sample by NanoDrop®ND-1000 (Nanodrop Technologies, Wilmington, USA) spectrophotometer to measure the absorbance of light at 260/280nm for RNA. Ultimately 260/280 ratio not only gives estimation for the RNA concentration but also purity of the RNA sample<sup>298, 299</sup>. The ratio that is given for a pure RNA sample is between 1.8 and 2.0<sup>299</sup>. Before any sample was quantified on the Nanodrop, DNase I (Qiagen Co., West Sussex, UK) treatment was performed on each sample after RNA extraction. DNase I treatment was carried out to manufacturer's instructions. DNase works by cleaving to DNA and disrupting the phosphodiester bonds. This extra step was performed to eliminate any DNA left over from the final washes; this treatment also improves the final 260/280 ratio.

### **2.5.5 RNA Extraction Procedure**

Samples from all studies based in Nottingham, U.K and Alberta, Canada were extracted using the RNeasy Plus Mini Kit (Qiagen, West Sussex, UK) with Tri Reagent (Sigma Chemical Co., Poole, UK). The procedure in Nottingham used 100mg-150mg/ml of pericardial, subcutaneous or omental adipose tissue from each sample. For the procedure in Alberta, retroperitoneal and epididymal fat depots in rats were used (same tissue mg/ml as Nottingham) for each sample. Following manufacturer's instructions, the process used 1mg/ml of Tri Reagent for each sample homogenised with the Dipso-Mix (Medic Tools, Zurich, Switzerland) in Nottingham and the MP- FastPrep®-24 (MP Biomedicals LLC, OH, United States) in Alberta.

### **2.5.6 Nottingham Study**

Pericardial, subcutaneous and omental adipose tissue samples were homogenised at 3000rpm with the Dispo-Mix (Medic Tools, Zurich, Switzerland) homogeniser and then placed into a water bath for 2 minutes at a constant temperature of 37°C, this allows for lipid breakdown. Following this, the sample is centrifuged at 12,000g for 10 minutes at room temperature, allowing for any insoluble material to be removed. The supernatant following centrifugation is transferred to a fresh 2.0ml eppendorf tube. 0.2ml of chloroform (Fisher Scientific, Leicestershire, UK) was added to each sample; vortexed till the solution was thoroughly mixed and then left to stand at room temperature for 15 minutes. The mixture is then centrifuged at 12,000g for 15 minutes at 4°C, following this centrifugation, the colourless upper aqueous solution which contains dissolved RNA is transferred to a fresh tube, this process is known as phase separation. Approximately 0.6ml of aqueous is pipetted into a gDNA Eliminator spin column (genomic deoxyribonucleic acid), centrifuged at 8,000g for 30 seconds at room temperature. The flow through from is saved and the column is discarded. The flow through is pipetted into a new 1.5ml eppendorf tube and 0.7ml of 70% ethanol added and vortexed for 15 seconds.

The solution is then transferred into a RNeasy spin column and placed in a 2ml eppendorf collection tube, centrifuged at 8,000g for 15 seconds at room temperature. The flow through is discarded as all the RNA is engaged within the column membrane. 0.7ml of buffer RW1 is added to the column and centrifuged at 8,000g for 15 seconds at room temperature with the flow through being discarded. 0.5ml of buffer RPE is then added to the column and

centrifuged at 8,000g for 2 minutes at room temperature with the flow through being discarded. The column is then transferred to a clean 2ml eppendorf collection tube and centrifuged at 8,000g for 1 minute at room temperature with the flow through being discarded. This dry spin allows for any leftover buffer to be collected and removed from any downstream RNA applications. The column is finally moved to a sterile 1.5ml eppendorf collection tube for a final elution step with 30µl of RNase free-water was added to the centre of the column and centrifuged at 8,000g for 1 minute. The final elution was repeated by taking the RNA and pipetting it back into the column and centrifuging again under the same conditions.

For accurate measurements of RNA yield, the Nanodrop®ND-1000 (Nanodrop Technologies, Wilmington, USA) spectrophotometer was used. To avoid degradation of RNA<sup>299</sup>, the RNA stock solution was aliquoted into 10µl batches and further diluted into 1µ/µl batches for each sample. This allowed for efficient and simple use when conducting RT-PCR processing. All RNA samples were stored in a -80°C freezer.

### **2.5.7 Alberta Study**

All the procedures outlined above were carried out to the same specification in Alberta, Canada, apart from the homogenisation. The MP- FastPrep®-24 (MP Biomedicals LLC, OH, United States) was used for homogenizing and lysing of all tissue instead of the Dipso-Mix (Medic Tools, Zurich, Switzerland).

## 2.6 Real Time PCR (real-time Polymerase Chain Reaction)

With the introduction of Real-time PCR, many problems such as contamination are reduced. The time taken by Real-time PCR is considerably shortened when compared to block based PCR as Real-time PCR quantifies reaction products from each sample of every cycle<sup>300</sup>.

Contamination is reduced as PCR tubes containing amplicons are not opened as gel electrophoresis is not required. Real-Time PCR generates quantitative results allowing standard curve generation, copy number calculation with a broad  $10^7$  fold range; all performed automatically<sup>300</sup>.

In these studies, SYBR® Green was used. This is a fluorogenic dye which displays slight fluorescence whilst in solution but releases an intense fluorescent signal upon binding to double stranded DNA (including non-specific amplification and primer-dimer complex). SYBR® Green is the cheaper alternative to the other chemistries but requires extensive optimisation.

As fluorescence technology is used to detect and quantify the samples, the signal is in proportion to the amount of template present. As each cycle in the reaction occurs, the signal is exponentially increased. The signal becomes detectable once it crosses a set certain baseline, the cycle number at which the signal crosses the baseline is called the cycle threshold/crossing point ( $C_t/C_p$ ). The software that analyses the Real-Time quantification calculations is Quansoft (Techne Inc., Burlington, USA).

Currently, there are two main methods used to calculate the results from Real-Time PCR; the comparative threshold method -  $C_t$  method and the standard

curve method; Quansoft uses a  $C_t$  method to calculate Real-Time PCR<sup>301</sup>. The slope that is produced by this method requires a range from -3.4 to -3.6 to prove a valid efficiency of 90%-100%. The slope is calculated using this formula:

$$\mathbf{Eff = 10^{(-1/slope)} - 1}$$

Eff (amplification efficiency) is calculated by working out a standard curve based on  $C_t$  cycle values against the log of cDNA concentrations<sup>301</sup>.

cDNA concentration calculations are performed during PCR reactions, as the PCR reactions exponentially increase the concentration of the reaction, the PCR data produces a sigmoid curve. The sigmoid curve exhibits a plateau after a certain concentration, the linear phase that is created allows for  $C_t$  values of each sample to be calculated. The calculation of DNA concentration in each sample is worked out by equating the standard curve of known standard concentrations.

The standard curve is calculated through dilutions performed from known standard concentrations of the DNA. The DNA concentration is then diluted to 1ng/ $\mu$ l. In order to perform a standard curve, further serial dilutions are made from  $1 \times 10^{-1}$  to  $1 \times 10^{-9}$ .

Analysis of  $C_p$  values also requires coefficient variance of each sample to be calculated. The coefficient variance allows us to evaluate the measure of precision from a set of  $C_p$  values. All graphs and results are expressed in CEL (Comparative expression level). The CEL equation is as follows:

$$\Delta C_p = (C_p \text{ of target gene} - C_p \text{ of 18s})$$

$C_p$  values were analysed for significance by performing a Kolmogorov-Smirnov test to calculate whether the data was normally distributed. If the data is normally distributed, parametric tests such as a t-test can be carried out, non-normally distributed data requires non-parametric tests such as Mann-Whitney.

This method of calculation allows for quantification of gene expression by using a reference gene to compare against. A reference gene is often referred to a gene that has the ability to be expressed relatively highly across all cells in various conditions, this allows for the possibility of the target tissue to be normalised. This calculation is based on the assumption that the efficiency of the PCR experiment is 100%, therefore each cDNA strand is replicated perfectly for each cycle. Efficiency is verified through evaluating the standard curve produced, accepted ranges of efficiency are generally between 90-105%<sup>302</sup>.

With fluorescent PCR chemistries such as SYBR green, issues often occur with primer dimer formation. These formations are non-specific dye-DNA complexes which SYBR green also binds to along with double stranded DNA and emit fluorescence. Therefore it is essential to evaluate the PCR product qualitatively to confirm the actual sequence targeted has been amplified. This is verified by adding an additional step to the PCR procedure, at the end of the final cycle, a melt-curve is performed. The melt-curve allows for the recording of temperature at integral stages of increasing °C, as the temperature increases it leads to the denaturing of the PCR product, this in turn leads decreased fluorescent signal. The PCR product melting curve should produce a specific



peak at a certain temperature depending on the base and length of the sequence. A melt curve analysis which shows one temperature peak means no primer dimer or possible contamination from DNA-complexes were present in the experiment.

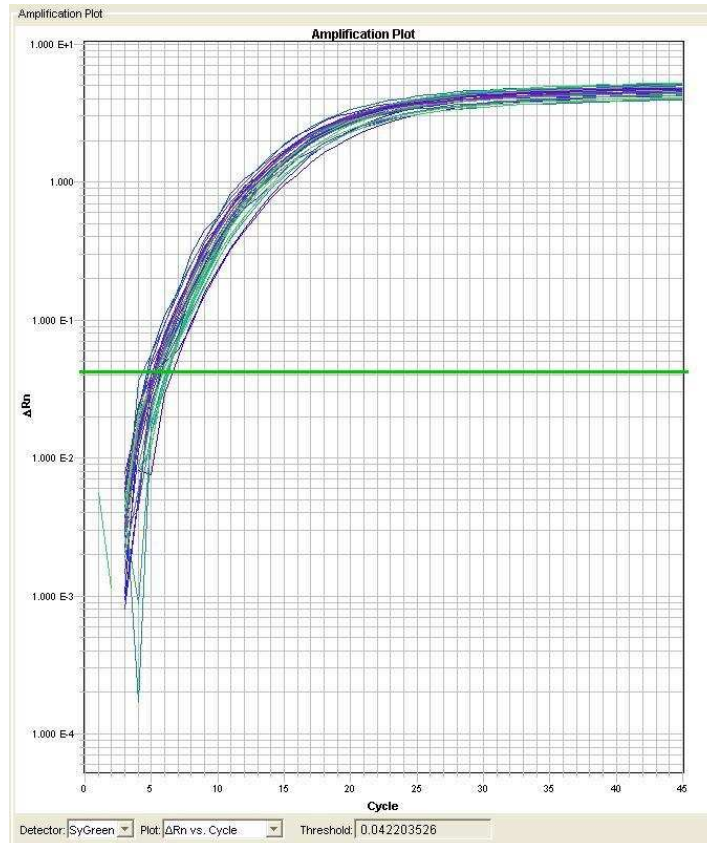


**Figure 13.5** - Real-Time PCR 18s samples using the StepOne Plus Real Time PCR System. Typical 'sigmoidal' curve in Q-PCR, the fluorescence signal crosses the threshold and increases exponentially until it reaches a plateau.

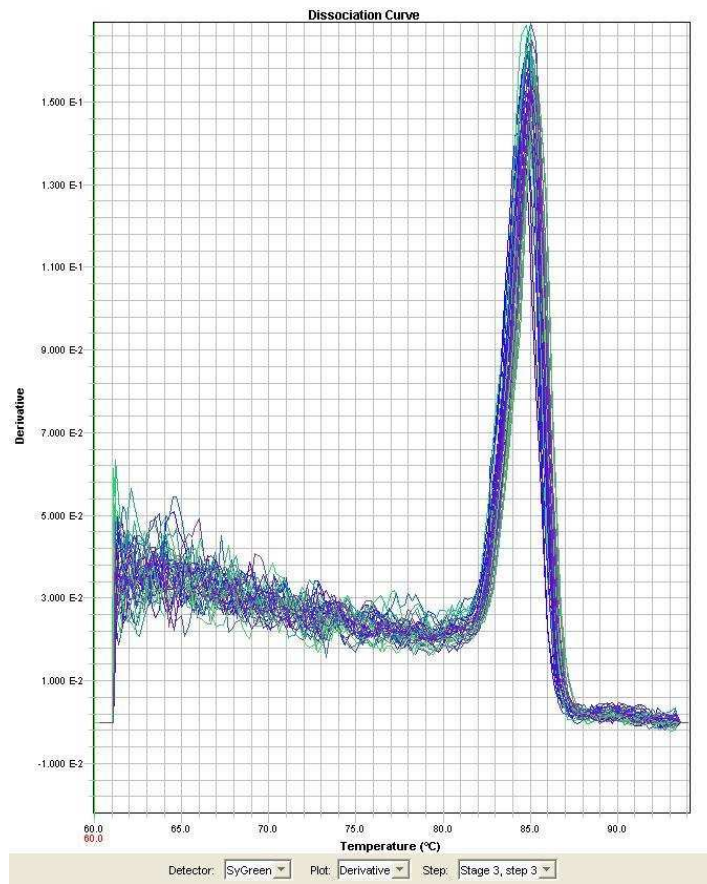


**Figure 14.6** - Melting curve using the StepOne Plus Real Time PCR System. A typical melt curve from Q-PCR, the single peak indicates the specificity of product amplified.

## **2.6.1 Primer Design**

### **Nottingham Study**

Primers for TNF $\alpha$ , leptin and insulin receptor were designed using Beacon Designer 4.0 software (Premier Biosoft, Palo Alto, USA). Primers designed for adiponectin were created using Primer3 (Whitehead Institute for Biomedical Research, USA).

In designing primers, the creation of primer dimers can restrict the efficiency of the PCR reaction. By using such specific programmes, the probability of primer dimer formation is greatly decreased. Primers were designed on the mRNA sheep, pig and cow sequences obtained from the NCBI (National Centre for Biotechnology Information) online database. Primers designed had introns spliced out and exon boundaries crossed, this allows for a greater specificity to the gene of interest and avoids amplification of gDNA (genomic DNA).

Along with minimal formation of primer dimer, primer design software also allows the user to determine the size of the amplicon. The optimum melting temperature for primers when used in a Real Time assay is approximately 60°C. The final condition that should be taken into consideration is C (cytosine) and G (guanine) content, the C and G optimum percentage per primer is 50% but percentages from 30 – 80% are acceptable.

Primers used in my project met the criteria described above. Leptin, IL-6, TNF $\alpha$  and Insulin receptor primers were designed by Dr. Melanie Hyatt, 18s primers were designed by Dr. Sylvain Sebert, MCP-1; TRL-4 primers were

designed by Dr. Don Sharkey, all other primers used in this study were designed by myself. All primers were acquired from Sigma-Genosys (Sigma Chemical Co., St. Louis, USA) and were diluted to a 1:40 dilution from a stock solution of 100 $\mu$ mol/l using of RNase free water (Ambion, Applied biosystems, Warrington, UK).

### **Alberta Study**

All primers designed for the Alberta study were based on mRNA from *Rattus Norvegicus* sequences obtained from the NCBI (National Centre for Biotechnology Information) online database. All primers were acquired from Sigma-Genosys (Sigma Chemical Co., St. Louis, USA) and were diluted to a 1:40 dilution from a stock solution of 100 $\mu$ mol/l using of RNase free water (Ambion, Applied biosystems, Warrington, UK) as previously prepared in Nottingham study.

**Table 2: List of primers used in the rat studies**

Name	Sequence	Accession Number
<b>18s Forward</b>	CGCGGTTCTATTTTGTGGT	NM_001142758
<b>18s Reverse</b>	AGTCGCCATCGTTTATGGTC	
<b>FTO Forward</b>	GCTGTGCCGTTGTGCATGGC	NM_001039713.1
<b>FTO Reverse</b>	GCCACGGCTGACCTGTCCAC	
<b>Adiponectin Forward</b>	AATCCTGCCCAGTCATGAAG	NM_144744.2
<b>Adiponectin Reverse</b>	TCTCCAGGAGTGCCATCTCT	
<b>Leptin Forward</b>	GAGACCTCCTCCATCTGCTG	NM_013076.3
<b>Leptin Reverse</b>	CTCAGCATTCAAGGCTAAGG	
<b>NF-kB Forward</b>	AGGCCATTGAAGTGATCCAG	XM_342346.4
<b>NF-kB Reverse</b>	CAGTGAGGGACTCCGAGAAG	
<b>IL-18 Forward</b>	AATGCGGAGCATAAATGACC	NM_019165.1
<b>IL-18 Reverse</b>	TAGGGTCACAGCCAGTCCTC	
<b>TNF-Alpha Forward</b>	ACTCCCAGAAAAGCAAGCAA	NM_012675.3
<b>TNF-Alpha Reverse</b>	CGAGCAGGAATGAGAAGAGG	
<b>MCP-1 Forward</b>	ATGCAGTTAATGCCCACTC	NM_031530.1
<b>MCP-1 Reverse</b>	TTCCTTATTGGGGTCAGCAC	
<b>GRP78 Forward</b>	TGCAGCAGGACATCAAGTTC	NM_013083.2
<b>GRP78 Reverse</b>	CTGCATGGGTGACCTTCTTT	
<b>IL-6 Forward</b>	CCGGAGAGGAGACTTCACAG	NM_012589.1
<b>IL-6 Reverse</b>	ACAGTGCATCATCGCTGTTC	
<b>CHOP Forward</b>	CCAGCAGAGGTCACAAGCAC	
<b>CHOP Reverse</b>	CGCACTGACCACTCTGTTTC	
<b>TLR4 Forward</b>	AGCTTTGGTCAGTTGGCTCT	
<b>TLR4 Reverse</b>	CAGGATGACACCATTGAAGC	
<b>IL-1B Forward</b>	CACCTCTCAAGCAGAGCACAG	
<b>IL-1B Reverse</b>	GGGTTCCATGGTGAAGTCAAC	

## 2.6.2 Reverse Transcription (RT-PCR)

Reverse transcription is used to produce cDNA (complimentary DNA); that can then be used in Real-Time PCR to analyse the expression of selected genes. In order to produce cDNA, single stranded RNA is reverse transcribed to produce double stranded cDNA with the use of a reverse transcriptase enzyme and DNA primers.

RT-PCR process works by random DNA primers annealing to the mRNA template to produce a complimentary sequence of the template mRNA with elongation and transcription occurring through a reverse transcriptase enzyme, this produces cDNA allowing for future PCR amplification.

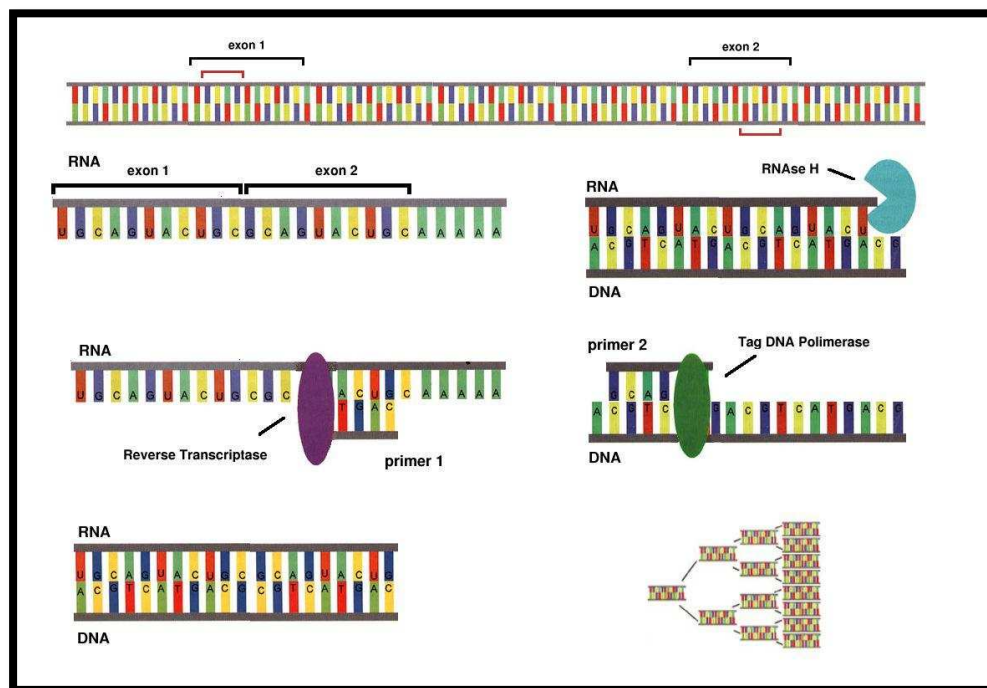


**Figure 15.7** - RT-PCR process step by step. A random primer binds to single stranded mRNA and the sequence is elongated by a transcriptase enzyme to create cDNA. Template of double stranded cDNA is then amplified by classic PCR.

### 2.6.3 Reverse Transcription Procedure

Reverse transcription is performed using Superscript II Reverse Transcriptase (Invitrogen Life Technologies, Paisley, UK). The programme used to perform the experiment is listed below.

Steps	Conditions
<b>Dilution</b>	Dilution of samples to obtain a concentration from 1 to 5 $\mu\text{g}/\mu\text{l}$ in RNASE free water
<b>Elongation Mix</b>	1 $\mu\text{l}$ of P(d)N6 ( random primers from Amersham pharmacia) 8 $\mu\text{l}$ of DEPC (diethylpyrocarbonate) water 1 $\mu\text{l}$ of RNA from a stock solution volume of 1 $\mu\text{g}/1\mu\text{l}$ – Total volume of 10 $\mu\text{l}$
<b>RNA elongation and random primer hybridization</b>	Incubation 10 minutes at 65°C in a thermocycler
<b>RNA elongation samples to be kept on ice</b>	
<b>RT master mix preparation</b>	DTT (Dithiothreitol) - 2 $\mu\text{l}$ 5X Buffer - 4 $\mu\text{l}$ DnTP (Deoxyribonucleotide triphosphate) -2 $\mu\text{l}$ RNase free water – 2.5 $\mu\text{l}$ Superscript - 2 $\mu\text{l}$ 10 $\mu\text{l}$ of master mix to be added to each RNA elongation sample
<b>Incubation</b>	45 minutes at 42°C in thermocycler Samples are stored in a -20°C freezer

Before the samples can be run with their gene of interest, the reverse transcriptase samples must be run along with their negative controls to check for possible genomic DNA expression. Negative samples are prepared as listed above but without Superscript II Reverse Transcriptase. All real time PCR experiments that were performed using cDNA samples were diluted from their concentrations obtained from reverse transcriptase to a 1:10 dilution.

#### 2.6.4 Real-Time PCR Procedure

Serial dilutions from  $1 \times 10^{-1}$  to  $1 \times 10^{-9}$  were made from the target cDNA template (1ng/ $\mu$ l) gene as a set of standards to be run for each Real-Time PCR experiment to calculate the efficiency of each experiment. The unknown samples were run alongside the standards for each experiment and gene analysis was calculated by using the housekeeping gene ribosomal 18s to normalise all the unknown cDNA samples present.

Real Time PCR assays were carried out using the programme listed below:

Step	Temperature	Time
<b>Denaturation</b>	94°C	15 minutes
<b>Denaturation</b>	94°C	10 seconds
<b>Annealing</b>	60°C	30 seconds
<b>Melt Curve</b>	75°C – 90°C	-
<b>Final Hold</b>	4°C	-

} 45 Cycles

All real time PCR assays were carried out using a total of 15 $\mu$  for each sample reaction. The samples included 1.5 $\mu$ l each of forward and reverse primers, 4.5 $\mu$ l of cDNA and 7.5 $\mu$ l of SYBR Green (Qiagen Co., West Sussex, UK). Each sample was run in duplicate on each plate of 96 wells. Controls included no template and no primer samples, also in duplicate. After each plate was successfully pipetted, plates were sealed using an Abgene plate sealer with individual thermal seals (Alpa Laboratories, Hampshire, UK) heat sealed onto each plate. Plates were then placed into the selected Real-Time PCR machine Quantica Q-PCR instrument (Techne) or the StepOne Plus Real Time PCR System (Applied Biosystems).



Real time PCR data analysis was carried out using Microsoft Excel (Microsoft Co., Redmond, USA), SPSS (SSPS Inc., Chicago, USA), Prism and Quansoft. Analysis of data from Quansoft can be easily exported into Microsoft Excel; Quansoft refers to  $C_t$  values as  $C_p$  (crossing points) values.

## **2.7 Histology**

Histology is known as the study of sectioned tissues through anatomical microscopy which facilitates visualisation of the cellular structure and composition, further enhanced through numerous histological stains. To preserve degradation of the tissue, it is essential to chemically fix the whole tissue before any histological procedure can proceed. Chemically fixing a tissue is performed by firstly placing it in formaldehyde, this process permanently cross-links the proteins in the tissue allowing preservation of the tissue<sup>303</sup>. For successful fixing, it is vital for the tissue to be encased within a holding matrix to help maintain its cellular and structural composition, this also aids in sectioning the tissue for microscopic analysis. The holding matrix in which the tissue is held must have certain properties that allow the fixing chemicals to flood and saturate the tissue and allow the tissue to solidify without damaging or disturbing the structure.

The most commonly used holding matrix for microscopy in histology is paraffin wax. Paraffin has hydrophobic properties which make it immiscible in water and therefore the tissue must undergo a dehydration step prior to embedding in the paraffin wax. The dehydration step is performed by

submerging the tissue in xylene (hydrophobic clearing chemical) and ethanol (dehydrating agent), the tissue is then ready to be sliced using a microtome.

### **2.7.1 Histological tissue processing**

Subcutaneous and omental adipose tissues from each animal based in Nottingham and retroperitoneal and epididymal adipose tissues from each rat situated at Alberta were treated with 10% formalin (10% v/v formaldehyde in 0.9 w/v sodium chloride/distilled water (Fisher Scientific) saline solution) for approximately 2-4 hours. Sections from each tissue sample were placed onto a Histosette II (Simport, Quebec, Canada) 30mm x 27mm x 5mm cassette and undergoes 6 steps of ethanol dehydration proceeded by 3 steps of ethanol-clearing with xylene (Fisher Scientific). The next three steps involved submerging the tissue sample in paraffin wax at 60°C and leaving to solidify the tissue sample overnight, using the Shandon Excelsior tissue wax processor (Fisher Scientific)

Sectioning the tissues was achieved by slicing each sample using a sledge microtome (Anglia Scientific, Cambridge, UK) at 5µm, 10 slides for each sample. The sectioned tissue was washed in 70% ethanol before being floated in water at 45°C, this allows for the sectioned wax tissue to stretch out via surface tension. The floating tissue sections were transferred onto Superfrost Plus slides (Menzel-Glaser Inc, Braunschweig, Germany) and left to dry on a heat rack for 15 minutes and placed into a drying oven for 24 hours at 37°C.

### **2.7.2 Haematoxylin and eosin staining**

Harris haematoxylin (also known as hematoxylin, C.I. 75290 or Natural Black 1) is aluminium based salt dye used for staining tissue. In its oxidised form, haematoxylin forms haematein. Haematein produces coloured complexes with specific metal ions such as aluminium and iron salts, therefore Harris haematoxylin is a suitable dye for staining tissues to visualise cellular nuclei. Harris haematoxylin is a regressive dye and decreases in intensity and its distinct blue colour is washed off by a weak alkali<sup>304, 305</sup>.

A contrasting dye used to visualise tissue architecture neighbouring the nuclei is Eosin Yellowish. Eosin Yellowish is an acidic based dye (defined as eosinophilic), known for binding to basic structures such as muscle fibres, cytoplasm, and collagen<sup>304</sup>. Eosinophilic formations are differentiated and visualised through various washes with water.

H&E (Haematoxylin and eosin) staining is a common method widely used in histology for examining structures of adipose tissue. The presence of crown-like structures and damage to adipocyte structure can be observed and measured through quantitative analysis<sup>210, 167</sup>.

### **2.7.3 H&E staining procedure**

A blinding process was implemented by assigning one slide per sample used via a random identifier; these slides were kept on a separate slide rack from other samples to ensure no bias. Slides underwent dewaxing by submersion into two xylene containers for 3 minutes each and then a further two stages of

submersion into 100% ethanol containers for rehydration followed by one stage of 70% ethanol submersion and a final stage of washing with distilled water.

The slides were firstly stained in Harris haematoxylin container (VWR Ltd, Lutterworth, UK) for approximately 5 minutes and washed with tap water to remove any excess dye. To implement the regression phase of haematoxylin staining, the slides were submerged into an acid-alcohol mixture (1% concentration hydrochloric acid in 70% ethanol) for 5 seconds and then washed with tap water and further submerged for 1 minute in a Scott's tap water container (0.2% sodium bicarbonate and 20% magnesium sulphate distilled water solution). Slides were then rinsed in tap water and placed into a 1% Eosin Yellowish stain trough (VWR Ltd, Lutterworth, UK) for 3 minutes and then rinsed in tap water to remove excess dye and allow for differentiation to occur of eosinophilic formations. The slides underwent a 2 stage dehydration phase by submerging them for 2 minutes in 100% ethanol container and then two 3 minutes submerging in xylene to remove any excess ethanol on the slides. The final step was to mount the slides with coverslips (VWR Ltd, Lutterworth, UK) using the DPX mounting solution (Fisher Scientific, Loughborough, UK) and then left to dry at room temperature overnight.

#### **2.7.4 Immunohistochemistry**

Albert H. Coons and his fellow colleagues were the first to successfully use a fluorescent dye to label antibodies in the identification of specific antigens in

tissue sections<sup>306, 307</sup>. Immunohistochemistry (IHC) is a process known for identifying and localising the antigen of interest from a tissue section by the aid of a specific reagents and labelled antibody via antigen-antibody interactions that can be visualised through markers such as enzymes, fluorescent dyes, colloidal gold and radioactive elements and used either an direct or indirect staining method.

The direct staining method involves only a one step approach which involves the labelled primary antibody binding directly to the specific antigen to generate a signal. While this method is fairly simple and quick, the sensitivity is much lower with direct staining as its signal amplification is lower.

Indirect staining requires the use of an unlabelled primary antibody and a labelled secondary antibody, the primary antibody is the first layer that binds to the specific antigen and the secondary antibody then binds to the first antibody, this method has a much higher specificity in comparison to the direct staining method<sup>308</sup>. The most widely used method for indirect IHC is a secondary antibody horseradish peroxidase (HRP) enzyme and when in the presence of 3,3 diaminobenzidine (DAB) it produces a brown formation, a chromogenic mixture via catalytic conversion<sup>309</sup>. Before any antibody exposure can begin, it is vital all sectioned slides are dewaxed and rehydrated, a comparable process to the histological staining method, this permits all IHC reagents to access the sectioned tissue. As previously described, formalin fixation of tissues develops in cross-linking of proteins, which in turns results in masking any viable antigenic sites. In order to disrupt the protein cross-links, samples are required to undergo a heat-induced epitope retrieval (HIER) process<sup>310</sup>.

### **2.7.5 IHC procedure**

A blinding process was implemented by assigning one slide per sample used via a random identifier; these slides were kept on a separate slide rack from other samples to ensure no bias and placed onto the Leica BondMax IHC slide processor (Leica Microsystems) and run via a software program (Vision Biosystems Bond version 3.4A) using Bond polymer refine detection reagents (Leica Microsystems).

Slides were treated with washes from xylene and ethanol for 1 minute each and then incubated at 95°C with epitope retrieval mixture. Slides were then treated at room temperature for 5 minutes with Peroxide Block. All slides excluding those for negative control were treated to 150µl of pre-optimised primary polyclonal anti-rabbit antibody (Abcam, Cambridge, UK) dilution (MCP-1 1:500, Abcam, GRP-78 1:150, Abcam) for 30 minutes before being treated to 150µl of HRP conjugated secondary anti-mouse and rabbit antibody polymer for 8 minutes. Slides were then treated with 3,3 DAB for 10 minutes until a brown precipitate has formed and then treated with Harris haematoxylin for 5 minutes. At the end of each stage the slides were automatically washed with Bondwash buffer and distilled water. The final step was to mount the slides with coverslips (VWR Ltd, Lutterworth, UK) using the DPX mounting solution (Fisher Scientific, Loughborough, UK) and then left to dry at room temperature overnight. The samples processed in the blinded process were observed using a 10x magnification and photographed for image analysis at 10 random areas. Volocity (Perkin Elmer, Cambridge, UK) imaging software was used to estimate positively stained cell percentage normalised against the total cell number present.

## **2.8 Bicinchoninic acid total protein determination**

The BCA assay method was used to calculate the total protein concentration from samples. The assay is based on a colourimetric reaction between BCA, proteins and copper sulphate<sup>311</sup>. The peptide bonds reduce  $\text{Cu}_{2+}$  to  $\text{Cu}_{1+}$  ions in proteins when incubated at a certain temperature. This activates the BCA reagent to form a chelation complex with the  $\text{Cu}_{1+}$  ions, which in turn results in a purple compound<sup>311</sup>. The colour change from the standard green to purple is equal to the proportion to the quantity of protein present in the selected sample, the wavelength at which absorbance is measured is at 526nm. The unknown concentrations are then quantified against the standard curve.

### **2.8.1 BCA assay procedure**

50ml of reagent A which contains 2% sodium carbonate, 1% bicinchoninic acid, 0.4% sodium hydroxide and 0.16% sodium tartrate was constituted to a final volume with distilled water and 10% sodium bicarbonate. 50ml of reagent B (4% copper sulphate solution) is made to a final volume with distilled water. Reagent C was produced by mixing reagents A and B together at a ratio of 100ml: 2ml, the solution was stored at 4°C until further use.

Eight bovine serum albumin (BSA) concentrations were used to produce standards ranging from 1.0 to 0.00 mg/ml; the standards were created in 0.9% saline. 2.5µl from each unknown protein sample was diluted to a ratio of 1:20 in 0.9% saline solution and constituted to a final volume of 50µl. For each standard, negative control and unknown sample, 10µl was pipetted into a 96-

well microplate followed by 200µl of reagent C to each well, the plate was then incubated at 37°C for 30 minutes in an orbital shaker. This final step allowed for colour development from green to purple and for measurement at wavelength 526nm. Each sample was replicated in duplicate with an acceptable level of 5% coefficient of variance only; any samples that were outside this range were repeated. For each sample reading, a 20x multiplication factor was formulated onto the recorded absorbance results to account for the primary dilution factor of 1:20.



## 2.9 Electrochemiluminescence

Electrochemiluminescence or electrogenerated chemiluminescence (ECL) is a novel approach to detecting antigens by generating luminescence via electrochemical reactions in mixtures. A highly exergonic reaction is produced with from electrochemically created intermediates in electrogenerated chemiluminescence, the reaction leads to an electronically heightened state of excitement which emits light<sup>312</sup>. The ECL excitation is a direct reaction lead by a redox reaction of electrogenerated species through a transfer of energetic electrons. This form of luminescence excitation is a type of chemiluminescence in which all or one of the reactants are generated electrochemically on the surface of electrodes<sup>313</sup>.

The ECL method has proven to be a very resourceful technique in analytical applications in highly sensitive and precise methods. ECL has the distinct advantages of chemiluminescent analysis (no background optical signal) and effortless control of the reaction through application of an electrode potential. Varying the electrode potential leads to an enhanced selectivity of ECL by controlling the species which are oxidised/reduced on the electrode and which species engage in the ECL reaction<sup>314</sup>.

ECL mechanism commonly uses Ruthenium complexes, in particular [Ru(bipy)3]Cl2 (this complex discharges a photon at ~620nm) which regenerates with TPA (Tripropylamine) in a liquid-solid or liquid mixture (See Figure 2.8).

## ECL Features

- The photon's emit light at ~620nm, therefore eradicating any issues with colour quenching.
- Background interference is minimal as the stimulation mechanism (electricity) leads to decoupling from the signal (light).
- Numerous excitation cycles from each label leads to an amplification of the signal, increased sensitivity and enhanced light levels.
- Carbon coated electrode surface allows for 10x greater binding ability compared to conventional polystyrene.

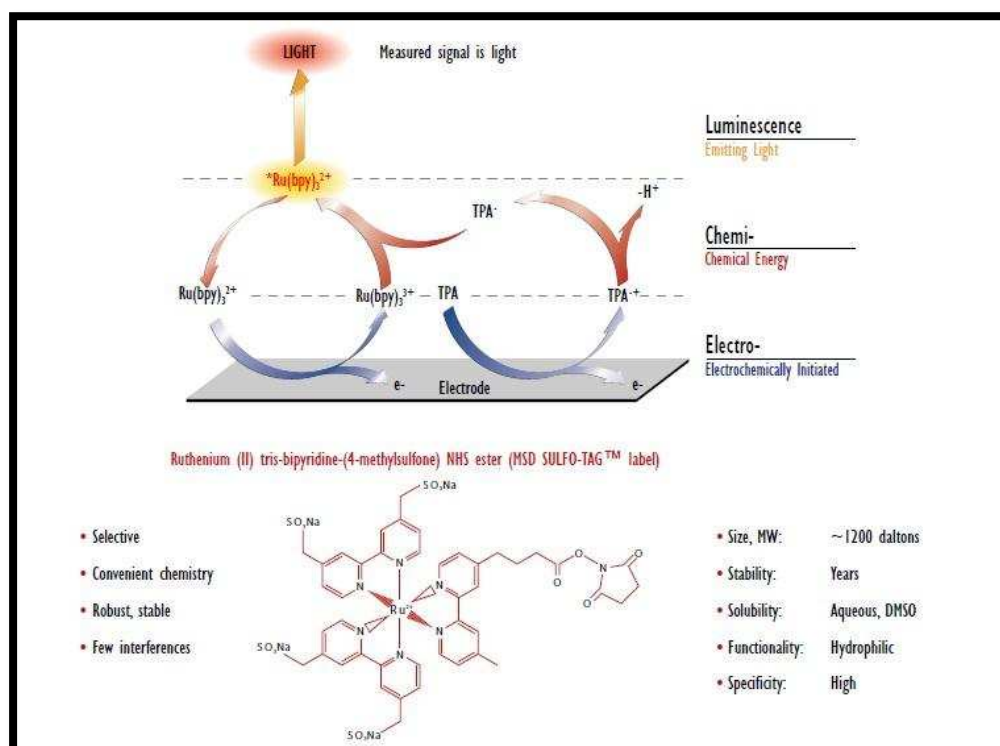


**Figure 16.8** - Electrochemiluminescence mechanism uses SULFO-TAG labels, which emit light upon electrochemical stimulation initiated at the electrode surfaces of MSD assay plates.

### 2.9.1 MSD Technology

MSD is a detection process by which ECL technology uses SULFO-TAG labels, that when excited by electrochemical stimulation emits light. Labels such as the SULFO-TAG are stable, non-radioactive and allow for a variety of choice for specific coupling chemistries. The electrochemical stimulation is initiated upon the electrode surface of multi-spot and multi-array plates.

MSD technology allows for quick and efficient method of analysing and measuring one or more proteins from a single small volume sample. MSD multi-array plates provide a platform for the construction of sandwich immunoassays. Uncoated plates are provided to the user, allowing the user to coat the assay with a capture antibody against a target protein specific to their experiment.

The sample is then added to the plate and a working solution comprising of the labelled detection antibody (MSD SULFO-TAG label, an anti-target antibody tagged with the electrochemiluminescent) are incubated over a period of time. The target which is present in the sample then binds to the capture antibodies present on the electrode surface; the immunoassay sandwich is finally complete by recruiting the labelled detection antibody to the target (See figure below).

A final MSD Read Buffer is added to the plate to allow for the correct chemical milieu for ECL to occur, the plate can then be loaded onto a MSD SECTOR for analysis. The SECTOR instrument is used to apply an electric voltage across the plate, which causes the electrode surface where the label

target is present to emit light. The SECTOR instrument processes the intensity of emitted light from the plate as a quantitative measure for the amount of target protein of interest in the sample.

### **2.9.2 ECL – MSD Multi-Array Procedure**

All instructions provided by MSD Technologies (Meso Scale Discovery, Maryland, USA) for the cytokine multi-plex plates were followed as suggested.

### **2.9.3 Solution preparation**

Preparation of solutions to the correct dilution and concentration was vital before prepping the MSD plate. All chemical solutions were provided by MSD Technologies (Meso Scale Discovery, Maryland, USA). The detection antibody solution was provided at 50X concentration, the final working concentration for the MSD plate should be 1X. For each plate used, 60µl of the stock solution (50X) was added to 2.94mL of Diluent 5, this brought the concentration to 1X. The read buffer which is added to the MSD plate at the end before reading in the SECTOR instrument is diluted to a working solution of 2X in deionized water. For each plate, 10mL of 4X read buffer was added to 10mL of deionized water. The MSD plates supplied required no pre-wetting as they were already pre-coated with the antibodies of the specific analyte chosen. The plates were also subjected to stabilizing treatment to ensure the stability of the immobilised antibodies.

## 2.9.4 Calibrator and standard solutions

All reagents were brought to room temperature with the stock solution of the calibrator allowed to thaw on ice. Calibrators are diluted in diluent 6, an 8-point standard curve consisting of 2 replicates for each point were used. Each well requires 25µl of calibrator standard. The correct setup required for each plate requires a 4-fold serial dilution with diluent 6 alone for the 8<sup>th</sup> step, set up as the blank.

<b>Standard</b>	<b>Concentration (pg/mL)</b>	<b>Dilution Factor</b>
<b>100X Stock</b>	1,000,000	
<b>STD-01</b>	40,000	25
<b>STD-02</b>	10,000	4
<b>STD-03</b>	2500	4
<b>STD-04</b>	625	4
<b>STD-05</b>	156	4
<b>STD-06</b>	39	4
<b>STD-07</b>	9.8	4
<b>STD-08</b>	0	n/a

For preparation of the 8-point standard curve:

1. To produce the highest point calibrator (STD-01), 10µl of the rat cytokine stock calibrator was added to 240µl of diluent 6 (dilution factor of 25)
2. The next step is to transfer 50µl of the STD-01 into 150µl of diluent 6. Repeat this 4-fold serial dilution step for the next 5 additional times to produce 7 calibrators.
3. The final STD-08 should be consisting of diluent 6 i.e. zero calibrator.

## **Assay protocol**

1. Dispense 25 $\mu$ l of diluent 6 into each well followed by sealing the plate with an adhesive plate seal and incubating for 30 minutes with vigorous shaking (300-1000rpm) at room temperature.
2. Pipette 25 $\mu$ l of calibrator controls into the selected wells followed by 25 $\mu$ l of sample into the remaining wells as planned. The plate is then sealed again and incubated for 2 hours with vigorous shaking (300-1000rpm) at room temperature.
3. Wash the plate 3 times with 200 $\mu$ l of PBS-T each time. After the wash, pipette 25 $\mu$ l of the 1X detection antibody solution into each well of the plate. Seal the plate with an adhesive plate seal and incubate for 2 hours with vigorous shaking (300-1000rpm) at room temperature.
4. Wash the plate 3 times with 200 $\mu$ l of PBS-T each time. After the wash add 150 $\mu$ l of 2X read buffer to each well and insert the plate into the SECTOR Imager. Preload the plate template onto the computer and analyse the plate. The plate must be read immediately after the addition of the read buffer into all the wells.

## 2.9.5 Analysis of results

All calibrator controls need to run in duplicate to produce a standard curve. The standard curve is modelled on using least squares fitting algorithms so that the signals processed from the samples of known levels of the analyte of interest can be used to calculate the concentration of the analyte in the sample. The assays have a wide range (3-4 logs), this allows for accurate quantitation in many samples without the need for dilution. The MSD analysis software supplied utilises a 4-parameter logistic model (or sigmoidal dose-response) and includes a  $1/Y^2$  weighting function. The weighting function is crucial as it provides a better fit of data over a wide dynamic range, particularly at the low end of the standard curve (See Fig 2.4.4).

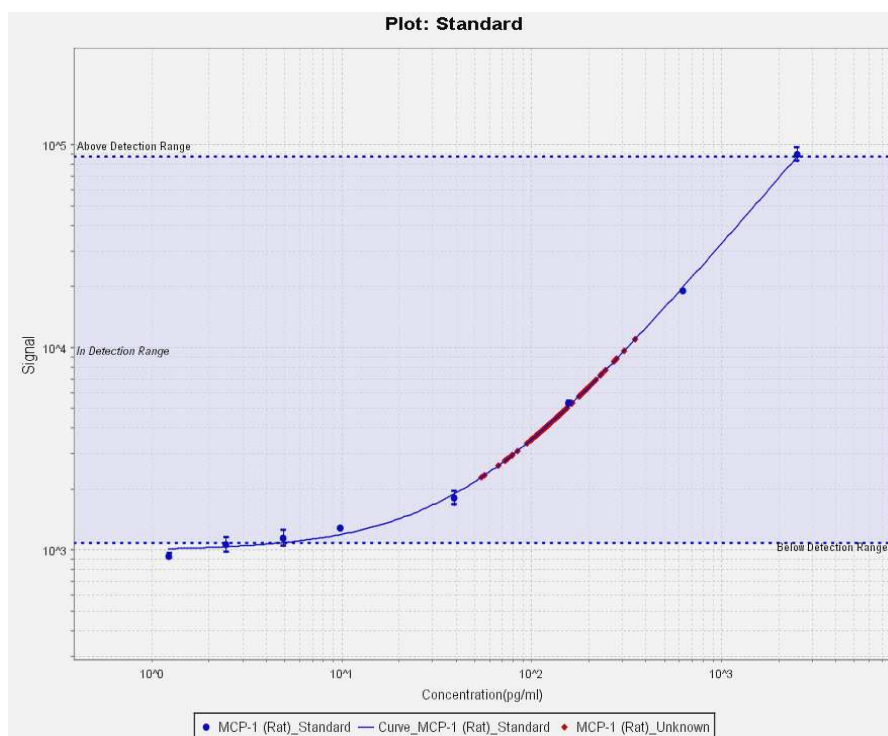


**Figure 17.9** – Typical standard curve from an MSD plate. The blue dots indicate the standards used to generate the standard curve, red dots are samples plotted against the curve to calculate concentration based on signal.

### **2.9.6 Statistical analysis**

Before any statistical analysis could be performed, the coefficient of variance for very duplicate sample used in the experiments was calculated. This was calculated on software package Microsoft Office Excel 2007 (Microsoft Corporation, Berkshire, UK), a spreadsheet program. To support accept reproducibility of the selected assay, the coefficient of variance had to be confirmed less than 5%. Data points that fell within the criteria of  $\leq 5\%$  were accepted for statistical analyses. All statistical analysis of data in all experiments was performed using Microsoft Excel 2007 and GraphPad Prism v5.01 (GraphPad Software, California, USA). All data points from experiments also underwent normality of distribution tests; the Kolmogorov-Smirnov normality test for parametric or non-parametric distribution was selected for this task. The Kolmogorov-Smirnov test concludes  $p \geq 0.05$  is determined as normality. For analysis of variance with comparable groups, they were assessed with a number of tests such as one or two-ANOVA for parametric data, for non-parametric data Kruskal-Wallis one-way analysis. For multiple group post hoc Dunn's or Bonferroni correction tests were applied. Graphs produced for all experiments were based on software package GraphPad Prism v5.01 (GraphPad Software, California, USA), to represent consistency within all data sets; the data was displayed as mean average  $\pm$  standard error of the mean (SEM). To yield a statistically significant result and have reason to justify the rejection the null hypothesis the p value must be less than 0.05.



# Chapter 3 – Early-to-mid gestational nutrient restriction

---

## 3.1 Introduction and aims

Pericardial adipose tissue is situated on the exterior of the parietal pericardium and is distinctly different in position and blood supply from epicardial adipose tissue<sup>315</sup>. Epicardial adipose tissue is located on the surface of the heart, with the ability to expand into the heart and integrate with the muscle fibers of the myocardium<sup>316</sup>. Studies reported in a recent review<sup>317</sup> demonstrated that depots of pericardial, epicardial and myocardial fat were associated with excess body weight<sup>21, 22</sup>, however the association between the fat depots and various measurements of body composition still remain questionable<sup>317</sup>.

The heart is covered by a layer called the pericardium. The pericardium is an unrestricting sac that wraps itself around the heart and the major blood vessels. Fat which is situated on the outer layer of the pericardium is called pericardial fat<sup>318</sup>. The pericardium is organised in two layers, the inner layer of visceral pericardium (or epicardium) and the outer layer of parietal pericardium that has a thicker structure and shapes itself to the chest cavity<sup>318</sup>. The epicardium lines the outer layer of the heart with a layer of flat mesothelial cells that are situated upon a fibrocollagenous support tissue and contains a variety of different cells along with large arteries and venous tributaries transporting blood to and from the heart wall<sup>319</sup>. Adipose tissue is surrounded by coronary arteries and veins which help expand the epicardium<sup>319</sup>. To prevent friction between the heart and the pericardium, there is a middle fluid layer which allows inhibited movement of the heart during its muscle contractions<sup>319</sup>.

### **3.2 Hypothesis**

This chapter therefore aims to investigate the extent to which alterations of pericardial adipose tissue inflammatory activity induced by prenatal nutrition could increase cardiovascular risk when it accompanies obesity may be critical to the understanding of the developmental origins of cardiovascular disease. My hypothesis therefore is that maternal nutrient restriction during the early to mid gestation period followed by juvenile obesity will results in a significant accumulation of fat mass and increased genetic inflammatory response as a result of this increased fat mass.

### 3.3 Material and methods

A fully detailed description of all the methods used in this chapter can be found in Chapter 2. The experimental set-up and model used to describe and illustrate and the result in this chapter can be observed in Figure 3.1. All animal experimentations that were reported i.e. tissue weights, plasma measurements and animal dissections were performed and supervised by Dr. D. Gardner and Dr. S. Sebert. For any sample or analytical exceptions are described in the results section of the relevant chapter. All statistical tests conducted in this chapter are detailed in Chapter 2.

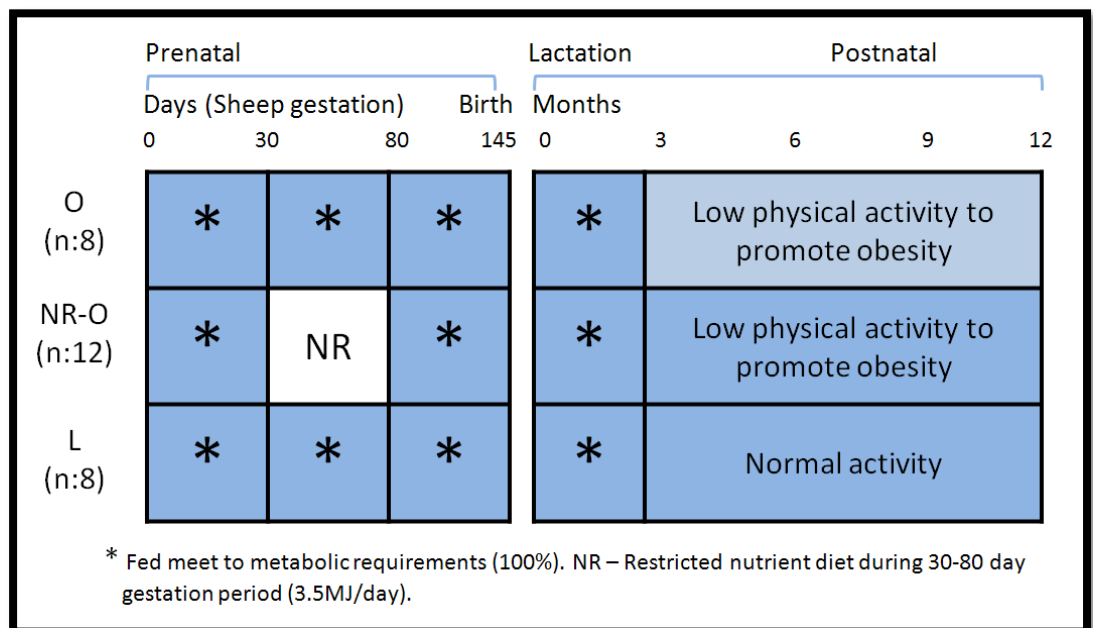


**Figure 18.1** – Sheep Study: Early to mid gestational nutrient restriction model.

O=Obese group, NR-O = Nutrient restricted-obese group, L = Lean group.

### 3.4 Results

#### 3.4.1 The effects of maternal nutrient restriction between early to mid-gestation on pericardial fat mass

Results showed there no difference in body weight at birth between both groups, this correlation continued until the time of dissection at 12 months of postnatal age. In addition there was a difference in pericardial fat mass ( $p < 0.05$ ; Fig 3.2) and pericardial % total fat ( $p < 0.05$ ; Fig 3.2.1) in sheep to subjected juvenile obesity.

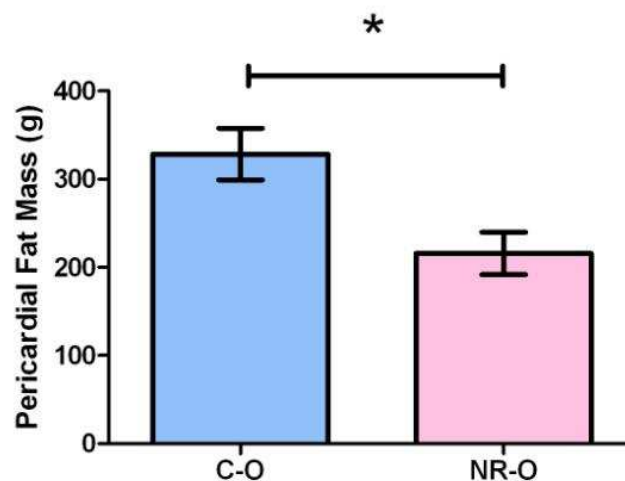


**Figure 19.2** - Pericardial fat mass (g) measurements of obese group (O, n=8) and nutrient restricted group (NR-O, n=12). Values are in mean  $\pm$  SEM; statistical differences are denoted by \*, where \* =  $p < 0.05$ . Analyses of pericardial fat mass (g) between the groups were treated with unpaired t-tests.

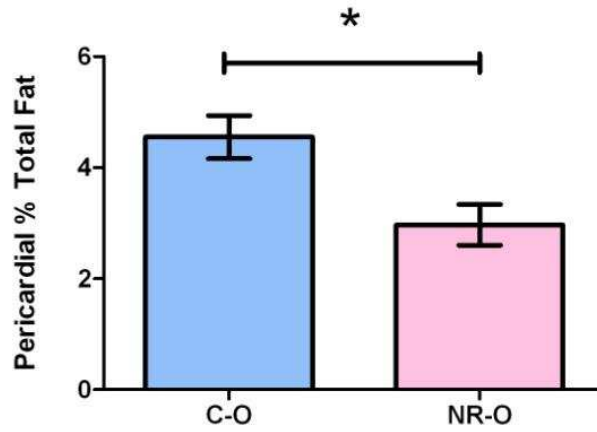


**Figure 20.2.1** – Pericardial % total fat measurements of obese group (O, n=8) and nutrient restricted-obese group (NR-O, n=12). Values are in mean ± SEM; statistical differences are denoted by \*, where \* =  $p < 0.05$ . Analyses of pericardial fat mass (g) between the groups were treated with unpaired t-tests.

### 3.4.2 Pericardial gene expression of pro-inflammatory markers interleukin-6 (IL-6) and interleukin 18 (IL-18)

As expected the analysis of pericardial mRNA expression of illustrated IL-6 ( $p < 0.05$ ) and IL-18 ( $p < 0.05$ ) identified a significant up regulation for the group subject to maternal nutrient restriction followed by juvenile obesity.

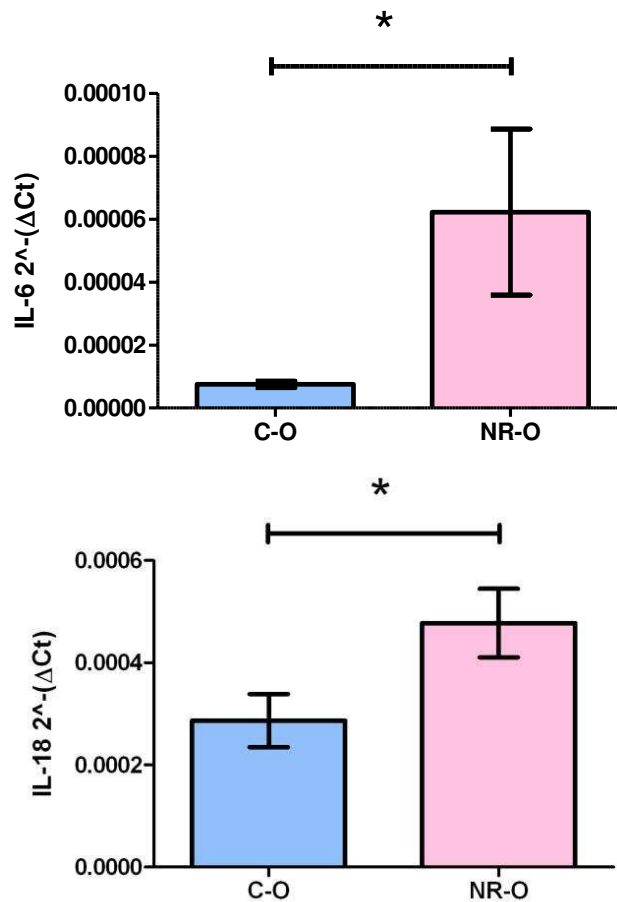


**Figure 21.2.2** – Interleukin-6 (IL-6) and Interleukin 18 (IL-18) mRNA expression values of the obese group (O, n=8) and nutrient restricted-obese group (NR-O, n=12). Values are in mean ± SEM; statistical differences are denoted by \* =  $p < 0.05$  (unpaired t-test).

### 3.4.3 Pericardial gene expression of 78 kDa glucose-regulated protein (GRP-78) and monocyte chemotactic protein-1 (MCP-1)

As expected the analysis of pericardial mRNA expression of illustrated MCP-1 ( $p < 0.05$ ) and GRP78 ( $p < 0.05$ ) identified a significant up regulation for the group subject to maternal nutrient restriction followed by juvenile obesity.

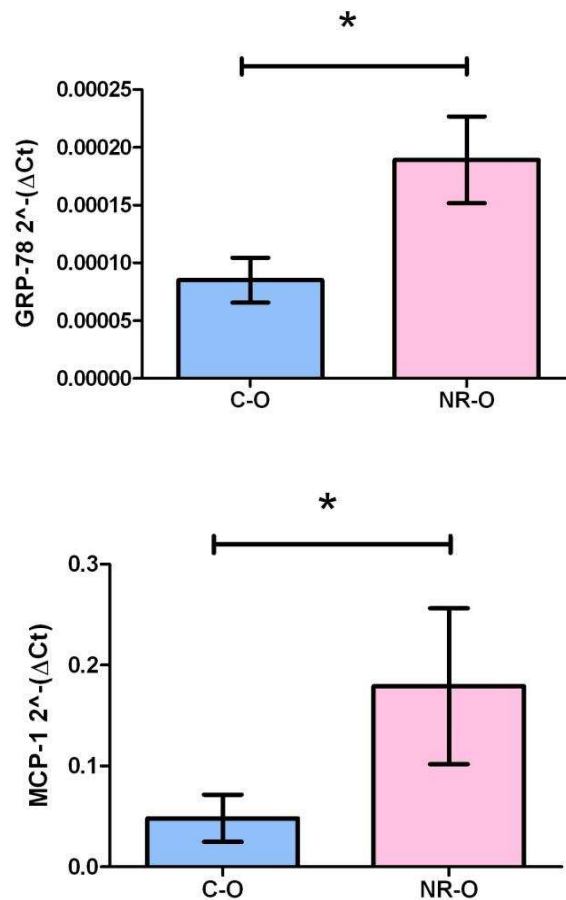


**Figure 22.2.3** – GRP-78 and MCP-1 mRNA expression values of the obese group (O, n=8) and nutrient restricted-obese group (NR-O, n=12). Values are in mean  $\pm$  SEM; statistical differences are denoted by \* =  $p < 0.05$  (unpaired t-test).

### 3.4.4 Pericardial gene expression of metabolic and inflammatory markers

After observing the difference in pericardial adipose tissue mass we decided to examine certain adiposity markers such as FTO, leptin and adiponectin. TNF-alpha which is also known for its regulating and modifying influence on adiponectin and other cytokines was also investigated. There was no change exhibited by the gene listed in Table 3.1. Other pro-inflammatory markers such as TLR4 were also tested for gene expression change but they were showed no significant change between the groups.

**Table 3:** Inflammatory and metabolic gene mRNA expression of O (obese group) and NR-O (nutrient-restricted obese group). Values are mean  $\pm$ SEM. NS = no significant difference (unpaired t-test)

Group	O (n=7)	NR-O (n=12)	p value
<b>Adiponectin</b>	1.69 $\pm$ 0.41	1.40 $\pm$ 0.43	ns
<b>FTO</b>	1.38 $\pm$ 2.60	1.10 $\pm$ 1.30	ns
<b>Leptin</b>	2.77 $\pm$ 0.86	4.55 $\pm$ 1.34	ns
<b>TNF-<math>\alpha</math></b>	0.10 $\pm$ 0.06	0.07 $\pm$ 0.03	ns
<b>TLR4</b>	0.003 $\pm$ 0.05	0.003 $\pm$ 0.06	ns



### 3.5 Discussion

Work previously carried out by the University of Nottingham Academic Division of Child Health on obese sheep, have developed models based on an amalgamation of maternal nutrition restriction followed by varying postnatal activity treatment<sup>157</sup>. The nutritional restriction stage was aimed at the in utero period of early to mid gestation (ovine organ- and embryogenesis period), gestational days 30-80 during pregnancy<sup>210</sup>. When analyzing the physiological adaptations of adipose tissue and renal function, the study was able to demonstrate that maternal nutrient restriction throughout this stage resulted in altered inflammatory and metabolic genetic-protein reaction in the kidney and perirenal adipose tissue depots for individuals in groups of lean, obese and nutrient restricted obese<sup>210, 320</sup>. Furthermore the study highlighted that the nutrient restricted obese group demonstrated enhanced metabolic dysfunction that were distinguished by increased apoptosis, renal oxidative stress along with increased renal lipid deposition<sup>321</sup>.

My study was able to supplement the evidence that maternal nutrition restriction in the early to mid gestation period leads to increased inflammatory expression of IL-6, IL-18, and macrophage related MCP-1 and ER stress related GRP78 chaperone genes in the maternal nutrient restricted obese group.

### **3.5.1 Fat mass accumulation following maternal nutrient restriction in juvenile obesity**

A recent study investigating the role of pericardial fat in relation to atherosclerotic processes in coronary arteries showed a direct correlation to pericardial fat independent of the measure of adiposity currently undertaken such as body mass index and waist circumference<sup>322</sup>. Data collected from cross-sectional studies have also shown pericardial fat (independent of body fat) correlated positively to coronary artery disease<sup>323 324</sup>.

Studies based on autopsy results have shown epicardial fat not be positively correlated to subcutaneous abdominal fat<sup>325</sup> but in vivo studies have demonstrated differences in correlations with differing strength<sup>317 326</sup>. Studies have shown visceral fat to be an independent marker of myocardial fat<sup>327</sup> with strong relationships with pericardial fat<sup>328</sup>.

In addition, studies involving myocardial, epicardial and pericardial fat depots have shown strong correlations with the components of metabolic syndrome such as type 2 diabetes mellitus<sup>327</sup>, increased triglycerides and hypertension<sup>324</sup>, raised fasting insulin and elevated waist circumference<sup>329 330</sup>. Studies investigating pericardial and epicardial fat have been able to conclude that excess fat may be a contributing factor in the pathogenesis of coronary heart disease<sup>317 324 325</sup>.

Current research concludes that epicardial is biochemically different from pericardial fat<sup>330</sup>, studies involving measuring fat thickness through echocardiography demonstrated the differences in epicardial and pericardial<sup>326</sup>. With epicardial echocardiography Iacobellis et al, were able to predict visceral

adiposity<sup>326 329</sup>, metabolic syndrome<sup>331</sup>, heart morphology<sup>332 333</sup>, fasting glucose<sup>334</sup>, insulin resistance<sup>330</sup>, liver enzymes<sup>334</sup> and sub-clinical atherosclerosis<sup>335</sup>. The body of evidence for epicardial fat as a predictor for such metabolic diseases is becoming more apparent, therefore more research and understanding must be gathered for pericardial fat.

My study was able to demonstrate changes in fat mass accumulation in pericardial adipose tissue resulting from juvenile obesity in comparison to maternal nutrient restriction followed by juvenile obesity. When reviewing my original hypothesis, I stated that individuals who were exposed to early to mid gestational nutrient restriction followed by juvenile obesity would accumulate more fat mass. The original hypothesis was based on the assumption that early to mid gestation would drive the fetus into a “catch up growth” phase during postnatal growth, a period of growth where food was not restricted.

However this was not demonstrated in pericardial fat and a possible reason for this may be the development of pericardial adipose tissue during early to mid gestation was severely inhibited and its ability to store fat was largely decreased. This may give an explanation to the number of inflammatory markers that up-regulated in pericardial adipose tissue from this study.

### **3.5.2 Expression of inflammatory markers following maternal nutrient restriction in juvenile obesity**

My study was able to display an up-regulation in inflammatory markers such as MCP-1, IL-6, GRP78 and IL-18. The inflammatory process was independent of fat mass accumulation as the control group which showed a statistically significant increase in fat mass but did not show any change in gene expression. A possible reason for the increase of inflammatory markers in a fat depot with lowered fat mass could be the maternal nutrient restriction during early to mid gestation causing a metabolic and physiological change on the outcome of pericardial adipose tissue functioning. This dysregulation during the gestational period may attribute to the inflammatory response as during postnatal growth, the individuals were forced into juvenile obesity through being maintained within a restricted activity environment and fed ad libitum. It is thus possible that the fat mass was unable to be stored successfully in the pericardial adipose tissue leading to inflammatory reactions and cell apoptosis.

### **3.6 Conclusion**

As previously described in the introduction chapter MCP-1 is known for its properties in macrophage recruitment to sites of cell stress. GRP-78 is an endoplasmic reticulum chaperone that is increased in expression during times of adipocyte stress, in order to promote cell survival it is activated by the UPR pathway to restore cellular homeostasis<sup>161</sup>. IL-18 is an inflammatory interleukin that is produced by macrophages<sup>336</sup> and IL-6 is well established for

its effects during an inflammatory response<sup>99</sup>. Therefore in conclusion, the study was able to demonstrate that pericardial adipose tissue inflammation can be changed by in utero nutritional manipulation.

However metabolic, appetite regulating and body mass related genes such as FTO, leptin and adiponectin were not shown to statistically significant between the groups. Limitations such as basing this conclusion on gene expression alone should be taken on board. Further research involving protein expression on inflammatory markers should be investigated before a concrete conclusion is theorized. Furthermore additional depots such as epicardial adipose tissue could also be investigated to evaluate the full extent of maternal nutrition restriction on cardiac physiology and function.

# Chapter 4 – Late gestational nutrient restriction

---

## 4.1 Introduction and aims

The correct amount and composition of nutritional intake is required during the rapid developmental periods for the fetus as well as to during their first years of life. The supply and demand for nutrient turnover in young infants and children when compared to adults is much higher due to the rapid rates of growth. Growth from pre to post natal life and into adolescence is outlined by specific developmental changes in multiple organ composition and function. A failure to supply the adequate nutritional needs during this phase is likely to lead to adverse consequences on metabolic development and growth.

Therefore providing the correct nutritional needs at the earliest stage possible – pregnancy, is essential. My previous chapter looked at inflammatory marker gene expression in pericardial adipose tissue and adaptations in its metabolism during nutrient restriction between early and mid-gestation followed by juvenile obesity. This chapter focuses on nutrient restriction in late gestation with or without accelerated postnatal growth in subcutaneous adipose tissue.

As highlighted earlier, with overwhelming evidence that VAT mass correlates with the progression towards CVD and T2DM via the development of insulin resistance and with little evidence supporting SAT's involvement<sup>35, 37, 38</sup>, SAT's suggested ability is to play a buffer or a sink to avidly absorb circulating FFAs and TGs in the postprandial period. However once this buffer reaches its capacity the cells lose their protective benefit and fat begins to accumulate

around tissues not suited for lipid storage<sup>337</sup>. Therefore I feel it is a depot that with current research can also play a vital role in the understanding of CVD and T2DM development<sup>49, 338</sup>.

This chapter details the changes that occur during the final stages of pregnancy, a period of when 70% of fetal growth occurs, and any changes of nutritional uptake during phase may have negative effects later in life.

## **4.2 Hypothesis**

My hypothesis was that fetal sheep exposed to a nutrient restricted diet in late gestation, that is followed by accelerated postnatal growth would exhibit increased gene expression of inflammatory and metabolic markers in subcutaneous adipose young adult offspring.



### 4.3 Materials and Methods

A fully detailed description of all the methods used in this chapter can be found in Chapter 2. The experimental set-up and model used to describe and illustrate the result in this chapter can be observed in Figure 4.1. All animal experimentations that were reported i.e. tissue weights, plasma measurements and animal dissections were performed and supervised by Dr. S. Sebert and Dr L Chan. For any sample or analytical exceptions are described in the results section of the relevant chapter. All statistical tests conducted in this chapter are detailed in Chapter 2.

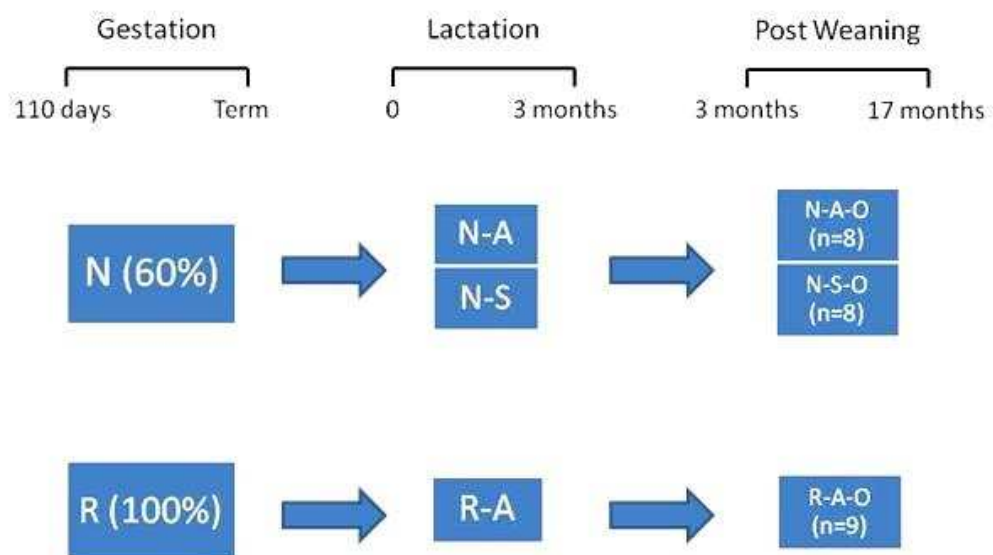


**Figure 23.1** - Late gestational nutrient restriction model, N = nutrient restricted (60% of normal energy requirements), R = fed to requirements (100% of normal energy requirements), A = fed to appetite (150% of normal energy requirements). During lactation, the N group were either raised as a singleton (-A = Accelerated growth raised without competition) or with a twin (-S = Standard growth raised as a twin). Post weaning phase, all groups were raised in an obesogenic environment.

## 4.4 Results

### 4.4.1 The effects of a nutrient restricted environment and their impact on body weight and fat mass accumulation

Weight measurements taken at the time of birth showed a reduced birth weight following maternal nutrition restriction (Fig 4.1.1). Both NA and NS groups were grouped together for the data shown in Fig 4.1.1, as the NA was treated the same as NS during gestation.

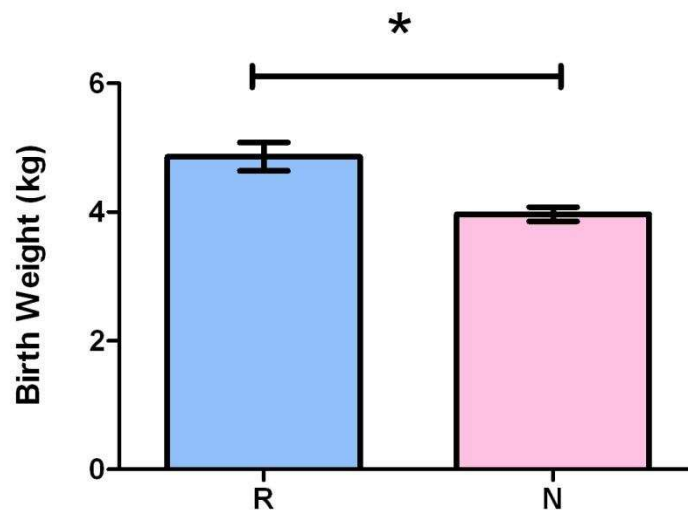


**Figure 24.1.1** - Birth weight measured following late gestational maternal nutrition restriction. N = nutrient restricted (60% of normal energy requirements, n=16), R = fed to requirements (100% of normal energy requirements, n=9). Values are in mean  $\pm$  SEM; statistical differences are denoted by \* =  $p < 0.05$  (unpaired t-test).

Following the difference observed in birth weight, I decided to look at the gestation weight gain between the groups. It was observed that low birth weight offspring (NS) exhibited a reduced weight gain throughout late gestation and did not display any signs of accelerated postnatal growth (Fig 4.1.2). Groups RA and NA weighed more at the end of lactation (90days) due to their groups being allowed to accelerate growth unlike NS (Fig 4.1.2).

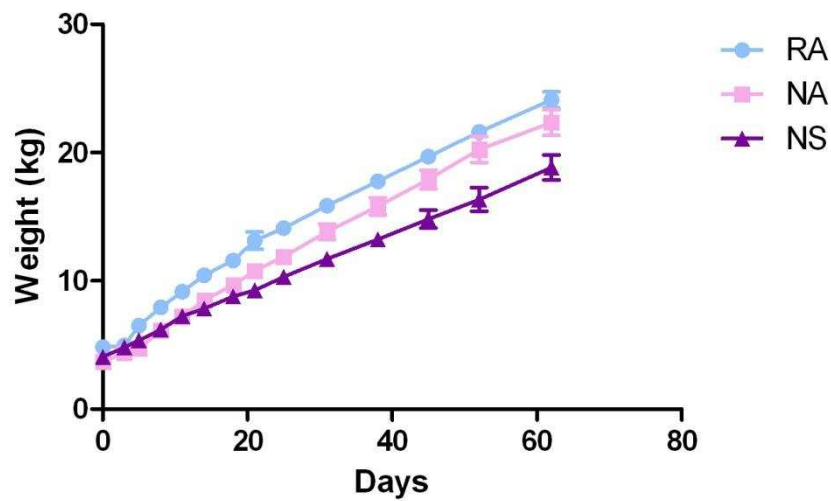


**Figure 25.1.2** – Early post-natal growth displayed in a time course from birth to the end of lactation (90 days) for the RA group (fed to 100% of energy requirements, raised without competition, n=9), NA group (fed to 60% of energy requirements, raised without competition, n=8), and the NS group (fed to 60% of energy requirements, raised with competition, n=8). Values are in mean  $\pm$  SEM; there were no statistical differences between the groups (Two way - ANOVA).

Following weaning, all offspring from nutrient restricted mothers needed an extra 4 months before their overall weight was within range of the other groups. This could be largely explained as a result from the reduced weight gain pre-weaning (Fig 4.1.1). The NS group did however show a faster rate of weight gain during post-weaning but no offspring group that underwent maternal nutrition restriction gained more weight than the control group at the final weigh (Fig 4.1.3). This was similarly observed between all groups when comparing total fat mass (Fig 4.1.4).

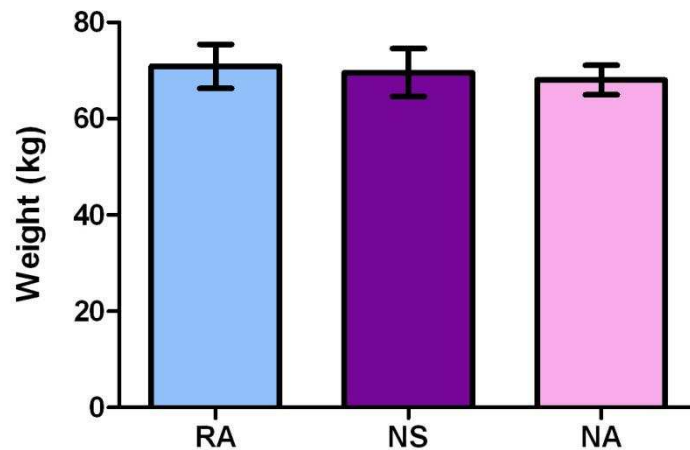


**Figure 26.1.3** – Graph of weight taken at 17 months of age. RA group (fed to 100% of energy requirements, raised without competition, n=9), NA group (fed to 60% of energy requirements, raised without competition, n=8), and the NS group (fed to 60% of energy requirements, raised with competition, n=8). Values are in mean  $\pm$  SEM; there were no statistical differences between the groups (ANOVA).

**Figure 4.1.4** Graph of total fat mass %

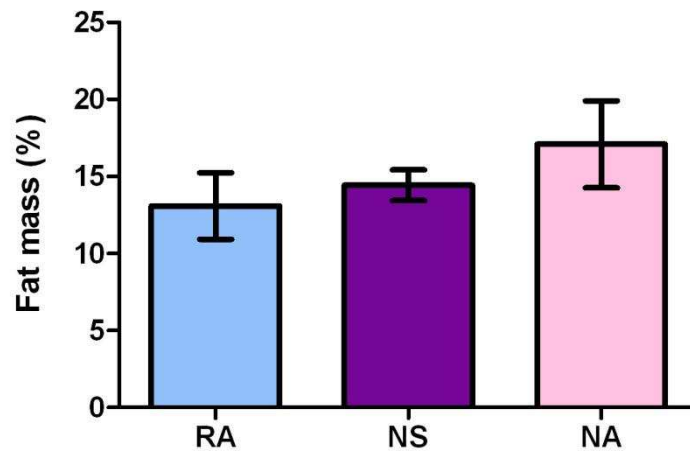


**Figure 27.1.4** – Graph of total fat mass % taken at 17 months of age, RA group (fed to 100% of energy requirements, raised without competition, n=9), NA group (fed to 60% of energy requirements, raised without competition, n=8), and the NS group (fed to 60% of energy requirements, raised with competition, n=8). Values are in mean  $\pm$  SEM; there were no statistical differences between the groups (ANOVA).

#### 4.4.2 Maternal gestational nutrition restriction effect on gene expression of metabolic and inflammatory markers from subcutaneous adipose tissue

From the previous results in birth weight and post-weaning weight gain, the metabolic marker leptin, which is associated with appetite regulation, was first investigated followed by adiponectin that has been seen to have increased gene expression in lean subjects. There was no gene expression difference observed between groups in leptin and adiponectin (Table 4.1). There were also no statistically significant differences in gene expression when groups were analyzed for gender differences (Table 4).

**Table 4:** mRNA gene expression values of inflammatory and metabolic markers on RA group (fed to 100% of energy requirements, n=9) compared to NA group (fed to 60% of energy requirements, n=8). Values are in mean  $\pm$  SEM; NS = no significant difference, S = significance ( $p < 0.05$ )

Group	RA (n=9)	NA (n=8)	p value	Gender
<b>Adiponectin</b>	3.75e-004 $\pm$ 1.7e-004	8.2e-004 $\pm$ 2.6e-004	ns	ns
<b>Leptin</b>	0.29 $\pm$ 0.1	0.36 $\pm$ 0.1	ns	ns
<b>IL-6</b>	8.2e-004 $\pm$ 1.3e-004	7.7e-004 $\pm$ 1.4e004	ns	S
<b>TNF-<math>\alpha</math></b>	8.8e-004 $\pm$ 2.5e-004	8.5e-004 $\pm$ 2.4e-004	ns	ns
<b>MCP-1</b>	6.0e-004 $\pm$ 2.3e-004	2.8e-004 $\pm$ 5.9e-004	ns	ns
<b>TLR-4</b>	9.2e-004 $\pm$ 2.0e-004	7.9e-004 $\pm$ 1.6e-004	ns	ns
<b>IL-18</b>	0.23 $\pm$ 0.1	0.06 $\pm$ 0.02	ns	ns
<b>GRP-78</b>	7.9e-004 $\pm$ 1.2e-004	9.2e-004 $\pm$ 1.4e-004	ns	ns
<b>FTO</b>	8.8e-004 $\pm$ 1.8e-004	5.6e-004 $\pm$ 4.0e-005	ns	S

The gene expression of IL-6 when analysed in mixed gender settings did not demonstrate any statistical difference between the groups (Table 4.1). However, when the group was analysed by gender, the females exhibited an up-regulation of IL-6 expression when fed to requirement during the gestation period (Fig 4.1.5). There was no statistically significant difference found in between males.

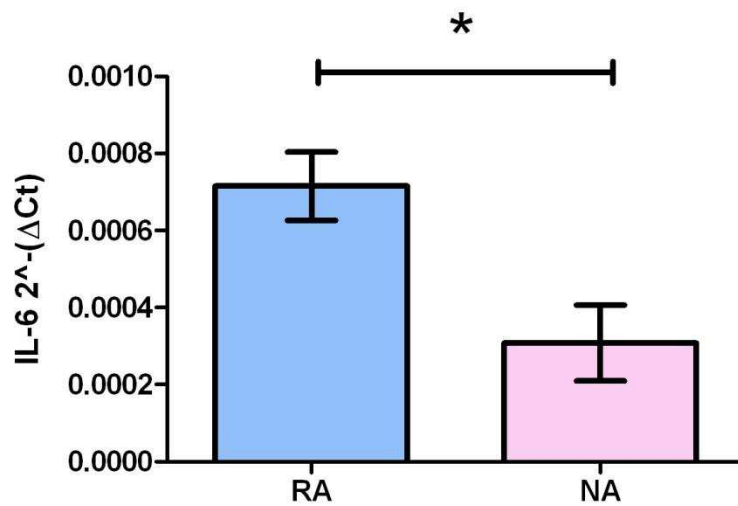


**Figure 28.1.5** - An up-regulation of IL-6 mRNA expression values in females from RA group (fed to 100% of energy requirements, raised without competition, n=9) compared to NA group (fed to 60% of energy requirements, raised without competition, n=8). Values are in mean  $\pm$  SEM; statistical differences are denoted by \* =  $p < 0.05$  (unpaired t-test).

When analyzing the gene expression of TNF- $\alpha$  and GRP-78, there are no statistically significant differences between the groups or gender. Other inflammatory markers such as IL-18, IL-18 along with MCP-1 and TLR-4 also did not exhibit and statically significant differences between groups or gender (Table 4.1).

However, the obesity gene related marker FTO did reveal differences gene expression and was statistically significant different when comparing between genders in groups but not mixed (Table 4.1). FTO showed an up-regulation of expression in the female groups only who were fed to requirement during the gestation period (Figure 4.1.6).

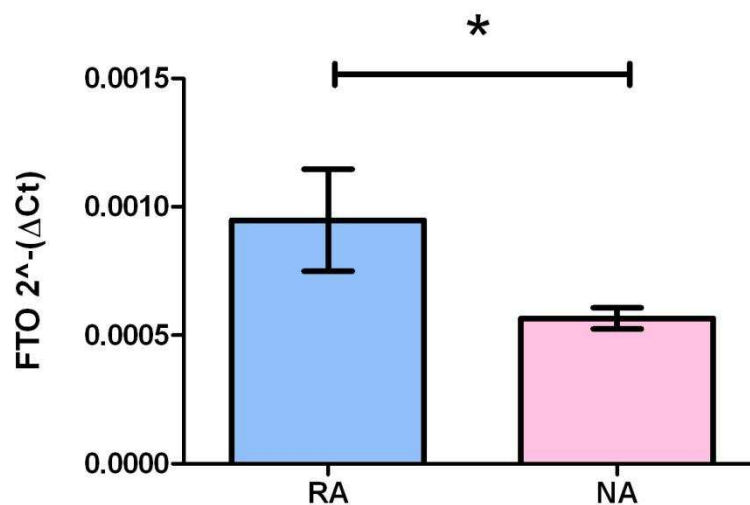


**Figure 29.1.6** - An up-regulation of FTO mRNA expression values in females from RA group (fed to 100% of energy requirements, raised without competition, n=9) compared to NA group (fed to 60% of energy requirements, raised without competition, n=8). Values are in mean  $\pm$  SEM; statistical differences are donated by \* =  $p < 0.05$  (unpaired t-test).



#### 4.4.3 The effects of postnatal accelerated growth on gene expression of inflammatory on subcutaneous adipose tissue

There were also no statistically significant differences in gene expression when groups were compared for gender (Table 5).

**Table 5:** mRNA gene expression values of inflammatory and metabolic markers on NS group (fed to 60% of energy requirements, n=8, raised with competition) compared to NA group (fed to 60% of energy requirements, n=9, raised without competition). Values are in mean  $\pm$  SEM; NS = no significant difference, S = significance ( $p < 0.05$ , unpaired t-test)

Group	NA (n=9)	NS (n=8)	p value	Gender
<b>Adiponectin</b>	0.0018 $\pm$ 0.0009	0.0032 $\pm$ 0.001	ns	S
<b>Leptin</b>	0.00077 $\pm$ 0.00031	0.00055 $\pm$ 0.00019	ns	ns
<b>IL-6</b>	0.0048 $\pm$ 0.00093	0.0063 $\pm$ 0.0048	ns	ns
<b>TNF-<math>\alpha</math></b>	1.2e-005 $\pm$ 3.0e-005	7.5e-006 $\pm$ 4.3e-005	ns	ns
<b>MCP-1</b>	3.7e-005 $\pm$ 2.3e-005	2.4e-005 $\pm$ 1.2e-005	ns	ns
<b>TLR-4</b>	0.00077 $\pm$ 0.00025	0.00035 $\pm$ 0.00023	ns	ns
<b>IL-18</b>	4.7e-005 $\pm$ 1.4e-005	2.1e-005 $\pm$ 6.2e-005	ns	ns
<b>GRP-78</b>	7.5e-005 $\pm$ 2.1e-005	2.4e-005 $\pm$ 5.5e-005	ns	ns
<b>FTO</b>	6.2e-005 $\pm$ 1.6e-005	7.5e-005 $\pm$ 2.1e-005	ns	ns

When analyzing the gene expression of TNF- $\alpha$ , FTO, GRP-78, no statistically significant differences were observed between groups or gender. Other inflammatory markers such as IL-18, IL-6 and macrophage recruiter such as MCP-1 and TLR-4 also did not exhibit any statically significant differences between groups or gender (Table 5).

The most striking result from the postnatal accelerated growth phase was for gene expression of the anti-inflammatory marker adiponectin that was found to be raised significantly in females but not males. The female group displayed a standard growth postnatal had a significantly increased gene expression (Fig 4.1.7).

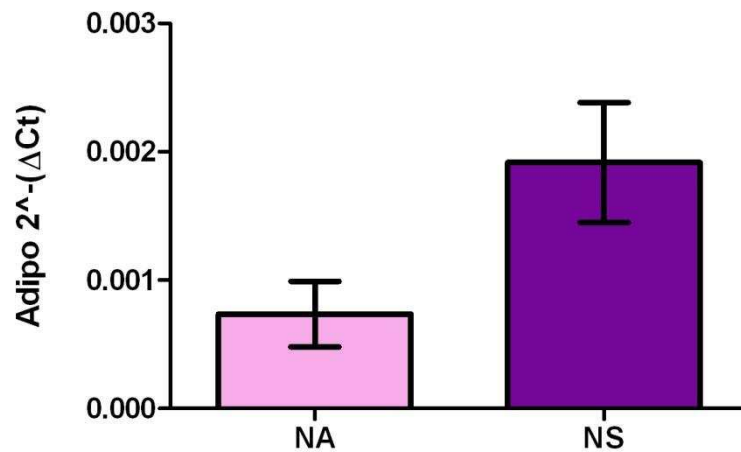


**Figure 30.1.7** - An up-regulation of adiponectin mRNA expression values in females from NS group (fed to 60% of energy requirements, raised with competition, n=9) compared to NA group (fed to 60% of energy requirements, raised without competition, n=8). Values are in mean  $\pm$  SEM; statistical differences are denoted by \* =  $p < 0.05$  (unpaired t-test).

#### **4.4.4 The effect of a maternal nutrient restricted environment during gestation followed by differing post-natal conditions on the development of adipose tissue**

Subcutaneous adipose tissue samples were taken from all three groups and histological analysis was performed as described in the methods chapter. For each group, a representative image is shown below.

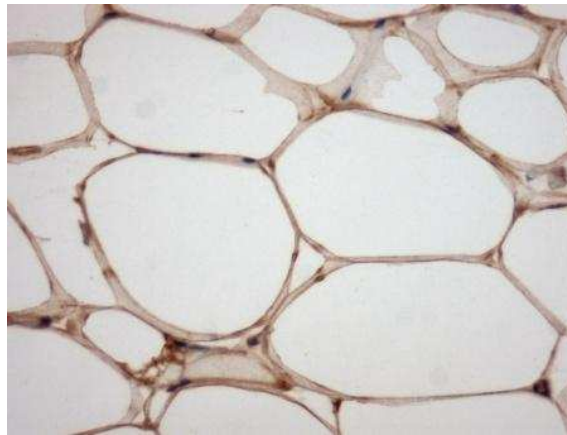


**Figure 31.1.8** – Representative of haematoxylin & eosin microscopic stained section of adipocytes from the RA group ((fed to 100% of energy requirements, raised without competition, n=9) at x40 magnification.

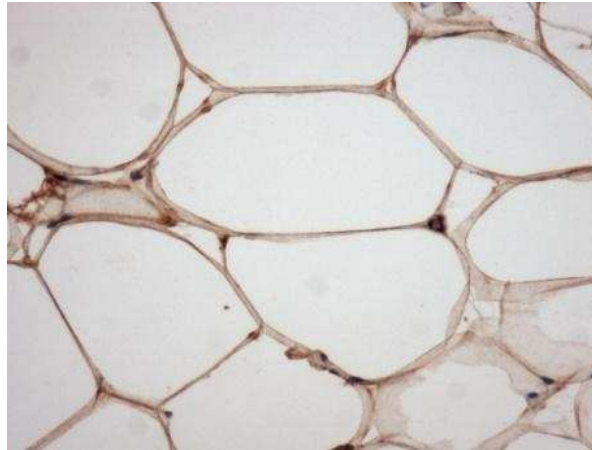


**Figure 32.1.9** – Representative of haematoxylin & eosin microscopic stained section of adipocytes from the NA group ((fed to 60% of energy requirements, raised without competition, n=8) at x40 magnification.

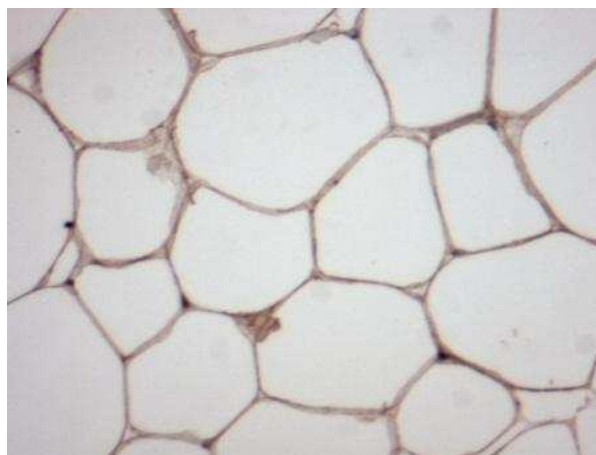


**Figure 33.2.0** – Representative of haematoxylin & eosin microscopic stained section of adipocytes from the NS group ((fed to 60% of energy requirements, raised with competition, n=8) at x40 magnification.

The adipose tissue was analyzed microscopically with cell size of each group calculated (adipocyte area  $\mu\text{m}^2$ ). There was no statistically difference between the groups or when separated between gender groups (Fig 4.1.7 – Fig 4.1.9).

When observing the tissue samples under the microscope using immunochemistry, there was no visible evidence of any infiltrated nucleated cellular structures or the possible development of crown-like structures present around the adipocytes. This removed the possibility of performing any quantification for the measurement of macrophage infiltration.

**Table 6:** Adipocyte area ( $\mu\text{m}^2$ ) of subcutaneous adipose tissue from NS group (fed to 60% of energy requirements, raised with competition, n=9), NA group (fed to 60% of energy requirements, raised without competition, n=8). RA group (fed to 100% of energy requirements, without competition, n=9). Values are in mean  $\pm$  SEM; NS = no significant difference (ANOVA).

Group	NA (n=9)	NS (n=8)	RA (n=9)	Gender
Cell Size (Area $\mu\text{m}^2$ )	142454 $\pm$ 27125	159329 $\pm$ 20673	151610 $\pm$ 24475	ns

#### **4.4.5 Discussion**

The rapid development of infants during the first year of life and continued infant life, although at lower rates, from the age of twelve months up to adolescence requires distinctive nutritional requirements. When comparing this nutrient requirement for growth to adults, infant requirement levels are much higher due to the increasing metabolic and nutrient turnover. This is because of the accompanying developmental changes in organ composition and function, therefore a failure to sustain or provide these nutrients during this crucial stage is likely to have adverse effects on development as well as growth. In conclusion, requirement of this nutritional demand, especially during early life, is therefore fundamental<sup>339</sup>.

#### **4.4.6 Nutrient restriction during late gestation and intra-uterine growth restriction**

The growth and development phase of the fetus is a specialized physiological process<sup>340</sup>. It is well known that maternal nutrition restriction during pregnancy reduces the rate of fetal growth, and is termed intrauterine growth restriction (IUGR)<sup>341</sup>. Studies have shown negative adaptations on the development of organs and tissues associated from low birth weight due to IUGR<sup>341, 342</sup>.

Recent experimental studies have been able to demonstrate the evidence of maternal nutrient restriction on the fetal cardiovascular system as well as possibly altering ovarian development in sheep<sup>343, 344, 345</sup>. These programmed alterations that are observed during maternal nutrient restriction may be the underlying

origin for metabolic diseases such as diabetes, hypertension, and cardiovascular disease in later adult life<sup>346</sup>.

Energy homeostasis of an individual is generated partly from the pre, post-natal and lactation stages of development<sup>347</sup>. From this aspect, it can be said that the last phase of gestation in both human and ovine models are significant in determining both birth weight and postnatal development.

The present study highlights a distinct nutritional scenario in young adult offspring life, where a 40% reduction in maternal nutrition uptake during late gestation (110 days to term), is preceded by an environment that challenges the potential for post-natal growth.

These changes are predicted to be damaging and increase the risk for damaging metabolic outcomes at the time of birth and throughout adult life, resulting in a predisposition for the onset of metabolic diseases.

#### **4.4.7 Changes in inflammatory gene expression**

IL-6 is a cytokine that spans a wide range of metabolic effects from inflammation to insulin resistance<sup>99</sup> with studies illustrating plasma levels positively correlating with obesity and insulin resistance<sup>62</sup>. It has been well established that approximately 25% of IL-6 secretion in the body is from adipose tissue<sup>99</sup>. Therefore during maternal nutrition restriction in late gestation, it would be more than likely that there would be detrimental effects on the development of adipose tissue, which could lead to the possible dysregulation of IL-6 secretion. However, in my study, IL-6 was not statistically different in groups experiencing such an environment during

gestation. Only when the groups are split by gender do you see an increase in the expression of IL-6 in females. More interestingly the group that was fed to requirement during gestation exhibited an increase in IL-6 expression, leading to the possible conclusion that nutrient restriction during late gestation may hinder the ability of adipose tissue to control secretion of IL-6 hence the increased levels.

The FTO gene is a recent addition to the appetite regulation and obesity associated cascade of genes. A common variant of the FTO gene was found to show strong relationships with the body mass index and prevalence from a young age<sup>159</sup>. FTO is expressed in a wide range of tissues and most importantly the hypothalamus, a region associated for its appetite regulation, where its expression is highly concentrated<sup>157</sup>.

My study was able to demonstrate the increased expression of the FTO gene within the group born to mothers fed to requirements, but was only observed in females. It is important to gain more information on this gene and its possible effects in the offspring following maternal nutrient restriction. As a recent European cohort study based on the original paper linking FTO to obesity, have shown the FTO gene to be linked with the predisposition of subjects to diabetes as a consequence of body mass<sup>348</sup>.

In conclusion, females born to mothers who were fed to requirements and then exhibited accelerated post-natal growth exhibited the greatest response in gene expression within their subcutaneous adipose tissue. This post-natal growth may therefore have a role in enhancing the gene expression of IL-6 and the FTO gene. The functional consequences remain to be elucidated. A possible



mechanism for the changes in gene expression being expressed only in females could be down to sex hormones. It could be suggested hormones such as oestrogen could play a role in this change compared to males. There are significant differences in fat distribution, adipose tissue and adipocyte function between women and men, which to a considerable extent, could result from gender differences in oestrogen receptor expression<sup>349</sup>. Oestrogen is a female hormone, which is produced largely by the ovaries, and during pregnancy, the placenta. Oestrogens are also produced by secondary sources such as the liver, breasts, adrenal glands, and fat cells in smaller amounts<sup>350</sup>. Studies have been able to highlight that adipose tissue and adipocyte oestrogen receptor alpha (ER $\alpha$ ) cooperate in preserving adipose tissue function and protecting against inflammatory damage<sup>351, 352</sup>. The studies also went on to suggest that ER $\alpha$  signalling is vital for the development of adipocyte hypertrophy and adipose tissue inflammation by concluding that higher expression of adipose tissue oestrogen receptors in females may be responsible for higher adipose tissue insulin sensitivity and lower susceptibility to inflammation compared to males<sup>349</sup>. By evaluating this current research and comparing the work carried out in this chapter, it could be suggested that the female hormone oestrogen may have played a role in the differences observed in IL-6, MCP-1, and adiponectin. However without work being carried out on protein expression, this remains only a possibility.

Whether oestrogen played a role in gender differences observed between IL-6, MCP-1, and adiponectin gene expression remains to be answered. However, it is an avenue of research that should be investigated to fully understand the mechanisms behind male and female differences in adipose tissue function.

#### **4.4.8 Accelerated post-natal growth and its effects on anti-inflammatory gene expression**

Early post-natal and intrauterine periods of growth have been recommended as possible windows for the increased risks of metabolic disease in later life<sup>176</sup>. Markers of nutrient restriction during pregnancy such as low birth and thinner size have been associated with such adverse outcomes as cardiovascular disease and metabolic syndrome in adults<sup>353, 354, 355, 356</sup>. Rapid weight gain during the postnatal phase has shown a relationship with greater risk for hypertension<sup>357</sup>, obesity<sup>188</sup>, cardiovascular disease<sup>358</sup> and insulin resistance<sup>193</sup>.

From the survey of literature above it can be seen that these two windows of early life growth are closely related because growth-restricted infants that underwent nutrient restriction during pregnancy usually offset this by displaying quick growth (catch up) in their first year of life after birth<sup>197</sup>. Studies have concluded that it is not low birth weight but more likely postnatal development that contributes more to the development towards metabolic disease in later adult life<sup>188, 183</sup>. Consequently, it has not yet been firmly established at which period during the postnatal window (early infancy or early childhood), that rapid weight gain is responsible for the development of long term metabolic risks. However, a recent Swedish cohort study investigated the longer term effects of weight gain during both early infancy and early childhood on fat mass at adolescent<sup>359</sup>. The study concluded that rapid weight gain during infancy was solely responsible for an increase in metabolic risk at 17 years of age. The study was able to show that this change was independent from a number of factors such gestational age, current height, rapid weight gain in childhood, birth weight and maternal fat mass along with

socioeconomic status<sup>197</sup>. These findings are also in unison with studies in murine studies<sup>360</sup> and infants born preterm<sup>361, 362, 362</sup> all concluding that rapid weight gain during early postnatal life could lead to increased risk in long term metabolic health outcomes<sup>363</sup>.

My study was able to show evidence that low birth weight following intra-uterine restriction can lead to a possible predisposition to accelerated postnatal growth. A key component towards explaining this response is the possible availability of food at the point of lactation. This difference is seen when the offspring are nurtured as a singleton which meant there was no overriding competition for milk from a sibling corresponding to the same age. The study was able to observe that prospective harmful metabolic outcomes were influenced by the time after birth in which growth was enhanced in growth restricted offspring. This time of rapid postnatal growth was also illustrative of that observed in human newborn who were small for gestational age<sup>364</sup>.

The evidence found in this study was also able to demonstrate that adiponectin had a higher gene expression in nutrient restricted females with a standard growth compared to those who underwent accelerated growth. Adiponectin is known for existing in low quantities in obese and overweight individuals, with protective properties against cardiovascular damage, inflammation and glucose intolerance<sup>110, 128, 365</sup>. My results suggests that if rapid weight gain (catch up growth) is not present, adiponectin expression is enhanced for these individuals leading to possible anti-inflammatory properties, irrespective of nutrient restriction in utero.

#### **4.4.9 Adipose tissue deposition and physiology**

The study did not show any statistically significant differences in other metabolic or inflammatory genes that were hypothesised. A possible explanation for the limited effect seen in gene expression during nutrient restriction in late gestation could be that subcutaneous adipose tissue is less metabolically active when compared to more visceral adipose tissue such as the main depot in the perirenal-abdominal region. A recent study was able to demonstrate a significant inflammation response in perirenal fat, a depot of visceral adipose tissue in response to nutrient restricted juvenile obesity<sup>210</sup>.

The ability to store lipids and convert them into energy in times of need for the body is seen as one of the main functions of adipocytes. When the detrimental metabolic effects of obesity take an accumulative effect on the body in the shape of intra-abdominal fat, it is reasoned that subcutaneous adipose tissue is no longer able to function correctly as the “energy sink”<sup>366</sup> for caloric excess resulting either surplus energy intake or decreased energy expenditure. This ultimately leads to a phenomenon called ectopic fat deposition<sup>366</sup>, whereby fat is accumulated at undesired locations such as the liver, muscle, heart etc. An increase in intra-abdominal fat mass should therefore be taken as warning to fat being accumulated at locations that could ultimately have harmful consequences such as increasing cardiovascular disease and diabetes. However, my study was not able to illustrate this theory as total fat mass in all groups were not significantly different between groups. Therefore, as there was no difference in total fat mass it was not possible to accept the hypothesis that subcutaneous adipose tissue dysfunction leads to ectopic fat deposition.

#### **4.5.0 Conclusion**

In conclusion, this study was able to demonstrate that subcutaneous adipose tissue gene expression after nutritional manipulation during late gestation exhibits only limited adaptations. However, statistically significant differences in gene expression were found in 3 different metabolic and inflammatory markers, IL-6, FTO, and adiponectin (female groups only). These were observed in subcutaneous adipose tissue even though total fat mass and final body weight showed no differences.

# Chapter 5 – Fructose fed mothers

---

## 5.1 Introduction and aims

Previous chapters have looked at the effect of maternal nutrition restriction during mid or late gestation on the offspring and the resulting development of inflammation and adaptations in metabolism and adipose tissue. The focus of the following chapters is to investigate the dietary impact of fructose feeding in mothers during pregnancy. From the introduction chapter, it was identified that obesity and weight gain are related to fructose intake during pregnancy and its possible role in the development of hyperglycemia and hyperinsulinemia in the mothers<sup>288</sup>. Most studies involving fructose intake in pregnancy are centred on a high-fructose diet, this study would investigate a low fructose intake of 10%, a diet close to complimentary daily human intake.

## 5.2 Hypothesis

The focus of this study was to investigate the effect of fructose consumption during pregnancy and its effect on fat mass and inflammatory markers. Despite the large amounts of evidence of potential adverse effects of fructose consumption, there have not been enough studies extensively looking into fructose consumption during pregnancy and its potential role with inflammatory markers. My hypothesis is a fructose intake during pregnancy will result in elevated inflammatory markers and increased fat mass compared to the control group.

### 5.3 Methods and materials

A fully detailed description of all the methods used in this chapter can be found in Chapter 2. The experimental set-up and model used to describe and illustrate the result in this chapter can be observed in Figure 5.1. All animal experimentations that were reported i.e. tissue weights, plasma measurements and animal dissections were performed and supervised by Dr. R.Bell and Abha Hoedl. For any sample or analytical exceptions are described in the results section of the relevant chapter. All statistical tests conducted in this chapter are detailed in Chapter 2, normalization of the mRNA gene expression results were calculated against one reference gene (r18s).

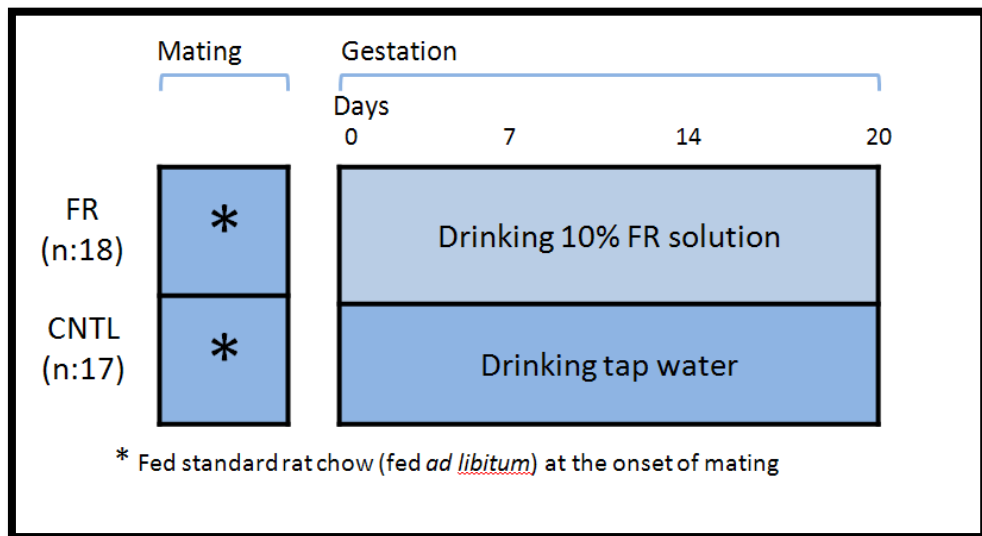


**Figure 34.1** - Rat Study: Fructose fed mothers model. FR group = Females fed 10% fructose water during pregnancy. CNTL group = females fed water. Both groups were fed chow (ad libitum) from the onset of mating.

## 5.4 Results

### 5.4.1 The effect of fructose feeding during pregnancy on body weight

At the start of the study body weights of female rats did not differ between diet groups. Both groups gained weight during pregnancy and there was no significant difference in final body weights between groups throughout gestation or at gestational day 20, the final day of the study. Adipose tissue mass (retroperitoneal) was significantly greater in the FR group compared to the Control group on gestational day 20 (See Table 7,  $p < 0.05$ )

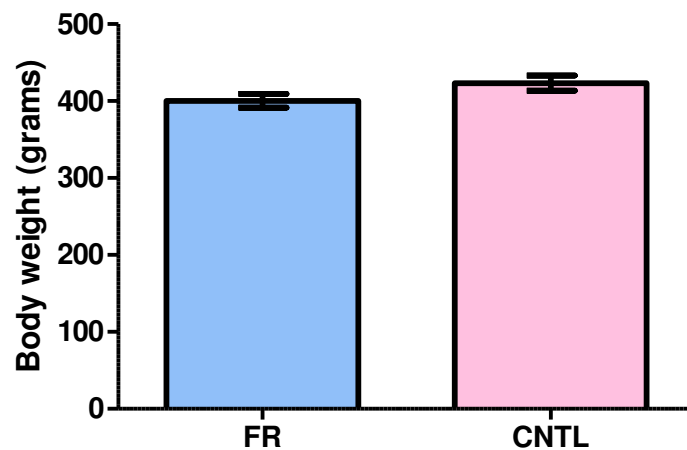


**Figure 35.2** - Graph of weight taken at gestation day 20. FR group (n=18) = Females fed 10% fructose water during pregnancy. CNTL group (n=17) = females fed water during pregnancy. Both groups were fed chow (ad libitum) from the onset of mating. Values are in mean  $\pm$  SEM; there were no statistical differences between the groups (Unpaired t-test).



### 5.4.2 Measurement of food and water intake during pregnancy

Overall, energy intake was significantly greater in the FR group compared to the Control group on the 2 days measured but did not differ significantly over time within each diet group.

**Table 7:** Measurements food and water intake along with body weight and adipose weight of the FR group (fed 10% fructose water, n=18) and CNTL group (fed water, n=17), values are in mean  $\pm$  SEM; statistical differences are denoted by \* =  $p < 0.05$  (unpaired t-test).

Characteristic	FR (n=18)	Control (n=17)
<b>Initial Body Weight (g)</b>	259.9 $\pm$ 6.7	259.5 $\pm$ 6.7
<b>End Body Weight (g)</b>	400.3 $\pm$ 8.10	423.2 $\pm$ 9.9
<b>Adipose Weight (g)</b>	4.95 $\pm$ 0.6*	3.20 $\pm$ 0.4
<b>Total Food Intake (g)</b>		
<b>7 Day Intake</b>	13.66 $\pm$ 1.2	24.62 $\pm$ 1.1*
<b>14 Day Intake</b>	19.28 $\pm$ 1.6	27.56 $\pm$ 1.5*
<b>Total 10% Fructose/Water Intake (ml)</b>		
<b>Gestation Day 7 Intake</b>	131.8 $\pm$ 14.3*	33.2 $\pm$ 3.5
<b>Gestation Day 14 Intake</b>	127.2 $\pm$ 11.8*	36.8 $\pm$ 3.8
<b>Total Kcal Intake</b>		
<b>Gestation Day 7 Intake</b>	97.8 $\pm$ 9.7	81.25 $\pm$ 3.6
<b>Gestation Day 14 Intake</b>	114.4 $\pm$ 10.0	91.0 $\pm$ 5.0

Total daily food intake was significantly lower on gestational days 7 and 14 in the FR group compared to the Control group (gestational day 7;  $p < 0.0005$ , gestational day 14;  $p < 0.0317$ ). Food intake increased as gestation progressed in the FR group (gestational day 14 vs. day 7;  $p < 0.031$ ); this however was not

observed in the Control group. Rats in the FR group consumed significantly more fluid on gestational days 7 and 14 (gestational day 7;  $p < 0.0001$ , gestational day 14;  $p < 0.0001$  respectively) compared with the Control group. Fluid intake was similar at each of these times within the diet groups. Overall, energy intake was not significantly greater in the FR group compared to the Control group on the 2 days measured but did not differ significantly over time within each diet group.

### 5.4.3 The effect of fructose intake during pregnancy on expression of metabolic markers

To determine the effect of fructose intake during pregnancy on gene expression of metabolic markers, mRNA gene expression analysis was performed on several key genes implicated in obesity regulated metabolic markers as previously discussed in the introduction chapter.

### 5.4.4 Gene expression of metabolic markers

Metabolic marker analysis showed a statistically significant up-regulation in leptin adipose tissue gene expression of fructose fed group compared to the control group ( $p < 0.05$ ). Figure 5.2.1

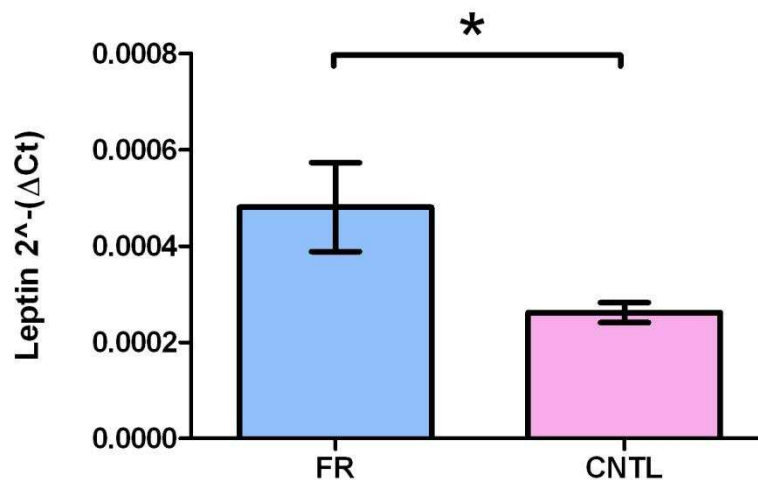


**Figure 36.2.1** - An up-regulation of leptin mRNA expression values of FR group ( $n=18$ ) = Females fed 10% fructose water during pregnancy compared to CNTL group ( $n=17$ ) = females fed water during pregnancy. Both groups were fed chow (ad libitum) from the onset of mating. Values are in mean  $\pm$  SEM; statistical differences are denoted by \* =  $p < 0.05$  (unpaired t-test).

FTO gene expression analysis showed the same significant trend where the fructose fed group showed a statistically significant up-regulation in comparison to the control group ( $p < 0.05$ ). Figure 5.2.2

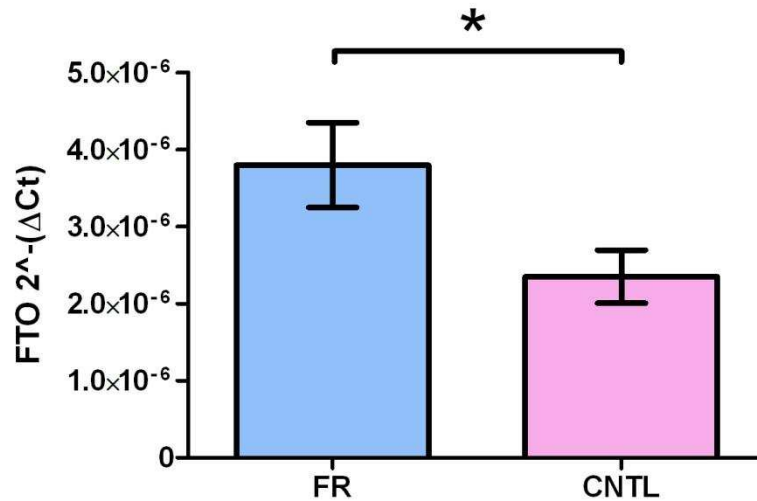


**Figure 37.2.2** - An up-regulation of FTO mRNA expression values of FR group (n=18) = Females fed 10% fructose water during pregnancy compared to CNTL group (n=17) = females fed water during pregnancy. Both groups were fed chow (ad libitum) from the onset of mating. Values are in mean ± SEM; statistical differences are denoted by \* =  $p < 0.05$  (unpaired t-test).

Adiponectin gene expression analysis showed the same significant trend where the fructose fed group showed a statistically significant up-regulation in comparison to the control group ( $p < 0.05$ ). Figure 5.2.3

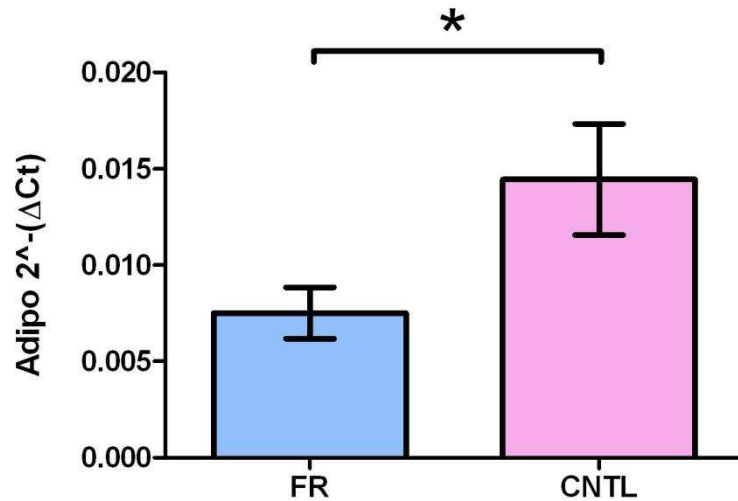


**Figure 38.2.3** - An up-regulation of adiponectin mRNA expression values of CNTL group ( $n=17$ ) = females fed water during pregnancy compared to FR group ( $n=18$ ) = Females fed 10% fructose water during pregnancy. Both groups were fed chow (ad libitum) from the onset of mating. Values are in mean  $\pm$  SEM; statistical differences are denoted by \* =  $p < 0.05$  (unpaired t-test).

#### 5.4.5 The effect of fructose intake during pregnancy on expression of pro-inflammatory markers

To determine the adipose inflammatory genotype, mRNA gene expression analysis was performed on several key genes implicated in obesity regulated inflammatory markers as previously discussed in the introduction chapter.

#### 5.4.6 Gene expression of inflammatory markers

Metabolic marker analysis showed a statistically significant up-regulation in NF- $\kappa$ B adipose tissue gene expression of fructose fed group compared to the control group ( $p < 0.05$ ). See Figure 5.2.4

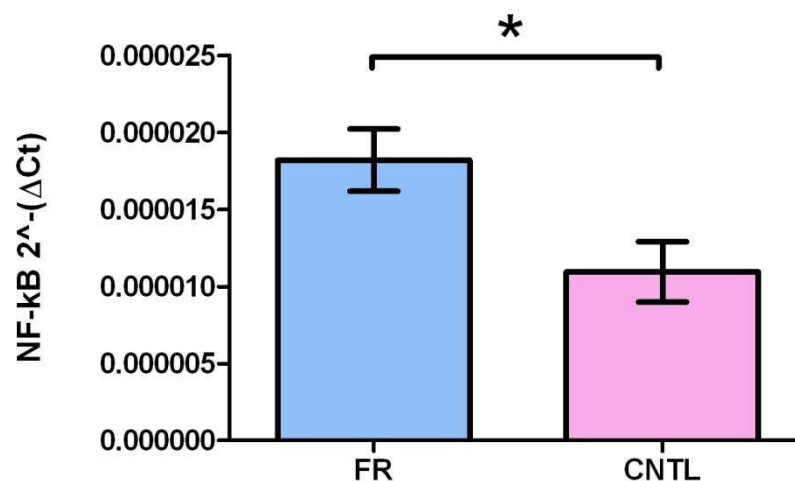


**Figure 39.2.4** - An up-regulation of Nf- $\kappa$ B mRNA expression values of FR group (n=18) = Females fed 10% fructose water during pregnancy compared to CNTL group (n=17) = females fed water during pregnancy. Both groups were fed chow (ad libitum) from the onset of mating. Values are in mean  $\pm$  SEM; statistical differences are denoted by \* =  $p < 0.05$  (unpaired t-test).

IL-18 gene expression analysis showed the same significant trend where the fructose fed group showed a statistically significant up-regulation in comparison to the control group ( $p < 0.05$ ), please see figure 5.2.5

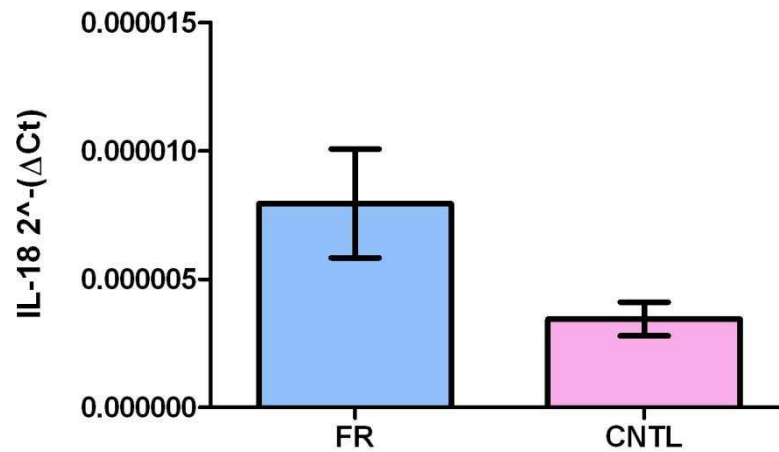


**Figure 40.2.5** - An up-regulation of IL-18 mRNA expression values of FR group (n=18) = Females fed 10% fructose water during pregnancy compared to CNTL group (n=17) = females fed water during pregnancy. Both groups were fed chow (ad libitum) from the onset of mating. Values are in mean ± SEM; statistical differences are denoted by \* =  $p < 0.05$  (unpaired t-test).

No additional statistical differences were observed in gene expression of MCP-1, IL-6 and GRP-78, see table 8

**Table 8:** mRNA gene expression values of inflammatory and metabolic markers on FR group (fed 10% fructose water, n=18) compared to CNTL group (fed water, n=17,. Values are in mean  $\pm$  SEM; NS = no significant difference between the groups (unpaired t-test).

<b>Group</b>	<b>FR (n=18)</b>	<b>CNTL (n=17)</b>	<b>p value</b>
<b>IL-6</b>	3.5e-006 $\pm$ 5.5e-007	2.3e-006 $\pm$ 3.4e-007	ns
<b>MCP-1</b>	2.7e-007 $\pm$ 2.0e-007	9.9e-007 $\pm$ 3.0e-007	ns
<b>GRP-78</b>	2.3e-006 $\pm$ 7.0e-007	4.4e-006 $\pm$ 1.0e-006	ns



### 5.4.7 Plasma triglyceride concentration

Triglyceride concentrations measured over 4 time periods during pregnancy displayed significant differences. The results identified a significant increase ( $p < 0.005$ ) of plasma triglyceride concentrations in the fructose group compared to the control group on days 19 and 20, following an smaller significant increase at day 12 ( $p < 0.05$ ) Figure 5.2.6

**Figure 5.2.6 Triglyceride concentrations measured during pregnancy**

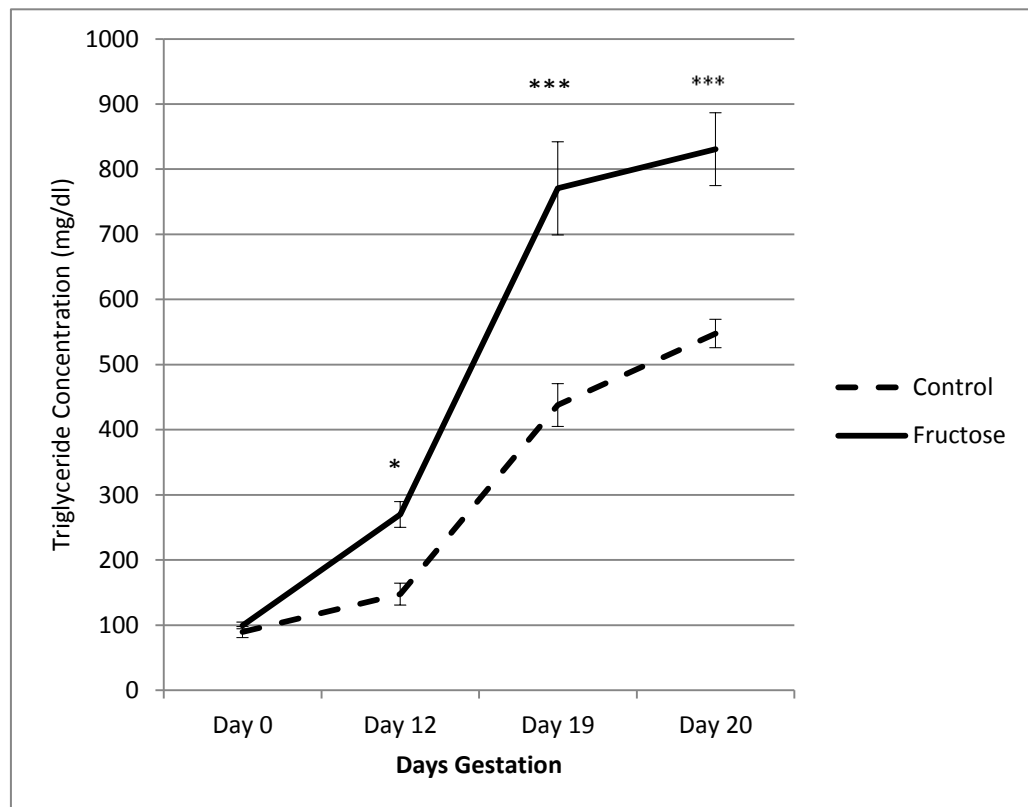


**Figure 41.2.6** – Representative of triglyceride concentrations measured during pregnancy for FR group (n=18) = Females fed 10% fructose water during pregnancy compared to CNTL group (n=17) = females fed water during pregnancy. Values are in mean  $\pm$  SEM; statistical differences are denoted by \* =  $p < 0.05$ ; \*\*\* =  $p < 0.01$  (Two way ANOVA with repeated measures)

## 5.5 Discussion

The main focus of our study was to investigate the effect of fructose intake during pregnancy and its effects on metabolite and inflammatory markers in the mother. Previous studies have consistently been able to show that fructose consumption in non-pregnant state results with increased fat mass and bodyweight changes along with an association to the development of metabolic syndrome. Our study was able to show that 10% fructose consumed during pregnancy produced a change in body composition with increased fat mass of the adipose depot (retroperitoneal) and significant changes in the mRNA expression of metabolic markers, inflammatory markers and triglyceride concentrations.

However, overall bodyweight was not different through pregnancy between groups but an increase in adiposity with fructose consumption was observed despite no difference in total daily energy intake observed either. This increase in adiposity is confirmed with the increased retroperitoneal fat mass within the fructose group during pregnancy. Results show that food and water intake during gestation can be a possible mechanism behind the increased fat mass. The fructose fed rats show a 4 fold increase in water intake during gestation with their food intake being compensated with a 2 fold decrease compared to the control group. This decrease in food intake by the fructose group may be largely down to the sweet and addictive taste that fructose provides over plain water, due to the large consumption of fructose the rats regulate their energy intake with a decreased amount of food intake. Fructose is a sugar that bypasses the normal regulatory enzymatic processes that glucose undergoes, therefore allowing fructose to contribute directly to increasing amounts of

triglycerides observed through pregnancy. The increased plasma triglyceride concentrations are features that are associated with hypertriglyceridemia. Studies described in the introduction relating to high-fructose intake during pregnancy leading to maternal hypertriglyceridemia<sup>286, 287</sup> also correlate with triglyceride results shown here. However, our study was able to show hypertriglyceridemia during late gestation which was not present in previous fructose intake studies, displaying instead hypotriglyceridemia in late gestation<sup>287</sup>. An explanation for hypertriglyceridemia could be the increased fructose intake which leads to an activation of de novo lipogenesis by increasing the amount of lipids present in blood often referred to as dyslipidemia. My study was able to show that during pregnancy, a low intake of fructose was able to demonstrate elevated triglyceride concentrations, similar to those found in studies investigating high fructose intake<sup>251, 254, 255</sup>.

### 5.5.1 Homeorhesis

During pregnancy the body switches from its normal control of metabolism, homeostasis, to homeorhesis<sup>367</sup>. This state allows for the body to accumulate weight gain or a long period of time without the normal response of metabolic stress. Homeorhesis is often referred to as “coordinated changes in metabolism of body tissues necessary to support a (dominant) physiological process”, these processes include lactation, a period where the mother is in requirement for her multiple organs to send nutrients to the mammary gland for milk synthesis<sup>367</sup>  
<sup>368</sup>.

During pregnancy the homeorhetic state allows for dramatic changes in metabolic and reproductive hormones such as leptin, estrogen, progesterone, cortisol, prolactin and placental lactogen<sup>369 370</sup>. These hormones play a vital role in simulating metabolic processes in the organs that regulate nutrient and energy supply to the fetus for development, furthermore these hormones also play a role in the initiation of lactation<sup>371 372</sup>.

During the onset of lactation, the female's body will co-ordinate various metabolic changes in multiple tissues via the endocrine system to allow for the increased requirement of nutritional intake whilst simultaneously balancing homeostasis in the animal<sup>373</sup>. These nutritional demands made during lactation are either supplemented through an increased dietary intake or drawn upon from stored nutrients in tissues<sup>374 375</sup>. During normal pregnancy there is an expected level of increased bodyweight weight with body composition therefore including an increase in body fat/adiposity<sup>376</sup>. With a supplemented

diet of fructose intake daily, this situation can lead to possible risk of obesity or excessive weight gain during pregnancy.

### **5.5.2 Pregnancy and inflammation**

Various studies in experimental animals have been able to demonstrate inflammation induced by fructose intake<sup>280, 281</sup>, in non-pregnant rodents. As previously stated in the introduction chapter, studies have been able to show that expression of MCP-1 in a range of cell types can be induced through intake of fructose<sup>283, 280</sup>. MCP-1 is seen as a key cytokine in the development of atherosclerosis and is involved in mediating an inflammatory response in symptoms related to metabolic syndrome. Studies investigating inflammatory markers in pregnancy have shown, MCP-1 was increased in pregnant women suffering from severe obesity<sup>377, 378</sup> and preeclampsia<sup>379</sup>.

A suggested mechanism behind raised inflammatory markers such as MCP-1 and IL-6 being stimulated during fructose intake can be accounted for through various factors such as the progression of dyslipidemia, insulin resistance, and excess uptake of fatty acids. The excess fat mass implicated from fructose intake causes an inhibitory effect by reducing adiponectin secretion in adipocytes and further increasing stimulation for the release of TNF- $\alpha$  and IL-6, thereby removing any inhibitory controls<sup>138</sup>. These circumstances can possibly lead to an elevated inflammatory response, specifically MCP-1, that as previously described, is known for stimulating and initiating the recruitment of other monocytes and macrophages to the stressed adipocytes<sup>285</sup>.

However, in my study MCP-1 was not up-regulated in gene expression neither were other inflammatory cytokines such as IL-6 and GRP78. A recent study

investigating inflammatory marker MCP-1 in pregnancy exhibited a reduced concentration in pregnancy under normal conditions giving a possible explanation that the reduction of MCP-1 may be a possible pathway to inhibit the characteristics from insulin resistance and homeostatic inflammation<sup>380</sup>. Limited research in this field makes validation for this theory complicated as only one report to date has been able to explain a peripheral decrease in serum concentration of MCP-1 during pregnancy<sup>381</sup>. The decrease in MCP-1 may be a possible adaptation known as homeorhesis which is described above, allowing a metabolic change in endocrine organs to prevent the activation of macrophages and monocytes in a pregnancy-induced insulin resistance. This, however, has only been represented in a study researching hypertensive rats, where the expression of MCP-1 was greatly increased in the kidney and decreased significantly soon after pregnancy, along with blood pressure<sup>382</sup>.

My study did, however, reveal increased expression of NF-kB, IL-18, FTO and leptin in the fructose fed group along with a decreased expression of adiponectin in the control group. Studies in non-pregnant rats have showed that fructose feeding leads to increased expression of classical inflammatory pathways such as NF-kB<sup>383</sup>. NF-kB is a protein whose activity is constant because it induces the expression of various genes which protect the cells from conditions that could cause cell apoptosis<sup>384</sup>. Studies have shown that during pregnancy NF-kB activity is raised and is essential to multiple pro-labour pathways<sup>384</sup>. Therefore increased fat mass during pregnancy would lead to an inflammatory response from NF-kB ultimately leading to increased expression of genes that prevent cell apoptosis. Studies involving IL-18 during pregnancy

have also highlighted increased serum concentrations during all periods of pregnancy and further increased during labour<sup>385</sup>.

Metabolic markers such as FTO and leptin showed that fructose intake during pregnancy lead to increased gene expression, both makers have been previously described as appetite regulators and FTO to be associated with body mass index and obesity. These markers show that not all pathways associated with the inflammation response are inhibited during pregnancy. Adiponectin expression levels decreasing during pregnancy do go to exhibit the effect of increased fat mass and circulating triglyceride concentrations on adipose tissue function, as the regular inhibitory pathway of TNF- $\alpha$  and IL-6 were not highly expressed in the fructose group<sup>138</sup>.

## 5.6 Conclusion

My study showed that fructose intake during pregnancy can lead to increased significant fat mass along with increased expression of metabolic markers related to appetite and body mass index, as well decreasing the expression of adiponectin. As hypothesised early that inflammatory markers would be elevated in expression and an increase in fat mass would be observed, it is observed that only a small inflammatory response was negated from this study. The possible reason being a homeorhesis reaction during pregnancy allows the mother to increase in size and therefore stop the normal potentially detrimental inflammatory pathways being activated.

A possible addition to the study to clarify the inflammatory response would be a third group that represented a non-pregnant fructose intake group; this would have been able to clarify fructose induced changes in comparison to pregnancy induced changes. A noteworthy explanation to the increased fat mass by fructose could be due to the increase in water content in tissue. As noted above in the results, fructose water intake was increased dramatically in FR groups.

A limitation that can be observed in this study was the single adipose depot studied; a further study may include the epididymal depot. Other factors to take into account are most conclusions in this study are drawn upon from evidence solely based on gene expression. Further research is required on the extent this has on protein expression, only then can a clear range of possible pathways be explained.

Whilst this study shows many inflammatory effects on the maternal adaptation of homeostasis during pregnancy along with a small inflammatory and



metabolic effect, it is crucial that more investigations are carried out to research into the possible harmful effects of low-fructose intake during pregnancy. As fructose intake increases in the western diet, it is vital to know the effects of this during pregnancy for the long term health of the mother.

# Chapter 6 – Effect of long-term fructose consumption

---

## 6.1 Introduction and aims

The final study in my thesis is based on fructose feeding during pregnancy and its long term effects on the offspring. The previous study investigated in chapter 5 examined the effect of fructose feeding during pregnancy on the mothers only. We observed changes in triglyceride concentrations, inflammatory markers and metabolic markers as well as homeorhesis pregnancy. However the previous study had limitations on its scope with fetal and offspring development not being further examined. Therefore this study will look at the metabolic effect on the offspring that occurs from early to later life following fructose intake in pregnancy. It has been well known that nutritional manipulation during various periods of pregnancy in animal and human models have shown increased risk of adverse effects on the offspring in later adult life<sup>170</sup>. This study is the first to explore the effects of fructose feeding during pregnancy and its long term effects on the offspring.

## 6.2 Hypothesis

My hypothesis is that fructose intake during pregnancy will lead to an increase inflammatory responses during early postnatal growth along with increased fat mass in the fructose fed group compared to the control. This will be evident in both adipose tissue depots with increased triglyceride concentrations and insulin levels calumniating from fructose feeding in pregnancy.

### 6.3 Methods and materials

A fully detailed description of all the methods used in this chapter can be found in Chapter 2. The experimental set-up and model used to describe and illustrate the result in this chapter can be observed in Figure 6.1. All animal experimentations that were reported i.e. tissue weights, plasma measurements and animal dissections were performed and supervised by Dr. R.Bell and Abha Hoedl and myself. For any sample or analytical exceptions are described in the results section of the relevant chapter. All statistical tests conducted in this chapter are detailed in Chapter 2, normalization of the mRNA gene expression results were calculated against one reference gene (r18s)

**Figure 6.1 Long term fructose consumption study model**

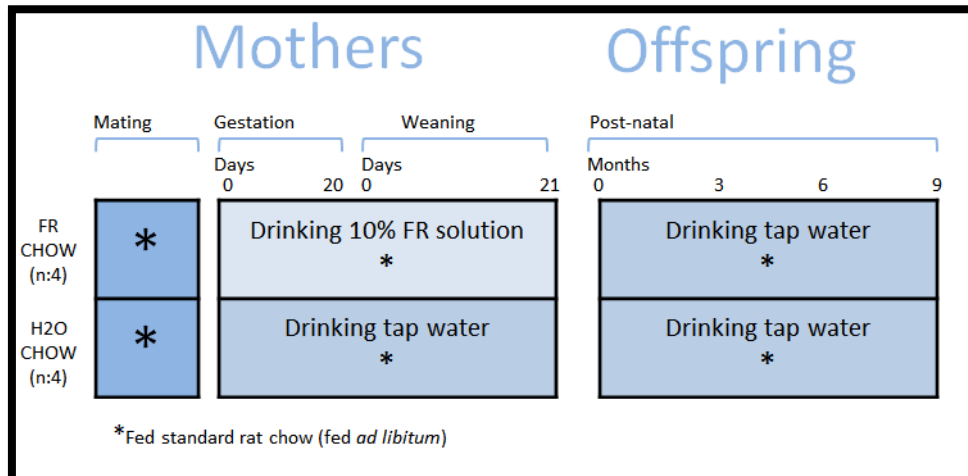


**Figure 42.1 - Rat Study: Effect of long term fructose consumption model.** FR CHOW group were fed 10% fructose water during gestation and weaning while H2O CHOW group were fed water during gestation and weaning. Offspring for both groups FR CHOW (n=21) and H2O CHOW (n=24) fed only water and chow during post-natal period.

## 6.4 Results

### 6.4.1 Long term body weight measurements and fat mass measure during fructose feeding in pregnancy in females

There were no observational differences in birth weight between the groups however 3 month body weight displayed statistical difference in weight gain from birth (p value =0.0163) . Results presented no other significant change in relation to fat mass apart from a significant increase of reproductive fat at 3 months in the fructose fed group (p value = 0.0036). See Table 9.

**Table 9:** Measurements of body weight and adipose weight of the FR CHOW group (fed 10% fructose water, n=18) and H2O CHOW group (fed water, n=17) were taken during the study, values are in mean  $\pm$  SEM; statistical differences are donated by \* = p<0.05 (unpaired t-test).

Characteristic	FR CHOW	H2O CHOW
<b>Weaning Weight (g)</b>	79.50 $\pm$ 3.2 (n=21)	75.30 $\pm$ 3.0 (n=24)
<b>3 Month Body Weight (g)</b>	274.9 $\pm$ 6.3* (n=21)	251.9 $\pm$ 6.6 (n=24)
<b>6 Month Body Weight (g)</b>	306.1 $\pm$ 9.2 (n=13)	304.7 $\pm$ 16.1 (n=15)
<b>9 Month Body Weight (g)</b>	337.5 $\pm$ 23.6 (n=6)	327.0 $\pm$ 40.9 (n=7)
<b>3 Month Retroperitoneal Fat (g)</b>	2.1 $\pm$ 0.2 (n=8)	2.5 $\pm$ 0.3 (n=9)
<b>6 Month Retroperitoneal Fat (g)</b>	6.2 $\pm$ 0.5 (n=7)	5.5 $\pm$ 0.3 (n=8)
<b>9 Month Retroperitoneal Fat (g)</b>	6.4 $\pm$ 1.0 (n=6)	3.8 $\pm$ 1.6 (n=7)
<b>3 Month Uterine Fat (g)</b>	5.0 $\pm$ 0.4* (n=8)	3.3 $\pm$ 0.3 (n=9)
<b>6 Month Uterine Fat (g)</b>	5.5 $\pm$ 0.1 (n=7)	6.0 $\pm$ 0.5 (n=8)
<b>9 Month Uterine Fat (g)</b>	7.8 $\pm$ 0.3 (n=6)	4.1 $\pm$ 1.6 (n=7)

#### 6.4.2 Long term body weight measurements and fat mass measure during fructose feeding in pregnancy in males

There were no observational differences in birth weight between the groups with 3 and 6 month body weight (3 month body weight p value = 0.0174, 6 month body weight p value = 0.0403) showing statistical difference in weight gain since birth. Results presented no other significant change in relation to fat mass apart from a significant increase of retroperitoneal fat at 3 and 6 months in the fructose fed group (3 month fat mass p value = 0.0174, 6 month fat mass p value = 0.0403).

**Table 10:** Measurements of body weight and adipose weight of the FR CHOW group (fed 10% fructose water, n=18) and H2O CHOW group (fed water, n=17) were taken during the study in males, values are in mean  $\pm$  SEM; statistical differences are denoted by \* = p<0.05 (unpaired t-test).

Characteristic	FR CHOW	H2O CHOW
<b>Weaning Weight (g)</b>	87.88 $\pm$ 4.1 (n=9)	81.96 $\pm$ 3.0 (n=12)
<b>3 Month Body Weight (g)</b>	506.7 $\pm$ 13.4* (n=9)	469.3 $\pm$ 7.4 (n=12)
<b>6 Month Body Weight (g)</b>	687.6 $\pm$ 17.8* (n=5)	631.9 $\pm$ 15.3 (n=8)
<b>9 Month Body Weight (g)</b>	752.5 $\pm$ 2.5 (n=2)	682.8 $\pm$ 26.0 (n=4)
<b>3 Month Retroperitoneal Fat (g)</b>	10.9 $\pm$ 1.5* (n=4)	6.3 $\pm$ 0.7 (n=4)
<b>6 Month Retroperitoneal Fat (g)</b>	15.1 $\pm$ 1.3* (n=3)	11.0 $\pm$ 0.9 (n=4)
<b>9 Month Retroperitoneal Fat (g)</b>	25.2 $\pm$ 5.5 (n=2)	16.9 $\pm$ 2.3 (n=4)
<b>3 Month Epididymal Fat (g)</b>	9.5 $\pm$ 1.9 (n=4)	6.9 $\pm$ 0.9 (n=4)
<b>6 Month Epididymal Fat (g)</b>	12.9 $\pm$ 1.2 (n=3)	9.9 $\pm$ 0.2 (n=4)
<b>9 Month Epididymal Fat (g)</b>	15.5 $\pm$ 1.9 (n=2)	12.4 $\pm$ 0.4 (n=4)

### 6.4.3 Measurement of food and water intake during pregnancy

Overall, energy intake was not significantly greater in the FR group compared to the Control group on the 2 days measured but did not differ significantly over time within each diet group.

#### Food and water intake during gestation for mothers

**Table 11:** Measurements food and water intake along with body weight and total Kcal intake of the FR group (fed 10% fructose water, n=18) and CNTL group (fed water, n=17) in mothers during pregnancy, values are in mean  $\pm$  SEM; statistical differences are denoted by \* =  $p < 0.05$  (unpaired t-test).

Characteristic	FR CHOW (n=4)	H2O CHOW (n=4)
<b>Total Food Intake (g)</b>		
Premating Intake	11.73 $\pm$ 1.9*	21.63 $\pm$ 0.8
7 Day Intake	12.17 $\pm$ 0.9*	24.33 $\pm$ 0.8
14 Day Intake	18.35 $\pm$ 1.7*	27.17 $\pm$ 1.2
<b>Total 10% Fructose/Water Intake (ml)</b>		
Premating Intake	118.8 $\pm$ 9.3*	37.50 $\pm$ 1.4
Gestation Day 7 Intake	160.0 $\pm$ 23.0*	55.00 $\pm$ 2.8
Gestation Day 14 Intake	141.7 $\pm$ 21.6*	55.00 $\pm$ 3.5
<b>Total Kcal Intake</b>		
Premating Intake	86.2 $\pm$ 8.2	77.86 $\pm$ 2.8
Gestation Day 7 Intake	102.0 $\pm$ 16.5	87.58 $\pm$ 2.8
Gestation Day 14 Intake	112 $\pm$ 14.3	97.81 $\pm$ 4.3

#### 6.4.4 The effect of fructose intake during pregnancy on expression of inflammatory markers on 3 month old offspring

To determine the adipose metabolite genotype, mRNA gene expression analysis was performed on several key genes implicated in obesity regulated metabolic markers as previously discussed in the introduction chapter.

#### 6.4.5 Gene expression of inflammatory markers on reproductive adipose tissue

No additional statistical differences were observed in gene expression of any inflammation markers in reproductive adipose tissue. Table 12.

**Table 12:** mRNA gene expression values of inflammatory and metabolic markers on FR CHOW (fed 10% fructose water, n=7) compared to H2O CHOW group (fed water, n=9) in reproductive adipose tissue at 3 months of age, Values are in mean  $\pm$  SEM; NS = no significant difference.

Group	FR CHOW (n=7)	H2O CHOW (n=9)	p value
<b>Adiponectin</b>	0.02 $\pm$ 0.01	0.03 $\pm$ 0.01	ns
<b>Chop</b>	1.2e-006 $\pm$ 3.7e-007	1.0e-006 $\pm$ 2.3e-007	ns
<b>FTO</b>	8.3e-006 $\pm$ 2.9e-006	8.3e-006 $\pm$ 2.8e-006	ns
<b>GRP78</b>	0.02 $\pm$ 0.01	0.03 $\pm$ 0.01	ns
<b>IL-6</b>	3.1e-008 $\pm$ 1.4e-008	2.4e-008 $\pm$ 1.3e-008	ns
<b>IL-18</b>	2.9e-006 $\pm$ 1.5e-006	1.6e-006 $\pm$ 7.2e-007	ns
<b>Leptin</b>	1.7e-004 $\pm$ 5.8e-005	1.9e-004 $\pm$ 9.0e-005	ns
<b>MCP-1</b>	1.1e-006 $\pm$ 4.1e-007	1.5e-006 $\pm$ 8.8e-007	ns
<b>TNF-<math>\alpha</math></b>	0.0002325 $\pm$ 6.5e-005	0.0001909 $\pm$ 2.9e-005	ns
<b>NF-kB</b>	9.5e-006 $\pm$ 3.1e-006	1.0e-005 $\pm$ 3.8e-006	ns

#### 6.4.6 Gene expression of inflammatory markers on retroperitoneal adipose tissue

No additional statistical differences were observed in gene expression of adiponectin; chop, GRP78, IL-6, IL-18, TNF- $\alpha$ .

**Table 13:** mRNA gene expression values of inflammatory and metabolic markers on FR CHOW (fed 10% fructose water, n=7) compared to H2O CHOW group (fed water, n=9) in retroperitoneal adipose tissue at 3 months of age, Values are in mean  $\pm$  SEM; NS = no significant difference. S = significance (p<0.05, unpaired t-test)

Group	FR CHOW (n=7)	H2O CHOW (n=9)	p value
<b>Adiponectin</b>	0.01664 $\pm$ 0.002	0.01026 $\pm$ 0.001	ns
<b>Chop</b>	4.3e-007 $\pm$ 8.1e-008	8.5e-007 $\pm$ 1.9e-007	ns
<b>FTO</b>	1.3e-004 $\pm$ 1.5e-005	8.2e-005 $\pm$ 9.2e-006	S
<b>GRP78</b>	0.0023 $\pm$ 0.0004394	0.0013 $\pm$ 0.0002975	ns
<b>IL-6</b>	1.4e-007 $\pm$ 1.3e-008	1.5e-007 $\pm$ 4.4e-008	ns
<b>IL-18</b>	8.4e-005 $\pm$ 1.3e-005	7.0e-005 $\pm$ 2.6e-005	ns
<b>Leptin</b>	0.0004 $\pm$ 5.2e-005	0.0002 $\pm$ 2.7e-005	S
<b>MCP-1</b>	1.2e-005 $\pm$ 1.1e-006	6.2e-006 $\pm$ 1.1e-006	S
<b>TNF-<math>\alpha</math></b>	1.5e-006 $\pm$ 2.7e-007	9.8e-007 $\pm$ 1.4e-007	ns
<b>NF-kB</b>	2.6e-005 $\pm$ 3.8e-006	1.4e-005 $\pm$ 8.3e-007	S



### 6.4.7 Gene expression of inflammatory markers on retroperitoneal adipose tissue

Metabolic and inflammatory marker analysis showed a statistically significant up-regulation in leptin, MCP-1, FTO, NF-Kb gene expression of fructose fed group compared to the control group ( $p < 0.05$ ) at 3 months of age.

**Figure 6.2 Up-regulation of Leptin, MCP-1, FTO, NF-Kb gene expression**

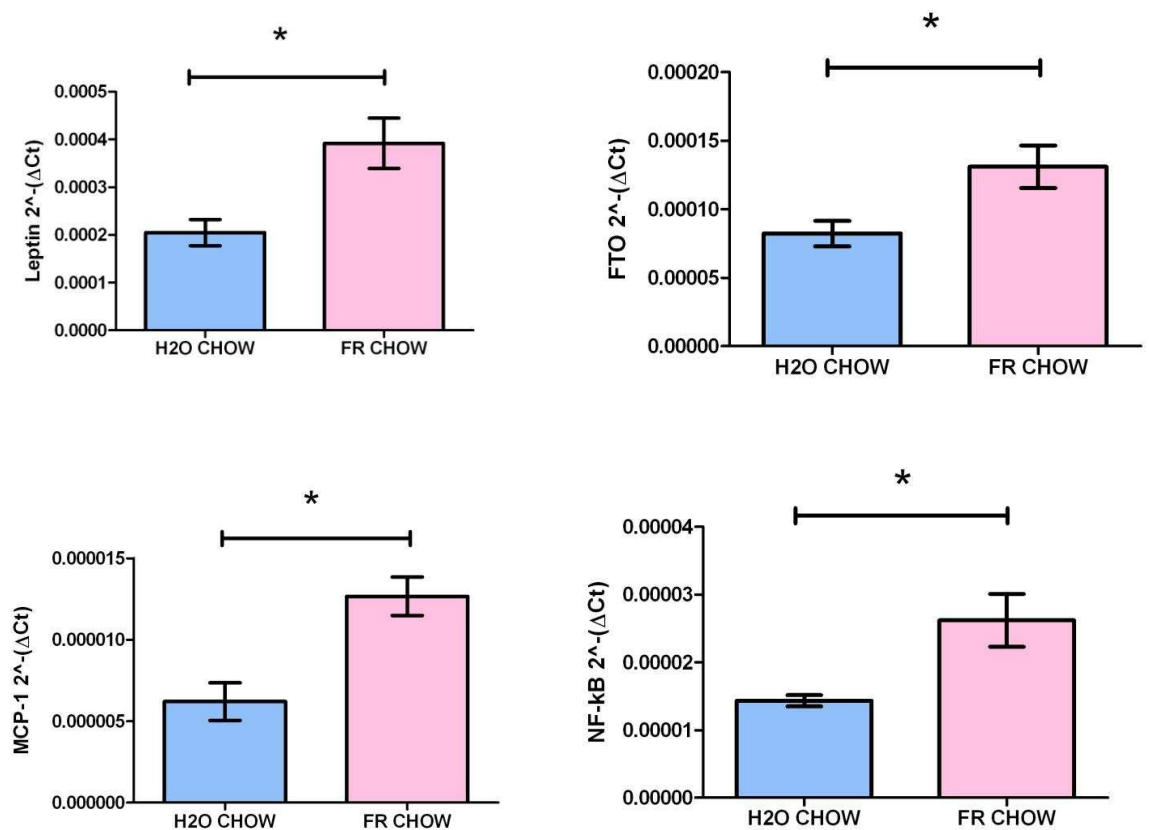


**Figure 43.2** - An up-regulation of Leptin, MCP-1, FTO, and NF-kB mRNA expression values of FR group offspring (n=8) compared to H2O group offspring (n=9) in retroperitoneal adipose tissue at 3 months of age. Values are in mean  $\pm$  SEM; statistical differences are denoted by \* =  $p < 0.05$  (unpaired t-test).

#### 6.4.8 The effect of fructose intake during pregnancy on expression of inflammatory markers on 6 month old offspring

To determine the adipose metabolite genotype, mRNA gene expression analysis was performed on several key genes implicated in obesity regulated metabolic markers as previously discussed.

##### Gene expression of inflammatory markers on reproductive adipose tissue

No additional statistical differences were observed in gene expression of adiponectin, chop, FTO, GRP78, IL-1B, IL-18, leptin, MCP-1, TNF- $\alpha$ , NF-kB and TLR-4. Table 6.6

**Table 14:** mRNA gene expression values of inflammatory and metabolic markers on FR CHOW (fed 10% fructose water, n=7) compared to H2O CHOW group (fed water, n=9) in reproductive adipose tissue at 6 months of age, Values are in mean  $\pm$  SEM; NS = no significant difference. S = significance (p=<0.05, unpaired t-test)

Group	FR CHOW (n=7)	H2O CHOW (n=8)	p value
<b>Adiponectin</b>	1.9e-006 $\pm$ 5.2e-007	1.6e-006 $\pm$ 3.1e-007	ns
<b>Chop</b>	1.4e-007 $\pm$ 4.9e-008	1.4e-007 $\pm$ 4.3e-008	ns
<b>FTO</b>	0.00014 $\pm$ 3.3e-005	0.00024 $\pm$ 7.3e-005	ns
<b>GRP78</b>	0.00026 $\pm$ 8.7e-005	0.00022 $\pm$ 8.8e-005	ns
<b>IL-1B</b>	4.8e-007 $\pm$ 1.7e-007	5.1e-007 $\pm$ 7.9e-008	ns
<b>IL-6</b>	6.5e-007 $\pm$ 1.1e-007	1.9e-007 $\pm$ 7.3e-008	S
<b>IL-18</b>	1.9e-006 $\pm$ 9.3e-007	3.7e-006 $\pm$ 1.2e-006	ns
<b>Leptin</b>	0.00021 $\pm$ 0.0001	0.00024 $\pm$ 6.8e-005	ns
<b>MCP-1</b>	4.2e-006 $\pm$ 1.7e-006	2.8e-006 $\pm$ 9.9e-007	ns

---

<b>TNF-<math>\alpha</math></b>	1.8e-006 $\pm$ 5.9e-007	4.5e-007 $\pm$ 1.4e-007	ns
<b>NF-Kb</b>	5.9e-006 $\pm$ 1.5e-006	7.6e-006 $\pm$ 2.5e-006	ns
<b>TLR4</b>	9.2e-006 $\pm$ 2.8e-006	1.9e-005 $\pm$ 5.9e-006	ns

---

#### 6.4.9 Gene expression of inflammatory markers on retroperitoneal adipose tissue

No additional statistical differences were observed in gene expression of FTO, GRP78, TNF- $\alpha$  and leptin. Table 15

**Table 15:** mRNA gene expression values of inflammatory and metabolic markers on FR CHOW (fed 10% fructose water, n=7) compared to H2O CHOW group (fed water, n=9) in retroperitoneal adipose tissue at 6 months of age, Values are in mean  $\pm$  SEM; NS = no significant difference. S = significance (p<0.05, unpaired t-test)

Group	FR CHOW (n=7)	H2O CHOW (n=8)	p value
<b>Adiponectin</b>	0.0074 $\pm$ 0.002	0.019 $\pm$ 0.004	S
<b>Chop</b>	3.3e-005 $\pm$ 7.4e-006	8.6e-006 $\pm$ 3.9e-006	S
<b>FTO</b>	8.5e-005 $\pm$ 1.5e-005	9.4e-005 $\pm$ 2.8e-005	ns
<b>GRP78</b>	8.5e-006 $\pm$ 3.0e-006	1.9e-006 $\pm$ 6.4e-007	ns
<b>IL-1B</b>	0.0028 $\pm$ 0.00083	0.00083 $\pm$ 0.00028	S
<b>IL-6</b>	8.5e-006 $\pm$ 1.3e-006	3.6e-006 $\pm$ 8.1e-007	S
<b>IL-18</b>	5.2e-005 $\pm$ 1.2e-005	1.9e-005 $\pm$ 5.5e-006	S
<b>Leptin</b>	0.00087 $\pm$ 0.00021	0.00047 $\pm$ 0.00016	ns
<b>MCP-1</b>	5.2e-005 $\pm$ 1.3e-005	1.6e-005 $\pm$ 6.2e-006	S
<b>TNF-<math>\alpha</math></b>	1.7e-005 $\pm$ 4.0e-006	9.5e-006 $\pm$ 3.3e-006	ns
<b>NF-Kb</b>	8.0e-005 $\pm$ 1.9e-005	2.8e-005 $\pm$ 5.7e-006	S
<b>TLR4</b>	0.00065 $\pm$ 0.00013	0.00023 $\pm$ 8.3e-005	S

#### **6.4.10 Gene expression of inflammatory markers on retroperitoneal adipose tissue**

Metabolic marker analysis showed a statistically significant up-regulation in adiponectin, CHOP, IL-1B, IL-18, IL-6, MCP-1, NF-kB and TLR4 gene expression of fructose fed group compared to the control group ( $p < 0.05$ ). See Figure 6.2.

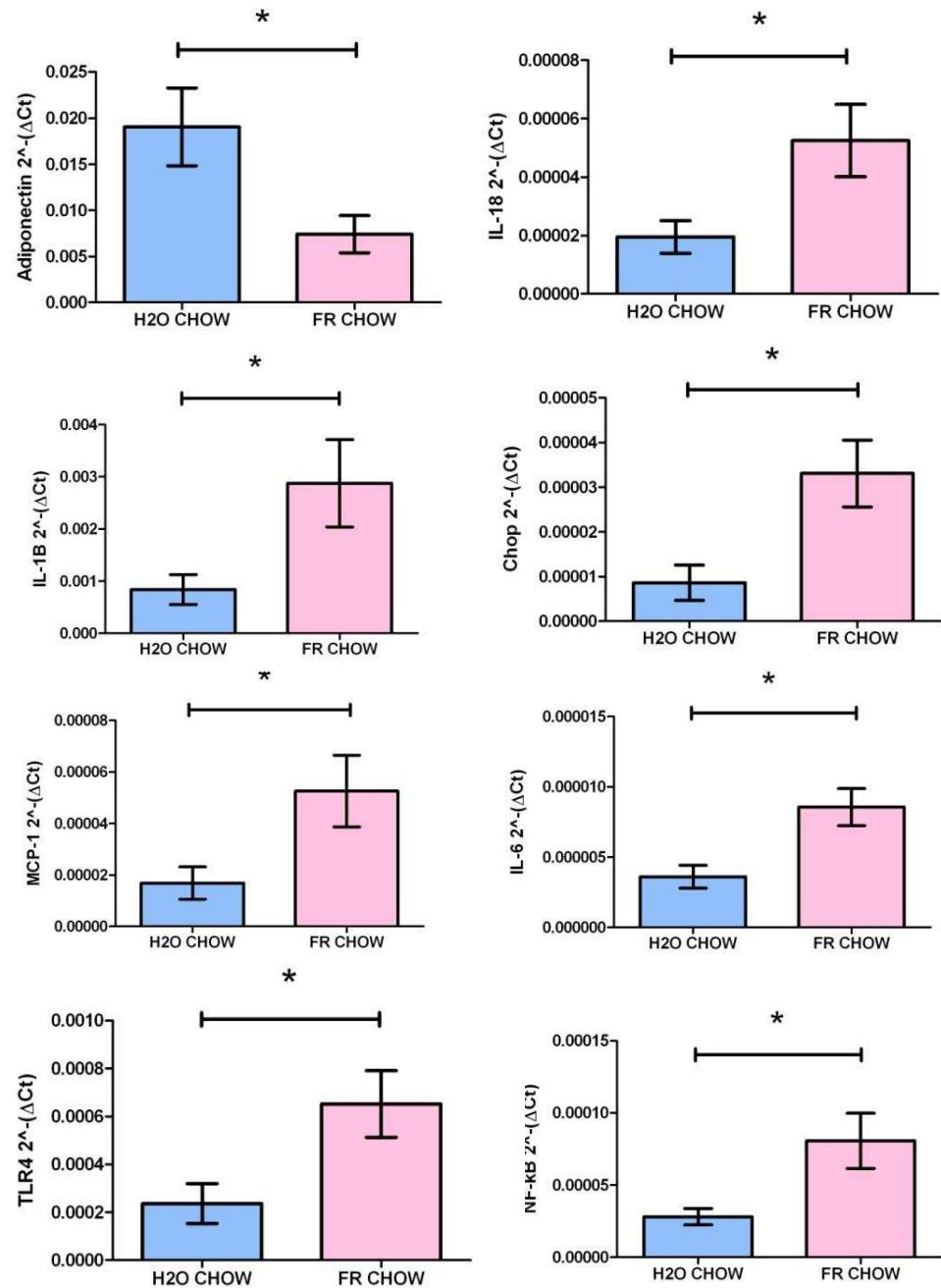


**Figure 44.2** - An up-regulation of CHOP, IL-1B, IL-18, IL-6, MCP-1, NF-kB and TLR4 mRNA expression values of FR group offspring (n=8) compared to H2O group offspring (n=9) in retroperitoneal adipose tissue at 6 months of age. Values are in mean  $\pm$  SEM; statistical differences are denoted by \* =  $p < 0.05$  (unpaired t-test).

#### 6.4.11 The effect of fructose intake during pregnancy on expression of inflammatory markers on 9 month old offspring

To determine the adipose metabolite genotype, mRNA gene expression analysis was performed on several key genes implicated in obesity regulated metabolic markers as previously discussed.

##### Gene expression of inflammatory markers on reproductive adipose tissue

No additional statistical differences were observed in gene expression of any inflammation markers in reproductive adipose tissue. Table 16.

**Table 16:** mRNA gene expression values of inflammatory and metabolic markers on FR CHOW (fed 10% fructose water, n=7) compared to H2O CHOW group (fed water, n=9) in reproductive adipose tissue at 9 months of age, Values are in mean  $\pm$  SEM; NS = no significant difference. S = significance (p<0.05, unpaired t-test)

Group	FR CHOW (n=6)	H2O CHOW (n=7)	p value
<b>Adiponectin</b>	0.001 $\pm$ 0.0002	0.002 $\pm$ 0.0003	ns
<b>Chop</b>	2.4e-008 $\pm$ 3.7e-009	3.4e-008 $\pm$ 6.9e-009	ns
<b>FTO</b>	2.1e-006 $\pm$ 3.7e-007	2.8e-006 $\pm$ 4.9e-007	ns
<b>GRP78</b>	3.4e-008 $\pm$ 2.5e-008	2.3e-008 $\pm$ 4.9e-009	ns
<b>IL-1B</b>	6.3e-005 $\pm$ 1.0e-005	5.7e-005 $\pm$ 1.6e-005	ns
<b>IL-6</b>	9.9e-008 $\pm$ 2.3e-008	1.4e-007 $\pm$ 4.7e-008	ns
<b>IL-18</b>	3.8e-006 $\pm$ 7.2e-007	3.4e-006 $\pm$ 6.8e-007	ns
<b>Leptin</b>	8.8e-006 $\pm$ 2.0e-006	1.5e-005 $\pm$ 3.7e-006	ns
<b>MCP-1</b>	3.7e-007 $\pm$ 1.0e-007	2.2e-007 $\pm$ 6.7e-008	ns
<b>TNF-<math>\alpha</math></b>	7.9e-008 $\pm$ 1.1e-008	9.7e-008 $\pm$ 2.1e-008	ns

<b>NF-Kb</b>	1.2e-006 ± 2.1e-007	1.9e-006 ± 2.8e-007	ns
<b>TLR4</b>	1.0e-007 ± 1.4e-008	1.6e-007 ± 2.8e-008	ns

#### 6.4.12 Gene expression of inflammatory markers on retroperitoneal adipose tissue

No additional statistical differences were observed in gene expression of adiponectin, CHOP, FTO, GRP78, IL-1B, IL-6, IL-18, leptin, MCP-1, TNF- $\alpha$ , NF-kB, TLR4.

**Table 17:** mRNA gene expression values of inflammatory and metabolic markers on FR CHOW (fed 10% fructose water, n=7) compared to H2O CHOW group (fed water, n=9) in retroperitoneal adipose tissue at 9 months of age, Values are in mean  $\pm$  SEM; NS = no significant difference. S = significance (p<0.05, unpaired t-test)

<b>Group</b>	<b>FR CHOW (n=6)</b>	<b>H2O CHOW (n=7)</b>	<b>p value</b>
<b>Adiponectin</b>	0.00089 ± 0.0001	0.00073 ± 0.0001	ns
<b>Chop</b>	1.0e-005 ± 2.4e-006	4.0e-006 ± 2.4e-006	ns
<b>FTO</b>	9.9e-006 ± 2.0e-006	7.1e-006 ± 1.1e-006	ns
<b>GRP78</b>	6.4e-006 ± 1.9e-006	6.5e-006 ± 5.5e-007	ns
<b>IL-1B</b>	0.00029 ± 9.6e-005	4.9e-005 ± 1.2e-005	ns
<b>IL-6</b>	3.3e-006 ± 1.0e-006	1.2e-006 ± 3.9e-007	ns
<b>IL-18</b>	1.8e-006 ± 7.0e-007	1.1e-006 ± 7.3e-007	ns
<b>Leptin</b>	2.3e-005 ± 5.7e-006	1.2e-005 ± 2.2e-006	ns
<b>MCP-1</b>	1.4e-005 ± 3.4e-006	2.7e-006 ± 4.2e-007	S
<b>TNF-<math>\alpha</math></b>	5.1e-006 ± 7.5e-007	1.1e-006 ± 2.3e-007	S



<b>NF-Kb</b>	2.0e-005 ± 4.1e-006	1.5e-005 ± 2.3e-006	ns
<b>TLR4</b>	1.5e-006 ± 3.8e-007	1.1e-006 ± 2.6e-007	ns

## 6.5 Electrochemiluminescence protein results on 3 months and 9 months offspring of gestational fructose feeding on retroperitoneal adipose tissue

MSD multiplex array plates were processed for the detection and quantification of cytokine concentration present in retroperitoneal adipose tissue. Plates were run for 3 months and 9 months, results for 6 months were omitted as due a technical error with the SECTOR instrument at the point of analysis.

### 6.5.1 3 Month Retroperitoneal MSD multiplex arrays

Inflammatory marker analysis showed a statistically significant up-regulation in IL-1B, protein expression of fructose fed group compared to the control group ( $p < 0.05$ ), see Figure 6.3.

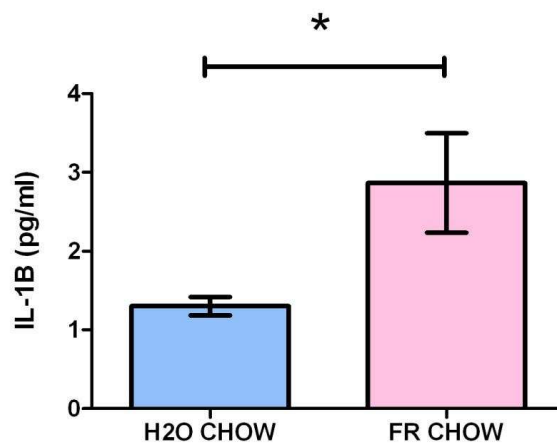


**Figure 45.3** - An up-regulation of IL-1B protein expression values of FR group offspring ( $n=8$ ) compared to H2O group offspring ( $n=9$ ) in retroperitoneal adipose tissue at 3 months of age. Values are in mean  $\pm$  SEM; statistical differences are denoted by \* =  $p < 0.05$  (unpaired t-test).

Inflammatory marker analysis showed no statistically significant up-regulation in IL-6, protein expression of fructose fed group compared to the control group.

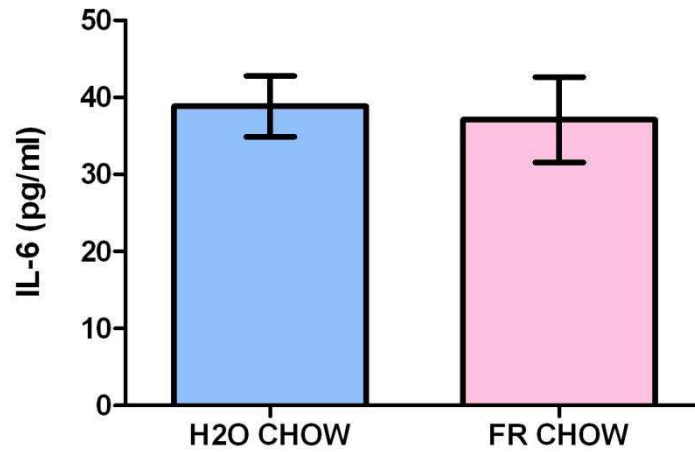


**Figure 46.4** - IL-6 protein expression values of FR group offspring (n=8) compared to H2O group offspring (n=9) in retroperitoneal adipose tissue at 3 months of age. Values are in mean  $\pm$  SEM; no statistical differences were observed (unpaired t-test).

Inflammatory marker analysis showed no statistically significant up-regulation in MCP-1, protein expression of fructose fed group compared to the control group.

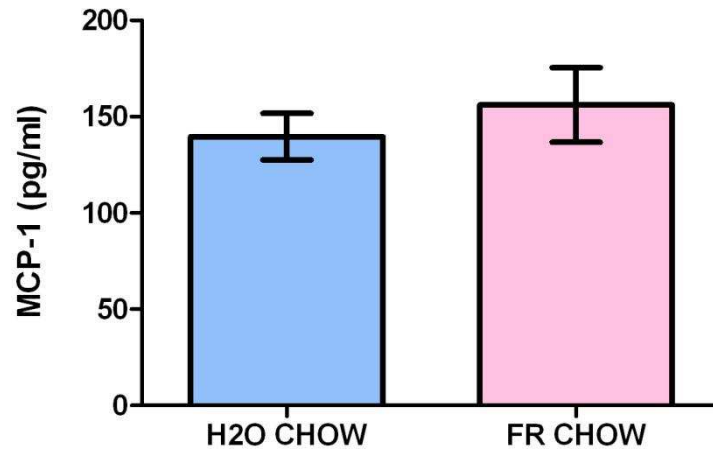


**Figure 47.5** – MCP-1 protein expression values of FR group offspring (n=8) compared to H2O group offspring (n=9) in retroperitoneal adipose tissue at 3 months of age. Values are in mean  $\pm$  SEM; no statistical differences were observed (unpaired t-test).

Inflammatory marker analysis showed no statistically significant up-regulation in TNF- $\alpha$ , protein expression of fructose fed group compared to the control group.

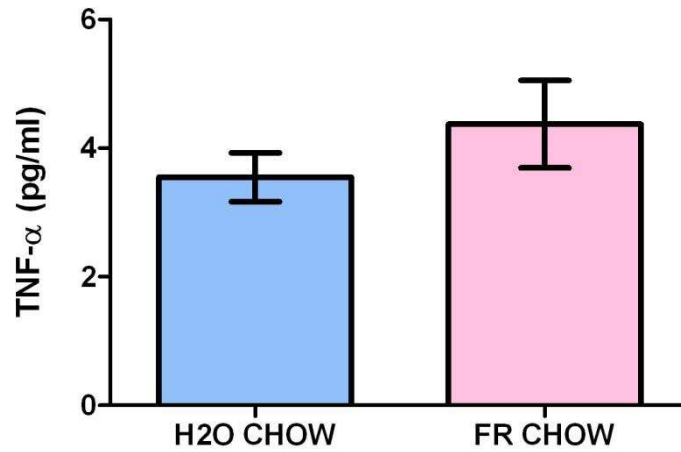


**Figure 48.6** – TNF- $\alpha$  protein expression values of FR group offspring (n=8) compared to H2O group offspring (n=9) in retroperitoneal adipose tissue at 3 months of age. Values are in mean  $\pm$  SEM; no statistical differences were observed (unpaired t-test).

### 6.5.2 9 Month Retroperitoneal MSD multiplex arrays

Inflammatory marker analysis showed a statistically significant up-regulation in IL-1B, protein expression of fructose fed group compared to the control group ( $p < 0.05$ ).

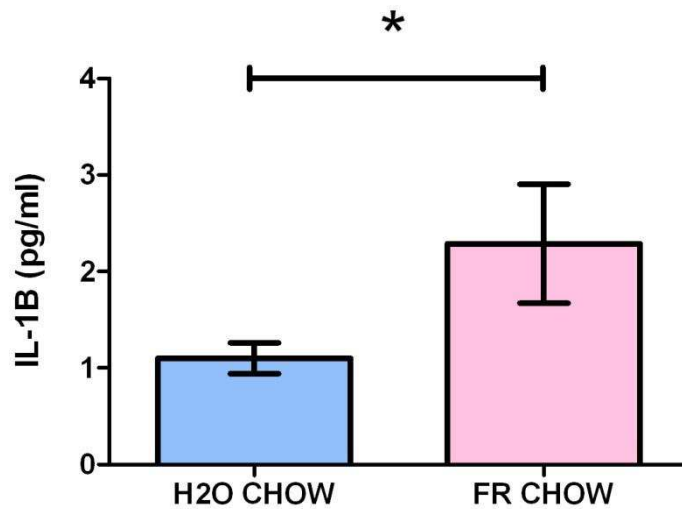


**Figure 49.7** – An up-regulation of IL-1B protein expression values of FR group offspring ( $n=6$ ) compared to H2O group offspring ( $n=7$ ) in retroperitoneal adipose tissue at 3 months of age. Values are in mean  $\pm$  SEM; statistical differences are denoted by \* =  $p < 0.05$  (unpaired t-test).

Inflammatory marker analysis showed a statistically significant up-regulation in IL-6, protein expression of fructose fed group compared to the control group ( $p < 0.05$ ).

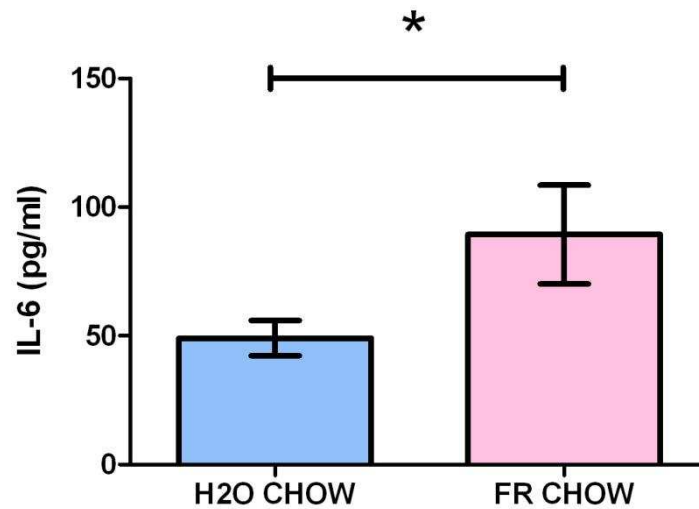


**Figure 50.8** – An up-regulation of IL-6 protein expression values of FR group offspring ( $n=6$ ) compared to H2O group offspring ( $n=7$ ) in retroperitoneal adipose tissue at 3 months of age. Values are in mean  $\pm$  SEM; statistical differences are denoted by \* =  $p < 0.05$  (unpaired t-test).

Inflammatory marker analysis showed a statistically significant up-regulation in MCP-1, protein expression of fructose fed group compared to the control group ( $p < 0.05$ ).

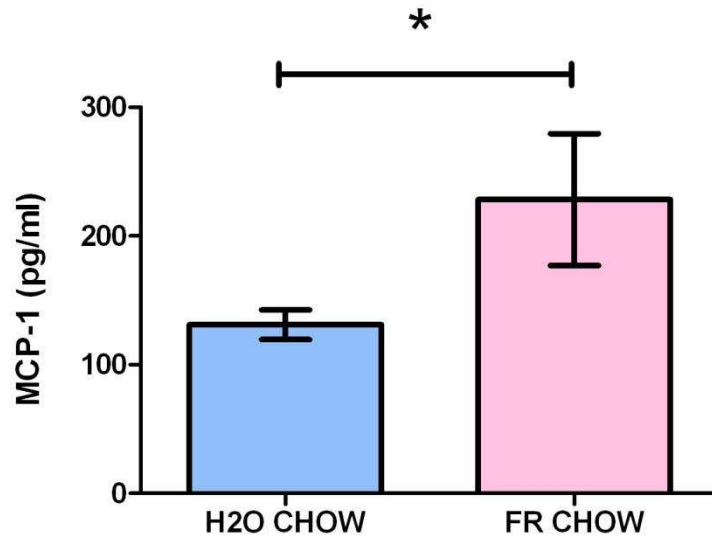


**Figure 51.9** – An up-regulation of MCP-1 protein expression values of FR group offspring ( $n=6$ ) compared to H2O group offspring ( $n=7$ ) in retroperitoneal adipose tissue at 3 months of age. Values are in mean  $\pm$  SEM; statistical differences are denoted by \* =  $p < 0.05$  (unpaired t-test).



Inflammatory marker analysis showed a statistically significant up-regulation in TNF- $\alpha$ , protein expression of fructose fed group compared to the control group ( $p < 0.05$ ).

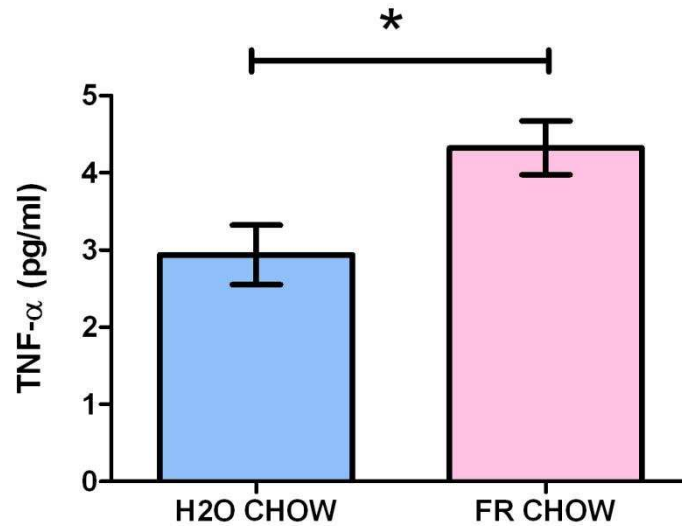


**Figure 52.10** – An up-regulation of TNF- $\alpha$  protein expression values of FR group offspring ( $n=6$ ) compared to H2O group offspring ( $n=7$ ) in retroperitoneal adipose tissue at 3 months of age. Values are in mean  $\pm$  SEM; statistical differences are denoted by \* =  $p < 0.05$  (unpaired t-test).

## 6.6 Triglyceride concentration, insulin plasma and glucose levels measured in gestational fructose fed offspring compared to the control group

We observed no statistical differences in the triglyceride, insulin or glucose levels of either group during the 9 months of this study.

**Table 18:** Measurements of triglyceride concentrations, insulin plasma, and glucose levels for the FR CHOW group (fed 10% fructose water) and H2O CHOW group (fed water) were taken during the study, values are in mean  $\pm$  SEM; NS = no significant difference. S = significance ( $p < 0.05$ , unpaired t-test).

Group	FR CHOW	H2O CHOW	p value
3 month insulin	0.56 $\pm$ 0.07 (n=21)	0.73 $\pm$ 0.08 (n=24)	ns
6 month insulin	0.66 $\pm$ 0.12 (n=13)	0.97 $\pm$ 0.25 (n=15)	ns
9 month insulin	2.0 $\pm$ 0.38 (n=6)	1.6 $\pm$ 0.21 (n=7)	ns
3 month glucose	167.9 $\pm$ 13.74 (n=21)	182.7 $\pm$ 12.56 (n=24)	ns
6 month glucose	155.8 $\pm$ 15.81 (n=13)	133.6 $\pm$ 10.99 (n=15)	ns
9 month glucose	191.9 $\pm$ 26.58 (n=6)	149.7 $\pm$ 13.02 (n=7)	ns
3 month triglycerides	106.1 $\pm$ 12.58 (n=21)	119.0 $\pm$ 13.16 (n=24)	ns
6 month triglycerides	91.97 $\pm$ 12.73 (n=13)	76.34 $\pm$ 10.16 (n=15)	ns
9 month triglycerides	102.4 $\pm$ 8.50 (n=6)	134.2 $\pm$ 13.31 (n=7)	ns

## 6.7 Discussion

The main focus of my study was to investigate the effect of fructose intake during pregnancy and its effects on the long term health of the offspring exposed to this nutrient manipulation during pregnancy.

From my previous chapter it was evident that raised fructose intake (10%) during pregnancy was able to show a change in body composition with increased fat mass of the adipose depot and significant changes in the mRNA expression of metabolic markers, inflammatory markers and triglyceride concentrations. Therefore it was crucial to investigate the longer term effects on the offspring and the metabolic adaptations they might occur later in life. Studies involving nutrient manipulation during pregnancy affecting the offspring in later life have already been conducted in humans and animals<sup>181, 157</sup>. However there has not been a study involving fructose feeding and its impact on offspring over a long period.

My study design was based on the set up as in chapter 5 but in this instance the offspring were allowed to be born and kept for periods of 3, 6 and 9 months. Rats reach puberty at 6 weeks of ages, at 6 months they have reached social maturity. equivalency to ~18 years of age in human years and at 9 months they are close to reaching 25 years in human terms<sup>386</sup>. This long term process allowed the study to investigate the offspring's full development from young infancy to full grown maturity<sup>386</sup>.

### **6.7.1 Body weight and fat mass measurements**

Body weight measurements recorded throughout the experiment were analysed separately as the huge weight differences became apparent once the rat offspring reached puberty, females grew to approximately maximum weight of ~300 grams with males reaching ~750 grams. My study showed that weaning weights were not statistically different between groups in both males and females. Body weights at 3 months showed a significant increase in the fructose fed group for both male and females. This pattern did not carry on for the females at 6 months, whereas the males still showed signs of increased body weight. Both groups showed no statistically difference at 9 months between fructose fed and control groups. This change in body weight could be a possible plateau reached in maximum growth for each gender. Females reached a plateau at around 300 grams which is first seen at 3 months in the fructose fed group, the control group reaches that threshold at 6 months, much later than the fructose fed group. The same was seen for males at 9 months. A possible explanation could be fructose feeding during pregnancy allows leads to increased weight gain during the postnatal growth period. This has previously been described in chapter 5 and documents a Swedish cohort study investigating the long effects of weight gain during both early infancy and early childhood on fat mass at adolescent<sup>359</sup>. The study concluded that rapid weight gain during infancy was solely responsible for an increase in metabolic risk at 17 years of age. The study was able to show that this change was independent from a number of factors such gestational age, current height, rapid weight gain in childhood, birth weight and maternal fat mass along with socioeconomic status<sup>197</sup>. These findings are also in unison with studies in

murine studies<sup>360</sup> and infants born preterm<sup>361, 362, 362</sup> all concluding that rapid weight gain during early postnatal life could lead to increased risk in long term metabolic health outcomes<sup>363</sup>.

When observing the weight measurements of adipose tissue depots in males, we can see a significant increase of retroperitoneal adipose tissue weight in the fructose fed group for 3 and 6 months age, once again coinciding with the same pattern of increase in body weight. No measureable difference was seen in epididymal adipose tissue. Females, however, only demonstrate an increase in uterine adipose tissue weight at 3 months in the fructose fed group. This also coincides with body weight increase, however no significant increase was observed with any retroperitoneal adipose tissue weight. A possible explanation for uterine fat increase could be the linked to the reproductive status of the female, as they fully developed and attained sexual maturity.

During measurements of food and fructose/water intake the study shows that pregnancy leads to increased quantities of fructose intake compared to water in correlation with decreased chow intake in the fructose group. However, overall energy intake was not statistically greater in the fructose fed group compared to controls, a similar result to that presented in chapter 5. The increased fructose intake could be a possible explanation to increased adiposity in 3 and 6 months of males and 3 months in females. Studies have shown that ad libitum consumption of fructose sweetened beverages was significantly increased in comparison to water and also affect food intake during this period for the control group<sup>387</sup>. However this increased consumption of fructose did not affect the body weight gain of rats, this was further supported by other studies reporting the same effect<sup>388</sup>.

It has been well established that children from mothers who are overweight, obese or have gestational diabetes mellitus have a higher chance of developing childhood metabolic syndrome features such as hypertension, glucose intolerance, insulin resistance and uncharacteristic lipid profiles<sup>389</sup>. As previously described, excess or high fructose diets have been associated with obesity and increased weight gain and with studies linking maternal obesity to the development of metabolic disease in offspring. It is therefore clinically significant to examine the effects of a high fructose-based diet during different gestational periods to investigate any changes in maternal and offspring metabolic phenotype.

An important finding from the study was the non-significant increase of triglyceride, insulin or glucose levels in the offspring from fructose fed mothers. Our previous study was able to show signs of hypertriglyceridemia in mothers, but none of these metabolic alterations have seemed to be present in the offspring of this study. However, there are only a limited number of studies in the current scientific domain that relate to maternal fructose intake. Studies using fructose solid diets of 78% and 50% during certain periods of pregnancy have demonstrated changes in offspring metabolism and also altered maternal hypertriglyceridemia<sup>286, 287</sup>.

The studies listed above used fructose solid diets of high concentrations; this is very unlikely to be seen even in a western diet, a more common strategy is using low fructose concentrations<sup>288</sup>. Our study as described in chapter 5 was able to show hypertriglyceridemia during the late gestation which was not present in previous fructose intake studies, displaying instead hypotriglyceridemia in late gestation<sup>287</sup>. Mainly studies involving fructose

intake combined with a high fat diet, which eliminates the contribution of fructose during this approach to the metabolic phenotype. Therefore fructose intake studies investigating long terms in offspring are not well known<sup>289</sup>. A possible explanation for the non-significant increase of triglyceride, insulin or glucose levels in the offspring could be due to the low fructose levels used (10% fructose used in study), studies using elevated levels of fructose as described above have shown significant changes.

### **6.7.2 Gene expression of inflammatory markers at 3, 6 and 9 months**

My study was able to demonstrate that reproductive adipose tissue was not different in any of the inflammatory markers that were tested between groups. However this is completely the opposite effect seen in retroperitoneal adipose tissue, metabolic and inflammatory marker analysis showed a statistically significant up-regulation in leptin, MCP-1, FTO, NF-Kb gene expression of fructose fed group compared to controls.

Furthermore at 6 month of age, metabolic and inflammatory marker analysis showed a statistically significant up-regulation in CHOP, IL-1B, IL-18, IL-6, MCP-1, NF-kB, TLR4 and decrease in adiponectin gene expression of fructose fed group in retroperitoneal adipose tissue. Only IL-6 was up-regulated in the reproductive adipose tissue, no other inflammatory or metabolic marker showed a significant increase.

A possible explanation for this increase in inflammatory response from the retroperitoneal adipose tissue and muted response from the reproductive fat is that retroperitoneal adipose tissue is a more metabolically active endocrine tissue. As previously described in chapter 4, subcutaneous adipose tissue is often seen as energy sink and when it undergoes metabolic dysregulation, it leads to increased cytokine production and greater fat mass accumulation in undesired locations. This could possibly be the case of retroperitoneal adipose tissue as its high specificity for raised expression of so many inflammatory genes could be a signal of dysregulation.

The cascade of inflammatory markers showing an increase in gene expression during 3 and 6 months could be a possible correlation to the increase in weight



gain seen male and females during that time period. As gene expression at 9 months in retroperitoneal adipose tissue is only raised for MCP-1 and TNF- $\alpha$  and reproductive adipose tissue is not significant in any inflammatory markers. Studies have shown that the expression of MCP-1 in various cell types is also induced through fructose intake<sup>283, 280</sup>.

This weight gain seen at 3 and 6 months from the fructose fed groups would go to demonstrate that not only does fructose cause long term health implications such as weight gain during early post natal growth but also elicit and underlying chronic inflammatory response in offspring of fructose fed mothers during pregnancy.

One highlighted cytokine was MCP-1 which was statistically significant in all three time periods of the study. Due to the weight gain over a long period, MCP-1 is activated to recruit more macrophages to infiltrate cells of stress and increases the chances of metabolic characteristics such as insulin resistance and metabolic syndrome. The increased fat mass from fructose intake leads to reduced adiponectin secretion in adipocytes and further stimulates the release of TNF- $\alpha$  and IL-6, due to the removal of any inhibitory controls<sup>138</sup>. These conditions lead to a possible elevated inflammatory response, in particular MCP-1 that as previously described, stimulates the recruitment of other monocytes and macrophages to the adipocyte of target<sup>285</sup>.

## **6.8 Protein expression of inflammatory markers at 3, and 9 months**

In addition to gene expression, I also conducted protein expression through the ECL method. I observed an increase in protein expression from the fructose fed group in 3 months and 9 months for proteins such as IL-1B at 3 months and IL-1B, MCP-1, TNF-  $\alpha$  and IL-6 protein expression at 9 months from the retroperitoneal adipose tissue. The raised abundance of these proteins expressed from the fructose fed group at 9 months was accompanied with enhanced MCP-1 and TNF- $\alpha$  gene expression. This gene-protein interaction gives more evidence to the theory that offspring from fructose fed mothers undergo chronic inflammation during early and later stages of life.

## **6.9 Conclusion**

My study was able to show that individuals whose mothers underwent fructose feeding during pregnancy are more than likely to develop chronic inflammation in retroperitoneal adipose tissue from early infancy to later adult life. The possible mechanisms for this process are still unknown and will require further investigative research.

As hypothesised earlier in the chapter, fructose intake during pregnancy will lead to an increase inflammatory response during early postnatal growth along with increased fat mass in the fructose fed group compared to the control. This will be evident in both adipose tissue depots with increased triglyceride concentrations and insulin levels calumniating from fructose feeding in pregnancy. However, this was not evident from all the findings and I concluded that only retroperitoneal adipose tissue was affected sufficiently to produce an inflammatory response to the fructose intake during pregnancy. Also triglyceride, insulin or glucose levels were not elevated in the fructose fed group. A possible explanation for this occurrence is that there was no activation of de novo lipogenesis pathway to inhibit triglyceride clearance.

# Chapter 7 – Conclusions

---

## **7.1 Conclusion**

### **7.1.1 General aims**

My study was structured to investigate the effects of maternal nutrient manipulation on adipose tissue induced inflammation and its contribution towards metabolic disease in later adult life. I achieved this by analysing and reviewing the metabolic homeostasis of male and female sheep exposed to nutrient restricted environment and varying postnatal conditions. I also studied the rat model and analysed and reviewed the effect of nutritional uptake during pregnancy and the possible implications on inflammatory processes on the adipose tissue. This chapter summary shows the key findings determined throughout the thesis.

### **7.1.2 Impact of gestational nutrient restriction on the sheep model**

From reviewing the literature it was suggested that for the development and growth of the offspring, the intrauterine environment plays a critical role. The frequency of adult disease increases in infants who have a suboptimal growth in utero<sup>181, 182</sup>. When looking at the effects of early life nutrition on growth and development, “programming” was defined as the lasting consequences of a stimulus or insult during a sensitive period in early life<sup>183</sup>. It is now well recognised that either throughout or at specific stages of pregnancy, changes in the macronutrient or micronutrient composition of the maternal diet can have significant effects on the fetus<sup>171</sup>. My study highlights distinct nutritional

scenarios in young adult offspring, a 40% reduction in maternal nutrition uptake during late gestation (110 days to term), proceeded by environments that challenge their potential for post-natal growth. These changes are predicted to be damaging and increasing the risk for detrimental metabolic results at the time of birth and throughout adult life, concluding in a predisposition for the onset of metabolic diseases. In conclusion, my study was able to demonstrate that subcutaneous adipose tissue gene expression after nutritional manipulation during late gestation suffers limited alterations. In contrast exposure to maternal nutrient restriction at the time of organogenesis resulted in raised markers of inflammation within pericardial adipose tissue despite a reduction in total fat mass.

### **7.1.3 Impact of gestational nutrient manipulation on the rat model**

The focus of first study was to investigate the effect of raised fructose consumption during pregnancy and its effect on fat mass and inflammatory markers. Despite the large amounts of evidence of increased fructose consumption, there have not been enough studies extensively looking into fructose consumption during pregnancy and its potential role with inflammatory markers. The second study was designed to examine the metabolic effects on the offspring that occurs from early to later life following fructose intake in pregnancy. It has been well known that nutritional manipulation during various periods of pregnancy in animal and human models have shown increased risk of adverse effects on the offspring in later adult life<sup>170</sup>. My study was able to show that individuals whose mothers

underwent fructose feeding during pregnancy are more than likely to develop chronic inflammation in retroperitoneal adipose tissue from early infancy to later adult life.

## **7.2 Study limitations**

### **7.2.1 Sheep model**

Using the sheep as a model for the nutrient restriction during pregnancy for translation research to humans does have some limitations. The sheep genome is still not fully encoded. This has a huge impact on the limitation of genes available and published for the analysis of mRNA expression in my study. An example at the time of the study was adiponectin receptor, a key receptor in the translation of adiponectin activity during weight gain/loss and inflammatory processes, yet many attempts to design primers based on limited genome code meant analysis was completed. The same limitations apply to NF-kB that is a key regulator of inflammatory pathways and transcribing their genes<sup>390</sup>.

### **7.2.2 Rat model**

The rat model has been widely used for experiments in a range of fields. Limitations for this model also rise in the form of short gestational period that is only 3 weeks compared to the sheep's 21 weeks (closer to humans), therefore selected periods of gestation are not readily available in the rat. Pups are born in large litters that can play a major role in lactation as there is more competition for milk and growth. Rat models are also distinctly different in maturity compared to sheep; they are fully sexually mature at 6 weeks. Tissue size is incredibly small compared to sheep, requiring no margin for error or even repeated experiments with the same tissue to verify results. Advantages such as handling size and cost efficiency per rat compared to sheep is affordable along full genome encoding allows for correct primer design.

### **7.3 Future work and perspectives**

In order to validate the findings of the studies conducted, it would be essential to complete further investigations into the rat model for a clearer understanding into fructose and inflammation during pregnancy. Suggestions are discussed below.

#### **7.3.1 Non-pregnant group**

During the study in chapter 5 and 6, it would have been useful to have a non-pregnant group undergoing fructose intake for the same length of time. This could provide a clearer picture to the effects of fructose feeding during pregnancy. It would determine if the inflammatory response seen in chapter 5 is really down to fructose or homeorhesis in pregnancy.

#### **7.3.2 Other adipose depots**

A possible analysis of other fat depots if possible might help explain the reason why reproductive fat was inhibited in response to increased weight gain and subsequent inflammatory response in chapter 6.

#### **7.3.3 Further protein work**

The cost of MSD protein plates did restrict the amount of protein work I could carry out in the limited time I had in Canada. A full range of metabolic and protein array multiplex plates would help further understand the inflammatory



process caused by fructose intake in pregnancy. Other methods for protein expression such as western blotting in addition to MSD protein plates could have been a beneficial advantage to this experiment and added more weight to the evidence provided.

#### **7.3.4 Final Remarks**

##### **Final Remarks**

This study highlighted that nutrient manipulation during different stages of gestation followed by obesity or postnatal activity contributes to the alterations of adipose tissue function and physiology in relation to inflammatory gene and protein responses. The research conducted in this study could play a role in help understanding the mechanisms and pathways that are involved in the inflammatory response during such situations.

# References

---

1. WHO. Obesity and overweight. Fact sheet N°311 ed: World Health Organization, 2006.
2. Judith Mackay GAM, Shanthi Mendis, Kurt Greenlund. The Atlas of Heart Disease and Stroke: World Health Organization, 2004.
3. Quetelet A. Antropométrie ou Mesure des Différences Facultés de l'Homme. Brussels, 1871.
4. WHO. Obesity: preventing and managing the global epidemic. Technical report series 894 ed: World Health Organization, 2000.
5. National Heart L, and Blood Institute. Clinical Guidelines on the Identification, Evaluation, and Treatment of Overweight and Obesity in Adults: International Medical Publishing, Inc., 1998.
6. TaskForce IO. Global Obesity Map. London: IOTF, 2007.
7. Prevention CfDCa. U.S. Obesity Trends 1985–2007, 2007.
8. Prevention CfDCa. About BMI for Children and Teens, 2008.
9. Prevention CfDCa. Childhood Overweight, 2007.
10. Health Do. Obesity General Information, 2008.
11. Miranda PJ, DeFronzo RA, Califf RM, Guyton JR. Metabolic syndrome: definition, pathophysiology, and mechanisms. *Am Heart J* 2005;149(1):33-45.
12. Southampton Uo. Metabolic Syndrome.
13. WHO. World Health Organisation. Definition, diagnosis and classification of diabetes. Geneva: World Health Organisation., 1999.
14. Ferrannini E, Natali A, Capaldo B, Lehtovirta M, Jacob S, Yki-Jarvinen H. Insulin resistance, hyperinsulinemia, and blood pressure: role of age and obesity. *European Group for the Study of Insulin Resistance (EGIR). Hypertension* 1997;30(5):1144-9.
15. Bays H, Mandarino L, DeFronzo RA. Role of the adipocyte, free fatty acids, and ectopic fat in pathogenesis of type 2 diabetes mellitus: peroxisomal proliferator-activated receptor agonists provide a rational therapeutic approach. *J Clin Endocrinol Metab* 2004;89(2):463-78.
16. Fruhbeck G, Gomez-Ambrosi J, Muruzabal FJ, Burrell MA. The adipocyte: a model for integration of endocrine and metabolic signaling in energy metabolism regulation. *Am J Physiol Endocrinol Metab* 2001;280(6):E827-47.
17. Ailhaud G, Grimaldi P, Negrel R. Cellular and molecular aspects of adipose tissue development. *Annu Rev Nutr* 1992;12:207-33.
18. Ailhaud G, Grimaldi P, Negrel R. A molecular view of adipose tissue. *Int J Obes Relat Metab Disord* 1992;16 Suppl 2:S17-21.
19. Himms-Hagen J. Brown adipose tissue thermogenesis: interdisciplinary studies. *FASEB journal : official publication of the Federation of American Societies for Experimental Biology* 1990;4(11):2890-8.
20. Cannon B, Nedergaard J. Brown adipose tissue thermogenesis in neonatal and cold-adapted animals. *Biochemical Society transactions* 1986;14(2):233-6.
21. Stock MJ, Rothwell NJ. Brown adipose tissue and the response to overfeeding. *Biochemical Society transactions* 1986;14(2):239-40.

22. Ricquier D, Bouillaud F. Mitochondrial uncoupling proteins: from mitochondria to the regulation of energy balance. *The Journal of physiology* 2000;529 Pt 1:3-10.
23. Cinti S. The role of brown adipose tissue in human obesity. *Nutr Metab Cardiovasc Dis* 2006;16(8):569-74.
24. Lab TA. Institute for Diabetes, Obesity and Metabolism.
25. Mitchell P. Coupling of phosphorylation to electron and hydrogen transfer by a chemi-osmotic type of mechanism. *Nature* 1961;191:144-8.
26. Jagendorf AT. Photophosphorylation and the chemiosmotic perspective. *Photosynth Res* 2002;73(1-3):233-41.
27. Morrison SF. Central pathways controlling brown adipose tissue thermogenesis. *News Physiol Sci* 2004;19:67-74.
28. Bouillaud F, Couplan E, Pecqueur C, Ricquier D. Homologues of the uncoupling protein from brown adipose tissue (UCP1): UCP2, UCP3, BMCP1 and UCP4. *Biochim Biophys Acta* 2001;1504(1):107-19.
29. Monemdjou S, Kozak LP, Harper ME. Mitochondrial proton leak in brown adipose tissue mitochondria of Ucp1-deficient mice is GDP insensitive. *Am J Physiol* 1999;276(6 Pt 1):E1073-82.
30. Argyropoulos G, Harper ME. Uncoupling proteins and thermoregulation. *J Appl Physiol* 2002;92(5):2187-98.
31. Kershaw EE, Flier JS. Adipose tissue as an endocrine organ. *J Clin Endocrinol Metab* 2004;89(6):2548-56.
32. Cousin B, Caspar-Bauguil S, Planat-Benard V, Laharrague P, Penicaud L, Casteilla L. [Adipose tissue: a subtle and complex cell system]. *J Soc Biol* 2006;200(1):51-7.
33. Bjorndal B, Burri L, Staalesen V, Skorve J, Berge RK. Different adipose depots: their role in the development of metabolic syndrome and mitochondrial response to hypolipidemic agents. *J Obes* 2011;2011:490650.
34. Zhang Y, Proenca R, Maffei M, Barone M, Leopold L, Friedman JM. Positional cloning of the mouse obese gene and its human homologue. *Nature* 1994;372(6505):425-32.
35. Wajchenberg BL. Subcutaneous and visceral adipose tissue: their relation to the metabolic syndrome. *Endocrine reviews* 2000;21(6):697-738.
36. Casteilla L, Penicaud L, Cousin B, Calise D. Choosing an adipose tissue depot for sampling: factors in selection and depot specificity. *Methods Mol Biol* 2008;456:23-38.
37. Chowdhury B, Sjostrom L, Alpsten M, Kostanty J, Kvist H, Lofgren R. A multicompartiment body composition technique based on computerized tomography. *International journal of obesity and related metabolic disorders : journal of the International Association for the Study of Obesity* 1994;18(4):219-34.
38. Hoffstedt J, Arner P, Hellers G, Lonnqvist F. Variation in adrenergic regulation of lipolysis between omental and subcutaneous adipocytes from obese and non-obese men. *Journal of lipid research* 1997;38(4):795-804.
39. Hajer GR, van Haefen TW, Visseren FL. Adipose tissue dysfunction in obesity, diabetes, and vascular diseases. *Eur Heart J* 2008;29(24):2959-71.

40. Yang YK, Chen M, Clements RH, Abrams GA, Aprahamian CJ, Harmon CM. Human mesenteric adipose tissue plays unique role versus subcutaneous and omental fat in obesity related diabetes. *Cell Physiol Biochem* 2008;22(5-6):531-8.
41. Deveaud C, Beauvoit B, Salin B, Schaeffer J, Rigoulet M. Regional differences in oxidative capacity of rat white adipose tissue are linked to the mitochondrial content of mature adipocytes. *Mol Cell Biochem* 2004;267(1-2):157-66.
42. Kraunsoe R, Boushel R, Hansen CN, Schjerling P, Qvortrup K, Stockel M, et al. Mitochondrial respiration in subcutaneous and visceral adipose tissue from patients with morbid obesity. *The Journal of physiology* 2010;588(Pt 12):2023-32.
43. Sramkova D, Krejbichova S, Vcelak J, Vankova M, Samalikova P, Hill M, et al. The UCP1 gene polymorphism A-3826G in relation to DM2 and body composition in Czech population. *Exp Clin Endocrinol Diabetes* 2007;115(5):303-7.
44. Arner P, Hellstrom L, Wahrenberg H, Bronnegard M. Beta-adrenoceptor expression in human fat cells from different regions. *The Journal of clinical investigation* 1990;86(5):1595-600.
45. Vidal-Puig AJ, Considine RV, Jimenez-Linan M, Werman A, Pories WJ, Caro JF, et al. Peroxisome proliferator-activated receptor gene expression in human tissues. Effects of obesity, weight loss, and regulation by insulin and glucocorticoids. *The Journal of clinical investigation* 1997;99(10):2416-22.
46. Jamdar SC. Glycerolipid biosynthesis in rat adipose tissue. Influence of adipose-cell size and site of adipose tissue on triacylglycerol formation in lean and obese rats. *The Biochemical journal* 1978;170(1):153-60.
47. Palou M, Priego T, Sanchez J, Rodriguez AM, Palou A, Pico C. Gene expression patterns in visceral and subcutaneous adipose depots in rats are linked to their morphologic features. *Cell Physiol Biochem* 2009;24(5-6):547-56.
48. Palou M, Sanchez J, Priego T, Rodriguez AM, Pico C, Palou A. Regional differences in the expression of genes involved in lipid metabolism in adipose tissue in response to short- and medium-term fasting and refeeding. *J Nutr Biochem* 2010;21(1):23-33.
49. Frayn KN. Adipose tissue as a buffer for daily lipid flux. *Diabetologia* 2002;45(9):1201-10.
50. Kelley DE, Thaete FL, Troost F, Huwe T, Goodpaster BH. Subdivisions of subcutaneous abdominal adipose tissue and insulin resistance. *American journal of physiology. Endocrinology and metabolism* 2000;278(5):E941-8.
51. Smith SR, Lovejoy JC, Greenway F, Ryan D, deJonge L, de la Bretonne J, et al. Contributions of total body fat, abdominal subcutaneous adipose tissue compartments, and visceral adipose tissue to the metabolic complications of obesity. *Metabolism: clinical and experimental* 2001;50(4):425-35.
52. Miyazaki Y, Glass L, Triplitt C, Wajcberg E, Mandarino LJ, DeFronzo RA. Abdominal fat distribution and peripheral and hepatic insulin resistance in type 2 diabetes mellitus. *American journal of physiology. Endocrinology and metabolism* 2002;283(6):E1135-43.

53. Walker GE, Verti B, Marzullo P, Savia G, Mencarelli M, Zurleni F, et al. Deep subcutaneous adipose tissue: a distinct abdominal adipose depot. *Obesity* 2007;15(8):1933-43.
54. Cnop M, Landchild MJ, Vidal J, Havel PJ, Knowles NG, Carr DR, et al. The concurrent accumulation of intra-abdominal and subcutaneous fat explains the association between insulin resistance and plasma leptin concentrations : distinct metabolic effects of two fat compartments. *Diabetes* 2002;51(4):1005-15.
55. Kadowaki K, Fukino K, Negishi E, Ueno K. Sex differences in PPARgamma expressions in rat adipose tissues. *Biol Pharm Bull* 2007;30(4):818-20.
56. Iacobellis G, Barbaro G. The double role of epicardial adipose tissue as pro- and anti-inflammatory organ. *Horm Metab Res* 2008;40(7):442-5.
57. Rabkin SW. Epicardial fat: properties, function and relationship to obesity. *Obesity reviews : an official journal of the International Association for the Study of Obesity* 2007;8(3):253-61.
58. Iacobellis G, Sharma AM. Epicardial adipose tissue as new cardio-metabolic risk marker and potential therapeutic target in the metabolic syndrome. *Curr Pharm Des* 2007;13(21):2180-4.
59. Sacks HS, Fain JN. Human epicardial adipose tissue: a review. *American heart journal* 2007;153(6):907-17.
60. Natale F, Tedesco MA, Mocerino R, de Simone V, Di Marco GM, Aronne L, et al. Visceral adiposity and arterial stiffness: echocardiographic epicardial fat thickness reflects, better than waist circumference, carotid arterial stiffness in a large population of hypertensives. *Eur J Echocardiogr* 2009;10(4):549-55.
61. Fantuzzi G. Adipose tissue, adipokines, and inflammation. *J Allergy Clin Immunol* 2005;115(5):911-9; quiz 20.
62. Pittas AG, Joseph NA, Greenberg AS. Adipocytokines and insulin resistance. *J Clin Endocrinol Metab* 2004;89(2):447-52.
63. Considine RV, Sinha MK, Heiman ML, Kriauciunas A, Stephens TW, Nyce MR, et al. Serum immunoreactive-leptin concentrations in normal-weight and obese humans. *N Engl J Med* 1996;334(5):292-5.
64. Tartaglia LA. The leptin receptor. *J Biol Chem* 1997;272(10):6093-6.
65. Takaya K, Ogawa Y, Isse N, Okazaki T, Satoh N, Masuzaki H, et al. Molecular cloning of rat leptin receptor isoform complementary DNAs-identification of a missense mutation in Zucker fatty (fa/fa) rats. *Biochem Biophys Res Commun* 1996;225(1):75-83.
66. Vaisse C, Halaas JL, Horvath CM, Darnell JE, Jr., Stoffel M, Friedman JM. Leptin activation of Stat3 in the hypothalamus of wild-type and ob/ob mice but not db/db mice. *Nat Genet* 1996;14(1):95-7.
67. Bjorbaek C, Uotani S, da Silva B, Flier JS. Divergent signaling capacities of the long and short isoforms of the leptin receptor. *J Biol Chem* 1997;272(51):32686-95.
68. Maffei M, Fei H, Lee GH, Dani C, Leroy P, Zhang Y, et al. Increased expression in adipocytes of ob RNA in mice with lesions of the hypothalamus and with mutations at the db locus. *Proc Natl Acad Sci U S A* 1995;92(15):6957-60.

69. Eleftheriou F, Takeda S, Ebihara K, Magre J, Patano N, Kim CA, et al. Serum leptin level is a regulator of bone mass. *Proc Natl Acad Sci U S A* 2004;101(9):3258-63.
70. Pelleymounter MA, Cullen MJ, Baker MB, Hecht R, Winters D, Boone T, et al. Effects of the obese gene product on body weight regulation in ob/ob mice. *Science* 1995;269(5223):540-3.
71. Ryden M, Arner P. Tumour necrosis factor-alpha in human adipose tissue - from signalling mechanisms to clinical implications. *J Intern Med* 2007;262(4):431-8.
72. Kern PA, Saghizadeh M, Ong JM, Bosch RJ, Deem R, Simsolo RB. The expression of tumor necrosis factor in human adipose tissue. Regulation by obesity, weight loss, and relationship to lipoprotein lipase. *J Clin Invest* 1995;95(5):2111-9.
73. Carswell EA, Old LJ, Kassel RL, Green S, Fiore N, Williamson B. An endotoxin-induced serum factor that causes necrosis of tumors. *Proc Natl Acad Sci U S A* 1975;72(9):3666-70.
74. Kriegler M, Perez C, DeFay K, Albert I, Lu SD. A novel form of TNF/cachectin is a cell surface cytotoxic transmembrane protein: ramifications for the complex physiology of TNF. *Cell* 1988;53(1):45-53.
75. Tang P, Hung MC, Klostergaard J. Human pro-tumor necrosis factor is a homotrimer. *Biochemistry* 1996;35(25):8216-25.
76. Black RA, Rauch CT, Kozlosky CJ, Peschon JJ, Slack JL, Wolfson MF, et al. A metalloproteinase disintegrin that releases tumour-necrosis factor-alpha from cells. *Nature* 1997;385(6618):729-33.
77. Ruan H, Lodish HF. Insulin resistance in adipose tissue: direct and indirect effects of tumor necrosis factor-alpha. *Cytokine Growth Factor Rev* 2003;14(5):447-55.
78. Hotamisligil GS. Inflammatory pathways and insulin action. *Int J Obes Relat Metab Disord* 2003;27 Suppl 3:S53-5.
79. Hotamisligil GS, Peraldi P, Budavari A, Ellis R, White MF, Spiegelman BM. IRS-1-mediated inhibition of insulin receptor tyrosine kinase activity in TNF-alpha- and obesity-induced insulin resistance. *Science* 1996;271(5249):665-8.
80. Kanety H, Hemi R, Papa MZ, Karasik A. Sphingomyelinase and ceramide suppress insulin-induced tyrosine phosphorylation of the insulin receptor substrate-1. *J Biol Chem* 1996;271(17):9895-7.
81. Fain JN, Madan AK, Hiler ML, Cheema P, Bahouth SW. Comparison of the release of adipokines by adipose tissue, adipose tissue matrix, and adipocytes from visceral and subcutaneous abdominal adipose tissues of obese humans. *Endocrinology* 2004;145(5):2273-82.
82. Wajchenberg BL. Subcutaneous and visceral adipose tissue: their relation to the metabolic syndrome. *Endocr Rev* 2000;21(6):697-738.
83. Locksley RM, Killeen N, Lenardo MJ. The TNF and TNF receptor superfamilies: integrating mammalian biology. *Cell* 2001;104(4):487-501.
84. Hehlgans T, Pfeffer K. The intriguing biology of the tumour necrosis factor/tumour necrosis factor receptor superfamily: players, rules and the games. *Immunology* 2005;115(1):1-20.

85. Naismith JH, Sprang SR. Modularity in the TNF-receptor family. *Trends Biochem Sci* 1998;23(2):74-9.
86. Banner DW, D'Arcy A, Janes W, Gentz R, Schoenfeld HJ, Broger C, et al. Crystal structure of the soluble human 55 kd TNF receptor-human TNF beta complex: implications for TNF receptor activation. *Cell* 1993;73(3):431-45.
87. Wajant H, Pfizenmaier K, Scheurich P. Tumor necrosis factor signaling. *Cell Death Differ* 2003;10(1):45-65.
88. Chen G, Goeddel DV. TNF-R1 signaling: a beautiful pathway. *Science* 2002;296(5573):1634-5.
89. Tartaglia LA, Ayres TM, Wong GH, Goeddel DV. A novel domain within the 55 kd TNF receptor signals cell death. *Cell* 1993;74(5):845-53.
90. Schulze-Osthoff K, Ferrari D, Los M, Wesselborg S, Peter ME. Apoptosis signaling by death receptors. *Eur J Biochem* 1998;254(3):439-59.
91. Yuasa T, Ohno S, Kehrl JH, Kyriakis JM. Tumor necrosis factor signaling to stress-activated protein kinase (SAPK)/Jun NH2-terminal kinase (JNK) and p38. Germinal center kinase couples TRAF2 to mitogen-activated protein kinase/ERK kinase 1 and SAPK while receptor interacting protein associates with a mitogen-activated protein kinase kinase upstream of MKK6 and p38. *J Biol Chem* 1998;273(35):22681-92.
92. Hsu H, Xiong J, Goeddel DV. The TNF receptor 1-associated protein TRADD signals cell death and NF-kappa B activation. *Cell* 1995;81(4):495-504.
93. Uysal KT, Wiesbrock SM, Hotamisligil GS. Functional analysis of tumor necrosis factor (TNF) receptors in TNF-alpha-mediated insulin resistance in genetic obesity. *Endocrinology* 1998;139(12):4832-8.
94. Uysal KT, Wiesbrock SM, Marino MW, Hotamisligil GS. Protection from obesity-induced insulin resistance in mice lacking TNF-alpha function. *Nature* 1997;389(6651):610-4.
95. Ruan H, Miles PD, Ladd CM, Ross K, Golub TR, Olefsky JM, et al. Profiling gene transcription in vivo reveals adipose tissue as an immediate target of tumor necrosis factor-alpha: implications for insulin resistance. *Diabetes* 2002;51(11):3176-88.
96. Bruun JM, Lihn AS, Verdich C, Pedersen SB, Toubro S, Astrup A, et al. Regulation of adiponectin by adipose tissue-derived cytokines: in vivo and in vitro investigations in humans. *Am J Physiol Endocrinol Metab* 2003;285(3):E527-33.
97. Saltiel AR, Kahn CR. Insulin signalling and the regulation of glucose and lipid metabolism. *Nature* 2001;414(6865):799-806.
98. Hotamisligil GS. The role of TNFalpha and TNF receptors in obesity and insulin resistance. *J Intern Med* 1999;245(6):621-5.
99. Papanicolaou DA, Wilder RL, Manolagas SC, Chrousos GP. The pathophysiologic roles of interleukin-6 in human disease. *Ann Intern Med* 1998;128(2):127-37.
100. Fried SK, Bunkin DA, Greenberg AS. Omental and subcutaneous adipose tissues of obese subjects release interleukin-6: depot difference and regulation by glucocorticoid. *J Clin Endocrinol Metab* 1998;83(3):847-50.

101. Senn JJ, Klover PJ, Nowak IA, Zimmers TA, Koniaris LG, Furlanetto RW, et al. Suppressor of cytokine signaling-3 (SOCS-3), a potential mediator of interleukin-6-dependent insulin resistance in hepatocytes. *J Biol Chem* 2003;278(16):13740-6.
102. Bastard JP, Jardel C, Bruckert E, Blondy P, Capeau J, Laville M, et al. Elevated levels of interleukin 6 are reduced in serum and subcutaneous adipose tissue of obese women after weight loss. *J Clin Endocrinol Metab* 2000;85(9):3338-42.
103. Vozarova B, Weyer C, Hanson K, Tataranni PA, Bogardus C, Pratley RE. Circulating interleukin-6 in relation to adiposity, insulin action, and insulin secretion. *Obes Res* 2001;9(7):414-7.
104. Kern PA, Ranganathan S, Li C, Wood L, Ranganathan G. Adipose tissue tumor necrosis factor and interleukin-6 expression in human obesity and insulin resistance. *Am J Physiol Endocrinol Metab* 2001;280(5):E745-51.
105. Pradhan AD, Manson JE, Rifai N, Buring JE, Ridker PM. C-reactive protein, interleukin 6, and risk of developing type 2 diabetes mellitus. *JAMA* 2001;286(3):327-34.
106. Vozarova B, Fernandez-Real JM, Knowler WC, Gallart L, Hanson RL, Gruber JD, et al. The interleukin-6 (-174) G/C promoter polymorphism is associated with type-2 diabetes mellitus in Native Americans and Caucasians. *Hum Genet* 2003;112(4):409-13.
107. Steensberg A, Fischer CP, Sacchetti M, Keller C, Osada T, Schjerling P, et al. Acute interleukin-6 administration does not impair muscle glucose uptake or whole-body glucose disposal in healthy humans. *J Physiol* 2003;548(Pt 2):631-8.
108. Wallenius V, Wallenius K, Ahren B, Rudling M, Carlsten H, Dickson SL, et al. Interleukin-6-deficient mice develop mature-onset obesity. *Nat Med* 2002;8(1):75-9.
109. Fasshauer M, Kralisch S, Klier M, Lossner U, Bluher M, Klein J, et al. Adiponectin gene expression and secretion is inhibited by interleukin-6 in 3T3-L1 adipocytes. *Biochem Biophys Res Commun* 2003;301(4):1045-50.
110. Fang X, Sweeney G. Mechanisms regulating energy metabolism by adiponectin in obesity and diabetes. *Biochem Soc Trans* 2006;34(Pt 5):798-801.
111. Scherer PE, Williams S, Fogliano M, Baldini G, Lodish HF. A novel serum protein similar to C1q, produced exclusively in adipocytes. *J Biol Chem* 1995;270(45):26746-9.
112. Hu E, Liang P, Spiegelman BM. AdipoQ is a novel adipose-specific gene dysregulated in obesity. *J Biol Chem* 1996;271(18):10697-703.
113. Maeda K, Okubo K, Shimomura I, Funahashi T, Matsuzawa Y, Matsubara K. cDNA cloning and expression of a novel adipose specific collagen-like factor, apM1 (AdiPose Most abundant Gene transcript 1). *Biochem Biophys Res Commun* 1996;221(2):286-9.
114. Nakano Y, Tobe T, Choi-Miura NH, Mazda T, Tomita M. Isolation and characterization of GBP28, a novel gelatin-binding protein purified from human plasma. *J Biochem* 1996;120(4):803-12.



115. Vasseur F. Adiponectin and its receptors: partners contributing to the "vicious circle" leading to the metabolic syndrome? *Pharmacol Res* 2006;53(6):478-81.
116. Kadowaki T, Yamauchi T. Adiponectin and adiponectin receptors. *Endocr Rev* 2005;26(3):439-51.
117. Berg AH, Combs TP, Du X, Brownlee M, Scherer PE. The adipocyte-secreted protein Acrp30 enhances hepatic insulin action. *Nature medicine* 2001;7(8):947-53.
118. Maeda N, Shimomura I, Kishida K, Nishizawa H, Matsuda M, Nagaretani H, et al. Diet-induced insulin resistance in mice lacking adiponectin/ACRP30. *Nat Med* 2002;8(7):731-7.
119. Fruebis J, Tsao TS, Javorschi S, Ebbets-Reed D, Erickson MR, Yen FT, et al. Proteolytic cleavage product of 30-kDa adipocyte complement-related protein increases fatty acid oxidation in muscle and causes weight loss in mice. *Proc Natl Acad Sci U S A* 2001;98(4):2005-10.
120. Waki H, Yamauchi T, Kamon J, Kita S, Ito Y, Hada Y, et al. Generation of globular fragment of adiponectin by leukocyte elastase secreted by monocytic cell line THP-1. *Endocrinology* 2005;146(2):790-6.
121. Ceddia RB, Somwar R, Maida A, Fang X, Bikopoulos G, Sweeney G. Globular adiponectin increases GLUT4 translocation and glucose uptake but reduces glycogen synthesis in rat skeletal muscle cells. *Diabetologia* 2005;48(1):132-9.
122. Fang X, Palanivel R, Zhou X, Liu Y, Xu A, Wang Y, et al. Hyperglycemia- and hyperinsulinemia-induced alteration of adiponectin receptor expression and adiponectin effects in L6 myoblasts. *J Mol Endocrinol* 2005;35(3):465-76.
123. Tsao TS, Tomas E, Murrey HE, Hug C, Lee DH, Ruderman NB, et al. Role of disulfide bonds in Acrp30/adiponectin structure and signaling specificity. Different oligomers activate different signal transduction pathways. *J Biol Chem* 2003;278(50):50810-7.
124. Tsao TS, Murrey HE, Hug C, Lee DH, Lodish HF. Oligomerization state-dependent activation of NF-kappa B signaling pathway by adipocyte complement-related protein of 30 kDa (Acrp30). *J Biol Chem* 2002;277(33):29359-62.
125. Oh DK, Ciaraldi T, Henry RR. Adiponectin in health and disease. *Diabetes Obes Metab* 2007;9(3):282-9.
126. Hug C, Wang J, Ahmad NS, Bogan JS, Tsao TS, Lodish HF. T-cadherin is a receptor for hexameric and high-molecular-weight forms of Acrp30/adiponectin. *Proceedings of the National Academy of Sciences of the United States of America* 2004;101(28):10308-13.
127. Qi Y, Takahashi N, Hileman SM, Patel HR, Berg AH, Pajvani UB, et al. Adiponectin acts in the brain to decrease body weight. *Nature medicine* 2004;10(5):524-9.
128. Shetty GK, Economides PA, Horton ES, Mantzoros CS, Veves A. Circulating adiponectin and resistin levels in relation to metabolic factors, inflammatory markers, and vascular reactivity in diabetic patients and subjects at risk for diabetes. *Diabetes Care* 2004;27(10):2450-7.
129. Hotta K, Funahashi T, Arita Y, Takahashi M, Matsuda M, Okamoto Y, et al. Plasma concentrations of a novel, adipose-specific protein,

- adiponectin, in type 2 diabetic patients. *Arterioscler Thromb Vasc Biol* 2000;20(6):1595-9.
130. Matsuzawa Y, Funahashi T, Kihara S, Shimomura I. Adiponectin and metabolic syndrome. *Arterioscler Thromb Vasc Biol* 2004;24(1):29-33.
  131. Yamauchi T, Hara K, Kubota N, Terauchi Y, Tobe K, Froguel P, et al. Dual roles of adiponectin/Acrp30 in vivo as an anti-diabetic and anti-atherogenic adipokine. *Curr Drug Targets Immune Endocr Metabol Disord* 2003;3(4):243-54.
  132. Pollin TI, Tanner K, O'Connell J R, Ott SH, Damcott CM, Shuldiner AR, et al. Linkage of plasma adiponectin levels to 3q27 explained by association with variation in the APM1 gene. *Diabetes* 2005;54(1):268-74.
  133. Ujiie H, Oritani K, Kato H, Yokota T, Takahashi I, Maeda T, et al. Identification of amino-terminal region of adiponectin as a physiologically functional domain. *J Cell Biochem* 2006;98(1):194-207.
  134. Wang Y, Lam KS, Chan L, Chan KW, Lam JB, Lam MC, et al. Post-translational modifications of the four conserved lysine residues within the collagenous domain of adiponectin are required for the formation of its high molecular weight oligomeric complex. *J Biol Chem* 2006;281(24):16391-400.
  135. Qiao L, Maclean PS, Schaack J, Orlicky DJ, Darimont C, Pagliassotti M, et al. C/EBPalpha regulates human adiponectin gene transcription through an intronic enhancer. *Diabetes* 2005;54(6):1744-54.
  136. Waki H, Yamauchi T, Kamon J, Ito Y, Uchida S, Kita S, et al. Impaired multimerization of human adiponectin mutants associated with diabetes. Molecular structure and multimer formation of adiponectin. *J Biol Chem* 2003;278(41):40352-63.
  137. Steffes MW, Gross MD, Schreiner PJ, Yu X, Hilner JE, Gingerich R, et al. Serum adiponectin in young adults--interactions with central adiposity, circulating levels of glucose, and insulin resistance: the CARDIA study. *Ann Epidemiol* 2004;14(7):492-8.
  138. Wang B, Jenkins JR, Trayhurn P. Expression and secretion of inflammation-related adipokines by human adipocytes differentiated in culture: integrated response to TNF-alpha. *Am J Physiol Endocrinol Metab* 2005;288(4):E731-40.
  139. Kern PA, Di Gregorio GB, Lu T, Rassouli N, Ranganathan G. Adiponectin expression from human adipose tissue: relation to obesity, insulin resistance, and tumor necrosis factor-alpha expression. *Diabetes* 2003;52(7):1779-85.
  140. Cnop M, Havel PJ, Utzschneider KM, Carr DB, Sinha MK, Boyko EJ, et al. Relationship of adiponectin to body fat distribution, insulin sensitivity and plasma lipoproteins: evidence for independent roles of age and sex. *Diabetologia* 2003;46(4):459-69.
  141. Arita Y, Kihara S, Ouchi N, Takahashi M, Maeda K, Miyagawa J, et al. Paradoxical decrease of an adipose-specific protein, adiponectin, in obesity. *Biochem Biophys Res Commun* 1999;257(1):79-83.
  142. Yamauchi T, Kamon J, Ito Y, Tsuchida A, Yokomizo T, Kita S, et al. Cloning of adiponectin receptors that mediate antidiabetic metabolic effects. *Nature* 2003;423(6941):762-9.

143. Rasmussen MS, Lihn AS, Pedersen SB, Bruun JM, Rasmussen M, Richelsen B. Adiponectin receptors in human adipose tissue: effects of obesity, weight loss, and fat depots. *Obesity (Silver Spring)* 2006;14(1):28-35.
144. Chinetti G, Zawadzki C, Fruchart JC, Staels B. Expression of adiponectin receptors in human macrophages and regulation by agonists of the nuclear receptors PPARalpha, PPARgamma, and LXR. *Biochem Biophys Res Commun* 2004;314(1):151-8.
145. Kharroubi I, Rasschaert J, Eizirik DL, Cnop M. Expression of adiponectin receptors in pancreatic beta cells. *Biochem Biophys Res Commun* 2003;312(4):1118-22.
146. Tomas E, Tsao TS, Saha AK, Murrey HE, Zhang Cc C, Itani SI, et al. Enhanced muscle fat oxidation and glucose transport by ACRP30 globular domain: acetyl-CoA carboxylase inhibition and AMP-activated protein kinase activation. *Proc Natl Acad Sci U S A* 2002;99(25):16309-13.
147. Yamauchi T, Kamon J, Waki H, Imai Y, Shimozawa N, Hioki K, et al. Globular adiponectin protected ob/ob mice from diabetes and ApoE-deficient mice from atherosclerosis. *J Biol Chem* 2003;278(4):2461-8.
148. Yamauchi T, Kamon J, Minokoshi Y, Ito Y, Waki H, Uchida S, et al. Adiponectin stimulates glucose utilization and fatty-acid oxidation by activating AMP-activated protein kinase. *Nat Med* 2002;8(11):1288-95.
149. Karpichev IV, Cornivelli L, Small GM. Multiple regulatory roles of a novel *Saccharomyces cerevisiae* protein, encoded by YOL002c, in lipid and phosphate metabolism. *J Biol Chem* 2002;277(22):19609-17.
150. Jiang Y, Zhu JF, Luscinskas FW, Graves DT. MCP-1-stimulated monocyte attachment to laminin is mediated by beta 2-integrins. *Am J Physiol* 1994;267(4 Pt 1):C1112-8.
151. Kanda H, Tateya S, Tamori Y, Kotani K, Hiasa K, Kitazawa R, et al. MCP-1 contributes to macrophage infiltration into adipose tissue, insulin resistance, and hepatic steatosis in obesity. *J Clin Invest* 2006;116(6):1494-505.
152. Uematsu S, Akira S. Toll-Like receptors (TLRs) and their ligands. *Handbook of experimental pharmacology* 2008(183):1-20.
153. O'Rourke AM, Mescher MF. T-cell receptor-activated adhesion systems. *Current opinion in cell biology* 1990;2(5):888-93.
154. Zhao W, Wang L, Zhang M, Wang P, Zhang L, Yuan C, et al. Peroxisome proliferator-activated receptor gamma negatively regulates IFN-beta production in Toll-like receptor (TLR) 3- and TLR4-stimulated macrophages by preventing interferon regulatory factor 3 binding to the IFN-beta promoter. *J Biol Chem* 2011;286(7):5519-28.
155. Akira S. The role of IL-18 in innate immunity. *Current opinion in immunology* 2000;12(1):59-63.
156. Netea MG, Joosten LA, Lewis E, Jensen DR, Voshol PJ, Kullberg BJ, et al. Deficiency of interleukin-18 in mice leads to hyperphagia, obesity and insulin resistance. *Nat Med* 2006;12(6):650-6.
157. Sebert SP, Hyatt MA, Chan LL, Patel N, Bell RC, Keisler D, et al. Maternal nutrient restriction between early and midgestation and its impact upon appetite regulation after juvenile obesity. *Endocrinology* 2009;150(2):634-41.

158. Gerken T, Girard CA, Tung YC, Webby CJ, Saudek V, Hewitson KS, et al. The obesity-associated FTO gene encodes a 2-oxoglutarate-dependent nucleic acid demethylase. *Science* 2007;318(5855):1469-72.
159. Frayling TM, Timpson NJ, Weedon MN, Zeggini E, Freathy RM, Lindgren CM, et al. A common variant in the FTO gene is associated with body mass index and predisposes to childhood and adult obesity. *Science* 2007;316(5826):889-94.
160. Hotamisligil GS. Endoplasmic reticulum stress and inflammation in obesity and type 2 diabetes. *Novartis Foundation symposium* 2007;286:86-94; discussion 94-8, 162-3, 96-203.
161. Ting J, Lee AS. Human gene encoding the 78,000-dalton glucose-regulated protein and its pseudogene: structure, conservation, and regulation. *DNA* 1988;7(4):275-86.
162. Xu C, Bailly-Maitre B, Reed JC. Endoplasmic reticulum stress: cell life and death decisions. *The Journal of clinical investigation* 2005;115(10):2656-64.
163. Schroder M, Kaufman RJ. ER stress and the unfolded protein response. *Mutat Res* 2005;569(1-2):29-63.
164. Shen X, Zhang K, Kaufman RJ. The unfolded protein response--a stress signaling pathway of the endoplasmic reticulum. *J Chem Neuroanat* 2004;28(1-2):79-92.
165. Ron D, Habener JF. CHOP, a novel developmentally regulated nuclear protein that dimerizes with transcription factors C/EBP and LAP and functions as a dominant-negative inhibitor of gene transcription. *Genes & development* 1992;6(3):439-53.
166. Urano F, Wang X, Bertolotti A, Zhang Y, Chung P, Harding HP, et al. Coupling of stress in the ER to activation of JNK protein kinases by transmembrane protein kinase IRE1. *Science* 2000;287(5453):664-6.
167. Murano I, Barbatelli G, Parisani V, Latini C, Muzzonigro G, Castellucci M, et al. Dead adipocytes, detected as crown-like structures, are prevalent in visceral fat depots of genetically obese mice. *Journal of lipid research* 2008;49(7):1562-8.
168. Cinti S, Mitchell G, Barbatelli G, Murano I, Ceresi E, Faloia E, et al. Adipocyte death defines macrophage localization and function in adipose tissue of obese mice and humans. *Journal of lipid research* 2005;46(11):2347-55.
169. Symonds ME, Stephenson T, Gardner DS, Budge H. Long-term effects of nutritional programming of the embryo and fetus: mechanisms and critical windows. *Reprod Fertil Dev* 2007;19(1):53-63.
170. Barker DJ. The developmental origins of adult disease. *J Am Coll Nutr* 2004;23(6 Suppl):588S-95S.
171. Roseboom T, de Rooij S, Painter R. The Dutch famine and its long-term consequences for adult health. *Early Hum Dev* 2006;82(8):485-91.
172. Ravelli AC, van der Meulen JH, Michels RP, Osmond C, Barker DJ, Hales CN, et al. Glucose tolerance in adults after prenatal exposure to famine. *Lancet* 1998;351(9097):173-7.
173. de Rooij SR, Painter RC, Roseboom TJ, Phillips DI, Osmond C, Barker DJ, et al. Glucose tolerance at age 58 and the decline of glucose tolerance in comparison with age 50 in people prenatally exposed to the Dutch famine. *Diabetologia* 2006;49(4):637-43.

174. Barker DJ. Fetal origins of coronary heart disease. *BMJ* 1995;311(6998):171-4.
175. Barker DJ, Eriksson JG, Forsen T, Osmond C. Fetal origins of adult disease: strength of effects and biological basis. *Int J Epidemiol* 2002;31(6):1235-9.
176. Lucas A. Programming by early nutrition in man. *Ciba Found Symp* 1991;156:38-50; discussion 50-5.
177. Keller G, Zimmer G, Mall G, Ritz E, Amann K. Nephron number in patients with primary hypertension. *N Engl J Med* 2003;348(2):101-8.
178. Phillips DI. Insulin resistance as a programmed response to fetal undernutrition. *Diabetologia* 1996;39(9):1119-22.
179. Hales CN, Barker DJ. Type 2 (non-insulin-dependent) diabetes mellitus: the thrifty phenotype hypothesis. *Diabetologia* 1992;35(7):595-601.
180. Barker DJ. Fetal growth and adult disease. *British journal of obstetrics and gynaecology* 1992;99(4):275-6.
181. Barker DJ. The effect of nutrition of the fetus and neonate on cardiovascular disease in adult life. *The Proceedings of the Nutrition Society* 1992;51(2):135-44.
182. Barker DJ. The fetal origins of diseases of old age. *European journal of clinical nutrition* 1992;46 Suppl 3:S3-9.
183. Lucas A, Fewtrell MS, Cole TJ. Fetal origins of adult disease-the hypothesis revisited. *BMJ* 1999;319(7204):245-9.
184. Barker DJ. Maternal and fetal origins of coronary heart disease. *Journal of the Royal College of Physicians of London* 1994;28(6):544-51.
185. Ravelli AC, van Der Meulen JH, Osmond C, Barker DJ, Bleker OP. Obesity at the age of 50 y in men and women exposed to famine prenatally. *The American journal of clinical nutrition* 1999;70(5):811-6.
186. Muhlhausler BS, Ritorto V, Schultz C, Chatterton BE, Duffield JA, McMillen IC. Birth weight and gender determine expression of adipogenic, lipogenic and adipokine genes in perirenal adipose tissue in the young adult sheep. *Domestic animal endocrinology* 2008;35(1):46-57.
187. Muhlhausler B, Smith SR. Early-life origins of metabolic dysfunction: role of the adipocyte. *Trends in endocrinology and metabolism: TEM* 2009;20(2):51-7.
188. Ong KK, Ahmed ML, Emmett PM, Preece MA, Dunger DB. Association between postnatal catch-up growth and obesity in childhood: prospective cohort study. *BMJ* 2000;320(7240):967-71.
189. Ong KK, Dunger DB. Thrifty genotypes and phenotypes in the pathogenesis of type 2 diabetes mellitus. *Journal of pediatric endocrinology & metabolism : JPEM* 2000;13 Suppl 6:1419-24.
190. Soto N, Bazaes RA, Pena V, Salazar T, Avila A, Iniguez G, et al. Insulin sensitivity and secretion are related to catch-up growth in small-for-gestational-age infants at age 1 year: results from a prospective cohort. *J Clin Endocrinol Metab* 2003;88(8):3645-50.
191. Singhal A, Cole TJ, Fewtrell M, Kennedy K, Stephenson T, Elias-Jones A, et al. Promotion of faster weight gain in infants born small for gestational age: is there an adverse effect on later blood pressure? *Circulation* 2007;115(2):213-20.

192. Singhal A, Wells J, Cole TJ, Fewtrell M, Lucas A. Programming of lean body mass: a link between birth weight, obesity, and cardiovascular disease? *The American journal of clinical nutrition* 2003;77(3):726-30.
193. Forsen T, Eriksson J, Tuomilehto J, Reunanen A, Osmond C, Barker D. The fetal and childhood growth of persons who develop type 2 diabetes. *Ann Intern Med* 2000;133(3):176-82.
194. Eriksson J, Forsen T, Tuomilehto J, Osmond C, Barker D. Size at birth, childhood growth and obesity in adult life. *Int J Obes Relat Metab Disord* 2001;25(5):735-40.
195. Eriksson JG, Forsen TJ, Osmond C, Barker DJ. Pathways of infant and childhood growth that lead to type 2 diabetes. *Diabetes Care* 2003;26(11):3006-10.
196. Vaag A. Low birth weight and early weight gain in the metabolic syndrome: consequences for infant nutrition. *International journal of gynaecology and obstetrics: the official organ of the International Federation of Gynaecology and Obstetrics* 2009;104 Suppl 1:S32-4.
197. Ekelund U, Ong KK, Linne Y, Neovius M, Brage S, Dunger DB, et al. Association of weight gain in infancy and early childhood with metabolic risk in young adults. *J Clin Endocrinol Metab* 2007;92(1):98-103.
198. Gardner DS, Van Bon BW, Dandrea J, Goddard PJ, May SF, Wilson V, et al. Effect of periconceptional undernutrition and gender on hypothalamic-pituitary-adrenal axis function in young adult sheep. *The Journal of endocrinology* 2006;190(2):203-12.
199. Aderem A, Ulevitch RJ. Toll-like receptors in the induction of the innate immune response. *Nature* 2000;406(6797):782-7.
200. Karopka T, Fluck J, Mevissen HT, Glass A. The Autoimmune Disease Database: a dynamically compiled literature-derived database. *BMC bioinformatics* 2006;7:325.
201. Madigan MT, Brock TD. *Brock biology of microorganisms*. 12th ed. San Francisco, CA: Pearson/Benjamin Cummings, 2009.
202. Baron S. *Medical microbiology*. 4th ed. Galveston, Tex.: University of Texas Medical Branch at Galveston, 1996.
203. Pickens CO. *Cell apoptotic signalling pathways*. New York: Nova Biomedical Books, 2007.
204. Vachharajani V. Influence of obesity on sepsis. *Pathophysiology : the official journal of the International Society for Pathophysiology / ISP* 2008;15(2):123-34.
205. Hotamisligil GS, Shargill NS, Spiegelman BM. Adipose expression of tumor necrosis factor-alpha: direct role in obesity-linked insulin resistance. *Science* 1993;259(5091):87-91.
206. Trayhurn P, Wood IS. Signalling role of adipose tissue: adipokines and inflammation in obesity. *Biochem Soc Trans* 2005;33(Pt 5):1078-81.
207. Roytblat L, Rachinsky M, Fisher A, Greemberg L, Shapira Y, Douvdevani A, et al. Raised interleukin-6 levels in obese patients. *Obes Res* 2000;8(9):673-5.
208. Eder K, Baffy N, Falus A, Fulop AK. The major inflammatory mediator interleukin-6 and obesity. *Inflammation research : official journal of the European Histamine Research Society ... [et al.]* 2009;58(11):727-36.

209. Juge-Aubry CE, Somm E, Pernin A, Alizadeh N, Giusti V, Dayer JM, et al. Adipose tissue is a regulated source of interleukin-10. *Cytokine* 2005;29(6):270-4.
210. Sharkey D, Gardner DS, Fainberg HP, Sebert S, Bos P, Wilson V, et al. Maternal nutrient restriction during pregnancy differentially alters the unfolded protein response in adipose and renal tissue of obese juvenile offspring. *FASEB journal : official publication of the Federation of American Societies for Experimental Biology* 2009;23(5):1314-24.
211. Fain JN. Release of inflammatory mediators by human adipose tissue is enhanced in obesity and primarily by the nonfat cells: a review. *Mediators of inflammation* 2010;2010:513948.
212. Ye J. Adipose tissue vascularization: its role in chronic inflammation. *Current diabetes reports* 2011;11(3):203-10.
213. Harle P, Straub RH. Leptin is a link between adipose tissue and inflammation. *Annals of the New York Academy of Sciences* 2006;1069:454-62.
214. Mangge H, Almer G, Truschnig-Wilders M, Schmidt A, Gasser R, Fuchs D. Inflammation, adiponectin, obesity and cardiovascular risk. *Current medicinal chemistry* 2010;17(36):4511-20.
215. Kahn BB, Flier JS. Obesity and insulin resistance. *J Clin Invest* 2000;106(4):473-81.
216. Mayfield J. Diagnosis and classification of diabetes mellitus: new criteria. *Am Fam Physician* 1998;58(6):1355-62, 69-70.
217. Kraegen EW, Clark PW, Jenkins AB, Daley EA, Chisholm DJ, Storlien LH. Development of muscle insulin resistance after liver insulin resistance in high-fat-fed rats. *Diabetes* 1991;40(11):1397-403.
218. Schinner S, Scherbaum WA, Bornstein SR, Barthel A. Molecular mechanisms of insulin resistance. *Diabet Med* 2005;22(6):674-82.
219. Ebbesson SO, Kennish J, Ebbesson L, Go O, Yeh J. Diabetes is related to fatty acid imbalance in Eskimos. *Int J Circumpolar Health* 1999;58(2):108-19.
220. Lovejoy JC. Dietary fatty acids and insulin resistance. *Curr Atheroscler Rep* 1999;1(3):215-20.
221. Kahn SE, Hull RL, Utzschneider KM. Mechanisms linking obesity to insulin resistance and type 2 diabetes. *Nature* 2006;444(7121):840-6.
222. Goodpaster BH, Kelley DE, Wing RR, Meier A, Thaete FL. Effects of weight loss on regional fat distribution and insulin sensitivity in obesity. *Diabetes* 1999;48(4):839-47.
223. Tappy L, Le KA. Metabolic effects of fructose and the worldwide increase in obesity. *Physiological reviews* 2010;90(1):23-46.
224. Elliott SS, Keim NL, Stern JS, Teff K, Havel PJ. Fructose, weight gain, and the insulin resistance syndrome. *The American journal of clinical nutrition* 2002;76(5):911-22.
225. Hanover LM, White JS. Manufacturing, composition, and applications of fructose. *The American journal of clinical nutrition* 1993;58(5 Suppl):724S-32S.
226. Agriculture USDo. Sugar and Sweeteners  
Yearbook Tables. Other Recommended Data Products. USA: United States Department of Agriculture, 2009.

227. Corpe CP, Burant CF, Hoekstra JH. Intestinal fructose absorption: clinical and molecular aspects. *Journal of pediatric gastroenterology and nutrition* 1999;28(4):364-74.
228. Douard V, Ferraris RP. Regulation of the fructose transporter GLUT5 in health and disease. *Am J Physiol Endocrinol Metab* 2008;295(2):E227-37.
229. Cui XL, Schlesier AM, Fisher EL, Cerqueira C, Ferraris RP. Fructose-induced increases in neonatal rat intestinal fructose transport involve the PI3-kinase/Akt signaling pathway. *American journal of physiology. Gastrointestinal and liver physiology* 2005;288(6):G1310-20.
230. Ferraris RP, Hsiao J, Hernandez R, Hirayama B. Site density of mouse intestinal glucose transporters declines with age. *Am J Physiol* 1993;264(2 Pt 1):G285-93.
231. Cheeseman CI. GLUT2 is the transporter for fructose across the rat intestinal basolateral membrane. *Gastroenterology* 1993;105(4):1050-6.
232. Colville CA, Seatter MJ, Jess TJ, Gould GW, Thomas HM. Kinetic analysis of the liver-type (GLUT2) and brain-type (GLUT3) glucose transporters in *Xenopus* oocytes: substrate specificities and effects of transport inhibitors. *The Biochemical journal* 1993;290 ( Pt 3):701-6.
233. Adelman RC, Ballard FJ, Weinhouse S. Purification and properties of rat liver fructokinase. *J Biol Chem* 1967;242(14):3360-5.
234. Heinz F, Lamprecht W, Kirsch J. Enzymes of fructose metabolism in human liver. *J Clin Invest* 1968;47(8):1826-32.
235. Hers HG, Kusaka T. [The metabolism of fructose-1-phosphate in the liver]. *Biochim Biophys Acta* 1953;11(3):427-37.
236. Iynedjian PB. Mammalian glucokinase and its gene. *The Biochemical journal* 1993;293 ( Pt 1):1-13.
237. Tornheim K, Lowenstein JM. Control of phosphofructokinase from rat skeletal muscle. Effects of fructose diphosphate, AMP, ATP, and citrate. *J Biol Chem* 1976;251(23):7322-8.
238. Bruynseels K, Bergans N, Gillis N, van Dorpen F, Van Hecke P, Stalmans W, et al. On the inhibition of hepatic glycogenolysis by fructose. A <sup>31</sup>P-NMR study in perfused rat liver using the fructose analogue 2,5-anhydro-D-mannitol. *NMR in biomedicine* 1999;12(3):145-56.
239. Cortez-Pinto H, Chatham J, Chacko VP, Arnold C, Rashid A, Diehl AM. Alterations in liver ATP homeostasis in human nonalcoholic steatohepatitis: a pilot study. *JAMA* 1999;282(17):1659-64.
240. Bar-On H, Stein Y. Effect of glucose and fructose administration on lipid metabolism in the rat. *The Journal of nutrition* 1968;94(1):95-105.
241. Clark DG, Rognstad R, Katz J. Lipogenesis in rat hepatocytes. *J Biol Chem* 1974;249(7):2028-36.
242. Tounian P, Schneiter P, Henry S, Delarue J, Tappy L. Effects of dexamethasone on hepatic glucose production and fructose metabolism in healthy humans. *Am J Physiol* 1997;273(2 Pt 1):E315-20.
243. Hellerstein MK, Neese RA, Schwarz JM. Model for measuring absolute rates of hepatic de novo lipogenesis and reesterification of free fatty acids. *Am J Physiol* 1993;265(5 Pt 1):E814-20.



244. Parks EJ, Skokan LE, Timlin MT, Dingfelder CS. Dietary sugars stimulate fatty acid synthesis in adults. *The Journal of nutrition* 2008;138(6):1039-46.
245. Postic C, Girard J. Contribution of de novo fatty acid synthesis to hepatic steatosis and insulin resistance: lessons from genetically engineered mice. *J Clin Invest* 2008;118(3):829-38.
246. Hudgins LC, Parker TS, Levine DM, Hellerstein MK. A dual sugar challenge test for lipogenic sensitivity to dietary fructose. *J Clin Endocrinol Metab* 2011;96(3):861-8.
247. White JS. Straight talk about high-fructose corn syrup: what it is and what it ain't. *The American journal of clinical nutrition* 2008;88(6):1716S-21S.
248. Havel PJ. Dietary fructose: implications for dysregulation of energy homeostasis and lipid/carbohydrate metabolism. *Nutrition reviews* 2005;63(5):133-57.
249. Le KA, Tappy L. Metabolic effects of fructose. *Current opinion in clinical nutrition and metabolic care* 2006;9(4):469-75.
250. Anderson JW, Story LJ, Zettwoch NC, Gustafson NJ, Jefferson BS. Metabolic effects of fructose supplementation in diabetic individuals. *Diabetes Care* 1989;12(5):337-44.
251. Bantle JP, Laine DC, Thomas JW. Metabolic effects of dietary fructose and sucrose in types I and II diabetic subjects. *JAMA* 1986;256(23):3241-6.
252. Bantle JP, Swanson JE, Thomas W, Laine DC. Metabolic effects of dietary fructose in diabetic subjects. *Diabetes Care* 1992;15(11):1468-76.
253. Bizeau ME, Pagliassotti MJ. Hepatic adaptations to sucrose and fructose. *Metabolism: clinical and experimental* 2005;54(9):1189-201.
254. Crapo PA, Kolterman OG. The metabolic effects of 2-week fructose feeding in normal subjects. *The American journal of clinical nutrition* 1984;39(4):525-34.
255. Macdonald I. Influence of fructose and glucose on serum lipid levels in men and pre- and postmenopausal women. *The American journal of clinical nutrition* 1966;18(5):369-72.
256. Fredrickson DS, Lees RS. A System for Phenotyping Hyperlipoproteinemia. *Circulation* 1965;31:321-7.
257. Kim JY, Nolte LA, Hansen PA, Han DH, Kawanaka K, Holloszy JO. Insulin resistance of muscle glucose transport in male and female rats fed a high-sucrose diet. *Am J Physiol* 1999;276(3 Pt 2):R665-72.
258. Chong MF, Fielding BA, Frayn KN. Mechanisms for the acute effect of fructose on postprandial lipemia. *The American journal of clinical nutrition* 2007;85(6):1511-20.
259. Parks EJ, Hellerstein MK. Carbohydrate-induced hypertriacylglycerolemia: historical perspective and review of biological mechanisms. *The American journal of clinical nutrition* 2000;71(2):412-33.
260. Hudgins LC, Hellerstein MK, Seidman CE, Neese RA, Tremaroli JD, Hirsch J. Relationship between carbohydrate-induced hypertriglyceridemia and fatty acid synthesis in lean and obese subjects. *Journal of lipid research* 2000;41(4):595-604.

261. Faeh D, Minehira K, Schwarz JM, Periasamy R, Park S, Tappy L. Effect of fructose overfeeding and fish oil administration on hepatic de novo lipogenesis and insulin sensitivity in healthy men. *Diabetes* 2005;54(7):1907-13.
262. Swarbrick MM, Stanhope KL, Elliott SS, Graham JL, Krauss RM, Christiansen MP, et al. Consumption of fructose-sweetened beverages for 10 weeks increases postprandial triacylglycerol and apolipoprotein-B concentrations in overweight and obese women. *The British journal of nutrition* 2008;100(5):947-52.
263. Drewnowski A, Bellisle F. Liquid calories, sugar, and body weight. *The American journal of clinical nutrition* 2007;85(3):651-61.
264. Berkey CS, Rockett HR, Field AE, Gillman MW, Colditz GA. Sugar-added beverages and adolescent weight change. *Obes Res* 2004;12(5):778-88.
265. Giammattei J, Blix G, Marshak HH, Wollitzer AO, Pettitt DJ. Television watching and soft drink consumption: associations with obesity in 11- to 13-year-old schoolchildren. *Archives of pediatrics & adolescent medicine* 2003;157(9):882-6.
266. Liebman M, Pelican S, Moore SA, Holmes B, Wardlaw MK, Melcher LM, et al. Dietary intake, eating behavior, and physical activity-related determinants of high body mass index in rural communities in Wyoming, Montana, and Idaho. *Int J Obes Relat Metab Disord* 2003;27(6):684-92.
267. Ludwig DS, Peterson KE, Gortmaker SL. Relation between consumption of sugar-sweetened drinks and childhood obesity: a prospective, observational analysis. *Lancet* 2001;357(9255):505-8.
268. Kvaavik E, Andersen LF, Klepp KI. The stability of soft drinks intake from adolescence to adult age and the association between long-term consumption of soft drinks and lifestyle factors and body weight. *Public health nutrition* 2005;8(2):149-57.
269. Rodriguez-Artalejo F, Garcia EL, Gorgojo L, Garces C, Royo MA, Martin Moreno JM, et al. Consumption of bakery products, sweetened soft drinks and yogurt among children aged 6-7 years: association with nutrient intake and overall diet quality. *The British journal of nutrition* 2003;89(3):419-29.
270. Forshee RA, Storey ML. Total beverage consumption and beverage choices among children and adolescents. *International journal of food sciences and nutrition* 2003;54(4):297-307.
271. Vartanian LR, Schwartz MB, Brownell KD. Effects of soft drink consumption on nutrition and health: a systematic review and meta-analysis. *American journal of public health* 2007;97(4):667-75.
272. Forshee RA, Anderson PA, Storey ML. Sugar-sweetened beverages and body mass index in children and adolescents: a meta-analysis. *The American journal of clinical nutrition* 2008;87(6):1662-71.
273. Tordoff MG, Alleva AM. Effect of drinking soda sweetened with aspartame or high-fructose corn syrup on food intake and body weight. *The American journal of clinical nutrition* 1990;51(6):963-9.
274. Raben A, Vasilaras TH, Moller AC, Astrup A. Sucrose compared with artificial sweeteners: different effects on ad libitum food intake and

- body weight after 10 wk of supplementation in overweight subjects. *The American journal of clinical nutrition* 2002;76(4):721-9.
275. Ashley JM, St Jeor ST, Perumean-Chaney S, Schrage J, Bovee V. Meal replacements in weight intervention. *Obes Res* 2001;9 Suppl 4:312S-20S.
  276. Ditschuneit HH, Flechtner-Mors M, Johnson TD, Adler G. Metabolic and weight-loss effects of a long-term dietary intervention in obese patients. *The American journal of clinical nutrition* 1999;69(2):198-204.
  277. Ebbeling CB, Feldman HA, Osganian SK, Chomitz VR, Ellenbogen SJ, Ludwig DS. Effects of decreasing sugar-sweetened beverage consumption on body weight in adolescents: a randomized, controlled pilot study. *Pediatrics* 2006;117(3):673-80.
  278. Dhingra R, Sullivan L, Jacques PF, Wang TJ, Fox CS, Meigs JB, et al. Soft drink consumption and risk of developing cardiometabolic risk factors and the metabolic syndrome in middle-aged adults in the community. *Circulation* 2007;116(5):480-8.
  279. Tonstad S, Thorsrud H, Torjesen PA, Seljeflot I. Do novel risk factors differ between men and women aged 18 to 39 years with a high risk of coronary heart disease? *Metabolism: clinical and experimental* 2007;56(2):260-6.
  280. Glushakova O, Kosugi T, Roncal C, Mu W, Heinig M, Cirillo P, et al. Fructose induces the inflammatory molecule ICAM-1 in endothelial cells. *Journal of the American Society of Nephrology : JASN* 2008;19(9):1712-20.
  281. Gaby AR. Adverse effects of dietary fructose. *Alternative medicine review : a journal of clinical therapeutic* 2005;10(4):294-306.
  282. Sumagin R, Lomakina E, Sarelius IH. Leukocyte-endothelial cell interactions are linked to vascular permeability via ICAM-1-mediated signaling. *Am J Physiol Heart Circ Physiol* 2008;295(3):H969-H77.
  283. Gersch MS, Mu W, Cirillo P, Reungjui S, Zhang L, Roncal C, et al. Fructose, but not dextrose, accelerates the progression of chronic kidney disease. *American journal of physiology. Renal physiology* 2007;293(4):F1256-61.
  284. Targher G, Chonchol M, Miele L, Zoppini G, Pichiri I, Muggeo M. Nonalcoholic fatty liver disease as a contributor to hypercoagulation and thrombophilia in the metabolic syndrome. *Seminars in thrombosis and hemostasis* 2009;35(3):277-87.
  285. Di Gregorio GB, Yao-Borengasser A, Rasouli N, Varma V, Lu T, Miles LM, et al. Expression of CD68 and macrophage chemoattractant protein-1 genes in human adipose and muscle tissues: association with cytokine expression, insulin resistance, and reduction by pioglitazone. *Diabetes* 2005;54(8):2305-13.
  286. Bourne AR, Richardson DP, Bruckdorfer KR, Yudkin J. The effects of feeding starch, sucrose, glucose or fructose to rats during pregnancy and early lactation. *The Proceedings of the Nutrition Society* 1975;34(2):80A-81A.
  287. Jen KL, Rochon C, Zhong SB, Whitcomb L. Fructose and sucrose feeding during pregnancy and lactation in rats changes maternal and pup fuel metabolism. *The Journal of nutrition* 1991;121(12):1999-2005.

288. Rawana S, Clark K, Zhong S, Buison A, Chackunkal S, Jen KL. Low dose fructose ingestion during gestation and lactation affects carbohydrate metabolism in rat dams and their offspring. *The Journal of nutrition* 1993;123(12):2158-65.
289. Vickers MH, Clayton ZE, Yap C, Sloboda DM. Maternal fructose intake during pregnancy and lactation alters placental growth and leads to sex-specific changes in fetal and neonatal endocrine function. *Endocrinology* 2011;152(4):1378-87.
290. Gardner DS, Tingey K, Van Bon BW, Ozanne SE, Wilson V, Dandrea J, et al. Programming of glucose-insulin metabolism in adult sheep after maternal undernutrition. *Am J Physiol Regul Integr Comp Physiol* 2005;289(4):R947-54.
291. Clause BT. The Wistar Institute Archives: rats (not mice) and history. *The Mendel newsletter; archival resources for the history of genetics & allied sciences* 1998(7):2-7.
292. Saiki RK, Scharf S, Faloona F, Mullis KB, Horn GT, Erlich HA, et al. Enzymatic amplification of beta-globin genomic sequences and restriction site analysis for diagnosis of sickle cell anemia. *Science* 1985;230(4732):1350-4.
293. Van Gelder RN. Applications of the polymerase chain reaction to diagnosis of ophthalmic disease. *Surv Ophthalmol* 2001;46(3):248-58.
294. Saiki RK, Gelfand DH, Stoffel S, Scharf SJ, Higuchi R, Horn GT, et al. Primer-directed enzymatic amplification of DNA with a thermostable DNA polymerase. *Science* 1988;239(4839):487-91.
295. Lodish HF. *Molecular cell biology*. 6th ed. New York: W.H. Freeman, 2008.
296. Chomczynski P, Sacchi N. Single-step method of RNA isolation by acid guanidinium thiocyanate-phenol-chloroform extraction. *Analytical biochemistry* 1987;162(1):156-9.
297. Chomczynski P. A reagent for the single-step simultaneous isolation of RNA, DNA and proteins from cell and tissue samples. *BioTechniques* 1993;15(3):532-4, 36-7.
298. Glasel JA. Validity of nucleic acid purities monitored by 260nm/280nm absorbance ratios. *BioTechniques* 1995;18(1):62-3.
299. Wilson K, Walker JM. *Principles and techniques of biochemistry and molecular biology*. 7th ed. Cambridge, UK New York: Cambridge University Press, 2009.
300. Bustin SA. Real-time, fluorescence-based quantitative PCR: a snapshot of current procedures and preferences. *Expert Rev Mol Diagn* 2005;5(4):493-8.
301. Pfaffl MW. A new mathematical model for relative quantification in real-time RT-PCR. *Nucleic Acids Res* 2001;29(9):e45.
302. Bustin SA. *A-Z of quantitative PCR*. La Jolla, CA: International University Line, 2004.
303. Werner M, Chott A, Fabiano A, Battifora H. Effect of formalin tissue fixation and processing on immunohistochemistry. *The American journal of surgical pathology* 2000;24(7):1016-9.
304. Bancroft JD, Stevens A. *Theory and practice of histological techniques*. 3rd ed. Edinburgh ; New York: Churchill Livingstone, 1990.

305. Kiernan JA. *Histological and histochemical methods : theory and practice*. 3rd ed. Oxford ; Boston: Butterworth Heinemann, 1999.
306. Coons AH, Leduc EH, Connolly JM. Studies on antibody production. I. A method for the histochemical demonstration of specific antibody and its application to a study of the hyperimmune rabbit. *J Exp Med* 1955;102(1):49-60.
307. Kaplan ME, Coons AH, Deane HW. Localization of antigen in tissue cells; cellular distribution of pneumococcal polysaccharides types II and III in the mouse. *J Exp Med* 1950;91(1):15-30, 4 pl.
308. Ramos-Vara JA. Technical aspects of immunohistochemistry. *Veterinary pathology* 2005;42(4):405-26.
309. Graham RC, Jr., Karnovsky MJ. The early stages of absorption of injected horseradish peroxidase in the proximal tubules of mouse kidney: ultrastructural cytochemistry by a new technique. *The journal of histochemistry and cytochemistry : official journal of the Histochemistry Society* 1966;14(4):291-302.
310. Shi SR, Key ME, Kalra KL. Antigen retrieval in formalin-fixed, paraffin-embedded tissues: an enhancement method for immunohistochemical staining based on microwave oven heating of tissue sections. *The journal of histochemistry and cytochemistry : official journal of the Histochemistry Society* 1991;39(6):741-8.
311. Sigma-Aldrich. Bicinchoninic acid protein assay kit. <http://www.sigmaaldrich.com/etc/medialib/docs/Sigma/Bulletin/bca1bul1.Par.0001.File.tmp/bca1bul.pdf>.
312. Kim J, Keyes T, Straub JE. Relationship between protein folding thermodynamics and the energy landscape. *Physical review. E, Statistical, nonlinear, and soft matter physics* 2009;79(3 Pt 1):030902.
313. Mauzeroll J, Bard AJ, Owhadian O, Monks TJ. Menadione metabolism to thiodione in hepatoblastoma by scanning electrochemical microscopy. *Proc Natl Acad Sci U S A* 2004;101(51):17582-7.
314. Fahnrich KA, Pravda M, Guilbault GG. Recent applications of electrogenerated chemiluminescence in chemical analysis. *Talanta* 2001;54(4):531-59.
315. McGavock JM, Victor RG, Unger RH, Szczepaniak LS. Adiposity of the heart, revisited. *Ann Intern Med* 2006;144(7):517-24.
316. Williams P. *Cardiovascular System*. Edinburgh: Churchill Livingstone, 1995.
317. Sacks HS, Fain JN. Human epicardial adipose tissue: a review. *Am Heart J* 2007;153(6):907-17.
318. Shabetai R. *The Pericardium*: Kluwer Academic Publishers, 2003.
319. Ross J. *Composition of the Heart*, 1999.
320. Sharkey D, Gardner DS, Symonds ME, Budge H. Maternal nutrient restriction during early fetal kidney development attenuates the renal innate inflammatory response in obese young adult offspring. *American journal of physiology. Renal physiology* 2009;297(5):F1199-207.
321. Hernan F. *Alterations induced by juvenile obesity on the renal tissue of nutrient restricted offspring*. University of Nottingham, 2010.
322. Ding J, Hsu FC, Harris TB, Liu Y, Kritchevsky SB, Szklo M, et al. The association of pericardial fat with incident coronary heart disease: the

- Multi-Ethnic Study of Atherosclerosis (MESA). *The American journal of clinical nutrition* 2009;90(3):499-504.
323. Jeong JW, Jeong MH, Yun KH, Oh SK, Park EM, Kim YK, et al. Echocardiographic epicardial fat thickness and coronary artery disease. *Circ J* 2007;71(4):536-9.
  324. Taguchi R, Takasu J, Itani Y, Yamamoto R, Yokoyama K, Watanabe S, et al. Pericardial fat accumulation in men as a risk factor for coronary artery disease. *Atherosclerosis* 2001;157(1):203-9.
  325. Rabkin SW. Epicardial fat: properties, function and relationship to obesity. *Obes Rev* 2007;8(3):253-61.
  326. Iacobellis G, Assael F, Ribaudo MC, Zappaterreno A, Alessi G, Di Mario U, et al. Epicardial fat from echocardiography: a new method for visceral adipose tissue prediction. *Obes Res* 2003;11(2):304-10.
  327. McGavock JM, Lingvay I, Zib I, Tillery T, Salas N, Unger R, et al. Cardiac steatosis in diabetes mellitus: a 1H-magnetic resonance spectroscopy study. *Circulation* 2007;116(10):1170-5.
  328. Wheeler GL, Shi R, Beck SR, Langefeld CD, Lenchik L, Wagenknecht LE, et al. Pericardial and visceral adipose tissues measured volumetrically with computed tomography are highly associated in type 2 diabetic families. *Invest Radiol* 2005;40(2):97-101.
  329. Iacobellis G, Ribaudo MC, Assael F, Vecci E, Tiberti C, Zappaterreno A, et al. Echocardiographic epicardial adipose tissue is related to anthropometric and clinical parameters of metabolic syndrome: a new indicator of cardiovascular risk. *J Clin Endocrinol Metab* 2003;88(11):5163-8.
  330. Iacobellis G, Leonetti F. Epicardial adipose tissue and insulin resistance in obese subjects. *J Clin Endocrinol Metab* 2005;90(11):6300-2.
  331. Iacobellis G, Willens HJ, Barbaro G, Sharma AM. Threshold values of high-risk echocardiographic epicardial fat thickness. *Obesity (Silver Spring)* 2008;16(4):887-92.
  332. Iacobellis G, Leonetti F, Singh N, A MS. Relationship of epicardial adipose tissue with atrial dimensions and diastolic function in morbidly obese subjects. *Int J Cardiol* 2007;115(2):272-3.
  333. Iacobellis G, Ribaudo MC, Zappaterreno A, Iannucci CV, Leonetti F. Relation between epicardial adipose tissue and left ventricular mass. *Am J Cardiol* 2004;94(8):1084-7.
  334. Iacobellis G, Barbaro G, Gerstein HC. Relationship of epicardial fat thickness and fasting glucose. *Int J Cardiol* 2008;128(3):424-6.
  335. Iacobellis G, Pellicelli AM, Sharma AM, Grisorio B, Barbarini G, Barbaro G. Relation of subepicardial adipose tissue to carotid intima-media thickness in patients with human immunodeficiency virus. *Am J Cardiol* 2007;99(10):1470-2.
  336. Yoshimoto T, Nakanishi K. Roles of IL-18 in basophils and mast cells. *Allergy international : official journal of the Japanese Society of Allergy* 2006;55(2):105-13.
  337. Freedland ES. Role of a critical visceral adipose tissue threshold (CVATT) in metabolic syndrome: implications for controlling dietary carbohydrates: a review. *Nutr Metab (Lond)* 2004;1(1):12.

338. Ibrahim MM. Subcutaneous and visceral adipose tissue: structural and functional differences. *Obesity reviews : an official journal of the International Association for the Study of Obesity* 2010;11(1):11-8.
339. Hills AP, King NA, Byrne NM. *Children, obesity and exercise : prevention, treatment, and management of childhood and adolescent obesity*. London: Routledge, 2007.
340. Gao FH, Xianzhi; Liu, Yingchun. Effect of intrauterine growth restriction on weight and cellularity of gastrointestinal tract in postnatal lambs. *Canadian Journal of Animal Science* 2008;88(1):6.
341. Robinson JJ, K. D. Sinclair and T. G. McEvoy. Nutritional effects on foetal growth. *Animal Science* 1999(68):315-31.
342. Osgerby JC, Wathes DC, Howard D, Gadd TS. The effect of maternal undernutrition on ovine fetal growth. *The Journal of endocrinology* 2002;173(1):131-41.
343. Edwards LJ, McMillen IC. Maternal undernutrition increases arterial blood pressure in the sheep fetus during late gestation. *J Physiol* 2001;533(Pt 2):561-70.
344. Vonnahme KA, Hess BW, Hansen TR, McCormick RJ, Rule DC, Moss GE, et al. Maternal undernutrition from early- to mid-gestation leads to growth retardation, cardiac ventricular hypertrophy, and increased liver weight in the fetal sheep. *Biology of reproduction* 2003;69(1):133-40.
345. Rae MT, Palassio S, Kyle CE, Brooks AN, Lea RG, Miller DW, et al. Effect of maternal undernutrition during pregnancy on early ovarian development and subsequent follicular development in sheep fetuses. *Reproduction* 2001;122(6):915-22.
346. Barker DJ. The long-term outcome of retarded fetal growth. *Schweizerische medizinische Wochenschrift* 1999;129(5):189-96.
347. Symonds ME, Sebert SP, Hyatt MA, Budge H. Nutritional programming of the metabolic syndrome. *Nature reviews. Endocrinology* 2009;5(11):604-10.
348. Frayling TM, McCarthy MI. Genetic studies of diabetes following the advent of the genome-wide association study: where do we go from here? *Diabetologia* 2007;50(11):2229-33.
349. Nilsson M, Dahlman I, Ryden M, Nordstrom EA, Gustafsson JA, Arner P, et al. Oestrogen receptor alpha gene expression levels are reduced in obese compared to normal weight females. *Int J Obes (Lond)* 2007;31(6):900-7.
350. Nelson LR, Bulun SE. Estrogen production and action. *J Am Acad Dermatol* 2001;45(3 Suppl):S116-24.
351. Davis KE, M DN, Sun K, W MS, J DB, J AZ, et al. The sexually dimorphic role of adipose and adipocyte estrogen receptors in modulating adipose tissue expansion, inflammation, and fibrosis. *Mol Metab* 2013;2(3):227-42.
352. Heine PA, Taylor JA, Iwamoto GA, Lubahn DB, Cooke PS. Increased adipose tissue in male and female estrogen receptor-alpha knockout mice. *Proceedings of the National Academy of Sciences of the United States of America* 2000;97(23):12729-34.
353. Barker DJ, Gluckman PD, Godfrey KM, Harding JE, Owens JA, Robinson JS. Fetal nutrition and cardiovascular disease in adult life. *Lancet* 1993;341(8850):938-41.

354. Hales CN, Barker DJ, Clark PM, Cox LJ, Fall C, Osmond C, et al. Fetal and infant growth and impaired glucose tolerance at age 64. *BMJ* 1991;303(6809):1019-22.
355. Phipps K, Barker DJ, Hales CN, Fall CH, Osmond C, Clark PM. Fetal growth and impaired glucose tolerance in men and women. *Diabetologia* 1993;36(3):225-8.
356. Lithell HO, McKeigue PM, Berglund L, Mohsen R, Lithell UB, Leon DA. Relation of size at birth to non-insulin dependent diabetes and insulin concentrations in men aged 50-60 years. *BMJ* 1996;312(7028):406-10.
357. Law CM, Shiell AW, Newsome CA, Syddall HE, Shinebourne EA, Fayers PM, et al. Fetal, infant, and childhood growth and adult blood pressure: a longitudinal study from birth to 22 years of age. *Circulation* 2002;105(9):1088-92.
358. Eriksson JG, Forsen T, Tuomilehto J, Winter PD, Osmond C, Barker DJ. Catch-up growth in childhood and death from coronary heart disease: longitudinal study. *BMJ* 1999;318(7181):427-31.
359. Ekelund U, Ong K, Linne Y, Neovius M, Brage S, Dunger DB, et al. Upward weight percentile crossing in infancy and early childhood independently predicts fat mass in young adults: the Stockholm Weight Development Study (SWEDES). *The American journal of clinical nutrition* 2006;83(2):324-30.
360. Ozanne SE, Hales CN. Lifespan: catch-up growth and obesity in male mice. *Nature* 2004;427(6973):411-2.
361. Singhal A, Fewtrell M, Cole TJ, Lucas A. Low nutrient intake and early growth for later insulin resistance in adolescents born preterm. *Lancet* 2003;361(9363):1089-97.
362. Singhal A, Cole TJ, Fewtrell M, Lucas A. Breastmilk feeding and lipoprotein profile in adolescents born preterm: follow-up of a prospective randomised study. *Lancet* 2004;363(9421):1571-8.
363. Singhal A, Cole TJ, Fewtrell M, Deanfield J, Lucas A. Is slower early growth beneficial for long-term cardiovascular health? *Circulation* 2004;109(9):1108-13.
364. Metcalfe NB, Monaghan P. Compensation for a bad start: grow now, pay later? *Trends in ecology & evolution* 2001;16(5):254-60.
365. Hotta K, Funahashi T, Bodkin NL, Ortmeier HK, Arita Y, Hansen BC, et al. Circulating concentrations of the adipocyte protein adiponectin are decreased in parallel with reduced insulin sensitivity during the progression to type 2 diabetes in rhesus monkeys. *Diabetes* 2001;50(5):1126-33.
366. Despres JP, Lemieux I. Abdominal obesity and metabolic syndrome. *Nature* 2006;444(7121):881-7.
367. Bauman DE, Currie WB. Partitioning of nutrients during pregnancy and lactation: a review of mechanisms involving homeostasis and homeorhesis. *Journal of dairy science* 1980;63(9):1514-29.
368. Bell AW, Bauman DE. Adaptations of glucose metabolism during pregnancy and lactation. *J Mammary Gland Biol Neoplasia* 1997;2(3):265-78.



369. Freeman ME, Kanyicska B, Lerant A, Nagy G. Prolactin: structure, function, and regulation of secretion. *Physiological reviews* 2000;80(4):1523-631.
370. Kelly PA, Bachelot A, Kedzia C, Hennighausen L, Ormandy CJ, Kopchick JJ, et al. The role of prolactin and growth hormone in mammary gland development. *Mol Cell Endocrinol* 2002;197(1-2):127-31.
371. Neville MC, Morton J, Umemura S. Lactogenesis. The transition from pregnancy to lactation. *Pediatr Clin North Am* 2001;48(1):35-52.
372. Tucker HA. Quantitative estimates of mammary growth during various physiological states: a review. *Journal of dairy science* 1987;70(9):1958-66.
373. Casey T, Patel O, Dykema K, Dover H, Furge K, Plaut K. Molecular signatures reveal circadian clocks may orchestrate the homeorhetic response to lactation. *PLoS One* 2009;4(10):e7395.
374. Oftedal OT. Use of maternal reserves as a lactation strategy in large mammals. *The Proceedings of the Nutrition Society* 2000;59(1):99-106.
375. Wheatley KE, Bradshaw CJ, Harcourt RG, Hindell MA. Feast or famine: evidence for mixed capital-income breeding strategies in Weddell seals. *Oecologia* 2008;155(1):11-20.
376. Augustine RA, Ladyman SR, Grattan DR. From feeding one to feeding many: hormone-induced changes in bodyweight homeostasis during pregnancy. *J Physiol* 2008;586(2):387-97.
377. Madan JC, Davis JM, Craig WY, Collins M, Allan W, Quinn R, et al. Maternal obesity and markers of inflammation in pregnancy. *Cytokine* 2009;47(1):61-4.
378. Basu S, Haghiac M, Surace P, Challier JC, Guerre-Millo M, Singh K, et al. Pregravid obesity associates with increased maternal endotoxemia and metabolic inflammation. *Obesity (Silver Spring)* 2011;19(3):476-82.
379. Lockwood CJ, Matta P, Krikun G, Koopman LA, Masch R, Toti P, et al. Regulation of monocyte chemoattractant protein-1 expression by tumor necrosis factor-alpha and interleukin-1beta in first trimester human decidual cells: implications for preeclampsia. *The American journal of pathology* 2006;168(2):445-52.
380. Naruse K, Noguchi T, Sado T, Tsunemi T, Shigetomi H, Kanayama S, et al. Chemokine and free Fatty Acid levels in insulin-resistant state of successful pregnancy: a preliminary observation. *Mediators of inflammation* 2012;2012:432575.
381. Kraus TA, Sperling RS, Engel SM, Lo Y, Kellerman L, Singh T, et al. Peripheral blood cytokine profiling during pregnancy and post-partum periods. *Am J Reprod Immunol* 2010;64(6):411-26.
382. Iacono A, Bianco G, Mattace Raso G, Esposito E, d'Emmanuele di Villa Bianca R, Sorrentino R, et al. Maternal adaptation in pregnant hypertensive rats: improvement of vascular and inflammatory variables and oxidative damage in the kidney. *American journal of hypertension* 2009;22(7):777-83.
383. Roglans N, Vila L, Farre M, Alegret M, Sanchez RM, Vazquez-Carrera M, et al. Impairment of hepatic Stat-3 activation and reduction of

- PPARalpha activity in fructose-fed rats. *Hepatology* 2007;45(3):778-88.
384. Lindstrom TM, Bennett PR. The role of nuclear factor kappa B in human labour. *Reproduction* 2005;130(5):569-81.
385. Ida A, Tsuji Y, Muranaka J, Kanazawa R, Nakata Y, Adachi S, et al. IL-18 in pregnancy; the elevation of IL-18 in maternal peripheral blood during labour and complicated pregnancies. *Journal of reproductive immunology* 2000;47(1):65-74.
386. Krinke G. *The laboratory rat*. San Diego, Calif.: Academic Press, 2000.
387. Botezelli JD, Dalia RA, Reis IM, Barbieri RA, Rezende TM, Pelarigo JG, et al. Chronic consumption of fructose rich soft drinks alters tissue lipids of rats. *Diabetology & metabolic syndrome* 2010;2:43.
388. Kanarek RB, Orthen-Gambill N. Differential effects of sucrose, fructose and glucose on carbohydrate-induced obesity in rats. *The Journal of nutrition* 1982;112(8):1546-54.
389. Boney CM, Verma A, Tucker R, Vohr BR. Metabolic syndrome in childhood: association with birth weight, maternal obesity, and gestational diabetes mellitus. *Pediatrics* 2005;115(3):e290-6.
390. Brasier AR. The NF-kappaB regulatory network. *Cardiovascular toxicology* 2006;6(2):111-30.